Tampere University

HANNA LUUKINEN

Novel Concepts of Mycobacterial Evasion Mechanisms

Tampere University Dissertations 739

Tampere University Dissertations 739

HANNA LUUKINEN

Novel Concepts of Mycobacterial Evasion Mechanisms

ACADEMIC DISSERTATION
To be presented, with the permission of
the Faculty of Medicine and Health Technology
of Tampere University,
for public discussion in the Jarmo Visakorpi auditorium
of the Arvo building, Arvo Ylpön katu 34, Tampere,
on March 17th 2023, at 12 o'clock.

ACADEMIC DISSERTATION
Tampere University, Faculty of Medicine and Health Technology
Finland

Responsible supervisor and Custos	Tenure track professor Mataleena Parikka Tampere University Finland	
Supervisor	Professor Vesa Hytönen Tampere University Finland	
Pre-examiners	Professor Bernadette Saunders University of Technology Sydney Australia	PhD Laura Savolainen University of Helsinki Finland
Opponent	Professor Antti Iivanainen University of Helsinki Finland	

The originality of this thesis has been checked using the Turnitin OriginalityCheck service.

Cover design: Roihu Inc.

ISBN 978-952-03-2744-6 (print)
ISBN 978-952-03-2745-3 (pdf)
ISSN 2489-9860 (print)
ISSN 2490-0028 (pdf)
http://urn.fi/URN:ISBN:978-952-03-2745-3

Carbon dioxide emissions from printing Tampere University dissertations have been compensated.

PunaMusta Oy – Yliopistopaino
Joensuu 2023

"Not resist, just exist"

(Jung et al., 2019)

ACKNOWLEDGEMENTS

This PhD thesis was conducted in the Infection Biology research group in the faculty of Medicine and Health Technology at Tampere University. I would like to express my greatest gratitude to all the people, core facilities and fish contributing to this thesis.

Finnish Cultural Foundation, Tampere Tuberculosis Foundation, Foundation of the Finnish Anti-Tuberculosis Association and Tampere University Doctoral School have supported this thesis by granting me personal scholarships – very much appreciated. The research has also been partially supported by Fimlab Laboratories.

This thesis was supervised by Associate Professor Mataleena Parikka and Professor Vesa Hytönen who both deserve a huge thanks for guiding and supporting me through this project and being my voice of sense. Thank you for sharing your scientific knowledge and finding the time to discuss with me, which is not always that easy in this hectic world. This journey has taught me to be a scientist and you have had a great role in it.

I am very honored to have Professor Antti Iivanainen from University of Helsinki as my opponent. Thank you for accepting this invitation. With your scientific background our discussion on the defense day will undoubtedly be fascinating. The pre-examiners of this thesis, Associate Professor Bernadette Saunders, and PhD Laura Savolainen, are acknowledged for their thorough review and excellent comments. Thank you for putting your time and effort on this thesis.

I would also like to thank my thesis follow-up group members Professor Olli Silvennoinen and Professor Ilkka Junttila for their valuable comments and scientific discussions during my years of PhD research.

The infection biology research group is a group of talented and often hilarious people and every one of them are appreciated. Especially, I would like to thank Milka Hammarén and Leena-Maija Vanha-aho for your friendship, brilliant mind, and laugh also outside work. Kirsi Savijoki, Saara Lehmusvaara, Lauri Paulamäki, Hannaleena Piippo, Aleksandra Svorjova, Alina Sillanpää and Rosa Korhonen – it has truly been a pleasure to work with you. I'm grateful for your sense of humor and all the help and support I have had.

The Zebrafish Core Facilities at Tampere University is acknowledged for taking good care of the zebrafish and keeping things organized. I would also like to thank my fellow fish researchers who had helped me countless times and understand that it is possible to hate and love fish at the same time.

Believe or not but there is also life outside the PhD project! The best way to have a good feeling is to play music with your friends and Torvikopla Big Band is a perfect example of this. Thank you, my dear friends, for lifting my spirit every Wednesday evening and sometimes other evenings as well.

Tiina, Emmi, Sofia, and Maaria – your friendship is so special and so much appreciated. It gives me strength to know that you are always there, all ups and downs, always. I'm also very grateful that I have become friends with your amazing families. My parents and my brothers, Matti, Jaakko, and Otto, with your families, you deserve a special thanks for giving me break-outs from the scientific world and for looking after the children when I needed extra working time.

I officially started my PhD work in 2015 and now seven years later I'm finishing the book. Lastly, I would like to thank my own little family; my dear husband Bruno and my beautiful kids Ahti and Kerkko. It is not easy to have a wife/mom with scientific ambitions and sometimes strange working hours but having your support and love means everything for me.

Hanna Luukinen
December 2022

ABSTRACT

Tuberculosis is caused by bacterium *Mycobacterium tuberculosis*, and it is currently the deadliest infectious disease worldwide. The standard antimicrobial regimen is a cocktail of antimicrobials taken for several months, which still does not guarantee a successful eradication of the bacteria. Treatment dropouts and the use of antimicrobials that are inefficient in eradicating the infection have led to emerged drug-resistance. Also, the lack of safe and effective vaccine makes the prevention of tuberculosis difficult. One reason for the challenges in both prevention and treatment of tuberculosis is the ability of mycobacterium to cause chronic infection and protect itself from environmental hazards such as active immune responses and antimicrobials.

The aim of this study was to examine mycobacterial evasion mechanisms against antimicrobials and immune responses and propose new intervention strategies. *Mycobacterium marinum* and zebrafish were used to study the interaction of the host and the pathogen. Mycobacterium can actively suppress immune responses and delay the onset of adaptive responses, and to prevent this immune evasion, an immunomodulation was tested. In the adult zebrafish population, around 10% of the population is able to naturally retain the *M. marinum* load below the detection limit of qPCR. This proportion could be increased up to 25% by priming with heat-killed *Listeria monocytogenes* prior the mycobacterial infection. The induced protective immune response significantly reduced mycobacterial loads after four weeks of infection and induced clearance in both wildtype and *rag1*$^{-/-}$ mutant fish showing the important role of innate immune responses in the sterilizing response. The protective immune response was characterized with an increased expression of *mpeg1, tnf* and *nos2b* and decreased expression of *sod2*. These results indicate early clearance mediated via pro-inflammatory responses and enhanced killing of mycobacteria. Importantly, the immunomodulation was ineffective if the infection was already established. However, a similar approach could be used as a prophylactic treatment in high burden areas.

Another mycobacterial evasion strategy is the formation of biofilms. After suppressing immune responses and establishing the infection, mycobacteria form bacterial communities in granulomas and produce extracellular matrix that gives

structure and protection for the bacterial population. The fast-growing *M. marinum* with a bioluminescent cassette was used to study the biofilm maturation and composition *in vitro*. The results showed that the biofilm maturation did not alter the minimum inhibitory concentration (MIC) but increased minimum bactericidal concentration (MBC) 63 times compared to planktonic cells within two days of biofilm culturing. It was further confirmed with repeated antimicrobial exposures that the increased tolerance of biofilm cultures was not due to genetic resistance. Degrading any of the major extracellular matrix components in combination with rifampicin reduced the number of live bacteria in a biofilm, demonstrating the important role of the biofilm matrix in the antimicrobial tolerance.

Time-kill curve analysis with a quick bioluminescence read-out was established to specifically measure the subpopulation of persister mycobacteria. In the analysis, the killing kinetics of a bacterial population was followed after the exposure to high concentration of a bactericidal antimicrobial, here rifampicin, to measure the persister subpopulation that can tolerate the drug for a prolonged time. For maturing *M. marinum* biofilm, the killing kinetics were significantly different after one week of culturing compared to planktonic cells, and the rifampicin concentration was saturated at 400 μg/ml after which increasing the antimicrobial concentration did not alter the killing kinetics. This method has a potential in screening for treatments that specifically target mycobacterial persisters.

Finally, sybodies against biofilm extracellular matrix proteins GroEL1 and GroEL2 were used to specifically target *M. marinum* and *M. tuberculosis* biofilms *in vitro* and in *ex vivo* zebrafish granulomas. Sybodies are synthetic molecules mimicking the binding domain of antibodies. The binding properties of the sybodies can be easily modified and screened against the wanted target in sybody libraries. The potential sybodies acquired from the screens were assessed by confocal imaging. Fluorescence labelled anti-GroEL sybodies were able to bound GroEL on both *in vitro* and *ex vivo* biofilms making sybodies an attractive molecular carrier to target mycobacterial biofilms. A treatment that specifically targets mycobacterial persisters in biofilms inside granulomas could enhance the efficacy of antimicrobial therapy and shorten the current treatment time. By understanding better, the mycobacterial evasion mechanisms, future treatments can more effectively be targeted against Mtb.

TIIVISTELMÄ

Mycobacterium tuberculosis -bakteerin aiheuttama tuberkuloosi on tällä hetkellä maailman tappavin infektiotauti. Nykyinen tuberkuloosin antibioottihoito on useamman lääkkeen yhdistelmä ja se kestää useita kuukausia, mutta ei siitäkään huolimatta takaa onnistunutta mykobakteerin häätämistä. Tehottomien antibioottien käyttö sekä pitkät hoitoajat keskeytyksineen edesauttavat antibioottiresistenttien kantojen syntyä. Lisäksi turvallisen ja tehokkaan rokotteen puute tekee tuberkuloosin ehkäisemisestä hankalaa. Yksi syy näihin haasteisiin tuberkuloosin ehkäisemisessä ja hoidoissa on mykobakteerin kyky kehittää krooninen infektio ja suojella itseään ympäristöhaitoilta kuten aktiiviselta immuunivasteelta sekä antimikrobiaalisilta lääkkeiltä.

Tämän tutkimuksen tavoitteena on tutkia mykobakteerin mekanismeja, joiden avulla se pystyy estämään antibioottien ja immuunivasteiden tehokkaan toiminnan, sekä etsiä uusia strategioita näihin mekanismeihin puuttumiseen. *Mycobacterium marinum* -bakteeria ja seeprakalaa käytettiin tutkimaan isännän ja patogeenin välistä vuorovaikutusta. Mykobakteeri kykenee aktiivisesti vaimentamaan immuunivasteita ja myöhästyttämään hankittujen immuunivasteiden alkamista. Tutkimuksessa testattiin immunomodulaation tehoa näiden mykobakteerin ominaisuuksien estämisessä. Ilman hoitoja noin 10 % aikuisista seeprakaloista pystyy luonnollisesti pitämään mykobakteerimäärän alle qPCR:n detektiorajan. Tätä osuutta voitiin kuitenkin nostaa 25 %:iin aktivoimalla immuunivaste lämpötapetulla *Listeria monocytogenes* -bakteerilla ennen mykobakteeri-infektiota. Aikaansaatu suojaava immuunivaste vähensi merkitsevästi mykobakteerimääriä mitattuna neljä viikkoa infektion jälkeen ja jopa steriloi mykobakteerin osasta populaatiota sekä villityypin kalassa että *rag1*$^{-/-}$ -mutanttikaloissa, mikä viittaa synnynnäisten immuunivasteiden tärkeään rooliin mykobakteerin steriloivassa vasteessa. Suojaavassa vasteessa *mpeg1, tnf* ja *nos2b* -geenien ilmentyminen oli merkitsevästi lisääntynyt, kun taas *sod2* oli vähentynyt verrattuna kontrolliryhmään. Nämä tulokset viittaavat mykobakteerin häätämiseen infektion varhaisessa vaiheessa lisääntyneen tulehdusvasteen ja tehokkaamman mykobakteerin tuhoamisen avulla. Huomattavaa on, että immunolodulaatio lämpötapettua *L. monocytogenes* -bakteeria hyödyntäen ei saanut aikaan suojaavaa vastetta, jos infektio oli jo olemassa. Vastaavaa immuuniterapiaa

voitaisiin kuitenkin käyttää ennaltaehkäisevänä menetelmänä korkean tuberkuloosi-ilmaantuvuuden alueilla.

Toinen tutkittu mykobakteerin suojautumiskeino on biofilmin muodostaminen. Immuunivasteiden heikentämisen ja infektion aikaansaamisen jälkeen mykobakteeri muodostaa bakteeriyhteisöjä granuloomissa ja tuottaa solunulkoista matriksia, joka antaa bakteeripopulaatiolle tukea ja suojaa. Nopeakasvuista bioluminoivaa *M. marinum* -bakteeria käytettiin biofilmin kypsymisen ja koostumuksen tutkimuksessa *in vitro*. Tulokset osoittivat, että biofilmin kypsyminen ei muuttanut rifampisiinin MIC-arvoa (minimum inhibitory concentration), mutta nosti MBC-arvoa (minimum bactericidal concentration) 63-kertaisesti verrattuna planktoniseen yksisoluisena kasvavaan mykobakteeriin kahden päivän biofilmin kasvattamisen jälkeen. Toistuvilla antibioottialtistuksilla pystyttiin varmistamaan, että biofilmin lisääntynyt antibioottitoleranssi ei johtunut geneettisestä resistenssistä. Elävien mykobakteerien lukumäärää biofilmissä pystyttiin vähentämään hajottamalla solunulkoisen matriksin tärkeimpiä polymeerejä yhdessä rifampisiini-hoidon kanssa, mikä osoitti biofilmin matriksin tärkeyden antibioottitoleranssissa.

Nopea bioluminesenssimittaukseen perustuva tappokäyräanalyysi validoitiin mittaamaan erityisesti persistoivien mykobakteerien alapopulaatiota. Analyysissa seurataan bakteeripopulaation tappokinetiikkaa korkealla antibioottikonsentraatiolla, ja voidaan mitata persisteribakteerien alapopulaatiota, joka kykenee sietämään antibioottia keskimääräistä pidemmän ajan. Tappokinetiikka oli merkitsevästi hitaampi yhden viikon ikäisellä *M. marinum* biofilmillä verrattuna planktoniseen yksisoluiseen kasvatukseen. Lisäksi rifampisiinin konsentraatio saturoitui 400 µg/ml:ssa, jonka jälkeen antibioottikonsentraation nostaminen ei nopeuttanut bakteerien tappoa. Tätä menetelmää on mahdollista käyttää seulomaan hoitoja, jotka vaikuttavat erityisesti persistoiviin soluihin.

Lopuksi tutkittiin mykobakteerin biofilmin solunulkoisen matriksin proteiineihin, GroEL1 ja GroEL2, kohdentuvia sybodeja *in vitro M. marinum* ja *M. tuberculosis* biofilmeissä sekä *ex vivo* seeprakalan granuloomissa. Sybodit ovat synteettisiä vasta-aineen sitoutumisosaa matkivia molekyylejä, jonka sitoutumista voidaan helposti muokata ja seuloa halutun kohteen mukaan olemassa olevista sybody-kirjastoista. Seulonnasta saatujen potentiaalisten sybodien sitoutumista mykobakteerin biofilmiin arvioitiin konfokaalimikroskopian avulla. Fluoresenssileimatut anti-GroEL-sybodit tunnistivat GroEL-proteiineja biofilmin päältä sekä *in vitro* että *ex vivo* tehden sybodista houkuttelevan vaihtoehdon erilaisten molekyylien kohdentamisessa mykobakteerin biofilmeihin. Nykyisiä antibioottihoitoja voidaan mahdollisesti tehostaa ja hoitojen pituutta lyhentää ottamalla huomioon granuloomien sisällä

biofilmeissä olevat mykobakteeripersisterit. Ymmärtämällä paremmin mykobakteerin menetelmiä, joilla se suojelee itseään ympäristön haittavaikutuksilta, tulevaisuuden hoitoja voidaan kohdentaa tehokkaammin *Mycobacterium tuberculosis* -bakteeria vastaan.

CONTENTS

List of Figures

List of Tables

ABBREVIATIONS

ADC	albumin, dextrose, catalase enrichment
APC	antigen presenting cell
ARG1	arginase 1
B.C.E.	before the common era
BCG	bacillus Calmette-Guérin
BSA	bovine serum albumin
CD	cluster of differentiation
CelA1	cellulase A1
CFP-10	10 kDa culture filtrate antigen
CFU	colony forming unit
CGB	corticosteroid-binding globulin
CTRL	control
DAPI	diamidino-2-phenylindole
DHEA	dehydroepiandrosterone
DPF	days post fertilization
ECM	extracellular matrix
eDNA	extracellular DNA (deoxyribonucleic acid)
EPS	extracellular polymeric substance
ESAT-6	6 kDa early secretory antigenic target
ESX	6 kDa early secretory antigenic target (ESAT6) protein family secretion
GroEL	chaperonin GroEL
HIV	human immunodeficiency virus
HKLm	heat-killed *Listeria monocytogenes*
HPA	hypothalamic-pituitary-adrenal
IFN	interferon
IGRA	interferon-gamma release assay
IL	interleukin
LPS	lipopolysaccharide
Lux	luciferase

MBC	minimum bactericidal concentration
MIC	minimum inhibitory concentration
MDR-Mtb	multi-drug resistant *Mycobacterium tuberculosis*
Mm	*Mycobacterium marinum*
MOI	multiplicity of infection
MPEG1	macrophage expressed gene 1
MPX	myeloid-specific peroxidase
Mtb	*Mycobacterium tuberculosis*
NK cell	natural killer cell
NOS2B	nitric oxide synthase 2b
OADC	oleic acid, albumin, dextrose, catalase enrichment
OD	optical density
PBS	phosphate-buffered saline
PCR	polymerase chain reaction
qPCR	quantitative polymerase chain reaction
RAG	recombination-activating gene
ROS	reactive oxygen species
RR-Mtb	rifampicin-resistant *Mycobacterium tuberculosis*
SEM	standard error of mean
SOCS3	suppressor of cytokine synthesis 3
SOD2	superoxide dismutase 2
TB	tuberculosis
Th cell	T helper cell
TLR	toll-like receptor
TNF	tumor necrosis factor
TST	tuberculin skin test
WHO	World Health Organization
WPI	weeks post infection

ORIGINAL PUBLICATIONS

Publication I **Luukinen H**, Hammarén MM, Vanha-aho L-M, Parikka M (2018) Modeling Tuberculosis in *Mycobacterium marinum* Infected Adult Zebrafish. J. Vis. Exp. (140), e58299, doi:10.3791/58299

Publication II **Luukinen H**, Hammarén MM, Vanha-aho L-M, Svorjova A, Kantanen L, Järvinen S, Luukinen BV, Dufour E, Rämet M, Hytönen VP, Parikka M (2018) Priming of Innate Antimycobacterial Immunity by Heat-killed *Listeria monocytogenes* Induces Sterilizing Response in the Adult Zebrafish Tuberculosis Model. Disease Models & Mechanisms 11: dmm031658 doi: 10.1242/dmm.031658

Publication III Savijoki K, Myllymäki H, **Luukinen H**, Paulamäki L, Vanha-aho LM, Svorjova A, Miettinen I, Fallarero A, Ihalainen TO, Yli-Kauhaluoma J, Nyman T, Parikka M. (2021) Surface-Shaving Proteomics of *Mycobacterium marinum* Identifies Biofilm Subtype-Specific Changes Affecting Virulence, Tolerance and Persistence. mSystems 29;6(3):e0050021. doi: 10.1128/mSystems.00500-21.

Manuscript Hammarén MM*, **Luukinen H***, Sillanpää A, Remans K, Lapouge K, Custodio T, Löw C, Myllymäki H, Montonen T, Seeger MA, Robertson J, Nyman T, Savijoki K, Parikka M. (2022) Proteomic analysis of Mycobacterial Biofilm Matrix and Development of Biofilm-binding Synthetic Nanobodies. Submitted.

*equal contribution

The publications are referred I-III or as manuscript in the following text.

AUTHOR'S CONTRIBUTION

Publication I Luukinen has participated in the development of the zebrafish study model introduced in the review article. In addition to presenting old data, the publication includes new data analysis of previously collected data, showing the spectrum of disease outcomes in adult zebrafish mycobacterial infection (Figure 2B). Luukinen has also written the manuscript.

Publication II Luukinen has had a significant contribution in all parts of the study: planning, performing the laboratory experiments (except the original screen of the immunomodulators), analyzing, and interpreting the results, writing, and editing the manuscript. Luukinen has designed, performed, and analyzed the laboratory experiments for all the major results described in the publication, except the original screen of the immunomodulators. The publication has also been published as a part of Milka Hammarén's PhD thesis.

Publication III Luukinen has designed, performed, and analyzed all antimicrobial tests made in the study (Figures 4C, 8 and S3). Luukinen has developed the biofilm culture protocol and optimized and validated the antimicrobial testing method. This data confirmed the importance of cellulose in the biofilm bacterial population and showed the role of maturing mycobacterial biofilms in the antimicrobial treatment. Luukinen has also participated in writing and editing the manuscript.

Manuscript Luukinen has participated in *in vitro* proteomics sample preparation and sample collection, method development and manuscript writing and editing. Particularly, Luukinen has designed, performed, and analyzed the functional analysis of the screened sybodies (Figures 4 and S4).

INTRODUCTION

Tuberculosis (TB) is an old disease caused by *Mycobacterium tuberculosis* (Mtb). It has been estimated that the first Mtb strain infecting humans is around 20,000 years old (Barberis et al., 2017). TB has been a health issue for a long time, and it has been reported in many historical documents the oldest known being dated 2,900 years B.C.E. (Cave & Demonstrator, 1939). Despite being such an old pathogen, TB still influences many lives today killing 1.5 million individuals each year (World Health Organization, 2021).

The long history with humans has made Mtb fluent in evading the host's immune responses and protecting itself from the environment. Co-evolution of Mtb with humans has finetuned the mechanisms on both sides but there is no winner in the competition. Mtb infection often leads to an asymptomatic chronic infection where the pathogen is sealed in granulomas, aggregations of host cells around the bacteria. In addition to asymptomatic chronic infection, mycobacterial infection can cause a range of different disease outcomes from active contagious disease to cleared infection. This heterogenous disease spectrum makes TB a complicated disease to model and the scientist to wander in a labyrinth of immunological networks. The current understanding of TB immunology is wide, but the details of the sterilizing immune responses are still unclear. The lack of knowledge on protective immune responses are seen in the lack of effective vaccines against TB. There is a high demand for new vaccines to replace BCG (bacillus Calmette-Guérin) vaccine that is ineffective for preventing infection and is partially protecting only young children (Mangtani et al., 2014).

In the granulomas, Mtb has its own niche where it can replicate and form bacterial communities, although the active immune responses and the endothelial layer around the granuloma limits the spread and replication of the bacteria. Mycobacteria are able to produce ECM (extracellular matrix) and develop biofilms in granulomas. These biofilms are known to increase the tolerance against drugs (Chakraborty et al., 2021). Drugs inefficient to eradicate the infection and easily disrupted long antimicrobial regimens enable the development of genetic antimicrobial resistance which has become an emerging issue. Without a doubt, there is a great need for better intervention strategies for preventing and treating TB.

The studies of this thesis aim in overcoming mycobacterial evasion mechanisms, either by inducing protective immune responses with immunomodulation, or by targeting mycobacterial biofilms to enhance the effect of antimicrobial treatment. The zebrafish–*M. marinum* pair is used here to model the natural interplay between mycobacteria and the host. In this work, the fish TB model has been found a potential approach for studying the details of the protective immune responses. In addition, the characteristics of mycobacterial antimicrobial tolerance were dissected and persisters, a subpopulation of phenotypically tolerant bacteria, were identified from the *M. marinum* biofilm. Finally, a nanobody-based targeting of mycobacterial biofilms *in vitro* and *ex vivo* was tested.

1 REVIEW OF THE LITERATURE

1.1 Tuberculosis epidemic

Currently TB is the deadliest infectious disease in the world infecting 10 million and killing 1.5 million individuals every year including 214,000 deaths with HIV (human immunodeficiency virus) co-infection (World Health Organization, 2021). The regional differences in the distribution of TB burden are large and it is most common in South-East Asia, Africa, and the Western Pacific (World Health Organization, 2021). The high death rates are affected by the fact that in high burden countries about one third of the TB patients seeking care did not have access to a proper healthcare system (Reid et al., 2019). It has also been estimated that half of the TB deaths are due to poor healthcare and drug availability (Kruk et al., 2018), which highlights the socioeconomic problems underlying the global TB epidemic. The social problems connected to TB are most visible in developing countries, but a similar trend is seen in industrial countries where social risk factors including education and housing were strong determinants of the risk of developing TB (Nguipdop-Djomo et al., 2020).

TB is an infectious disease caused by *Mycobacterium tuberculosis* (Mtb). It can be treated with antimicrobial, but the standard regimen lasts for six months and includes several antimicrobials. The long antimicrobial regimen easily leads to treatment dropouts and the development of antimicrobial-resistant strains. Dropouts are understandable especially among the poorest that might need to spend over 50% of their yearly incomes on the treatment in developing countries (Reid et al., 2019). In addition to dropouts, a long antimicrobial regimen with ineffective drugs or too low antimicrobial concentration can enrich the population of resistant mycobacteria within the host that can also potentially transmit the resistant bacteria to new hosts.

Antimicrobial-resistance of Mtb is an emerging issue and drugs that are better available and more effective against mycobacteria are in great need. The three countries with the highest prevalence of antimicrobial-resistant TB are India, China and the Russian Federation (World Health Organization, 2021). Worldwide there are almost 0.5 million antimicrobial-resistant TB cases yearly of which 78% are caused by multi-drug resistant strains (World Health Organization, 2020). The incidents

with antimicrobial-resistant strains are predicted to increase in the future and in 30 years, a quarter of the TB-related deaths are estimated to be caused by antimicrobial-resistant Mtb (O'Neill, 2016)

Vaccination against TB would be a cost-effective way to tackle the pathogen. The oldest and the only TB vaccine in use, BCG (bacillus Calmette-Guérin), gives very variable protection in human and as a live-attenuated vaccine it is not considered safe, and it cannot be recommended to HIV-infected or immunocompromised individuls (Reid et al., 2019). Despite all the efforts, designing a better vaccine has not been successful so far, even though the requirements for the potential protection does not have to be high. It has been estimated that a vaccine that would produce protection against active TB in 60% of the vaccinated individuals, would reduce the number of new cases by 40% when given to only 20% of the adults with the risk of TB (Knight et al., 2014).

The World Health Organization has set an ambitious End TB -strategy to reduce the TB-related deaths by 95% and new cases by 90% in 20 years compared to 2015 rates (World Health Organization, 2014). There has been some progress and the total number of new TB cases has indeed reduced 6.3% from 2015 to 2018 and deaths by 11%, but to hit the WHO's End TB -strategy goal the reduction should have been 20% and 35%, respectively (World Health Organization, 2019), which is far behind the set milestones. Also, the COVID-19 pandemic starting in the late 2019 has had a negative impact on the number of people seeking for medical help and the new TB cases have been underdiagnosed (World Health Organization, 2021). This has also reflected on the number of TB-related deaths. The first time since 2005 there is an increase in the number of TB deaths reversing three years of improvement (World Health Organization, 2021).

1.2 Tuberculosis as a disease

TB is caused by *Mycobacterium tuberculosis* complex bacteria most commonly *Mycobacterium tuberculosis* (Mtb). Mtb infection can lead to a spectrum of different disease outcomes from latent TB to disseminated active infection. There is a model that estimates that about ¼ of the human population has latent TB (Houben & Dodd, 2016). Latent TB is termed as condition where the Mtb-infected patient has an immune reaction against Mtb antigens but has no symptoms of active TB (World Health Organization, 2018). Although these patients do not show any signs of infection, they still have live bacteria in their body. Some of the bacteria can be in a

dormant state, in which the bacterium has reduced its metabolic activity and replication rate and has increased tolerance against drugs (Lipworth et al., 2016). Mycobacterium can stay in dormancy for years but can also reactivate later leading to an active TB, for example, if the immune system is compromised. An old epidemiological estimation states that 5-10% of all latent TB will reactivate during lifetime (Comstock et al., 1974). This group of patients that are termed as latently infected individuals may include persons that have active infection but do not have any symptoms of active TB or persons that have sterilized the infection and anything between these two disease states.

It has been estimated that only about 5% of the infected individuals are primary progressive patients that develop an active TB after infection (Tsenova & Singhal, 2020). These persons are unable to control the bacterial growth or restrict the bacteria in granulomas at this stage and are in a risk of dying of TB. In the case of latent TB, the clinical signs are the same – no symptoms. Active TB, on the other hand, can be found in many types and severities. The most common form of TB among adults is pulmonary TB (Alcaïs et al., 2005) but about 15% of the actively infected individuals have extrapulmonary disease such as meningeal TB (World Health Organization, 2019). Especially immunocompromised individuals have a greater risk of developing disseminated disease but at the same time, 20% of patient with disseminated disease do not have any immunodeficiencies (Sharma et al., 2016). Other risk factors in addition to immune deficiencies include malnutrition, diabetes, and poor lifestyles such as smoking and heavy alcohol consumption (World Health Organization, 2019).

The common symptoms of active pulmonary TB may include shortness of breath, weight loss, persistent cough, weakness, fever, and night sweats. The bloody cough is a typical symptom often described for TB and it is due to uncontrolled bacterial growth, caseation of granulomas and their cavitation into the lung in the later stages of pulmonary TB. TB patients also suffer from severe weight lost, wasting, that is connected to the altered metabolic status of the patient. Cavitation of granulomas and extensive inflammation can cause accumulation of liquid into the lungs eventually leading to lung failure.

1.2.1 Diagnostics of tuberculosis

The symptoms of active TB are common for many diseases, which makes diagnosing of TB difficult. The lack of signs in latent TB and the variety of symptoms in

extrapulmonary TB further reduces the number of diagnosed TB cases. TB is often underdiagnosed, and it is estimated that 35% of all TB cases are not diagnosed or treated for other reasons (Reid et al., 2019). The diagnostic methods of TB include imaging lung abnormalities of pulmonary TB by chest X-ray, measuring immune reaction against mycobacterial antigens or detecting the presence of Mtb either by PCR (polymerase chain reaction) or by smear microscopy of acid-fast bacilli and culture. Additionally, antimicrobial susceptibility can be determined by culture-based methods or by specific PCR methods targeting known Mtb resistance genes.

Although there are many diagnostic tests for TB, only active TB is possible to diagnose undoubtedly as the diagnosis can be confirmed bacteriologically. Tuberculin skin test and IGRA (interferon-γ release assay) are tests that measure existing immune responses, and they can be positive due to ongoing active infection, latent disease, or immunization after resolved infection. Tuberculin skin test may give a false-positive result if the patient has been recently vaccinated with BCG or has non-tuberculous mycobacterial infection (Mckay et al., 1999). IGRA has been developed to overcome these specificity problems but although it is currently the best method to diagnose latent TB, it cannot be used to interpret how active the disease is, how likely it is to reactivate or have the person already cleared the infection. Currently there is no tool for distinguishing between latent and sterilized infection and the efficacy of the TB treatments cannot be exclusively assessed.

1.2.2 Antimicrobial treatment of tuberculosis

TB requires a long and intensive antibiotic regimen. It lasts for total of six months starting with an intensive treatment with four different antibiotics for the first two months. These antibiotics are rifampicin, isoniazid, pyrazinamide, and ethambutol. The regimen is followed by rifampicin and isoniazid alone for the next four months. Even longer treatments are required if the infection is more severe such as in the case of disseminated TB, infection by drug-resistant Mtb or if the patient is HIV-positive or pregnant (Centers for Disease Control and Prevention, 2016). The long treatment time is problematic as it can easily lead to interruptions. Also, the use of suboptimal drugs in a long regimen increases the possibility of emerging of new drug-resistant strains.

The antibiotics that are used in the standard antibiotic regimen are called first-line drugs, but multidrug-resistant strains that need additional drugs are increasingly common. In 2019, which is the latest year that was not affected by the COVID-19

pandemic, it was estimated that there were 500,000 drug-resistant TB cases, of which 78% were caused by multi-drug resistant (MDR) strains (World Health Organization, 2020). These strains are genetically resistant to both isoniazid and rifampicin (Centers for Disease Control and Prevention, 2016), the two most commonly used antibiotics against Mtb. If treating susceptible Mtb is difficult, treating drug-resistant strains are even harder and the success rate of the antibiotic treatment in MDR-TB drops from 85% to 59% (World Health Organization, 2021). Drug-resistant Mtb strains are treated with second-line drugs. All TB drugs may cause severe side-effects forcing to end the regimen prematurely, but the second-line drugs are the most toxic, which makes the treatment of drug-resistant TB extremely difficult.

In addition to multi-drug resistant strains, extensively drug-resistant (XDR-TB) strains have been emerged. XDR-TB strains are resistant also against at least two second-line TB antibiotics such as fluoroquinolones, capreomycin, amikacin and kanamycin (Centers for Disease Control and Prevention, 2016). For example, fluoroquinolones are recommended to be used for treating isoniazid-resistant Mtb strains (World Health Organization, 2017). The number of MDR-TB cases has remained rather constant over the past few years consisting only 3-4% of the new TB cases, but the MDR-TB is enriched to 18-21% among the patients that have relapsed TB (World Health Organization, 2021). Luckily, more recent TB antibiotics bedaquiline and delamanid and repurposed antibiotics linezolid and clofazimine have helped in the treatment of drug-resistant TB (Furin et al., 2019).

All in all, the antibiotic treatment of TB is challenging with the current drugs available, and the actual number of drug-resistant cases remains an estimate as all TB cases are not tested in low-income countries. The antibiotics are ineffective in eradicating the infection and require long treatment time causing harmful side-effects and emerging antibiotic resistance.

1.2.3 Vaccines in tuberculosis prevention

BCG (bacillus Calmette-Guérin) is the oldest and the most often used TB vaccine. BCG is a live-attenuated strain of *Mycobacterium bovis* which has been developed by serial passages to loss the virulence factors. Although previous Mtb infection gives protection against re-infection in non-human primates (Cadena et al., 2018), the effectiveness of BCG vaccine varies greatly between different groups. A meta-analysis of BCG efficacy studies showed that the overall BCG protection varies between 0-100% (Rodrigues et al., 1993). The same meta-analysis revealed that the

protection against miliary and meningeal TB has the smallest deviation, the protection being 75% on average in case-control studies (Rodrigues et al., 1993). In children under age 16, BCG gives 19% protection against Mtb infection and 58% protection against the disease (Roy et al., 2014), but it has only little effect in the transmission of the pathogen as it protects such a limited number of TB cases (Angelidou et al., 2020). BCG is mostly given intradermally, but recent studies have pointed out that intravenous route can be more effective. In non-human primates, 60% of the animals were able to sterilize the infection after intravenous BCG vaccination and 90% could control the infection (Darrah et al., 2020).

M. bovis BCG is a live bacterium, and it is possible that the vaccinated person develops BCG disease, especially if the person is immunocompromised. One study concluded that about 1% of HIV-positive infants vaccinated with BCG got disseminated BCG disease (Hesseling et al., 2009). Due to its risk–benefit ratio, BCG has now been excluded from many national vaccination programs as unnecessary risk. When considering the variable efficacy of BCG and its safety-issues, better vaccines are needed against TB to effectively control the epidemic.

Currently there are about 150 on-going clinical trials of different TB vaccine candidates (Medicine, ClinicalTrials.gov, 2020). These vaccine candidates include both booster vaccines for BCG and vaccines to replace BCG. Most promising vaccine candidate (M72/AS01E) from GlaxoSmithKline has shown 50% protection against active disease in latently infected patients (Tait et al., 2019; van der Meeren et al., 2018). The M72/AS01E vaccine is a recombinant protein vaccine including two *Mtb* proteins and a liposomal adjuvant (Tait et al., 2019).

1.3 Pathogenesis of tuberculosis

Both host and pathogen factors affect the pathogenesis of TB. At the host side, there are few gene deficiencies related to immune responses that are known to increase the susceptibility to TB and the severity of the disease (Abel et al., 2018). Also, the overall wellbeing of the host also affects the probability of getting active TB. For example, malnutrition and environmental factors such as pollution can reduce the function of the immune system and hence affect the susceptibility to TB and the development of the disease. However, even without increased host susceptibility, Mtb infection can lead to serious disease, although the infectiveness of Mtb is rather low. One study reported that eventually only around 34% of children under five

years living with a household contact of active TB will get infected (Singh et al., 2005).

Mtb has several mechanisms to evade host's immune responses, which greatly affects the disease progression. It seems that both the host and the pathogen have powerful mechanisms and the fight of these two factors leads to most often chronic infection and granuloma formation but also active or sterilized infection depending on the balance of the forces.

1.3.1 Characteristics of *Mycobacterium tuberculosis*

Mtb is an acid-fast rod-shaped bacterium that has a high content of lipids around the cell. This mycobacterial cell structure consists of a plasma membrane and a cell wall that has arabinogalactan and peptidoglycan as its main components (Daffé & Marrakchi, 2019). The cell wall also has an outer membrane that is often called mycomembrane. The inner part of the mycomembrane contains mostly of the mycobacterial cell membrane lipids such as mycolic acids whereas the outer part of the membrane has a smaller percentage of different lipids, most importantly trehalose mycolic acids (Augenstreich & Briken, 2020; Ortalo-Magné et al., 1996). Many mycobacterial antibiotics inhibit mycolic acid synthesis, which highlights the importance of mycolic acids for mycobacteria (Lehmann et al., 2018; Schroeder et al., 2002). On top of the mycomembrane, Mtb also have a capsule that has a composition of carbohydrates, proteins, lipopolysaccharide, and limited amount of lipids (Daffé & Marrakchi, 2019). This unique cell envelope structure protects Mtb against different kind of environmental stresses.

It has already been mentioned that Mtb infection can result in different disease outcomes. Both host and mycobacterial heterogeneity affect the outcome of Mtb infection and how the disease progresses. *Mycobacterium tuberculosis* complex bacteria are genetically relatively homogenous and there are only small differences between the strains (Frothingham et al., 1994). One reason is that Mtb do not use horizontal gene transfer (Gutacker et al., 2002) but the genetic variation is due to the single nucleotide polymorphisms (Homolka et al., 2012). Even though the genetic differences are small, they might have a clinical impact (Jong et al., 2008; Reed et al., 2007) and indeed certain Mtb strains are reported to be more virulent than others (Hernández-Pando et al., 2012; Nicol & Wilkinson, 2008). Interestingly, it has been noticed by sequencing several individual mycobacterial cells from one patient that the majority of the mutations in this cell population show changes typically caused

by oxygen damage, which has led to a hypothesis that the host's reactive oxygen species (ROS) has contributed to these mutations (Liu et al., 2020). The same was not seen with HIV-positive patients further supporting the role of immune responses in the generation of the mutations (Liu et al., 2020). The mycobacterial genetic variation remains rather low but the mycobacterial phenotypic variation on the other hand can be high and the host determinants have a great contribution to this, which is important for the pathogenesis of the disease.

The phenotypic variation is distinct from genetic variation, and it is the cell's way to react to different environmental conditions. It is driven by the environment, and it is influenced for example by the anatomical location of the infection, availability of oxygen and nutrients, the local immune responses and whether the mycobacterium are found in an intracellular or extracellular niche or within granulomas (Dhar et al., 2016). Also, single cell's characteristics like size, age, growth rate, cell organelle composition and available components and molecules are connected to different phenotypes (Schwabe & Bruggeman, 2014). In the case of TB, especially the activation of the host's immune response has been linked with increased mycobacterial phenotypic variation (Dhar & Manina, 2015). An active immune response was able to induce the formation of dormant mycobacteria that are non- or slowly replicating and have reduced metabolic activity. Dormancy can be induced basically by any harmful condition such as low pH, iron deficiency, short of nutrient or oxygen (reviewed in (Sarathy & Dartois, 2020)). However, even when there are no problems with the growth conditions, the mycobacterial population has a small subpopulation of non-growing mycobacteria (Kussell et al., 2005).

1.3.2 Early infection and innate immune responses

The transmission occurs when droplets containing Mtb coughed by a patient with active TB are inhaled. The initial infection dose can be as low as one bacterium. Epithelial cells of the airways are the first encounters of Mtb. In addition to acting as a physical barrier, epithelial cells can produce for example antimicrobial peptides (Li et al., 2012; Rivas-Santiago et al., 2005) and complement proteins (Fehrenbach, 2001). Virulent Mtb strains can utilize epithelial cells as resident cells and induce their cell death to promote mycobacterial spreading (Dobos et al., 2000). Epithelial cells can also produce a variety of cytokines, chemokines, and growth factors to recruit and activate immune cells to kill the bacteria (Scordo et al., 2016).

In the lungs, Mtb is recognized by several innate receptors such as toll-like receptors (TLR), NOD-like receptors (NLR), c-type lectins and retinoic acid-inducible gene (RIG)1-like receptors (RLRs) located both on cell membrane and in cytosol of innate immune cells (Mortaz et al., 2015). Innate cell receptors recognize pathogen-associated molecular patterns (PAMPs) that are commonly found repetitive structures on pathogens. One way mycobacterium can evade immune responses is by physical hiding from the recognition by immune receptors using its mycomembrane. These mycomembrane lipids form a protective layer around the bacteria, which also slows down the influx of nutrients and hence the replication rate (Brennan & Nikaido, 1995). One group of membrane lipids, called phthiocerol dimycoceroserates (PDIM), are reported to specifically prevent the recognition by certain innate receptors (Cambier et al., 2014). These molecules also have an impact on the recruitment of new macrophages by shifting the phenotype of the local macrophage population towards less bactericidal (Cambier et al., 2014).

Alveolar macrophages, neutrophils, NK cells and dendritic cells play an important role in the early immune response as they are among the first immune cells encountered by Mtb. Macrophages consist of up to 95% of the immune cells in the alveolar space making them the most abundant innate cell type in the first encounter of host's immune response and Mtb (Srivastava et al., 2014). They take up Mtb by phagocytosis and try to kill them by fusing phagosomes with lysosomes containing reactive oxygen species (ROS) and antimicrobial peptides in an acidic environment.

Even though mycobacterium is recognized and phagocytosed by innate immune cells, it has ways to survive inside the endosome. Controversially, mycobacterium promotes phagosome fusion with early endosomes by its PIM (phosphatidylinositol mannoside) molecule (Vergne et al., 2004). However, Mtb is capable of arresting the later phagolysosome maturation by its LAM (lipoarabinomannan) molecule (Vergne et al., 2003). It has been speculated that the reason for enhancing early endosome fusion is to gain access to nutrients and iron located in the endosomes (Vergne et al., 2004). Mycobacterial PIM molecule can inhibit the reduction of pH in phagosomes by preventing the recruitment of vacuolar ATPase and GTPase that pump H^+ ions into the phagosome (Via et al., 1998). Prevention of phagolysosome fusion is a key point in the survival of mycobacterium within the host and it is thought to lead to translocation to cytosol and rapid bacterial growth phase inside the macrophage before escaping from the host cell (Sturgill-Koszycki et al., 1994).

In addition to inhibiting the acidification of the phagosomes, the attack of reactive oxygen (ROS) and nitrogen species (RNS) from lysosomes is prevented by

mycobacteria. The production of ROS and RNS during the infection is a common antimicrobial defense mechanism by innate immune cells but mycobacterium is able to resist this harmful environment for a long period. The mycobacterial ROS and RNS resistance mechanisms include for example the mechanical protection obtained via the strong cell wall and the production of scavenger enzymes for ROS (Voskuil et al., 2011).

Mycobacterial secretion systems, ESXs (6 kDa early secretory antigenic target (ESAT6) protein family secretion system), have a great role in the virulence of the pathogen. ESX is a transmembrane multiprotein apparatus that transports different molecules through the inner cell membrane of mycobacteria (Gröschel et al., 2016). Mycobacteria have five secretion systems, ESX-1 to 5, of which ESX-1 is the best-known in the context of immune evasion (Gröschel et al., 2016). ESX-1 is part of the RD1 (region of difference 1) gene locus which is removed from the avirulent BCG vaccine strain (Etna et al., 2015). ESX-1 secretion system has long been known to be essential in breaking down the phagosome and releasing mycobacteria into the cytosol (McDonough et al., 1993). ESX-1 has also been shown to break down whole host cells enabling the spreading of the bacteria into new host cells (Augenstreich et al., 2017; Conrad et al., 2017; Mahairas et al., 1996).

1.3.2.1 The role of other innate immune mechanisms

In addition to the well-known macrophages and their intracellular killing properties, other innate mechanisms contribute to the mycobacterial control as well such as innate lymphoid cells (ILC) and a phenomenon called xenophagy which can be described as autophagy against non-self-material. There are several pieces of evidence that xenophagy is an important defence mechanism against intracellular infections (Siqueira et al., 2018) and mycobacterium has developed an ESX-1-based method to hamper autophagy (Romagnoli et al., 2014), which supports the importance of the mechanisms in the protection against mycobacterial infections.

ILCs are unconventional lymphocytes commonly found on mucosal tissues and have characteristics from both innate and adaptive immunity. These cells are maturing from the lymphoid lineage, but they do not have functional machinery to undergo somatic recombination and thus are missing lymphocyte antigen receptors (T and B cell receptors) (Spits et al., 2013). Innate lymphoid cells can be divided into three groups that mimic the features of T helper cells (Th1, Th2 and Th17) of adaptive immunity described later (Spits et al., 2013). The role of unconventional T cells in TB is less studied but it has been shown in a mouse model that the ILC

population reacts to the mycobacterial infection and differentiate towards pro-inflammatory ILC1-like cells on mucosal tissues (Corral et al., 2022). Also, ILCs producing interleukin (IL) 17 and IL22 (group 3) has been reported to be important in the control of Mtb growth in the early mycobacterial infection (Ardain et al., 2019).

Natural killer (NK) cells are included in the ILC group 1. NK cells have a direct killing capacity to eliminate infected host cells, but they can also react directly against Mtb (Esin et al., 2013). Another important mechanism in mycobacterial infections mediated by NK cells is the secretion of different cytokines such as IL22 (Dhiman et al., 2009) and IFNγ (Schierloh et al., 2005) that activate macrophages to kill intracellular Mtb. NK cells have a role in the protection against TB and there is a correlation between disease severity and the number of available NK cells (Moreira-Teixeira et al., 2020). Also, the function of NK cells is affected in the early phase of the infection (Bozzano et al., 2009), which may be due to mycobacterial evading mechanisms.

Whereas the protective role of NK cells in TB is largely accepted, the role of neutrophils remains controversial. They are part of the innate repertoire, and they phagocytose mycobacteria during innate and adaptive responses (de Martino et al., 2019). Insufficient numbers of neutrophils in the early infection have been connected to the progression of the disseminated disease in a mouse model (Pedrosa et al., 2000). On the other hand, high numbers of neutrophils are associated with worsen disease outcome (Moreira-Teixeira et al., 2020; Panteleev et al., 2017) and neutrophils are commonly utilized by Mtb as host cells during active TB (Eum et al., 2010). It has been shown that Mtb is capable of inducing necrosis of neutrophils by a RD-1 (region of difference) dependent manner and promoting mycobacterial spreading into new host cells (Corleis et al., 2012). Altogether, it seems that the kinetics of the neutrophil number during Mtb infection is an important factor of TB pathogenesis (Hult et al., 2021; Pedrosa et al., 2000).

1.3.3 Establishing the infection and adaptive immune responses

Antigen presenting cells (APC), especially dendritic cells, leave the site of infection via draining lymphatics to lymph nodes after phagocytosing mycobacteria. In lymph nodes, they prime naïve T cells specific for their peptide antigen presented on HLA type II -molecule, which actives T cells and enhances T cell proliferation leading to activated adaptive immune system. The prevention of immune functions by mycobacterium is focused on innate responses, which greatly affect the course of

infection by ensuring the survival of the pathogen and by delaying adaptive immune responses. In addition, mycobacterial infection disturbs the transportation of the HLA type II -molecules from endosomes to cell membrane. Unloaded HLA molecules are detected on the cell surface of innate immune cells quickly after mycobacterial infection and at the same time the synthesis of new HLA type II -molecules is prevented (Hava et al., 2008). The overall result is that the transportation of APCs and mycobacterial antigens into lymph nodes and the initiation of adaptive responses is delayed compared to other infectious diseases, which gives mycobacteria more time to replicate (Gallegos et al., 2008). The delay of the onset can be significant, and it can take 2-6 weeks after the infection until the adaptive responses can be measured (de Martino et al., 2019).

1.3.3.1 Evading adaptive responses

The effector functions of the mammalian adaptive immune system are powerful, and it is important for mycobacterium to suppress these mechanisms to ensure its survival. There are indications that mycobacteria produce antigens to mislead T cell responses (Goldberg, Saini, and Porcelli 2014), which may also explain why Mtb has evolutionarily conserved antigens that are recognized by T cells in humans (Comas et al. 2010).

$CD4^+$ cells, so called helper T cells (Th cell), are one type of T cells. Their main job is to help other immune cells to get activated by secreting cytokines. The importance of $CD4^+$ cells in the control of TB is highlighted in HIV-positive patients who have a 19 times higher risk of developing TB (World Health Organization, 2019). HIV infects human $CD4^+$ cells and macrophages and reduces these cell populations. 8.2% of new TB cases were among HIV-positive patient but the percentage of HIV-positive cases increases to 15% when considering TB deaths (World Health Organization, 2020). $CD4^+$ cells are further divided into subtypes that all have a role in inducing specific types of immune responses. Of these subtypes only Th1 and Th2 are further discussed in the context of TB.

Traditionally, mycobacterium is thought to only reside in intracellular niches inside macrophages, where it is not exposed to humoral immune responses and therefore the focus of TB research has been on macrophages and Th1 cells that that activates macrophages to enhance their killing mechanisms against intracellular pathogens. However, various studies have yielded inconsistent results regarding the role of Th1 cells, varying from Th1 cells mediating detrimental effects to no effect or protective responses (reviewed in (Jasenosky et al., 2015)). Th1 and Th2 has been

described as one another's counterparts where expression of Th1 markers inhibit the expression of Th2 markers and vice versa but a more recent view accepts plasticity and co-expression between Th subsets (Zhu, 2018). In a zebrafish study, higher Th2/Th1 balance was connected to controlled mycobacterial infection (Hammaren et al., 2014). Another study revealed that IFNγ and IgA levels against mycobacteria were lower in patients with active TB and higher with protective responses (Belay, Legesse, Mihret, Ottenhoff, et al., 2015), which suggests that Th1 and Th2 inductions at the same time is both possible and beneficial in the fight against mycobacterial infection.

B cells and the differentiated form, plasma cells, are professional antibody producing cells. As so many other immune mechanisms, the role of antibodies in the pathogenesis and the protection against TB, is controversial. This might be because an early studies of TB serum therapy gave variable results (Glatman-Freedman & Casadevall, 1998). Later it has been noticed that the functional part of the antibody may affect the protection. IgA against Mtb prevented the *in vitro* cell line infection of mycobacterium but IgG enhanced the infection (Zimmermann et al., 2016). In addition to a diminished number of B cells in the blood of active TB patients, the remaining cells have dysfunctional proliferation and the production of immunoglobulins and cytokines (Joosten et al., 2016), which might be due to Mtb immune evasion strategies.

In addition to interrupting specific immune mechanisms, mycobacteria can also generate a regulatory environmental niche. It has been noticed that the number of regulatory T cells is increased in the mycobacteria-infected lungs, inhibiting the adaptive immune responses (Kursar et al., 2007). Regulatory T cells have an inhibitory role in inflammation and infection, and they maintain tolerance against own tissues. Although, it is important to prevent tissue disruption and excessive inflammation, these mechanisms can also prevent beneficial immune responses. Mycobacterium has evolved to take advantage of some of these inhibitory mechanisms, and it is known that they can, for example, manipulate a variety of immune cells to produce IL10 (Abdalla et al., 2016).

Host's innate and adaptive immune responses work hard to eliminate pathogens but in the case of Mtb the prevention mechanisms of the bacteria are strong and diverse, which often leads to a compromise between the host and the pathogen. In most of the TB patients, this compromise is seen as the establishment of chronic infection and the formation of granulomas.

1.3.4 Granulomatous lesions – survival after immune responses

Within a host, mycobacterium is often seen in granulomas when the immune response fails to resolve the infection. Granuloma is a typical pathological structure common in TB patients and it is considered as the hallmark of TB. However, granulomas can form also in other diseases when the source of infection or inflammation cannot be eliminated. The TB granuloma is a dynamic structure of aggregated host immune cells around a mycobacterial core where mycobacteria attach to each other including some immune cells moving around the granuloma (Cronan et al., 2018). The granuloma consists of innate immune cells such as macrophages, monocytes, dendritic cells, and neutrophils but also T and B cells of the adaptive immune response (Mattila et al., 2013; Wolf et al., 2007). A fibrous capsule surrounds the structure and seals mycobacteria inside (Cyktor et al., 2013).

The formation of a granuloma starts when infected and inflammatory macrophages cluster together (Bhavanam et al., 2016). New immune cells are recruited to the site to join the initial granuloma after which adaptive immune cells starts to aggregate to form a mature granuloma (Bhavanam et al., 2016). A mature granuloma is a tight structure where some of the macrophages have switched their phenotype to epithelioid macrophages with adherens junctions (Cronan et al., 2016). Macrophages can also be seen as multinucleated giant cells of fused macrophages. The development of giant cells is initiated by the signal from CD40-CD40 ligand interaction and sufficient amount of IFNγ produced by T lymphocytes (Sakai et al., 2012). The function of giant cells is unknown, but they are thought to be important in restricting the mycobacterial dissemination (Cronan et al., 2016). Interestingly, these cells are not able to phagocytose (Lay et al., 2007). Foamy macrophage is another modified macrophage type in granulomas. The characteristic of foamy macrophage is visible lipid droplets inside the cell. Foamy macrophages are developed when the host's lipid metabolism is altered leading to accumulation of lipids in the cytosol and giving the cells their foamy appearance (Kim et al., 2010). Large amounts of lipids inside the host cell can provide a source of nutrient for mycobacteria (Peyron et al., 2008).

Even though the host promotes granuloma formation to seal the pathogen in one place and to prevent the spreading of the disease, granulomas may also help mycobacteria to grow safely inside these structures (Cronan et al., 2016; Davis & Ramakrishnan, 2009). Macrophage morphological changes into epithelioid macrophages, giant cells and foamy macrophages are all connected to mycobacterial antigens (Johansen et al., 2018; Rhoades et al., 2005), which implies that

mycobacteria may actively enhance granuloma formation. Also, induction of granuloma blood vascularization by mycobacterium promotes mycobacterial growth (Oehlers et al., 2017). Mycobacterial antigens' capability of modifying granuloma formation shows that mycobacterium can utilize granuloma environment for its own use.

Granulomas have different maturation states. Granuloma can be found in a solid form where the centre of the granuloma is compact, but it can also mature further into a caseous granuloma and even liquify the centre of the granuloma when the infection proceeds. Formation of foamy macrophages can be considered as an early state of caseous granuloma (Kaplan et al., 2003). In some cases, the caseotic granuloma center with foamy macrophages can eventually develop into a necrotic granuloma center, where the core includes dead and dying host cells and live mycobacteria.

Like TB itself, granulomas are very heterogenous in nature. Only one bacterial cell can originate a granuloma (Lin et al., 2014) and within a patient, different granulomas are independent in their maturation (Subbian et al., 2015). Thus, granulomas can be found in many forms and maturation state within a patient. It has also been shown that separate granulomas can fuse together forming complex structures of multifocal granulomas (Cronan et al., 2018).

In addition to histological differences, the inflammatory environment can vary within a granuloma and inflammatory mediators differ between different granuloma sections. The centre of a granuloma has a pro-inflammatory profile and towards the edges anti-inflammatory environment takes place (Marakalala et al., 2016). Even though granulomas are formed when the source of infection cannot be eliminated and mycobacteria is known to take advantage of this situation, it has been shown that about 10% of the granulomas are sterilized by four weeks in a macaque model (Lin et al., 2014). The local granuloma immune responses determine the bacterial killing and can lead to different outcomes independently from other granulomas of the same individual (Gideon et al., 2015; Lin et al., 2014; Martin et al., 2017).

1.3.4.1 Mycobacterial biofilm

The initial steps in the TB pathogenesis include intracellular phases but mycobacteria can survive outside the host cell as well as already discussed in the previous section. Mycobacterial cords, long tight bacterial bundles, have been visualized *in vitro* already by Robert Koch (Koch, 1882) and the formation of biofilms has later been seen in human granulomas (Chakraborty et al., 2021). The aggregation of bacterial cells and

the production of ECM (extracellular matrix) is a natural phenomenon typical for bacteria. Biofilms are well-defined bacterial communities where the bacteria are adhered to each other and the ECM they have produced around them (Vestby et al., 2020). They can also attach to live or artificial surfaces (Vestby et al., 2020). Extracellular polymeric substance (EPS) originating from the bacteria can include proteins, lipids, nucleic acids, and polysaccharides that are known to be involved in the mycobacterial ECM structure (Chakraborty & Kumar, 2019). Cellulose is one component of the Mtb biofilm ECM in human granulomas that has also shown to have an impact on drug tolerance in mouse model (Chakraborty et al. 2021).

The bacteria also communicate with each other in biofilms, a phenomenon called quorum sensing, and several mycobacterial molecules have been identified to signal changes in the environment (Hegde, 2019). Environmental stress such as a reductive agent can induce the mycobacterial biofilm formation *in vitro* (Trivedi et al., 2016), which might be possible also in the *in vivo* situation where immune responses attack against the pathogen. Biofilm gives protection for the bacterial population and mycobacterium grown in a biofilm has an increased drug tolerance (Ojha et al., 2008). The importance of mycobacterial biofilms has been shown in experimental Mtb infection models, where they have been connected to higher virulence and more severe infection outcome (Arias et al., 2020; Chakraborty et al., 2021).

Biofilm lifestyle leads to heterogeneity of the bacterial population and the development of subpopulations within the biofilm. Persisters, a subpopulation of tolerant cells, have been identified in *Staphylococcus aureus* infections a long time ago (Hobby et al., 1942) but the terminology is often inconsistent, and tolerance, persistence and resistance are often used as synonyms in the literature. According to Brauner et. al, the term resistance is used for genetic resistance that can be measured by the increased MIC (Brauner et al., 2016). Tolerance is surviving in a lethal drug concentration for a long period of time without altering the MIC on the population level, whereas persistence is a character of a subpopulation of cells that are non-heritable tolerant to the drug (Brauner et al., 2016). Phenotypic cell-to-cell differences within the bacterial population are often associated with the metabolic status of the bacteria and their entry into dormancy (Cadena et al., 2017). While dormancy is an important way for mycobacteria to protect against harsh conditions, this is not the only means. It has been shown that the bacterial population has sub-populations within biofilm which alter by their metabolic activity, cell division rate and/or drug tolerance (reviewed in Bisht & Wakeman, 2019). However, the mycobacterial population in thiol-induced biofilm was shown to be metabolically active and still have increased drug tolerance (Trivedi et al., 2016).

1.4 Protective immune responses

Many cytokines are shown to be important in the control of TB. Immunosuppressant studies in humans and genetic deficiencies connected to TB have broadened the understanding of protective immune responses in TB. For example, the lack of IL12 or IFNγ is a determining factor of TB progression (Alcaïs et al., 2005) and the amount of produced IFNγ correlates negatively with the severity of the disease (Abebe et al., 2017; Belay, Legesse, Mihret, Bekele, et al., 2015). It has been shown that blocking pro-inflammatory TNF increases the risk of active TB in humans (Keane et al., 2001; Navarra et al., 2014). Also, IL1 receptor genetic deficiency is detrimental in TB (Fremond et al., 2007). As these studies indicate, deficiency in one cytokine or mechanism can lead to the progression of the disease but it is unlikely that there is a single factor that could protect against Mtb infection. The question is what kind of cocktail of immune cells and molecules is needed for the protection in different disease states.

Both TNF and IFNγ are cytokines that are acknowledged as key players in the immune response against Mtb. They are produced by several immune cell types in response to infection and they promote inflammation and immune reactions. The lack of either of the cytokines leads to more severe disease but also if they are produced extensively. The right balance of TNF (Roca & Ramakrishnan, 2013) and IFNγ (Sakai et al., 2016) during infection has been connected to better controlled bacterial burdens. Similar kind of balance is required in T cell subsets. The importance of $CD4^+$ cells in the control of TB has been demonstrated in HIV-TB co-infected patients but it has been a long debate whether Th1 or Th2 cells are more effective in protecting against TB. Increasing amount of evidence suggest that Th1 and Th2 responses together provides the best protection (Abebe, 2019; Hammaren et al., 2014).

It is known that some individuals are able to sterilize Mtb infection. These individuals are often called 'resisters'. The eradication of the bacteria can happen before the onset of adaptive immune responses and relies mostly on innate responses. This phenomenon is referred as early clearance. Delayed clearance is mediated by an effective combination of innate and adaptive responses (Verrall et al., 2014), which is seen for example as sterilized granulomas (Lin et al., 2014). A complete delayed clearance of Mtb can be detected only postmortem in human as latent and cleared infection are impossible to distinguished with diagnostics (Verrall et al., 2014). However, spontaneous clearance of mycobacteria has been shown in

adult zebrafish where about 10% of population cleared the mycobacterial infection without antibiotics or vaccinations (Hammaren et al., 2014).

One of the first studies of the resisters was reported already in 1930s where about 5% of highly Mtb-exposed nursing students remained tuberculin skin test (TST) negative (Badger & Spink, 1937), which is an indirect indication of the early clearance and the absence of the adaptive responses. The prevalence of resisters varies between different studies from 5% to 35% depending on the duration of the Mtb exposure, genetic background of Mtb and the host, the intensity of the exposure and the length of the study follow-up (reviewed in (Simmons et al., 2018)).

A more recent study followed household-contacts of active TB patients in Uganda and showed that 8.3% of the individuals with repeated high Mtb exposure did not develop reaction in IGRA-test (interferon-gamma release assay) (Lu et al., 2019). As the IGRA result indicates, these resisters did not produce IFNγ but instead had IFNγ-independent immune responses. Even though the resisters did not have IFNγ production, they had similar antibody responses to individuals with latent TB (Lu et al., 2019). In an *in vitro* study, blood immune cells from latent TB patients restricted the growth of BCG, whereas cells from patients with active TB did not (Joosten et al., 2018). It is also known that having latent Mtb infection partially protects against progressive disease in reinfection, and therefore $CD4^+$ and IFNγ, seen in the individuals infected for the first time, have been thought to be the cornerstones of the protective immune response (Andrews et al., 2012). However, this is in some extent contradictory to the observation that a stronger reaction in the TST is associated with higher likelihood of active TB in the future (Comstock et al., 1974; Doherty et al., 2002). Previously IGRA- and TST-negative persons have been categorized as individuals that do not have adaptive immune responses against Mtb. The Uganda cohort clearly indicates that the interpretation of the IGRA results is not that straightforward, and it is possible for IGRA-negative individuals to recognize Mtb antigens and develop antibodies against the pathogen.

For a long time, it has been known that resisters exist, but the protective immune mechanisms are still under investigation. The development of new TB prevention strategies would greatly benefit from broader understanding of the mechanisms of both early and delayed clearance.

1.5 Zebrafish model of tuberculosis

1.5.1 Overview of animal models to study tuberculosis

Many animal models have helped to understand mycobacterial infections and they all have given valuable information about the host and pathogen interactions. Modelling TB in animals has not been easy. All models have their pros and cons, and the animal model should be chosen according to the research question. Mtb is a very old human pathogen that has co-evolved with its host and developed specific immune evasion mechanisms. This has made the pathogen very host-specific, and even though it can infect other species as well, the development of the whole disease spectrum of TB is only seen in non-human primates, in addition to the human host. Especially, necrotic cavitary granulomas, aerosol transmission and post-primary steps of the infection with latent infection are hard to model in animals (Basaraba & Hunter, 2017). The primary phases of the Mtb infection are often described in animal models but many of the animals in use are either hyposensitive or hypersensitive to the mycobacteria and unable to resolve the infection or limit it by developing latency. After all, latent infection consists of a major part of human infections, and it would be important to model experimentally.

Non-human primates are considered the most accurate model to mimic human TB. They are anatomically and physiologically close to humans and they have similar immunological and pathological reactions against mycobacteria (Pena & Ho, 2015). The aerosol infection with Mtb develops, depending on the infection route and dose, into a spectrum of disease outcomes from progressive infection to latent disease (Lin et al. 2009). Macaque has indeed been used to study the heterogeneity of the granulomas within a single host (Lin et al., 2014; Martin et al., 2017). One difference between human and non-human primate infection is the prevalence of latency among infected individual which also varies between macaque species from 10 to 40% of the infected individuals versus up to 90% latency in humans (Pena & Ho, 2015). Another drawback in the use of non-human primates is the obvious ethical issues along with high costs and issues of ensuring safe handling of the animals.

Mice are the most commonly used animal model in the TB research offering a great variety of different research tools. A major disadvantage in the use of mice is that Mtb is not a natural pathogen of mice, and the course of the infection does not resemble in every aspect the mycobacterial infection seen in humans (Cooper, 2015). For example, the latent phase of the infection is often created by using antibiotics or

vaccination to kill the actively dividing bacteria that would otherwise proceed replicating eventually killing the animal (Shi et al., 2011). The inbred mouse strains have different susceptibility to Mtb infection some being resistant and the others very sensitive, which affects the progression of the disease (Medina & North, 1999). Even though the disease pathogenesis in mice differs from human infection, it is still the golden standard in TB drug and vaccine preclinical testing.

Guinea pigs and rabbits have also been routinely used as TB models. Guinea pigs are relatively susceptible for Mtb infections and produce an active gradually progressive disease with necrotic granulomas (Sakamoto, 2012). Compared to mice, guinea pigs are bigger in size, and hence more operations can be performed per one animal (Singh & Gupta, 2018). Unlike mice, guinea pigs can be used to study dissemination and transmission of TB (Smith et al., 1970), but in the other hand they lack the latent disease state (Riley, 1957). While guinea pigs are susceptible to the Mtb infection and mice can be either sensitive or resistant depending on the strain in use, rabbits can develop latent TB (Sakamoto, 2012). In addition, rabbits produce cavitary granulomas not seen in mice and model the transmission of the disease similar to guinea pigs (Peng et al., 2015). However, the lack of research tools for both rabbits and guinea pigs may reduce their use as TB models.

Mycobacterium bovis causes bovine TB in cattle. Over 50% of cattle and buffalo herds were tested to be infected by *M. bovis* in Amazon regions (Carneiro et al., 2019), which provides a large reservoir of zoonotic *M. bovis* infections for humans. It is a very common disease and clearly bovine TB needs resolving as an issue on its own, but it can also be used as a TB model of a natural host–pathogen interaction. Cows are large animals, and the disease progression is slow, which might reduce its practicality as a TB model, but the disease has many pathological similarities with human TB (van Rhijn et al., 2008). Unlike rodent models where the infection often spreads into other organs, *M. bovis* infection is mostly found in lungs. A natural *M. bovis* infection can start just from one to three bacteria but variable infection doses are used to modify the disease severity experimentally (van Rhijn et al., 2008). Granulomas are also hallmarks of bovine TB and the formation and the pathology of the granulomas are very similar to human TB (Palmer, 2018). In addition, latency is seen in the bovine TB, which has been detected by the absence of culturable bacteria but positivity in the IFNγ releasing assay (Pollock et al., 2000). Interestingly, the immune responses against *M. bovis* in cattle vary between the individuals and it is known that only maximum of 30% of the herd get the disease, resembling the heterogeneity of TB transmission in a human population (Phillips et al., 2003).

Drosophila melanogaster is a widely used model for many cellular and molecular phenomena. It has also been utilized as a model organism for innate immune responses and different aspects of infection diseases such as *Candida albicans* (Sampaio et al., 2018), *Yersinia pestis* (Ludlow et al., 2019), *Zika virus* (Y. Liu et al., 2018) and trypanosomatid infection (Hamilton et al., 2015). *M. marinum* has been used to study TB. *D. melanogaster* has only innate immune system which limits the use of the model to early mycobacterial infection. The lack of adaptive immune responses also makes drosophila a very susceptible to *M. marinum* infection and only few bacteria can lead to lethal disease within a couple of weeks (Dionne et al., 2003). In drosophila, *M. marinum* is capable of preventing acidification of the phagosomes, remaining alive in the phagocytes (Dionne et al., 2003) and induce wasting (Dionne et al., 2006) similarly to mammal TB models. The *M. marinum–D. melanogaster* model lacks some important aspects of the TB pathogenesis, but it is genetically tractable, rapid, and low-cost model, which is ideal for large-scale screening.

Amoeba is another invertebrate that has been used to study TB. It is a single-cell organism that is found in forest soil and water, and it is a possible natural source of non-tuberculous mycobacteria (Mba Medie et al., 2011). *Dictyostelium discoideum* can be infected by both Mtb and *M. marinum* (Hagedorn et al., 2009; Solomon et al., 2003). As a single-cell organism, amoeba can be compared to a macrophage that phagocytose material and degrade it and model these events of human TB. In addition, mycobacterial spreading from one cell to another is a nonlytic process has been modelled in amoeba infection (Hagedorn et al., 2009). The very early events of the mycobacterial infection can be studied in amoeba but in the absence of multiple mammalian cell types and tissues, it cannot fully model the pathogenesis of TB.

1.5.2 *Mycobacterium marinum* and zebrafish

Zebrafish (*Danio rerio*) infected with *Mycobacterium marinum* is a recently established TB model and a natural host–pathogen pair. The advantages of zebrafish include its small size, small space requirement and low cost. It also produces numerous offspring, and it is a well-known model often used in developmental biology. In comparison to many other laboratory animals, zebrafish populations are heterogenic in nature. Zebrafish lines are not inbred and hence remain genetically heterogeneous (Brown et al., 2012; Guryev et al., 2006). The heterogeneity of the population increases variation in the experimental results, but it also models the variation seen in the human population.

On the other hand, zebrafish is not a mammalian species, and its anatomical differences can affect the results. The infection route in the experimental zebrafish model differs from how humans get infected, as in the absence of the lungs, zebrafish are infected via injection. When adult zebrafish are infected by an intraperitoneal injection, the bacteria enter the blood circulation and the primary location of the experimental infection is the internal organs such as the spleen, the liver, the gonads, and the pancreas (Parikka et al., 2012). The location of the infection in internal organs after intraperitoneal injection and the lack of lungs prevent the modelling of air-borne transmission in zebrafish, which is a big drawback in TB research. Another disadvantage of the zebrafish model is the limited availability of research tools as compared to the often-used mouse model. For example, antibodies against zebrafish molecules and zebrafish cell lines are not commonly available.

The genomes of *M. tuberculosis* and *M. marinum* are 85% identical (Stinear et al., 2008). Most of the differences are due to *M. marinum* partial genome duplication and its adaptation for environmental niches (Tobin & Ramakrishnan, 2008). Both zebrafish larva and adult zebrafish are used as a TB model. Zebrafish larva is a transparent organism that enables visualization of the infection with fluorescence techniques. Zebrafish larva develop quickly, and intravenous injection can be performed already for one-day-old embryos. Also, drug treatments can be done by simply adding the compound into the fish water making large-scale screens feasible to perform. The ease of handling and genetic manipulation techniques have made zebrafish larva a popular model in TB research.

The fact that zebrafish larva is still a developing animal can be a problem in some cases. For example, larva does not have a full set of adaptive immune responses and its organs are still maturing (Trede et al., 2004). Adult zebrafish does not have this problem, but the wildtype fish lacks the easy imaging and genetic manipulation techniques used for larva, although optically transparent casper mutant zebrafish line has enabled imaging of adult fish as well. A major advantage in adult zebrafish is its fully developed innate and adaptive immune systems. It has been shown that a small infection dose of under 50 cfu (colony forming unit) produces spontaneous latent disease with stable *M. marinum* burden and dormant mycobacteria in the majority of adult fish (Hammaren et al., 2014; Parikka et al., 2012). The granuloma structure in zebrafish is highly similar to human granulomas (Swaim et al., 2006). In zebrafish larvae, early granulomas start to form already few days after the infection as an aggregation of *M. marinum*–infected macrophages and recruited neutrophils (Davis et al., 2002; Yang et al., 2012). In adult zebrafish, mature granulomas form within

few weeks with necrotic core, immune cell aggregation and epithelioid capsule (Parikka et al., 2012; Volkman et al., 2010).

Despite all the pros and cons in the use of zebrafish, most importantly, zebrafish is an ethical model to study TB as it is the least neuro–physiologically developed organism of the TB animal models that still has a full immune system with innate and adaptive branches (van der Sar et al., 2004) and can model the whole spectrum of mycobacterial infection outcomes.

1.5.3 Zebrafish immune system

As a vertebrate, zebrafish shares many features of the immune system with human but there are few important differences as well. The organization of lymphoid tissues in human and zebrafish are somewhat different. The primary lymphoid organs in adult zebrafish are the kidney and the thymus (Uribe et al., 2011) compared to human bone marrow and thymus where the hematopoiesis occurs. Secondary lymphoid organs are sites where mature lymphocytes meet antigens and innate cells and get activated. The human secondary lymphoid organs are lymph nodes, spleen, Peyer's patches, tonsils and appendix. Zebrafish do not have lymph nodes or Peyer's patches, which is one of the biggest differences to the mammalian immune system, but the spleen and the gut-associated lymphoid tissues function as secondary lymphoid organs in zebrafish (Lieschke & Trede, 2009; Renshaw & Trede, 2012).

Zebrafish larva do not yet have adaptive immune responses as the adaptive mechanisms are still developing. However, innate cells and their functions have been conserved during the evolution and zebrafish larvae have early macrophages already at one day post fertilization (Langenau et al., 2004). For historical reasons, all mononuclear cells found in zebrafish larvae are called macrophages despite their localization to tissues or circulation (Herbomel et al., 1999, 2001). Neutrophils can be detected soon after macrophages and they are the major granulocytes in zebrafish larva as eosinophils are only found in adult zebrafish and basophils are not known to be present in fish (Balla et al., 2010; Lieschke et al., 2002). However, a small number of mast cells have been identified in zebrafish larva (Dobson et al., 2008). These fish innate cells have several PRR types commonly found in mammals for the recognition of foreign molecules such as toll-like receptors, RIG-I-like receptors, scavenger receptors, NOD-like receptors and C-type lectin receptors (Masud et al., 2017). In addition to cell mediated innate responses, zebrafish also has soluble factors of the complement system which can be transferred from the mother either

as a protein or a mRNA before the onset of protein production (Zhang & Cui, 2014). Overall, it is known that the innate responses are stronger in fish than in mammals and these mechanisms are important even when adaptive responses are already functioning (Magnadóttir, 2006).

The first T cell progenitors appear as early as three days after fertilization, but it takes up to four weeks to have fully functioning lymphocytes (Langenau et al., 2004). Mature B cells with capability of producing antibodies can be detected 20 days post-fertilization (Page et al., 2013). The antibody classes of zebrafish are more limited than in mammals. Mammals have five different antibody subclasses whereas zebrafish has only IgM and IgD similar to mammals and IgZ which is a fish specific subclass. Like in humans, alternative splicing of mRNA is used to produce IgM and IgD antibodies but also IgZ (Lieschke & Trede, 2009; Zimmerman et al., 2011). The fish-specific antibody class IgZ has been suggested to be a counterpart of the mammalian IgA molecule in the mucosal immune system (Zhang et al., 2010). Although, there is no class-switching in zebrafish (Stavnezer & Amemiya, 2004) they show memory response in the re-exposure of a pathogen by quickly elevating antibody titers (Jørgensen et al., 2018).

1.5.4 Important TB findings made in the zebrafish–*Mycobacterium marinum* model

The zebrafish–*M. marinum* model has been used to understand the TB pathogenesis and several findings have been discovered utilizing this natural host-pathogen interaction. To verify the use of the zebrafish model, *M. marinum* infection of an adult zebrafish has been compared to human TB by several research groups, pinpointing many similarities between human and fish diseases from the formation of hypoxic granulomas to latent infection with dormant mycobacteria (Myllymäki et al., 2018; Parikka et al., 2012; Swaim et al., 2006).

The easy access to the granulomas in fish and their close resemblance to human granulomas has made it a good model to study the characteristics and the dynamics of a granuloma. It has been shown in fish that the formation of the granuloma is supported by mycobacterium, which has given new knowledge about the balance of granuloma protectivity between the host and the pathogen (Cronan et al., 2016; Davis & Ramakrishnan, 2009; Volkman et al., 2010). During the granuloma maturation, mycobacterium induces the formation of vascularization and by inhibiting this angiogenesis it is possible restrict mycobacterial growth (Oehlers et

al., 2017). This observation made in zebrafish highlights the large size and the complicated structure of the granulomas. Similarly, the epithelial reprogramming of granuloma macrophages (Cronan et al., 2016) and role of foamy macrophages in the granulomas have been studied in zebrafish (Johansen et al., 2018).

Zebrafish has also been a useful model to study immune responses against mycobacteria. Zebrafish has revealed the importance of the right amount of TNF during the infection both too high and too low being detrimental (Roca & Ramakrishnan, 2013). The early mycobacterial infection has been dissected in the zebrafish larva and has shown that macrophages are crucial in restricting the growth of the bacteria but also help spreading the bacteria into deeper tissues (Clay et al., 2007). The adaptive immunity of the adult zebrafish has shown for example how the balance between Th1 and Th2 cells associates with controlling of infection (Hammaren et al., 2014). Also, antituberculous drug activity and the formation of drug tolerance through mycobacterial efflux pumps in macrophages has been identified in zebrafish (Adams et al., 2011). Both adult zebrafish and zebrafish larvae have been used to model human TB successfully and it has been acknowledged as a well-established, informative, and accurate TB model that has been used to discover many details of the TB pathogenesis.

2 AIMS OF THE STUDY

Mycobacteria have developed many ways to evade immune responses, which has made mycobacterium a successful pathogen that survives within the host and causes a chronic latent disease in the majority of the infected individuals. One of the aims of this thesis was to explore methods for preventing the immune evasion and to understand the mechanisms responsible for the protective immune responses, knowing that some individuals can sterilize Mtb infection naturally in the early infection.

Another mycobacterial evasion strategy, in addition to actively preventing immune responses, is its ability to increase the drug tolerance by forming biofilm. Biofilm gives an effective protection against host immunity and drugs, and it greatly reduces the effectiveness of antimicrobial therapies. Genetically resistant bacterial strains are a widely occurring issue but the phenotypic tolerance and the existence of persister bacteria in an antibiotic sensitive population are not routinely taken into account in clinical settings. After all, persister cells can have an impact on the development of chronic infections and treatment failure and increase the possibility of genetic resistance.

The specific aims to study the interventions strategies for mycobacterial evasion mechanisms are listed below.

- To evaluate the disease spectrum of the *M. marinum*–zebrafish TB model and the natural clearance of mycobacteria in the zebrafish population

- To study immunomodulation prior to mycobacterial infection to prevent bacterial immune evasion strategies and induce sterilizing immune responses

- To characterize the *M. marinum* biofilm formation, maturation, and composition and to establish a molecular technique to specifically target mycobacterial biofilms

3 MATERIALS AND METHODS

3.1 Zebrafish lines, housing, and ethics statement (I, II)

All the zebrafish (*Danio rerio*) experiments and the facilities of Tampere University (Finland) have been approved by the Animal Experimental Board under the Regional State Administrative Agency in Finland (licenses: ESAVI/6407/04.10.03/2012, ESAVI/8245/04.10.07/2015, ESAVI/10079/04.10.06/2015 and ESAVI/17803/2019). Zebrafish were kept under standard conditions (Westerfield, 2000) in water-recirculating systems (Aquatic habitats and Aquatic Schwarz) with a light-dark cycle of 10h/14h.

AB wildtype and *rag1*$^{-/-}$ (hu1999) mutant zebrafish lines were used. The zebrafish lines were purchased from the European Zebrafish Resource Center (Karlsruhe Institute of Technology, Germany). For adult zebrafish experiments, 3–10 months-old fish were used.

3.2 Mycobacterial strains (I-III and manuscript)

Mycobacterium marinum wildtype strain ATCC 927 from the American Type Culture Collection (ATCC) (VA, USA) was used in all *M. marinum* experiments. In addition to wildtype bacteria, in-house-made wasabi fluorescent (pTEC15), tomato fluorescent (pTEC27) and bioluminescent *M. marinum* strains were used in the experiments. pTEC15 and pTEC27 fluorescent plasmids were purchased from Addgene (MA, USA) (plasmids #30174 and #30182 (Takaki et al., 2013)), and electroporated into *M. marinum* ATCC 927 as previously reported (Aspatwar et al., 2017). The bioluminescent *M. marinum* strain has a plasmid with pMV306hsp+LuxG13 cassette (Andreu et al., 2010). pMV306hsp+LuxG13 plasmid was a gift from Brian Robertson & Siouxsie Wiles (Addgene plasmid #26161). An avirulent *Mycobacterium tuberculosis* H37Ra strain (ATCC 25177) was used in *in vitro* testing of sybodies. Mycobacterial strains used in the thesis are listed in the Table 1.

Table 1. Bacterial strains used in the experiments

Bacterium	Strain	Specifications
Mycobacterium marinum	ATCC 927	Wildtype
Mycobacterium marinum pTEC15	ATCC 927 + pTEC15 (Addgene #30174)	Wasabi fluorescence
Mycobacterium marinum pTEC27	ATCC 927 + pTEC27 (Addgene #30182)	Tomato fluorescence
Mycobacterium marinum lux	ATCC927 + pMV306hsp + LuxG13 (Addgene #26161)	Bioluminescence
Mycobacterium tuberculosis	H37Ra (ATCC 25177)	Avirulent

3.3 Experimental *Mycobacterium marinum* infections of adult zebrafish (I, II and manuscript)

M. marinum strains were first cultured on Middlebrock 7H10 agar plate (Sigma-Aldrich, MO, USA) supplemented with 0.5% glycerol (Sigma-Aldrich) and 10% OADC enrichment (Becton, Dickinson and Company (BD), NJ, USA) for 1–2 weeks at 29°C in the dark. An inoculation of the bacterial mass was transferred into Middlebrook 7H9 medium (Sigma-Aldrich) supplemented with 10% of ADC enrichment (BD), 0.2% of glycerol (Sigma-Aldrich) and 0.2% of Tween80 (Sigma-Aldrich), and cultured for 3 days at 29°C. The liquid culture was further diluted to starting OD_{600} of 0.07 in the same medium and culturing was continued for 2 days to reach the OD_{600} of 0.4–0.6. If transgenic fluorescent *M. marinum* strain was used, 75 μg/ml of hygromycin was added into the culturing media. To prepare the bacterial suspension for experimental infection of zebrafish, 1 ml of *M. marinum* culture was transferred into a microcentrifuge tube and centrifuged 3 min at 10,000 g. The supernatant was discarded, and the bacterial pellet was resuspended into sterile 1x phosphate buffer saline (PBS) (Sigma-Aldrich) with 0.3 mg/ml of phenol red (Sigma-Aldrich) as a tracer to ensure a successful injection. Before infections, the bacterial suspension was slowly put through an HSW Fine Jet 27G needle (Henke Sass Wolf, Germany) 3 times to dissociate possible clumps of the bacteria. The prepared injection solution was used within two hours. Several samples of the *M. marinum*

solution were plated on 7H10 agar supplemented with 10% OADC (BD) to verify the infection dose throughout the infection procedure.

Adult zebrafish were anaesthetized with 0.02% of 3-aminobenzoic acid ethyl ester (Sigma-Aldrich) (pH 7.0) in the tank water. The fish were positioned ventral side up and 5 µl of the bacterial solution were injected between the pelvic fins intraperitoneally with an Omnican 100 30G insulin needle (Braun, Germany). After injection, the fish were quickly transferred into fresh tank water for recovery and for monitoring the well-being of the fish. The infection doses were 34±15 cfu in the publication I, ranging between 12–75 cfu with an average deviation of 24% in the publication II and in the manuscript the infection dose was 63±9 cfu per fish. From the previous experimental studies, it has been concluded that an infection dose between 10 and 100 cfu will induce a latent *M. marinum* infection in the majority of the adult zebrafish.

3.4 Experimental *Mycobacterium marinum* infections of zebrafish larvae (II)

M. marinum was cultured and prepared similarly for larval infections as described in the section "4.3 Experimental Infections of Adult Zebrafish" except 0.6 mg/ml of phenol red (Sigma-Aldrich) was used to prepare a colourful bacterial solution and 75 µg/ml of hygromycin (Invivogen, CA, USA) was used to culture fluorescent *M. marinum* strains. If fluorescent *M. marinum* was used, larvae were dechorionated at 1 dpf (days post fertilization) and kept in E3 medium with 0.0045% 1-phenyl-2-thiourea (Sigma-Aldrich) to prevent the development of pigmentation. 1 nl of *M. marinum* suspension were used to infect anesthetized larvae with an aluminosilicate glass capillary needle (Harvard Apparatus, MA, USA) using micromanipulator (Narishige International, UK) and PV830 Pneumatic PicoPump microinjector (World Precision Instrument, FL, USA). The infection site of the intravenous injection was the caudal vein for 1 dpf larvae and the blood valley for 2 dpf larvae. Infected larvae were kept separately on a 24-well plate in E3 medium at 29°C and the survival of the larvae were monitored daily. When the fluorescence signal of the bacteria was measured, the larvae were anesthetized with 0.02% of 3-aminobenzoic acid ethyl ester (Sigma-Aldrich) (pH 7.0) in E3 medium and embedded in 1% low-melt agarose on a black 96-well proxiplate (Perkin Elmer, MA, USA). The solidified agarose was covered with E3 medium with 0.02% of 3-aminobenzoic acid ethyl ester (Sigma-Aldrich) (pH 7.0) to prevent drying. The fluorescence signal from the

infected zebrafish larva was measured with 2104 EnVision plate reader (Perkin Elmer) by scanning individual wells three times 5x5 dots 0.5 mm apart from each other with 500 flashes per dot (measurement height 6.5 mm, excitation 490 nm, emission 509 nm). An average of the three repeats subtracted by a background signal from healthy non-infected larvae are shown in the results.

3.5 Preparing heat-killed *Listeria monocytogenes* for priming immune responses (II)

To prepare heat-killed *Listeria monocytogenes* (10403S), an inoculation from the bacterial glycerol stock was transferred into BHB (Sigma-Aldrich) and cultured at 37°C until the OD_{600} reached 0.9-1.0. The bacterial concentration was checked on LB agar plate and heat-killed by autoclaving 120°C for 20 min. The sterility of the bacterial suspension was checked on LB plate incubated at 37°C overnight. If soluble and insoluble *L. monocytogenes* molecules were required, the suspension was centrifuged at 15,000g for 10 min after autoclaving and diluted to 1xPBS to match the *L. monocytogenes* concentration of $1x10^6$ cfu/µl. For all experiments, the dose of heat-killed *L. monocytogenes* was $0.5x10^7$-$1x10^7$ cfu per fish.

3.6 Extraction of bacterial biomolecules for priming experiments (II)

3.6.1 Enzymatic treatments of heat-killed *Listeria monocytogenes*

The effect of different compounds of *L. monocytogenes* as a priming agent was tested by enzymatically treating heat-killed *L. monocytogenes* with either a combination of DNase and RNase or with proteinase K (Sigma-Aldrich). To degrade nucleic acids, heat-killed *L. monocytogenes* was first treated with 10 µg/ml of RNase A (Thermo Fisher Scientific, NH, USA) at 37°C for 18 h following by an incubation with 83 U/ml of DNase I (Thermo Fisher Scientific, NH, USA) at 37°C for 30 min and inactivation of the enzymes with 5 mM of EDTA with further incubation at 65°C for 10 min. A separate sample of heat-killed *L. monocytogenes* was treated with 10 µg/ml proteinase K (Thermo Fisher Scientific, NH, USA) and incubated at 37°C for

18 h to degrade proteins from the samples. Before injecting into zebrafish, the bacterial preparation was inactivated at 70°C for 15 min.

3.6.2 Extraction of lipids from *Listeria monocytogenes*

To test the properties of *L. monocytogenes* lipids as a priming agent, a method modified from Bligh and Dyer (Bligh & Dyer, 1959) was utilized. *L. monocytogenes* was first cultured to OD_{600} of 0.5 in BHB (Sigma-Aldrich) at 37°C. The bacteria were then centrifuged at 10,000g for 3 min and the pellet was collected and washed twice with sterile 1xPBS. After washing, the bacteria pellet was resuspended into lysis buffer including 20 mM TrisHCl (pH 8) and 1 mM EDTA. The bacteria were heat-killed for 20 min at 120°C and cooled on ice. To degrade the bacterial cell wall, lysozyme (Sigma-Aldrich) was added into the suspension at the final concentration of 20 mg/ml. After overnight incubation at 37°C, the samples were further homogenized by sonicating for 9 min. For 100 µl of cell lysate, 375 µl of chloroform:methanol (1:2) mixture was added and the suspension was vortexed for 15 min. Additional 125 µl of chloroform was added to the mixture and vortexed for 1 min. Finally, 125 µl of sterile water was added and again vortexed for 1 min. After the extraction steps, the suspension was first centrifuged at 800g for 6 min and then at 1500g for 5 min at room temperature to separate the molecular phases. The lower phase including the lipids was carefully transferred through the protein phase into a new weighted tube and dried in a miVac DUO concentration (GeneVac). The dry lipid pellet was weighted, and the mass of the lipids was calculated. The samples were stored at -20°C upon use.

The dried *L. monocytogenes* lipid samples were hydrated before use with sterile water using heat-freeze cycles: 5–10 min at 37°C heat-block, 0.5–1 min of vortexing and freezing in liquid nitrogen for total of 5 times. After the last cycle, the suspension was put through a 30G needle several times to produce a homogenous suspension. The lipid samples were hydrated just before the use.

3.7 Determination of mycobacterial counts from infected adult zebrafish (I and II)

At desired timepoint, adult zebrafish were euthanized with an overdose of 3-aminobenzoic acid ethyl ester (Sigma-Aldrich) (pH 7.0). The abdominal cavity was

opened with a surgical knife and all internal organs were detached and transferred into a homogenization tube. The tissue samples were quickly frozen on dry ice to prevent sample degradation. All instruments were rinsed in 70% ethanol between handling of individual fish. Nucleic acids were extracted from the sample with TRIreagent (Sigma-Aldrich). First, zebrafish tissue samples were homogenized in 1 ml of TRIreagent using 6 ceramic beads (2.8 mm diameter) (Mobio, CA, USA) with FastPrep homogenizator (MP Biomedicals, CA, USA) at 6.5 m/s for 2 times 40 s. The samples were cooled with dry ice during the procedure. After the homogenization, samples were further sonicated in a water bath at room temperature for 9 min. The TRIreagent RNA–DNA co-extraction protocol was continued according to manufacturer's orders (Sigma-Aldrich). Nucleic acids were dissolved in sterile water and the concentration of nucleic acids, and the purity of the samples were measured using NanoDrop (Thermo Fisher Scientific, NH, USA).

Extracted DNA was used to determinate the *M. marinum* load of a zebrafish. To do this, no-ROX SensiFAST qPCR kit (Bioline, UK) was used according to manufacturer's orders with *M. marinum* specific primers (MMITS1) that detect a sequence of *M. marinum* internal transcribed spacer (ITS) between 16S-23S genes. The primer sequences are found from the Table 2. The quantitative polymerase chain reaction (qPCR) program (Table 3) was run with a CFX96 thermal cycler (BioRad, CA, USA). The samples were measured as duplicates and a standard curve of a known amount of *M. marinum* was used to calculate the mycobacterial load in a fish.

3.8 Gene expression analysis of zebrafish genes (II)

RNA samples extracted with TRIreagent, as described above, were first treated with DNase I (Thermo Fisher Scientific, NH, USA) according to manufacturer's orders to remove possible traces of genomic DNA from the sample. The RNA samples were then converted to cDNA by reverse transcriptase (Fluidigm, CA, USA) and the gene expressions were measured with SsoFast Eva Green (Bio-Rad, CA, USA) qPCR kit according to the manufacturer's orders. qPCR was performed with a CFX96 thermal cycler (BioRad, CA, USA) and the results were normalized against a housekeeping gene (*loopern4*) and analysed relative to a pooled RNA sample of healthy non-infected fish. The primer sequences are shown in the Table 2 and the used qPCR program in the Table 4.

Table 2. Primers used in the study

Gene	Gene ID	Sequences
16S–23S ITS (MMITS1)	Locus AB548718	F: CACCACGAGAAACACTCCAA R: ACATCCCGAAACCAACAGAG
loopern4	Expressed repetitive elements	F: TGAGCTGAAACTTTACAGACACAT R: AGACTTTGGTGTCTCCAGAATG
tnf	ZDB-GENE-050317-1	F: GGGCAATCAACAAGATGGAAG R: GCAGCTGATGTGCAAAGACAC
arg1	ZDB-GENE-040724-181	F: TGGGAATAATAGGCGCTCCGTTC R: TCCTTCACCACACAACCTTGC
mpeg1	ZDB-GENE-081105-5	F: CTTCTGTTTCAGCATCAGCCG R: ATAAAGCTCCTCCGTGGCTC
mpx	ZDB-GENE-030131-9460	F: AACACTGAACTAGCCCGCAA R: CAACCTATCGCCATCTCGGA
nos2b	ZDB-GENE-080916-1	F: TCACCACAAAAGAGCTGGAATTCGG R: ACGCGCATCAAACAACTGCAAA
ifnγ1-1	ZDB-GENE-060210-1	F: CCAGGATATTCACTCAGTCAAGGC R: TGTGGAGGCCCGATAATACACC
ifnγ1-2	ZDB-GENE-040629-1	F: GGGCGATCAAGGAAAACGACCC R: TAGCCTGCCGTCTCTTGCGT
sod2	ZDB-GENE-030131-7742	F: GGCCATAAAGCGTGACTTTG R: GCTGCAATCCTCAATCTTCC

Table 3. qPCR program for measuring *M. marinum* load in zebrafish.

Step	Time	Temperature
1.	3 min	95 °C
2.	5 s	95 °C
3.	10 s	65 °C
4.	5 s	72 °C (fluorescence detection)
5.	Go to step 2. 39 times	
6.	Melting curve analysis	55–95°C with 0.5°C intervals
7.	Forever	4 °C

Table 4. qPCR program for measuring the gene expression from a zebrafish sample.

Step	Time	Temperature
1.	30 s	95 °C
2.	12 s	95 °C
3.	30 s	Annealing T (fluorescence detection)
4.	Go to step 2. 38 times	
5.	Melting curve analysis	65–95°C with 0.5°C intervals
6.	Forever	4 °C

3.9 Oxygen consumption measurements of RAW cells (II)

RAW264.7 (ATCC TIB-71) cells were used to measure changes in the oxygen consumption after priming with heat-killed *L. monocytogenes*. The cells were cultured in Dulbecco's modified Eagle's medium with 4.5 g/L D-glucose and L-glutamine (Gibco, NH, USA) supplemented with 10% of heat-inactivated fetal bovine serum (Gibco, NH, USA) and 100 U/ml of penicillin-streptomycin mixture (Thermo Fisher Scientific, NH, USA) at 37°C with 5% CO_2. Heat-killed *L. monocytogenes* was added on cell in MOI of 530 and incubated for 19–24 hours. 50 ng/ml of LPS was used as a control. After incubation, the media was changed, and new priming agents were added. The cells were allowed to settle for a minimum of 30 min after which a Clark electrode (Hansatech, UK) was used to measure oxygen consumption at 37°C in the culture media. Background oxygen consumption was measured by blocking the respiratory chain complex III with 150–279 nM of antimycin (Sigma-Aldrich). The background value was subtracted to get the actual oxygen consumption of the mitochondrial respiration.

3.10 Determination of minimum inhibitory concentration (MIC), and minimum bactericidal concentration (MBC) for *Mycobacterium marinum* biofilm (III)

Bioluminescent *M. marinum* (ATCC 927) with pMV306hsp+LuxG13 plasmid was used in the antibiotic tolerance testing. Bioluminescent *M. marinum* was pre-cultured on Middlebrook 7H10 agar (Sigma-Aldrich) including 0.5% (vol/vol) glycerol

(Sigma-Aldrich) and 10% (vol/vol) OADC enrichment (BD). The cultures were kept at 29°C for 7 days and protected from light. For liquid cultures of *M. marinum* biofilm, bacterial mass was suspended in Middlebrook 7H9 medium (Sigma-Aldrich) supplemented with 10% (vol/vol) of ADC enrichment (BD) to the starting OD_{600} of 0.1. Planktonic cultures were treated similarly to biofilm cultures, but the medium contained additional supplements of 0.2% (vol/vol) of glycerol (Sigma-Aldrich) and 0.2% (vol/vol) of Tween80 (Sigma-Aldrich).

M. marinum suspensions were divided on white 96-well plate (Perkin Elmer) 192 µl per well in triplicates, sealed with parafilm and cultured at 29°C in the dark to different ages. 8 µl of sterile rifampicin solution (TOKU-E, WA, USA) in water at the desired concentration was added to the bacterial suspension and incubated at 29°C. If DNase1 (Thermo Scientific), proteinase K (Thermo Scientific) or cellulase from Trichoderma sp. (Sigma-Aldrich) were used, the enzymes were diluted into 7H9 medium and added on 4-day-old biofilm together with rifampicin. For this experiment, the final concentrations were 0.1 mg/ml DNase1, 1 µg/ml proteinase K, 10 mg/ml cellulase and 8 µg/ml rifampicin.

To determine minimum inhibitory concentration (MIC), bioluminescence was measured with 2104 EnVision plate reader (Perkin Elmer) 3 times for 3 seconds (measurement height 6.5 mm) per well daily. For measuring minimum bactericidal concentration (MBC) for rifampicin, after 7 days of antibiotic treatment, 10 µl samples from the total volume of 200 µl were plated on Middlebrook 7H10 agar supplemented with 0.5% glycerol and OADC enrichment and cultured at 29°C in the dark up to 2 weeks. Mycobacterial counts under 100 cfu were considered negative, which refers to killing capacity of over 99.9%.

3.11 Time-kill curve analysis for *Mycobacterium marinum* biofilm (III)

The planktonic and biofilm *M. marinum* were cultured similarly except the addition of 0.2% (vol/vol) of glycerol and 0.2% (vol/vol) of Tween80 in the planktonic growth media as explained in section 4.10. Briefly, the starting bacterial amount in both liquid cultures was set to OD_{600} of 0.1 in 7H9 media. The bacterial suspensions were divided onto white 96-well plate (Perkin Elmer) 192 µl per well, sealed with parafilm, and let to grow to desired age at 29°C in the dark. 8 µl of rifampicin water solution (TOKU-E) in different concentrations was added into the bacterial liquid cultures and incubated for 7 days with daily bioluminescence measurement with 2104

EnVision plate reader (Perkin Elmer) 3 times for 3 seconds per well. Background signal from the wells containing only media were subtracted from the average result of the three technical and three biological repeats. The bioluminescence results were also normalized against the 0-day reading before the antibiotic has been added to show the reduction in a time-killing curve.

To test the phenotypic tolerance of pellicle and submerged biofilms separately, bioluminescent *M. marinum* was pre-cultured in liquid culture tubes in a total volume of 5 ml of 7H9 media supplemented with 10% of ADC (BD) at the starting OD_{600}-value of 0.1. The caps of the tubes were sealed with parafilm. After 2 weeks of culturing, the pellicles and submerged biofilms were collected separately from the tubes by lifting the pellicle with a 1 µl inoculation loop and carefully pipetting into weighted tubes. Pellicle and submerged biofilms from different tubes were then pooled and diluted into spent 7H9 growth media according to their biomass. The suspensions were vortexed briefly and divided on white 96-well plate (Perkin Elmer) 192 µl of *M. marinum* in spent media together with 8 µl of different concentration of sterile rifampicin water solution (TOKU-E) per well. Cultures were incubated for 7 days at 29°C and the bioluminescence signal were measured daily with 2104 EnVision plate reader (Perkin Elmer) 3 times for 3 seconds per well.

3.12 Proteomic sample preparation of *Mycobacterium marinum* biofilm for mass spectrometry analysis (Manuscript)

To find surface-exposed mycobacterial biofilm proteins, 5-week-old *M. marinum* biofilm was biotinylated. The biofilm was prepared as explained in the section 4.10. and both pellicle and submerged biofilms were used in the experiment. First the biofilm was collected by centrifugation and resuspended in BupH-PBS (Thermo Scientific). The biofilm ECM was briefly lysed in BupH-PBS with six ceramic beads using FastPrep homogenizator (MP Biomedicals, CA, USA) at 6.5 m/s for 2 times 40 s to get more homogenous suspension.

Sulfo-NHS-LC-Biotin (Pierce, Rockford, IL) was used to biotinylate proteins on the surface of the intact *M. marinum*. 1 mg of sulfo-NHS-LC-biotin was added in BupH-PBS per 150 mg of *M. marinum* biofilm. The bacteria were biotin labeled for 30 min at room temperature with gentle agitation and washed two times with BupH-PBS with 10 mg/ml glycine following by two washes with BupH-PBS. Labeled but intact bacteria were resuspended in urea lysis buffer including 7 M urea, 150 mM

NaCl, 20 mM Na_2HPO_4, 0.05% (vol/vol) Tween-20 (Sigma-Aldrich) and 0.2% (w/v) CHAPS at pH 7.3. The bacteria were then disrupted by bead milling with PowerBead tubes with 100-μm glass beads (Qiagen, Germany). After the homogenization, the insoluble particles were removed by centrifugation and the supernatant was collected for protein purification.

M. marinum biofilm cells that were lysed before the biotinylation step was used as a comparison. To expose both extracellular and intracellular proteins, the biofilm were homogenized in urea lysis buffer using FastPrep homogenizator (MP Biomedicals, CA, USA) at 6.5 m/s for 2 times 40 s with 100-μm glass beads with dry ice and sonicated for 10 min. The bacterial cells were further disrupted with 20 mg/ml of lysozyme in BupH-PBS for 2h at 37°C and centrifugated to remove insoluble particles. The biotinylation of the lysed biofilms were performed as for the intact cells described above but after biotinylation, lysed biofilm samples were dialyzed with Slide-A-Lyzer cassette (3,500 MWCO) (Thermo Scientific) in BupH-PBS with stirring at 4°C for first 1h and then over-night in fresh buffer.

Biotinylated proteins from both intact and lysed biofilms were purified by affinity purification with streptavidin-coated magnetic beads (Dynabeads MyOne Streptavidin C1) (Invitrogen, MA, USA) in low-binding SafeSeal microcentrifuge tubes (BioScience, UT, USA). The biotinylated proteins were incubated with the streptavidin-coated magnetic beads for 30 min at 4°C. The samples were then washed three times using a magnetic stand with a buffer containing 1.75 M urea, 150 mM NaCl, 20 mM Na_2HPO_4, 0.05% (vol/vol) Tween 20 and 0.05% (w/vol) CHAPS at pH 7.3. The washes were continued with two times a buffer containing 150 mM NaCl, 20 mM Na_2HPO4 and 0.05% (vol/vol) Tween 20 (pH 7.2) and once with 50 mM NH_4HCO_3 solution (pH 7.8). Before storing the protein samples by flash freezing, the pH was increased to 7.8 by adding NH_4HCO_3. The mass spectrometric analysis was performed by the Oslo proteomics core (Norway) by analyzing the trypsin digested peptides in a nanoElute nanoflow ultrahigh pressure liquid chromatography (Bruker Daltonics) together with a timsTOF fleX mass spectrometer (Bruker Daltonics).

3.13 Confocal imaging of *Mycobacterium marinum* and *Mycobacterium tuberculosis* biofilm-targeted sybodies *in vitro* (Manuscript)

According to the proteomics data, GroEL1 and GroEL2 were found to be among the most abundant proteins in *M. marinum* biofilm that also have orthologues in Mtb. These proteins also have known protein sequences and structures making them possible to produce in *E. coli* for sybody screening. Sybodies against GroEL1 and GroEL2 were screened and produced in EMBL PEPCORE (Heidelberg, Germany) (Zimmermann et al. 2020; 2018). Details of the proteomic analysis and sybody production can be found in the manuscript. To test the binding of these GroEL1- and GroEL2-targeted sybodies, 2-week-old *M. marinum* biofilm was cultured as described in the section 4.10. Avirulent Mtb biofilm was cultured similarly but the pre-culturing on 7H10 agar plates lasted three weeks and the culturing temperature was 37°C. The biofilms were collected by briefly spinning the bacterial suspension and 7H9 medium was removed by washing the bacterial mass three times with PBS. The intact biofilm was then blocked by 2% BSA (bovine serum albumin) (Sigma-Aldrich) in PBS at room temperature for 30–60 min. The BSA solution was removed by a brief spinning and 1 μM sybody in 0.1% BSA-PBS was added. The sybodies were incubated with the biofilms at room temperature for 1.5 h, after which the biofilms were washed twice with 2% BSA-PBS.

The biofilm-bound sybodies were labelled with 5 μg/ml of Myc Tag Monoclonal Antibody (Myc.A7), DyLight 488 (Invitrogen) at 4° for 0.5–1 h. The excess antibody was washed twice with PBS and once with distilled water. To visualize the bacterial cells of wildtype *M. marinum* and avirulent Mtb, ProLong Diamond Antifade Mount with DAPI (Invitrogen) was used. The confocal imaging was done using Nikon A1R+ and 60x oil immersion objective at the Tampere University imaging core. Fiji-ImageJ (64bit) (NIH, USA) were used to analyze the images.

3.14 Confocal imaging of *ex vivo* zebrafish granulomas with biofilm-targeted sybodies (Manuscript)

Adult zebrafish were infected with tdTomato (pTEC27) fluorescent *M. marinum* strain as described in the section 4.3. At 8 wpi, the fish were euthanized with an overdose of 3-aminobenzoic acid ethyl ester (Sigma-Aldrich) (pH 7.0). The abdominal cavity was opened, and the granulomas were carefully collected under a

stereomicroscope with tweezer using Nightsea lamp with green color and 600 nm filter (Electron Microscopy Sciences). Granulomas were stored at -80°C for later use.

To produce a small molecular weight sybody with fluorescence signal that could enter the granulomas, the sybodies against GroEL1 and GroEL2 were labelled with Alexa Fluor 488 carboxylix acid, succinimidyl ester (Invitrogen). The stain was dissolved in DMSO (Sigma-Aldrich) and incubated with the sybody in a double molar excess of the dye in PBS with gentle agitation covered from light at room-temperature for 1 hour. 10 mg/ml glycine were added to stop the esterification reaction of the dye and incubated at room-temperature for 10 min. The labelled sybodies were then dialyzed in PBS 1h and overnight at 4 °C to get rid of the unbound fluorescence dye.

Prior to the sybody staining, the granulomas were blocked in 2% BSA in PBS at room-temperature for 2 hours. The granulomas were then briefly spinned, the blocking solution removed, and the granulomas were incubated in 6 µM solution of fluorescence labelled sybody covered from light at 4°C for four days. After the staining, the granulomas were washed twice with PBS and once with distilled water. The granulomas were mounted with ProLong Diamond Antifade Mount with DAPI (Invitrogen) and imaged with Nikon A1R+ confocal microscopy and 60x oil immersion objective at the Tampere University imaging core. Fiji-ImageJ (64bit) (NIH, USA) was used to analyze the images.

3.15 Statistical comparisons (I-III and manuscript)

Statistical analyses were performed using Microsoft Excel, IBM SPSS Statistics and GraphPad Prism. The mycobacterial loads and the gene expression were compared between the experimental groups with unpaired two-tailed Mann-Whitney test followed by Bonferroni's correction when needed. Fisher's test was used to compare qualitative results of the experimental groups. In survival experiments of either zebrafish or *M. marinum in vitro*, Log-rank (Mantel-Cox) test was used to evaluate differences between the treatments. Unpaired two-tailed Mann Whitney U-test was used to compare maximum intensity projections of the fluorescence microscope images between control samples and sybody-stained samples to calculate the effect of autofluorescence and unspecific background staining. P-values of under 0.05 was considered significant.

4 SUMMARY OF THE RESULTS

4.1 Spectrum of the disease outcomes of the *Mycobacterium marinum* infected adult zebrafish (I)

As an ethical TB model, zebrafish, and its natural pathogen *Mycobacterium marinum* were chosen for studying mycobacterial immune evasion strategies. Adult zebrafish has both innate and adaptive immune system, and it has been reported to develop chronic mycobacterial infection with granulomas (Parikka et al., 2012).

A group of adult zebrafish were infected by an intraperitoneal injection with a low dose of *M. marinum* to study the natural heterogeneity of the mycobacterial infection. The results show that *M. marinum* infection spontaneously causes many disease outcomes in the zebrafish population (Figure 1). A small subpopulation (7%) is unable to limit the bacterial growth eventually dying of the mycobacterial infection before 8 wpi (weeks post infection). These individuals are called primary progressive. Majority of the population (65%) develops latent disease and is still alive showing no symptoms during the 32-week-long experiment. 18% of the population reactivate the latent disease and have symptoms of the infection after 8 wpi. 10% of the total population survive the whole 32 weeks of infection but unlike fish that have latent disease, these individuals do not have detectable amounts of mycobacteria.

Table 5. The detection limit of *M. marinum* qPCR tested in adult zebrafish homogenate

Added CFU in fish homogenate	***M. marinum* positive fish in qPCR (positive/total amount of samples)**
2000	2/2
500	4/4
100	2/3

To evaluate the sensitivity of the methodology in measuring mycobacterial loads, the detection limit of *M. marinum* -specific qPCR was determined. A known number of bacteria was added into fish samples before homogenization and DNA extraction.

By calculating the loss of the sample from fish homogenate to qPCR reaction, the detection limit was estimated to be 100 cfu. The same limit was observed in the spiking experiment where two fish samples out of three were *M. marinum* positive when 100 cfu was added into the sample (Table 5).

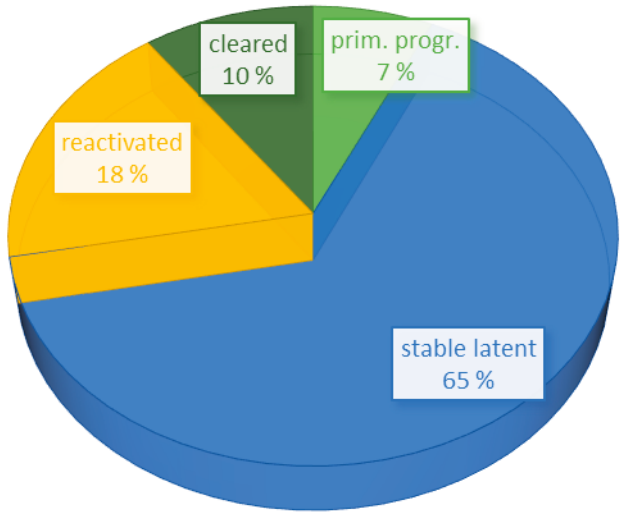

Figure 1. The proportions of different disease outcomes in the adult zebrafish population infected with a small dose of *M. marinum*. The population were divided into primary progressive (7%), reactivated (18%), latent (65%) and cleared (10%) individuals. Primary progressive individuals died between 0–8 wpi and reactivated between 8–32 wpi. The individuals that had stable latent disease were alive after 32 wpi and had detectable bacterial loads measured with qPCR. Cleared individuals were alive after 32 wpi but did not have detectable mycobacteria. The infection dose was 34±15 cfu. Modified from original publication I.

4.2 Protective immunity induced by heat-killed *Listeria monocytogenes* (II)

Knowing that mycobacteria have many immune evasion mechanisms, different immunomodulators such as known TLR ligands and heat-killed bacteria were tested to examine what kind of immune activation is needed in order to induce better control over the infection. In the screen, heat-killed *Listeria monocytogenes* (HKLm) was shown to reduce mycobacterial loads in adult zebrafish (Original Publication II). Exposing fish to HKLm 1 day prior to *M. marinum* infection reduced the mycobacterial loads significantly after 4 weeks of infection compared to PBS primed group (P=0.0013). The outline of the experimental setup is shown in the Figure 2.

It was tested that priming with HKLm 1 day prior the infection was more effective compared to mock injection than priming 1 week (publication II). Some individuals were able to control the infection below the detection limit and they did not show detectable mycobacteria at 4 wpi (Figure 3AB). In these experiments, around 4–10% of the population can naturally control the infection in a low dose *M. marinum* infection of 20–50 cfu without an immunomodulation. This proportion can be increased up to 25% by priming with HKLm.

Rag1$^{-/-}$ mutant fish were used to determine the role of adaptive responses in the HKLm-induced clearance. *Rag1*$^{-/-}$ mutants do not have functional adaptive immune cells, but the protective response induced by HKLm is also seen in these mutant fish implicating that the protective immune response is driven via innate mechanisms. 17% of the *rag1*$^{-/-}$ mutant fish primed with HKLm sterilized the infection in a pooled result of four independent experiment whereas all individuals from the mock injected *rag1*$^{-/-}$ mutant group still had detectable *M. marinum* at 4 wpi (Figure 3CD). The protective HKLm priming did not, however, work in zebrafish larvae; neither priming one day prior the infection or co-injection of HKLm and *M. marinum* did not protect against the infection (Figure 4), which might be due to still maturing immune system of the larvae or technical differences of the injections between larvae and adult fish.

Figure 2. Outline of the zebrafish priming experiments. Adult zebrafish were primed with heat-killed *L. monocytogenes* (HKLm) one day before infecting with 20-50 cfu of *M. marinum*. The HKLm dose corresponds to $0.5x10^7$-$1x10^7$ cfu of live bacteria per fish. The mycobacterial loads were measured at 4 weeks after infection with qPCR. Modified from original publication II.

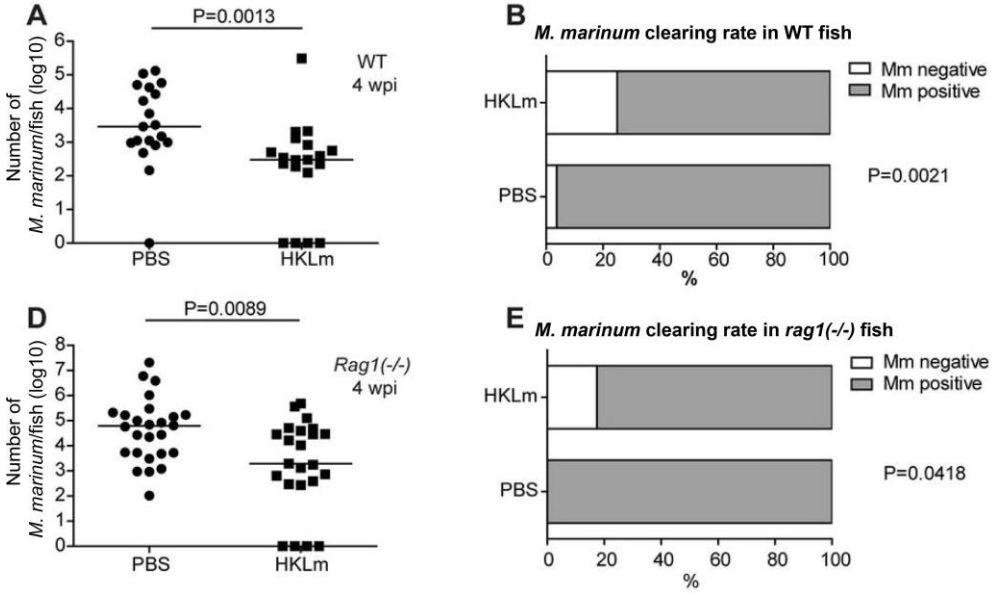

Figure 3. Heat-killed *L. monocytogenes* (HKLm) priming reduces the mycobacterial loads and induces clearance both in wildtype and *rag1*$^{-/-}$ mutant zebrafish. A) Adult wildtype (AB) zebrafish were primed with HKLm (0.5×107 cfu) 1 day prior the infection (27±2 cfu) and the mycobacterial loads were measured at 4 wpi by qPCR (PBS: n=19, HKLm: n=19). The bacterial loads were significantly lower in HKLm primed fish (P=0.0013). Two-tailed Mann-Whitney test and Bonferroni correction was used to evaluate the significance of the results. Medians are shown in the figure. B) HKLm priming induces sterilizing response in 25% of the population compared to mock injection of sterile 1xPBS (clearance in 3.7%), P=0.0021. The result consists of four independent experiments with infection doses of 27±2 cfu, 26±13 cfu, 75±13 cfu and 26±8 cfu. (PBS: n=54, HKLm: n=56). Fisher's test was used evaluate the significance of the results. C) *Rag1* $^{-/-}$ mutant zebrafish show reduction in the mycobacterial loads at 4 wpi when primed with HKLm 1 day prior the infection. The result consists of two independent experiments with infection doses of 48±8 cfu and 27±2 cfu (PBS: n=26, HKLm: n=23). Two-tailed Mann-Whitney test and Bonferroni correction was used to evaluate the significance of the results. Medians are shown in the figure. D) 17% of the *rag1* $^{-/-}$ mutant zebrafish is able to sterilize *M. marinum* infection when primed with HKLm 1 day prior the infection compared to PBS injected group (P=0.0418). There were no sterilized individuals in the control group that was injected with sterile 1xPBS. The result consists of two independent experiments (infection doses 48±8 cfu and 27±2 cfu) (PBS: n=26, HKLm: n=23). Fisher's test was used evaluate the significance of the results. PBS=phosphate-buffered saline, HKLm=heat-killed *Listeria monocytogenes*, WT=wild-type, wpi=weeks post infection, Mm=*Mycobacterium marinum*, *Rag1*=recombination-activating gene 1. Modified from original publication II.

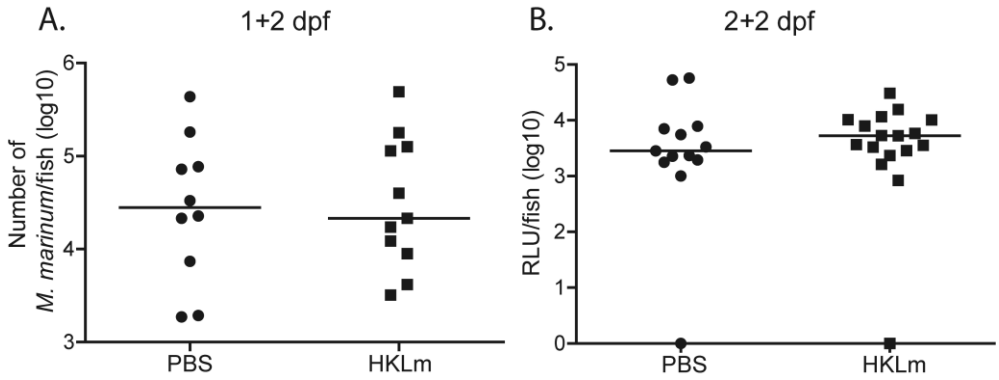

Figure 4. The heat-killed *L. monocytogenes* (HKLm) priming does not reduce the *M. marinum* loads in zebrafish larva. A) Zebrafish larvae were primed with HKLm corresponding to 240 cfu at 1 dpf and infected with 39±13 cfu of *M. marinum* at 2 dpf. The bacterial loads were measured with qPCR (PBS: n=10, HKLm: n=11). B) Co-injecting with 490 cfu of HKLm and with 39±16 cfu of *M. marinum* at 2 dpf did not reduce the bacterial loads. The bacterial loads were measured with EnVision plate reader from embedded larvae (PBS: n=13, HKLm: n=17). Two-tailed Mann-Whitney test and Bonferroni correction was used to evaluate the significance of the results. Medians are shown in the figure. PBS=phosphate-buffered saline, HKLm=heat-killed *Listeria monocytogenes*, dpf=days post fertilization, RLU=relative light unit. Modified from original publication II.

4.3 Priming effect of heat-killed *Listeria monocytogenes* components (II)

The protective effect of HKLm priming was induced when the heat-killed bacterial suspension included all bacterial biomolecules and the growth medium. To find the component of *L. monocytogenes* that generates the protective immune response against mycobacterial infection, soluble molecules secreted by listeria into the medium were first separated from the insoluble bacterial mass and tested as a priming agent in zebrafish. The secreted molecules from the growth medium did not induce protection and hence the protective component must be part of the bacteria (Figure 5A).

Knowing that the protective component is found in listeria itself, the washed and heat-killed bacteria mass was centrifuged with high-speed to separate soluble and insoluble phases of listeria biomolecules. Both phases were tested as immunomodulators in adult zebrafish, and it was concluded that the protection is mediated via insoluble molecules of listeria (P=0.0138, Figure 5B).

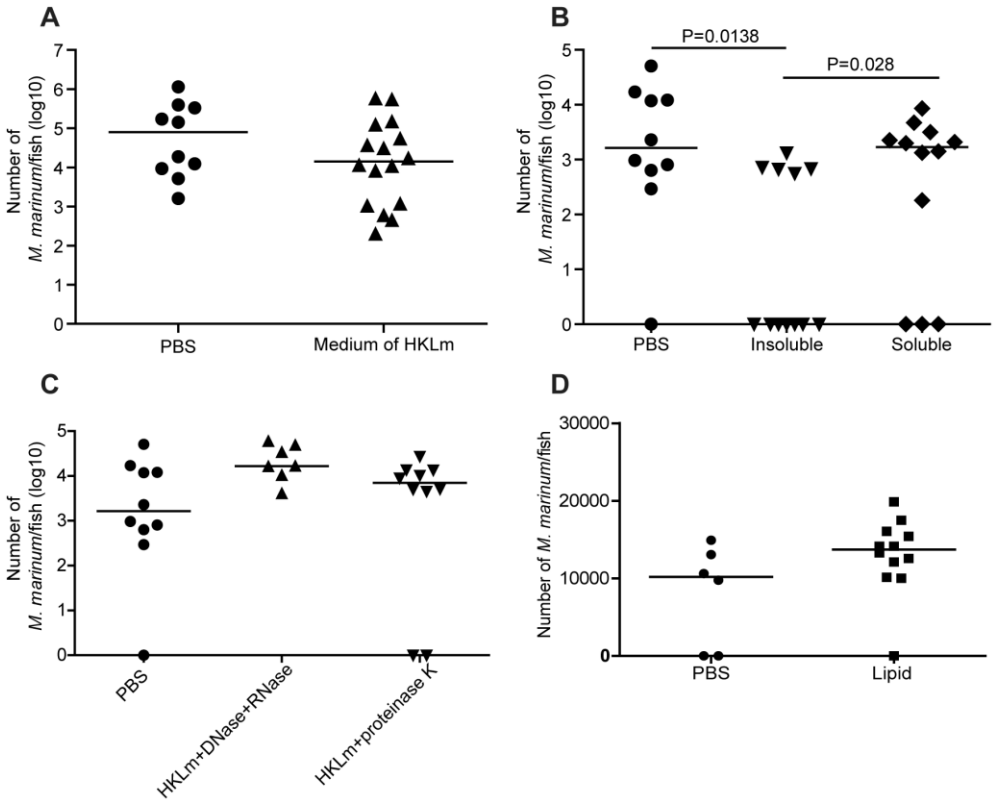

Figure 5. The protective component of the heat-killed *L. monocytogenes* (HKLm) suspension is either a nucleic acid or a protein or a combination of these. A) Growth medium that included molecules secreted by *L. monocytogenes*, did not influence the mycobacterial loads at 4 wpi when primed 1 day before infection. P=0.1005 (infection dose 26±6 cfu) (PBS: n=10, Medium of HKLm: n=16). B) The protective component of HKLm is in the insoluble phase after heat-killing (infection dose 33±11 cfu) (PBS: n=10, insoluble n=12, soluble: n=12). C) Treating HKLm either with nucleases or protease abolished the protective effect (infection dose: 33±11 cfu) (PBS: n=10, DNase and RNase: n=7, proteinase K: n=8). D) Extracted *L. monocytogenes* lipids do not induce protective responses in adult zebrafish when primed 1 day prior the *M. marinum* infection (12±4 cfu) (PBS: n=6, Lipid: n=13). 11 µg of extracted lipids were injected per fish corresponding to $5x10^9$ cfu of *L. monocytogenes*. For all experiments, adult wildtype zebrafish were primed at 1 day before infection and the samples were collected at 4 wpi. Two-tailed Mann-Whitney test and Bonferroni correction was used to evaluate the significance of the results. Medians are shown in the figure. PBS=phosphate-buffered saline, HKLm=heat-killed *Listeria monocytogenes*. Modified from original publication II.

As the protection was given by the insoluble phase of the heat-killed bacterial lysate, and traditional biomolecule separation methods do not have a good resolution for aggregated molecules, an enzymatic approach was used to selectively eliminate certain biomolecules from the listeria lysate including also secreted molecules and the removal of either nucleic acids or proteins was tested. It seemed that treating HKLm with both DNase and RNase or proteinase K erases the protective effect (Figure 5C). The immunomodulatory effect of lipids was tested in a separate experiment where the lipids were extracted from HKLm and injected into adult zebrafish prior to the *M. marinum* infection. Lipids of HKLm showed no protection against mycobacterial infection (P=0.1242) (Figure 5D). These results suggest that the component of HKLm protecting against mycobacterial infection is either a nucleic acid or a protein or a combination of those.

4.4 Immune responses relating to protective response against *Mycobacterium marinum* (II)

A panel of genes was analysed to evaluate their expressions in HKLm-primed fish. RNA samples were collected one day after the *M. marinum* infection of HKLm or PBS injected fish and analyzed using qPCR method. A neutrophil marker *myeloid-specific peroxidase* (*mpx*), M2-polarized macrophage marker *arginase 1* (*arg1*), and *interferon-γ* (*ifn*) *1-1* and *1-2* did not differ between the treatments (Figure 6). Gene expression levels of a macrophage marker *macrophage-expressed gene 1* (*mpeg1*) (P=0.0352), pro-inflammatory cytokine *tumor necrosis factor* (*tnf*) (P=0.0043), antimicrobial *nitric oxide synthase 2b* (*nos2b*) (P=0.0001) and mitochondrial *superoxide dismutase 2* (*sod2*) (P=0.0022) controlling the levels of toxic ROS (reactive oxygen species) (Peterman et al., 2015) were all differentially expressed in HKLm primed fish compared to mock injection.

The nature of the immune response seen after HKLm priming was further examined by measuring the oxygen consumption of RAW264.7 macrophages *in vitro*. It is known that the differentially polarized macrophages have distinct metabolic status, and pro-inflammatory (M1) macrophages use glycolysis as their major energy source, whereas alternatively activated (M2) macrophages rely on oxidative phosphorylation (Viola et al., 2019). In this experiment, macrophages activated with either LPS or HKLm showed significantly lower oxygen consumption compared to nontreated cells (Figure 6I), which implies a polarization towards M1 type

macrophages after HKLm priming. In summary, these findings indicate that HKLm increases the number of macrophages and enhances the pro-inflammatory responses.

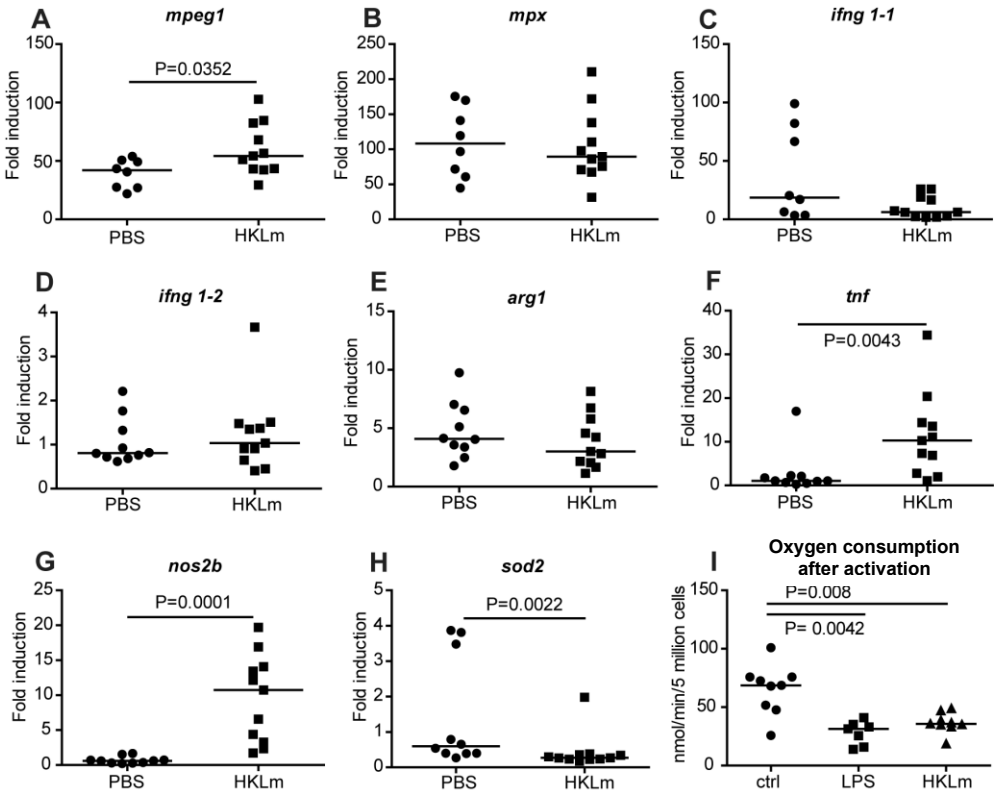

Figure 6. The heat-killed *L. monocytogenes* (HKLm) priming altered the gene expression of *mpeg1*, *tnf, nos2b* and *sod2,* and reduced the oxygen consumption of HKLm treated RAW264.7 cells. The expression of *mpeg1*, *tnf* and *nos2b* were upregulated, *sod2* was downregulated and the expression of *mpx*, *ifng1-1* and *ifng1-2* were not affected by the HKLm priming (A–H). The zebrafish were primed with HKLm 1 day before infection, infected with 67±16 cfu of *M. marinum* and the RNA was collected one day after the infection (PBS: n=10, HKLm: n=11). I) The oxygen consumption of RAW264.7 macrophages was significantly reduced after 19–24 hours activation with 50 ng/ml LPS or HKLm corresponding to MOI of 530. The panel I represents a pooled result of three independent experiment. Two-tailed Mann-Whitney test was used to evaluate the significance of the results with Bonferroni correction when needed. Medians for all groups are shown. PBS=phosphate-buffered saline, HKLm=heat-killed *Listeria monocytogenes*, LPS=lipopolysaccharide, ctrl=control. Modified from original publication II

4.5 HKLm does not protect against established mycobacterial infection (II)

The timing of the immune system activation in the *M. marinum* infection is crucial for inducing protection. As shown above, HKLm treatment can significantly (P=0.0013) reduce *M. marinum* loads at 4 wpi compared to the mock injection and induces sterilizing response in 25% of the population when injected one day prior to the infection (Figure 3). If the HKLm injection is given 2 weeks after the *M. marinum* infection (22±6 cfu) and mycobacterial counts are measured at 4 wpi, the HKLm treatment does not induce protection (Figure 7A). Similarly, HKLm priming does not have an effect on the bacterial burdens at 4 wpi if the *M. marinum* infection dose is as high as 4883±919 cfu (Figure 7B). However, the fish primed with HKLm showed significantly better survival (P=0.0245) even in a high dose infection (4883±919 cfu) that was approximately 10-times higher than the experimental low dose (20-50 cfu) used in the majority of the experiments (Figure 7C).

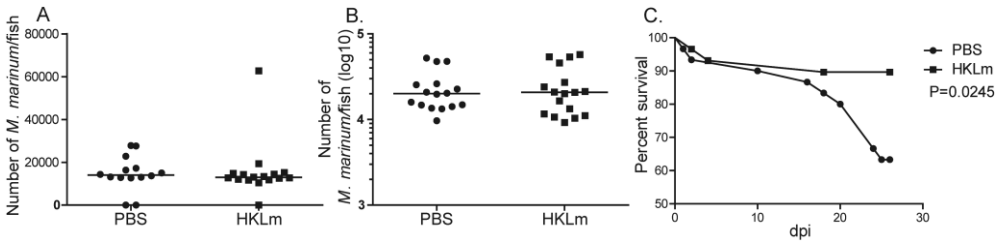

Figure 7. Protective immune responses cannot be induced with heat-killed *L. monocytogenes* (HKLm) in established *M. marinum* infection or in high-dose *M. marinum* infection. A) HKLm injection does not have an effect in established infection (22±6 cfu) (P=0.2704, two-tailed Mann-Whitney test). The HKLm injection was given 2 weeks after the *M. marinum* infection, and the DNA samples were collected at 4 wpi. (PBS:n=14, HKLm: n=16). B) HKLm priming one day before infecting the fish does not affect the *M. marinum* burden at 4 wpi if the *M. marinum* infection dose is high (4883±919 cfu) (P=0.9856, two-tailed Mann-Whitney test) (PBS:n=16, HKLm: n=17). C) HKLm priming 1 day prior to the infection significantly affects the survival in high dose *M. marinum* infection (4883±919 cfu) (P=0.0245, Log-Rank (Mantel-Cox) test) (PBS: n=30, HKLm: n=30). PBS=phosphate-buffered saline, HKLm=heat-killed *Listeria monocytogenes*. Modified from original publication II

4.6 *Mycobacterium marinum* naturally produces biofilms *in vitro* showing high antimicrobial tolerance (III)

M. marinum forms biofilms in a liquid culture without an external trigger. The biofilm formation starts early, and a visible submerged biofilm is detectable on the bottom of the tubes in couple of days. After around one week of culturing, the pellicle starts to form in the air–liquid interphase as a thin plastic-like layer or few bigger islands. Slowly both biofilm types grow thicker and increase their biomass (Figure 8).

The role of the biofilm formation in the antimicrobial tolerance was tested by determining minimum inhibitory concentration (MIC) for rifampicin by utilizing bioluminescent *M. marinum* that was pre-cultured to different ages. Different concentrations of rifampicin were added on the biofilm and the bioluminescence signal was measured up to 7 days. By comparing the bioluminescence signal to the starting value, it was concluded that MIC itself does not change with biofilm age (Figure 9). However, even when the bioluminescence signal drops dramatically after treating with high concentrations of rifampicin for 7 days, a persistent bacterial subpopulation remains in the solution. This population is viable and able to re-grow on an agar plate after removing the antimicrobial.

The proportion of persistent cells in the bacterial population increases during biofilm maturation, which is seen as an increasement of minimum bactericidal concentration (MBC) from 2 days to 1 week (Figure 10A). The biofilm was first cultured in suspension to certain ages and treated with different concentrations of rifampicin for 7 days. After the treatment, samples of the bacterial suspension were plated on agar plate and colonies were allowed to grow for two weeks to let them recover from the antimicrobial treatment. Planktonic and biofilm *M. marinum* behave differently in the MBC testing and already 2-day-old cultures showed remarkable difference; biofilm has 63 times higher MBC than the planktonic cultures (400 vs. 6.3 μg/ml of rifampicin) (Figure 10A). Planktonic cells were cultured with Tween80 which is a commonly used detergent in culture media to prevent aggregation of the bacteria. It inhibits the formation of the mycobacterial capsule (Sani et al., 2010) and alters the cell metabolisms (Pietersen et al., 2020). In addition to *M. marinum* biofilm, planktonic culture also increased its tolerance against rifampicin in two weeks indicating that it might have the ability to produce loosely-formed extracellular matrix and bacterial communities even in the presence of Tween80. In the following experiments, only 2-day-old planktonic culture was used as a control.

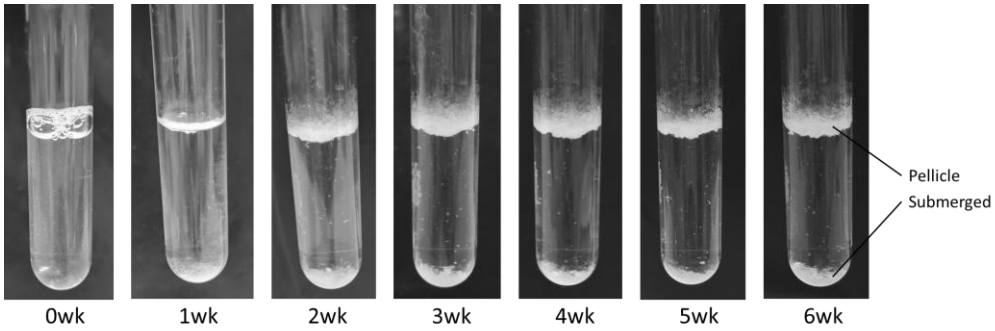

Figure 8. *M. marinum* liquid biofilm cultures show maturing pellicle and submerged biofilms. 5 ml of *M. marinum* culture from the starting OD_{600} of 0.1 was followed for total of 6 weeks in a sealed tube. The bacteria were cultured in 7H9 medium with 10% of ADC enrichment at 29°C in the dark without shaking.

A.

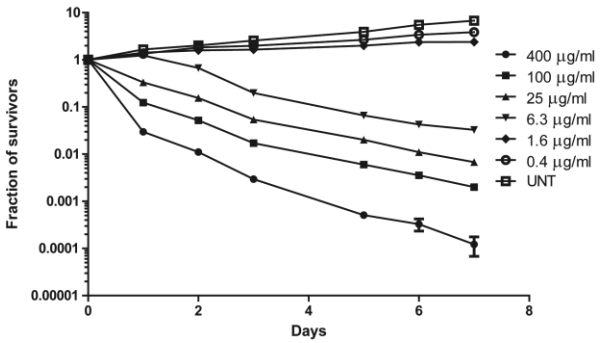

B.

Biofilm age	MIC, μg/ml
2d	1.6 - 6.3
4d	1.6 - 6.3
1wk	1.6 - 6.3
2wk	1.6 - 6.3

Figure 9. MIC (minimum inhibitory concentration) for rifampicin does not change during the biofilm maturation. A) A representative result of the bioluminescence signal of rifampicin-treated *M. marinum* biofilm (2-day-old) in relative to the starting bioluminescence value. Each concentration includes three biological replicates. Average and SEM of the signal are shown. B) MIC of different aged *M. marinum* biofilms for rifampicin remains the same over time. The MIC was identified between the shown range by measuring bioluminescence from three biological replicates.

A.

Planktonic					Biofilm				
Wiltype					Wildtype				
RIF, µg/ml	2d	4d	1wk	2wk	RIF, µg/ml	2d	4d	1wk	2wk
400	-	-	-	-	400	-	+	+	+
100	-	-	-	+	100	+	+	+	+
25	-	-	+	+	25	+	+	+	+
6.3	-	-	+	+	6.3	+	+	+	+
1.6	+	+	+	+	1.6	+	+	+	+
UNT	+	+	+	+	UNT	+	+	+	+

B.

Planktonic					Biofilm				
CelA1					CelA1				
RIF, µg/ml	2d	4d	1wk	2wk	RIF, µg/ml	2d	4d	1wk	2wk
400	-	-	-	-	400	-	-	+	+
100	-	-	-	-	100	-	+	+	+
25	-	-	-	+	25	+	+	+	+
6.3	-	-	+	+	6.3	+	+	+	+
1.6	+	+	+	+	1.6	+	+	+	+
UNT	+	+	+	+	UNT	+	+	+	+

Figure 10. Minimum bactericidal concentration (MBC) is higher with *M. marinum* biofilm than with planktonic bacteria, or CelA1 overexpression strain, and it increases when biofilm matures. A) A comparison of antimicrobial tolerance of wildtype *M. marinum* including PTEC27 tdTomato fluorescence plasmid and B) cellulase (CelA1) overexpression strain in a PTEC27 vector. Lowering antimicrobial tolerance is associated with cellulose degradation. The culturing was started from OD_{600} of 0.1 at day 0 for both planktonic and biofilm. The bacterial amount per well was normalized to starting bioluminescence value at the time of adding rifampicin and samples of the bacterial suspension was plated on 7H10 agar plate after 7 days of rifampicin treatment. Negative growth was determined by cfu count of under 100 which refers to over 99.9% killing capacity. Samples were prepared in triplicates. Modified from original publication III

4.7 Increased minimum bactericidal concentration (MBC) of mycobacterial biofilm is due to phenotypic tolerance

Long antimicrobial treatments are prone to promote the development of genetic resistance, and the possibility of genetic changes accounting for the enhanced antimicrobial tolerance seen in biofilm cultures was tested. The development of genetic antimicrobial resistance in *M. marinum* biofilm cultures was evaluated in liquid cultures with repeated rifampicin treatments using a bioluminescent *M. marinum* strain. At the first step, over 90% of the bacterial population was killed, mostly including actively dividing bacteria. After treating the cells with high concentrations

of rifampicin, the antimicrobial was removed and the cells washed, and the bacteria were let to regrow in a fresh media. Second rifampicin challenge was introduced, and similar killing kinetics was observed as with the first challenge. The tolerance against rifampicin was not enhanced after the first rifampicin treatment indicating phenotypic tolerance rather than genetic resistance in the remaining population (Figure 11).

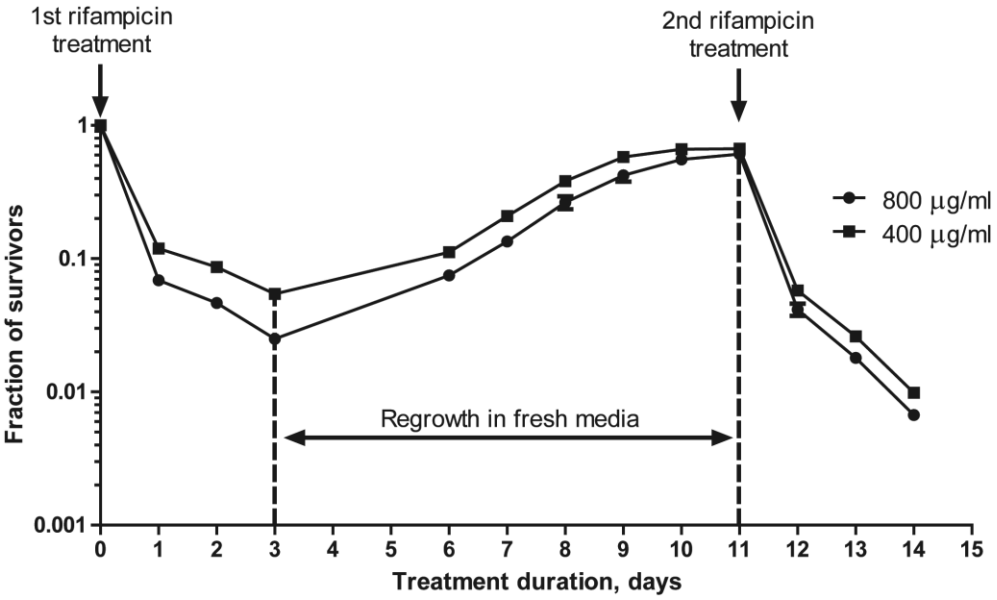

Figure 11. Rifampicin treatment does not increase the genetic resistance of *M. marinum* biofilm. A similar killing kinetics was observed after the 1st and the 2nd exposure of 800 and 400 µg/ml of rifampicin by measuring bioluminescence signal. Average and SEM of 12 replicates are shown in the figure.

Knowing that the tolerance in *M. marinum* biofilm is due to phenotypic changes, degrading the biofilm extracellular matrix was tested as an adjunctive treatment. Proteinase K, DNase1 and cellulase were added on a 4-day-old *M. marinum* biofilm or 2-day-old planktonic culture with or without 8 µg/ml of rifampicin. Figure 12 shows how the bioluminescence signal increased or reduced at day 6 compared to day 0 due to different treatments. The enzyme treatments alone had only a small effect on the planktonic bacteria but especially cellulase reduced the bioluminescence signal of the biofilm culture to similar level than 8 µg/ml of rifampicin. Planktonic

A.

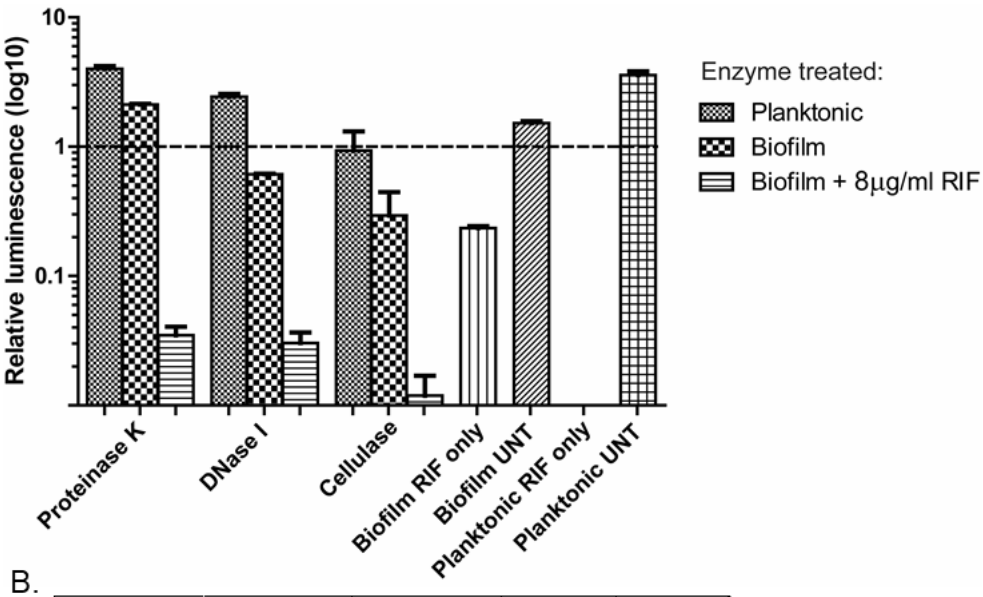

B.

		RIF	ENZ	RIF+ENZ
Plankt.	Protease	n/a	+4.0x	n/a
	DNase	n/a	+2.4x	n/a
	Cellulase	n/a	-1.1x	n/a
Biofilm	Protease	-5.6x	+2.1x	-29.4x
	DNase	-4.9x	-1.6x	-34.4x
	Cellulase	-4.3x	-4.7x	-102.1x

Figure 12. Treating developing biofilm with ECM-degrading enzymes potentiates the effect of rifampicin. 4-day-old biofilms or 2-day-old planktonic *M. marinum* in the logarithmic growth phase were treated with either 10 mg/ml cellulase, 0.15 mg/ml DNase1 or 1 µg/ml Proteinase K with or without 8 µg/ml of rifampicin. The viability of *M. marinum* was evaluated at day 6 by measuring the endpoint bioluminescence and normalized to the starting luminescence signal on day 0. A. Mean + SEM luminescence values of two biological replicates for enzyme treated samples and six replicates for rifampicin only and untreated groups at day 6. The dashed line represents the comparison point at day 0. B. Relative reduction or increasement of the bioluminescence values at day 6 compared to day 0. "RIF" refers to *M. marinum* cultures treated only with 8 µg/ml of rifampicin, "ENZ" to cultures treated only with a degrading enzyme and "RIF+ENZ" shows the effect of 8 µg/ml rifampicin and a degrading enzyme together. If the bioluminescence signal drops below the detection limit, the result is marked "n/a".

M. marinum cultures were so susceptible to rifampicin that the measured bioluminescence signals were under the detection limit after 6 days of treatment, which prevented further analysis of the role of degrading enzymes in the co-treatment group for planktonic *M. marinum*.

In biofilm groups, all adjunctive enzyme treatments with rifampicin reduced the bioluminescence signal several times more compared to rifampicin only or enzyme only treatments, cellulase showing the greatest effect by reducing the bioluminescence signal by over 100x compared to 0 day (Figure 12B). The effect of cellulase in degrading extracellular matrix was further examined with a *M. marinum* strain overexpressing mycobacterial cellulase (*celA1*). The results showed in line with the enzyme testing experiments that the overexpression strain was more susceptible to rifampicin than the wildtype *M. marinum* (Figure 10B).

4.8 Time-kill curve analysis for testing antimicrobials on *Mycobacterium marinum* biofilm (III)

Susceptible bacterial population has phenotypically different subpopulations that react to antimicrobials differently – some being more susceptible and some more tolerant against antimicrobials. Persisters are a subpopulation of bacterial cells that is able to tolerate antimicrobials for a prolonged time (Brauner et al., 2016). These persister are likely to be important in biofilms. The presence of persisters can be visualized as a biphasic killing curve where susceptible bacteria die quickly and persisters require a longer treatment time to be eradicated. If the whole bacterial population was phenotypically tolerant, the killing curve would not be biphasic.

As a quick bioluminescence-based method, time-kill curve analysis was established for measuring the killing of the *M. marinum* persisters in biofilms. The outline of the experiment is shown in the Figure 13. First, 1-week-old biofilm was treated with rifampicin concentrations ranging from 50 μg/ml to 800 μg/ml. The changes in the proportion of persistent cells in the mycobacterial population were studied by determining time-killing curve by measuring bioluminescence relative to the starting value. The figure 14A shows similar killing kinetics for the biofilms treated with 400 or 800 μg/ml of rifampicin suggesting that the killing time has been saturated and further increasing of the antimicrobial concentration does not speed up the killing. At these high concentrations (over 64 x MIC, minimum inhibitory concentration), the killing curves show biphasic nature revealing the presence of persister cells in the *M. marinum* biofilm; the most sensitive actively growing

mycobacteria died quickly and the persisters survived longer, which forms a biphasic killing curve of steep beginning continuing with a gentler slope. 400 µg/ml of rifampicin was chosen for the following experiments. As a control, the bioluminescence signal from untreated *M. marinum* biofilm was measured over time, which showed that at one week the biofilm is still growing and metabolically active (Figure 14B).

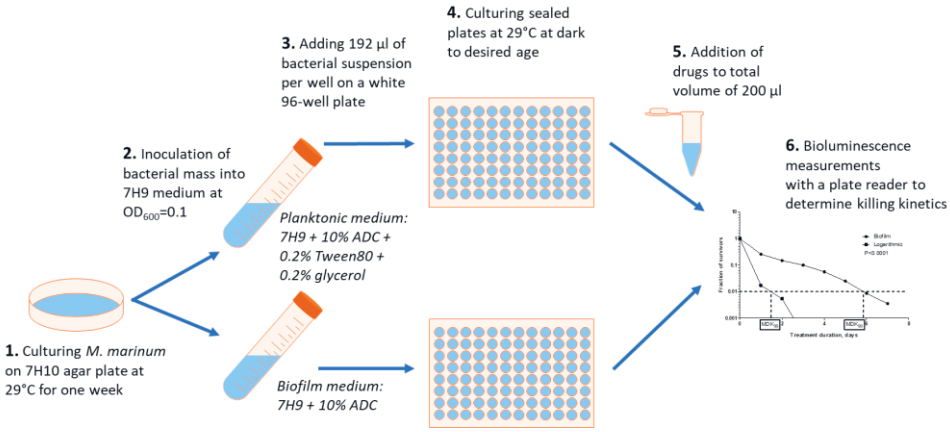

Figure 13. Outline of the time-kill curve analysis methodology to measure killing kinetics of bioluminescent *M. marinum*.

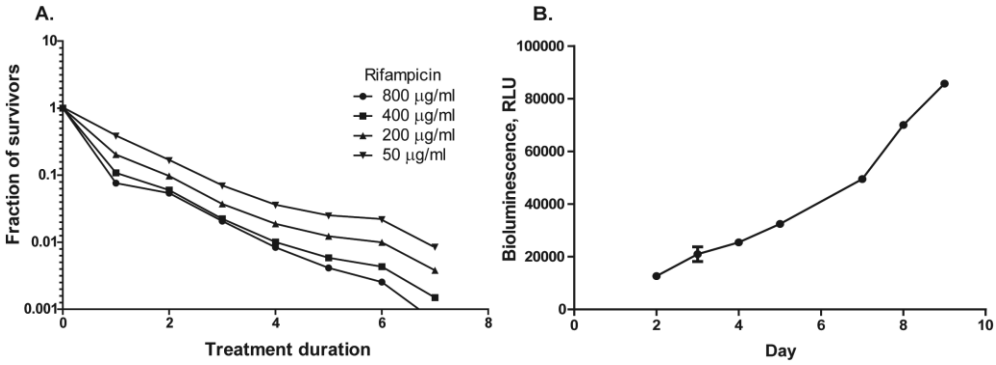

Figure 14. Metabolically active *M. marinum* biofilm reached a saturated rifampicin concentration at 400 µg/ml. A) Time-kill curve of 1-week-old *M. marinum* biofilm treated with 50–800 µg/ml of rifampicin. B) Untreated biofilm shows increasing bioluminescence signal over time. Mean and SEM are shown in the figures. Modified from original publication III.

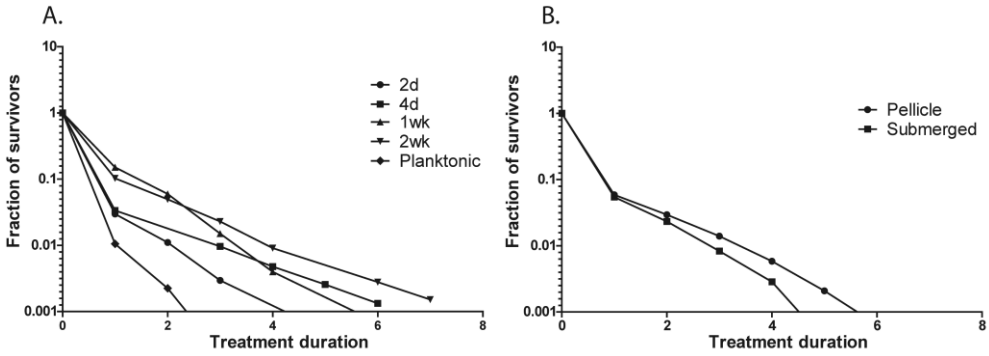

Figure 15. Maturing *M. marinum* biofilm shows increasing amount of persister bacteria for both pellicle and submerged biofilm subtypes. A) Time-kill curves of biofilm of different ages and 2-day-old planktonic *M. marinum*. Log-Rank test P=0.0002 (plankt. vs 1wk biofilm). B) 2-week-old pellicle vs submerged biofilm show no difference in the antimicrobial persistence (P=0.51, Log-Rank test). Mean and SEM of three biological replicates are shown in the figures. Modified from original publication III.

Next, the maturation of the phenotypic antimicrobial persistence of *M. marinum* was tested on biofilm cultures of different ages. This was done by measuring bioluminescence signal over time by comparing 2-day-old planktonic liquid culture in the logarithmic phase to different aged biofilm cultures. The only difference in the growth conditions between planktonic and biofilm was the addition of Tween80 and glycerol in the planktonic culture media. Aging *M. marinum* biofilm showed increasing antimicrobial resistance (P=0.0002) from 7 days onward compared to 2-day-old planktonic (Figure 15A). By combining the results of five independent experiments, it can be concluded that 11±3% of the 1-week-old *M. marinum* biofilm population consist of persisters that show slower killing kinetics after one day of rifampicin treatment.

The submerged biofilm in a steady liquid *in vitro M. marinum* culture is the first biofilm subtype that appears at the bottom of the culture, but a visible pellicle starts to form in the air-liquid interface around one week of culturing. To test whether one of these biofilm forms is more tolerant against drugs, 2-week-old pellicle and submerged biofilms were separated and their sensitivity against rifampicin was tested using time-kill curve analysis. The results showed no differences between pellicle and submerged biofilm in the drug susceptibility (Figure 15B). In conclusion, the results indicate that 1-week-old *M. marinum* biofilm is more tolerant against rifampicin than planktonic bacteria growing in the logarithmic growth phase. The phenotypic

antimicrobial tolerance increases over time and is characterized by an increased proportion of persister cells in both pellicle and submerged biofilms.

4.9 Mycobacterial biofilm targeted by sybodies (Manuscript)

In the proteomics data, where extracellular and intracellular proteins of *M. marinum* biofilm were compared, it was concluded that GroEL1 and GroEL2 could be potential targets of mycobacterial biofilms as they were among the 10 proteins giving the highest intensities in mass spectrometry analysis, the protein structures were known, and they were also present in Mtb. Hence, it was set out to produce synthetic nanobodies, sybodies, against these proteins (Manuscript).

Using confocal imaging and fluorescent labelled antibody against the Myc-tag of the sybodies, the binding to GroEL1 and GroEL2 in the biofilm of both *M. marinum* and Mtb was evident (Figure 16). In the experiment, samples treated only with antibodies against the Myc without the sybodies were used as a control. The difference of the maximum intensity projections of the green fluorescence signals between the controls and the samples stained with sybodies was statistically significant ($P<0.001$) proving binding of the sybody to mycobacterial biofilm.

Both Mtb and *M. marinum in vitro* biofilms can be found in many shapes and they resemble each other by the physical appearance. At the two-week timepoint, they both showed cord-like structures and they had produced excessive amounts of extracellular matrix (green) where the mycobacterial cells (blue) are embedded (Figure 16). However, the cords in the avirulent Mtb biofilm were much shorter than in *M. marinum* and Mtb seemed to have a tendency to form larger and more compact structures with less organized orientation.

Two different staining protocols of the sybodies were used. In the Figure 16, *in vitro* biofilm samples were treated first with GroEL-sybodies and thereafter stained with anti-Myc Alexa488 antibody. In the Figure 16 A&B, GroEL-sybodies were first labelled by the Alexa488-fluorophore with the covalent NHS-linkage and then used to target the *in vitro* biofilms. As the *M. marinum* biofilms were the same age, the only difference between the Figures 16E&F and 17A&B was the sybody staining protocol and it can be concluded that pre-labelled GroEL-sybodies give higher green fluorescence signal in the confocal imaging.

For the granuloma samples, the adult zebrafish were infected with tomato-fluorescent *M. marinum* and the red fluorescence signal was used to collect the granulomas at 8 wpi for the *ex vivo* sybody-testing. The pre-labelled sybodies were

used to target *ex vivo M. marinum* biofilms in granulomas. The sybody+Alexa488 combination is a smaller molecule in size than the sybody+antibody+Alexa488 complex and thus it is more likely to cross the outer layers of the granulomas and bind the biofilm itself. The sybody against GroEL1 was first tested on extracted granuloma biofilm where the outer layer of the granuloma was removed prior the staining. The sybody showed strong green fluorescence signal throughout the biofilm mass proving the presence of GroEL1 in *in vivo M. marinum* biofilms (Figure 17 C).

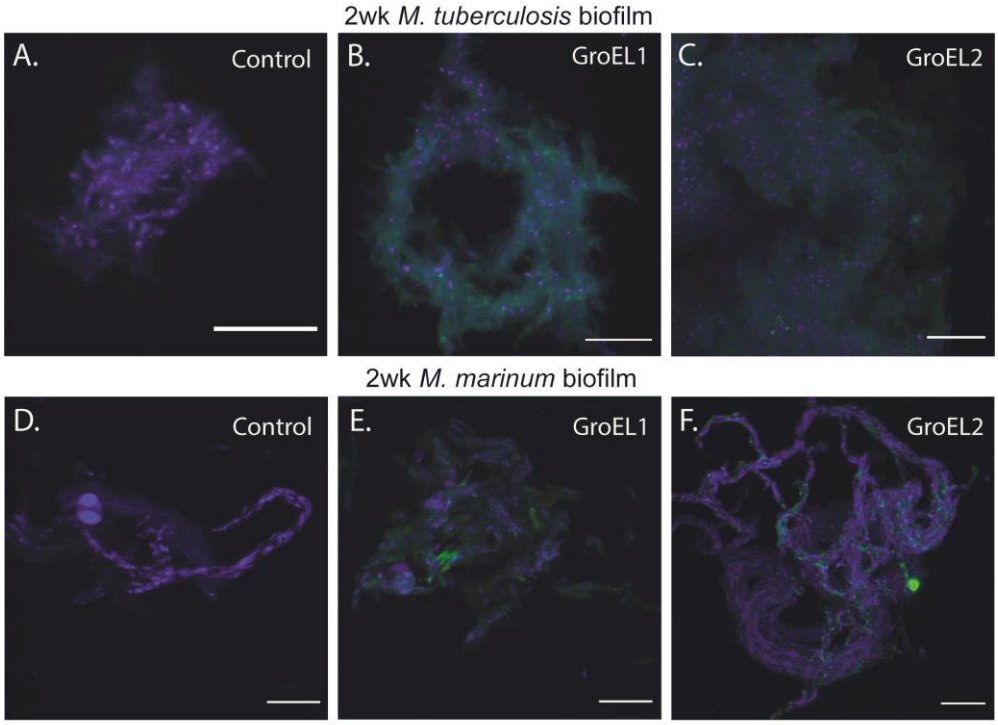

Figure 16. Synthetic sybodies against GroEL1 and GroEL2 specifically bind to *M. tuberculosis* and *M. marinum in vitro* biofilms. The 2-week-old biofilm of both *M. tuberculosis* and *M. marinum* were targeted with either GroEL1 or GroEL2 sybodies with Myc-tag (B, C, E and F). The sybodies were then stained with anti-Myc Alexa488-antibody (green) and DAPI was used to visualize mycobacterial cells (blue). Control samples (A and D) were stained without sybody using only anti-Myc antibody and DAPI. Scale bars are 10 µm for all images.

The pre-labelled Alexa488 GroEL-sybodies were also tested on intact zebrafish *M. marinum* granulomas and showed that it is able to penetrate through the protective host cell layers of the granuloma (Figure 17 D-G). Figure 17 D&E represent a 2D-captures through the surface of the round-shaped granuloma and Figure 17 F&G a zoomed layer-view of the granuloma edge where the sybody labelled with green is localized between the red-labelled mycobacteria and the blue-labelled host cells.

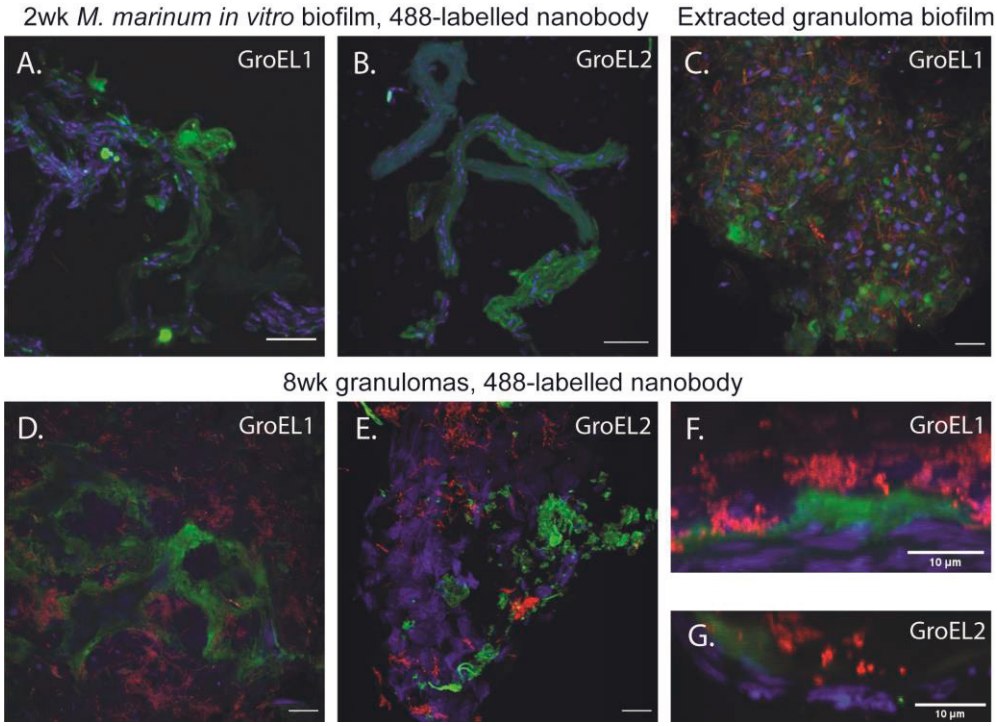

Figure 17. Fluorescent-labelled synthetic sybodies against GroEL1 and GroEL2 bound to *M. marinum* biofilm *in vitro* and to *ex vivo* zebrafish granulomas. 2-week-old *M. marinum* biofilm was stained with NHS-linked Alexa488-labelled GroEL1 (A) and GroEL2 (B) sybodies (green) and with DAPI to visualize mycobacterial cells (blue). Green fluorescent sybodies were also used to stain biofilm in *ex vivo* zebrafish granulomas of tomato-fluorescent *M. marinum* (C-G). The granulomas were collected at 8 wpi with the help of the red-fluorescence.

5 DISCUSSION

5.1 Heterogeneity of the disease outcomes in the zebrafish–*Mycobacterium marinum* TB model

TB shows a heterogenous nature in the human population. The exposure of just a few mycobacteria can lead to very different disease outcomes from active infection to latency. In active Mtb infection, the patient has symptoms of TB, actively dividing bacteria, and the ability to transmit the bacteria further. 5-10% of Mtb-infected individuals develop primary active disease, the remaining, up to 95%, accounting for cleared and latent infections (Biraro et al., 2016). Latent TB is an asymptomatic form of the disease that includes a range of different disease stages. Instead of categorizing TB to only latent and active infections, it has been suggested that latent infection should be divided into latent, incipient and subclinical TB, where the groups are classified according to the microbiological and radiographical status and the likelihood of developing an active infection (Drain et al., 2018). A large share of the active TB cases appear within the first years after the primary infection, but a significant proportion of active cases is due to reactivation of the latent TB, which is a major public health issue (World Health Organization, 2018). The risk of reactivating latent TB during a lifetime is 5-10% (Comstock et al., 1974).

The diversity in TB disease spectrum has been explained by environmental factors and by the genetics of the host or the pathogen. In the laboratory setting, where the environment, the infection dose and the bacterial strain are controlled, the host's genetic factors are more likely to contribute to the variation. Zebrafish populations are known to be genetically heterogenous (Balik-Meisner et al., 2018) and the variation seen in the development of the mycobacterial infection in this thesis (Figure 1) can be explained mostly by the genetic diversity of the zebrafish population.

The variation in the disease outcomes of *M. marinum* -infected adult zebrafish resembles the variation seen in human TB disease. When exposed to Mtb, about 5% of humans (7% of *M. marinum* -infected zebrafish) develop active disease (Tsenova & Singhal, 2020). Resisters, that are able to clear the infection in the early phase, accounts for 5-35% of human population (Simmons et al., 2018) (zebrafish 10%)

and individuals eventually reactivating the latent infection for 5-10% (Comstock et al., 1974) (zebrafish 18%). Calculated from these numbers, the proportion of latently infected humans would range between 50-85% of individuals infected with Mtb. In our zebrafish population, 65% of infected fish develop latent disease in a 32-week experiment. The natural host–pathogen pair that can be formed by using *M. marinum* and zebrafish can partially explain the high similarity between human and fish TB disease spectrum and pathogenesis.

5.2 Inducing sterilizing response against mycobacteria

A lot is known about the immune responses against Mtb; what is beneficial and what is needed to maintain the infection in a resting stage. However, it is unknown which immunological factors are crucial for the clearance of mycobacteria. Mycobacteria is famous for successfully evading host's immune response, which often leads to a chronic infection – a compromise between the wellbeing of host and the bacterium.

In our research group, a set of different heat-killed bacteria and immunoactivators were tested for their potential to beneficially modulate the immune response in order to prevent the evading mechanisms and to eradicate mycobacteria. In the screen, heat-killed *L. monocytogenes* (HKLm) was found to be the most promising agent (Original publication II), and here it was studied further. In our zebrafish population, 10% of the individuals can naturally clear the *M. marinum* infection of 20-50 cfu. Priming with HKLm one day prior the infection increased the percent of individuals able to sterilize mycobacteria, resisters, from 10% to 25% and reduced the overall mycobacterial loads significantly by 4 wpi (Figure 3AB).

L. monocytogenes is a gram-positive bacterium that survives inside a host cell. HKLm is known for being a common immunoactivator used to activate especially TLR2 which induces the production of pro-inflammatory cytokines (Flo, Halaas et al. 2000). The ligands for TLR2 receptor include polysaccharides, proteins and glycolipids (Oliveira-Nascimento et al., 2012). Here, lipids from *L. monocytogenes* did not show any protective effect but protection was mediated via nucleic acid and/or protein (Figure 5C&D). The exact HKLm component inducing the sterilizing response remained unknown for technical reasons.

It was shown with *rag1*$^{-/-}$ mutant fish lacking adaptive immunity that the innate immune responses were responsible for the protective effect of HKLm priming. 17% of the *rag1*$^{-/-}$ mutant fish were able to clear the low dose *M. marinum* infection when without priming there was no clearance in any of the individuals (Figure 3CD).

The induced clearance rates in the absence of adaptive responses in the *rag1*$^{-/-}$ mutants strongly indicates that the clearance seen in the fish population after HKLm priming is so-called early clearance and mediated via innate immune responses.

Zebrafish larvae do not develop functional adaptive responses until 3 to 4 weeks after fertilization (Langenau et al., 2004; Page et al., 2013) hence it can be used to study innate responses separately. Knowing from the rag-experiments that the HKLm induces early clearance, zebrafish larva was tested as an *in vivo* model. After testing 1 and 2 dpf larvae with separate and co-injection of HKLm and live *M. marinum*, it was concluded that unlike adult *rag1*$^{-/-}$ fish, zebrafish wildtype larva is not able to sterilize mycobacteria even with the help of HKLm pre-treatment (Figure 4). Zebrafish larva has innate immune responses but at such an early age the cells and tissues are developing and some crucial mechanisms for the mycobacterial sterilization may still be absent.

In the adult zebrafish experiments, the mycobacterial loads were measured with qPCR. Mycobacteria is almost entirely found in the internal organs of adult zebrafish (Parikka et al., 2012) and this was chosen as the material to determine mycobacterial loads. Even though all internal organs of the fish were used, there is still a detection limit of 100 cfu when the loads are measured by qPCR, which is an important fact when determining clearance. The detection limit depends on the sample lost and dilution during the homogenization of the tissues, DNA extraction and qPCR. The calculated theoretical detection limit seemed to hold true in the zebrafish samples as tested with a spiking experiment (Table 5), where two out of three of the 100 cfu samples were positive in qPCR. For higher bacterial loads, all samples were measurable. It was technically challenging to show that the fish have sterilized the infection completely, and we were not able to execute cfu plating or reactivation experiments to conclude the clearance finding. Due to the detection limit of qPCR, it is possible that there are small amounts of remaining *M. marinum* cells in the fish.

5.2.1 Innate responses after HKLm priming

The results from *rag1*$^{-/-}$ mutants showed that the clearance after HKLm priming is early clearance and due to innate responses. Hence, the expression of several genes involved in the innate immune responses were measured one day after the *M. marinum* infection. The sterilizing response induced by HKLm priming was characterized by the increased expression of *mpeg1*, *tnf* and *nos2b* genes and decreased expression of *sod2* (Figure 6). Mpeg1 is a marker for macrophages and higher *mpeg1*

expression indicates higher numbers of macrophages. The neutrophil marker *mpx* was not altered. The actual cell numbers were not examined and there are no prior studies assessing whether *mpeg1* or *mpx* expression stay constant during the cell activation or development, or if the genes reflect activation status of the cells. The expressions of pro-inflammatory cytokine *tnf* and *nos2b* producing microbicidal free radicals were also higher in the HKLm primed group showing a strong pro-inflammatory reaction against mycobacteria. *Sod2* is a mitochondrial enzyme that reduces the amount of free radicals by converting them to a less toxic form. A temporary reduction in the expression of *sod2*, might help the immune system to maintain higher amounts of ROS and effectively kill the bacteria.

Surprisingly, the expression levels of *ifnγ* did not differ between HKLm primed individuals and the control group even though both gene copies, *ifnγ1-1* and *ifnγ1-2*, found in the zebrafish genome were tested. The role of IFNγ in TB has been extensively investigated and many studies have shown the harmful effect in the absence of IFNγ (Cooper et al., 1993; Flynn et al., 1993). These results have strengthened the simplified classification of Mtb being an exclusively intracellular pathogen. Later, the importance of the balance and the timing of the IFNγ production has been understood. Although, IFNγ is an essential cytokine in the control of TB, IFNγ deficiency does not affect the mycobacterial burden in the early phase of the infection (Pearl et al., 2001), which is in line with the results shown in this thesis.

Macrophages have been traditionally categorized into classically activated pro-inflammatory M1 cells and alternatively activated (sometimes described as anti-inflammatory) M2 cells similarly to Th1/Th2 classification of T cells (Mills et al., 2000). These polarized cells from both extremes have been studied in the context of TB and it has been reported that M1 macrophages are important in the early clearance of mycobacteria (Viola et al., 2019). M1 macrophages have the ability to produce elevated levels of NO and pro-inflammatory cytokines including TNF (Chávez-Galán et al., 2015), molecules that were affected also by HKLm priming.

The expression of *arg1*, a commonly used marker for M2 macrophages, was not altered by HKLm priming. Arg1 uses arginine as a precursor to produce mediators for the tissue remodelling in granulomas and prevents the use of arginine for NOS production promoting anti-inflammatory responses (Park et al., 2021). Mtb is known for taking advantage of the macrophage balance by manipulating the M1/M2 polarization towards M2-biased response (Shi et al., 2016). The M1/M2 balance has been connected to different disease states, and decreased M1/M2a ratio of blood

monocytes can be used to predict active disease and reactivation of latent TB (Chen et al., 2020).

In addition to different immunological responses, M1 and M2 cells also differ by their metabolic status. M1 macrophages use glycolysis for their energy source whereas M2 cells rely on oxidative phosphorylation (O'Neill & Pearce, 2016). This phenomenon was seen after HKLm stimulation of macrophages *in vitro*, where macrophages significantly reduced their oxygen consumption (Figure 6I) supporting the result that HKLm activates M1 macrophages, and these cells are especially important in the sterilizing response against Mtb in the early infection.

Macrophages, their polarization, and pro-inflammatory response are important for the control of TB. However, when looking at the whole picture, both M1 and M2 macrophages are important in the control against TB; M1 for their microbicidal pro-inflammatory response and M2 for restricting Mtb growth inside granulomas. Several studies together indicate that heterogenous response of several cell types and corrected timing are the key to sterilizing response (Clay et al., 2007; Pearl et al., 2001; Pedrosa et al., 2000; Verrall et al., 2020), and there is no single cell type or response that would alone be beneficial in all situations.

5.2.2 Trained immunity in mycobacterial infection

Immunological memory has traditionally been a characteristic of adaptive responses. However, innate immune memory, often called trained immunity, has been acknowledged as a novel way to pass information via epigenetic programming such as through molecular modification of histones and DNA. The epigenetic reprogramming of trained immunity makes the genes involved in innate immune responses better available for transcription and the protection long-lasting (Kleinnijenhuis et al., 2012). Many factors affect the epigenetics, which is considered as the memory on a gene level, and it was studied whether HKLm priming could induce trained immunity.

Trained immunity has been first described after BCG vaccination. BCG has shown variable efficacy against Mtb, but epidemiological studies of BCG have also revealed a nonspecific protection against other infections (Aaby et al., 2011). It has been reported that these protective immune mechanisms are not specific to certain pathogen, and they are not mediated by lymphocytes but rather by trained immunity (Kleinnijenhuis et al., 2012). The role of innate responses in the protection against mycobacteria was also seen in HKLm priming. Although, it is still not known, how

long these trained immunity mechanisms can last (Hamada et al., 2019), it is reported that individuals able to resist the Mtb infection have epigenetic modifications in their genome (Seshadri et al., 2017). In the case of HKLm priming, 1-day and 1-week timepoints were tested prior the infection. One day was shown to have a greater sterilizing effect over mock injection and was used in the follow-up experiments (publication II). However, fish has been shown to have robust and long-lasting innate immune responses that have been utilized in the vaccination of fish by unspecific antigens (Tafalla et al., 2013; Uribe et al., 2011), which also makes even longer HKLm priming timepoints potential to consider. The possibility to utilize trained immunity in the prevention of human TB have also been suggested (Choreño-Parra et al., 2020).

Trained immunity has been characterized by metabolic changes (Riksen & Netea, 2021), such as the Warburg effect (Cheng et al., 2014). In the Warburg effect, despite the presence of oxygen the cell relies on fermentation as an energy production method (Warburg, 1956). The reduced oxygen consumption induced by HKLm may be an indication of trained immunity in the HKLm-induced protection against mycobacteria.

HKLm priming before infection can potentially prevent a range of different evasion mechanisms and this approach could be used as an effective prophylactic immunotherapy. A typical infection dose in human is small, just few bacteria, and small infection dose was used in the fish model to create a similar course of infection. High infection dose causes active disease with progressive amounts of bacteria in the adult zebrafish (Parikka et al., 2012) and it was determined that HKLm priming is not effective against such high-dose infection. The same was observed for established mycobacterial infection where HKLm was tested for treating *M. marinum* infection. In both cases, it is possible that the mycobacterial evasion mechanisms are either too strong or well established to overcome with immune activation. It seems that mycobacterial manipulation over immune system is so effective that in our zebrafish TB model, boosting the immune responses in an on-going infection is not the solution. In addition to active manipulation of immune reactions, the structure of mycobacteria and the extracellular matrix can also physically block immune responses and the effect of antimicrobials. The formation of the extracellular matrix and its effects on drug treatments in mycobacteria are discussed in the following chapter.

5.3 Characteristics of mycobacterial biofilms

Mycobacteria can tolerate many environmental conditions often leading to chronic diseases in a host. The mycobacterial cell envelope is a waxy double-layer structure that has a low permeability to many antimycobacterial drugs creating a phenotypic tolerance against a range of antimicrobials (Batt et al., 2020). Mtb can also modulate its cell envelope to create an even less permeable capsule in response to the presence of antimicrobials (Sebastian et al., 2020).

In addition to the bacteria itself, a cumulative amount of information has indicated that the bacterial biofilm influences drug susceptibility (Defraine et al., 2018; Gold & Nathan, 2017) and recently, Mtb biofilms have been discovered in mice and human granulomas (Chakraborty et al., 2021). In this thesis, planktonic and biofilm *M. marinum* showed a clear difference in their tolerance against antimicrobial. The MBC (minimum bactericidal concentration) was 63 times higher in mycobacterial biofilm than in planktonic cultures of logarithmic growth phase where the bacterial population is kept single-celled in the presence of detergent (Figure 10). Despite the evidence showing increased drug tolerance of mycobacteria in biofilms, biofilms have not been taken into account during drug development.

In mycobacterial *in vitro* studies, pellicle form of biofilm has been more studied (Chakraborty & Kumar, 2019), but the results of this thesis show that drug tolerance is developing already before the pellicle is visible and the increased tolerance is due to maturing submerged biofilm during the first days of liquid culture. Also, pellicle and submerged biofilm had no difference in drug susceptibility at two weeks according to time-kill curve analysis (Figure 15B), which highlights the importance of both biofilm types. Currently, there are no studies showing which biofilm type resembles the *in vivo* situation better, hence both pellicle and submerged biofilm should be considered when studying *in vitro* mycobacterial biofilms.

5.3.1 Degradation of mycobacterial biofilm extracellular matrix as an adjunctive therapy

Mycobacterial biofilms have been identified in many TB animal models and in human TB (Chakraborty et al., 2021; Sarathy et al., 2018). Compared to single-celled planktonic bacteria, biofilms are more resistant to environmental hazards and immune responses, which can also decrease the effectiveness of antimicrobials and vaccinations (Kumar et al., 2017). Biofilm formation decreases mycobacterial

response to antimicrobial treatment (Ojha et al., 2008). Respectively, by weakening the biofilm architecture, it is possible to improve the response (Ackart et al., 2014). This has drawn interest in the composition of the extracellular matrix (ECM) and quorum sensing network as potential drug targets.

Cellulose, proteins, mycolic acid and eDNA have been identified as the ECM components of the mycobacterial biofilm (Chakraborty et al., 2021; Ilinov et al., 2021; Ojha et al., 2008; Trivedi et al., 2016). Thus, degrading enzymes were tested for their ability to potentiate antimicrobial treatment in *M. marinum* biofilm. Cellulase, DNase1 and proteinase K all, together with rifampicin, significantly enhanced the bacterial killing compared to a group that received only rifampicin, which shows the importance of the biofilm ECM in the susceptibility to antimicrobials (Figure 12).

The ECM composition of the pellicle and the submerged biofilms differs to some extent. Lipids are the major component of pellicle biofilms whereas submerged biofilms are rich in polysaccharides (Chakraborty & Kumar, 2019). However, also eDNA and proteins play a role especially in the submerged biofilm as degrading these polymers had an effect on developing submerged biofilm when the pellicle biofilm is still absent. Cellulose has been identified as one of the major components of mycobacterial biofilm (Chakraborty et al., 2021; Trivedi et al., 2016) and degrading cellulose was the most effective adjunctive treatment with rifampicin, but additional factors may have an impact to the tolerance as well. A cellulase overexpression *M. marinum* strain had higher sensitivity to rifampicin in biofilm and in planktonic cultures but the tolerance still increased with age (Figure 10). It is possible that both biofilm subtypes have factors other than cellulose that contribute to the tolerance. Whether these factors are part of the biofilm architecture, quorum sensing, other biofilm dynamics or something else requires further examination.

5.3.2 Persistence in mycobacterial biofilm

Biofilms have gradients of energy source and oxygen supply, which leads to a heterogenous population of bacteria (Rani et al., 2007). The bacterial population within a biofilm includes metabolically active and dormant bacteria both having further subpopulations with altered drug-susceptibility. MIC did not change during the maturation of the mycobacterial biofilm but after a week of antimicrobial treatment there was an increasing number of live bacteria. The low MIC concentration of rifampicin may inhibit the growth, but a subpopulation of tolerant mycobacteria remains after drug treatment and accounts for the increased MBC.

This subpopulation is metabolically active, able to regrow on agar and in medium, and shows similar killing kinetics in repeated antimicrobial exposures, which indicates towards phenotypic tolerance rather than genetic resistance of the bacteria. These survivors, that are able to tolerate the antimicrobial treatment for a prolonged time, are called persisters.

MIC is a commonly used method for testing resistance for antimicrobials on clinical bacterial strains, but this technique does not take into account the persister cell populations, even though persisters have been identified for example in bacterial populations of *S. aureus* (Bryson et al., 2020), *E. coli* (Brauner et al., 2017) and *M. tuberculosis* (Vijay et al., 2021). Here, time-kill curve analysis was used to measure the amount of persisters in mycobacterial biofilms. The bacterial population was exposed to high concentration (63x MIC) of rifampicin and the killing rate was followed by measuring bioluminescence signal over time. When the antimicrobial was removed, the persistent *M. marinum* subpopulation regrew back into heterogenous population of antimicrobial-sensitive and persistent cells similar to the parental strain (Figure 11), which is a feature of persisters by definition (Brauner et al., 2016).

The time-kill curve analysis utilized a bioluminescent *M. marinum* strain. This approach enabled a quick method to measure the number of live mycobacteria in the sample. The two enzymes producing bioluminescence, luciferases A and B, and their three substrates in the LuxABCDE cassette are all produced under constantly active promoters and unlike a stable fluorescent protein, the bioluminescence signal ends when the substrates are consumed reflecting rapid changes in the bacterial numbers, which is good when measuring killing kinetics of the bacterial population.

In traditional plating or OD-based methods, the mycobacterial tendency to form aggregation in the liquid may disturb the measurement and the actual cell number will not be detected by these techniques whereas light-based methods are sensitive to physical barriers such as the ECM in the case of biofilm. It is possible that different amounts of biofilm can lead to different levels of light inhibition. In addition to physical barriers, bioluminescence is sensitive to the metabolic state of the cell. Mycobacteria can reduce its metabolic activity and even enter dormancy, which is a known way to tolerate environmental hazards. The effect of dormant cells in the *M. marinum* biofilm was excluded as the bioluminescence signal increased in untreated cultures for at least nine days of biofilm liquid culturing. Both the metabolic status and the thickness of the biofilm argue to use as young biofilm as possible. For this reason, one-week-old biofilm was used in this setup, even though the biofilm mass visible increases for several weeks.

This method was shown to be an easy and quick way to measure the killing kinetics of microbes grown in *in vitro* biofilms and could be used to screen antimicrobial compounds against persister cells, which could greatly improve the treatment outcome of the current drugs.

5.3.3 Targeting mycobacterial biofilms by synthetic single domain antibodies, sybodies

Sybodies were produced to demonstrate that it is possible to specifically target mycobacterial biofilms and to carry small molecules to close contact with the biofilm. Sybody is a synthetic polypeptide resembling the variable part of the antibody heavy chain of camelids (nanobody), which makes it a relatively small protein with possible very high binding affinity to its target and better tissue penetrance and stability compared to antibodies (Panikar et al., 2021). It is also possible to manipulate sybodies binding properties and they are easy to produce in *E. coli* (Zimmermann et al. 2020).

There has been a great interest in using nanobodies as a replacement for monoclonal antibodies. Currently, nanobodies have been used for diagnostics, imaging techniques and several molecules are in clinical trials, and one has already been approved by the FDA to prevent blood coagulation in acquired thrombotic thrombocytopenic purpura (reviewed in Jovčevska and Muyldermans 2020). The only drawback of nanobodies compared to traditional antibodies is their short half-life in the circulation due to their small size, which can be modified by adding an extra domain or conjugate to increase the molecular size of the complex and change the molecular properties (Harmsen et al., 2005; Vugmeyster et al., 2012; Xenaki et al., 2021).

Various techniques can be used to attach molecules to nanobodies via chemical bonding (Merkul et al., 2019; Panikar et al., 2021), which enables the utilization of nanobodies as carriers to transport molecules to a specific location. Important questions are how many pieces of cargo can be attached, what is the choice of method and most importantly, how the conjugation changes the functionality of the nanobody and is the cargo needed to detach from the nanobody in the destination. Here we were able to successfully conjugate Alexa488-fluorophore to the sybody by NHS-linkage but in theory this conjugated molecule could have been a therapeutic molecule. Targeting therapeutic molecules to a specific location makes the therapy possible more effective and reduces the side effects (Bathula et al., 2021).

In this thesis, GroEL1- and GroEL2 were selected as a sybody targets as they were found to be present in the *M. marinum* biofilm with high intensity in a proteomic analysis. GroEL1 and 2 are mycobacterial protein chaperons, and especially GroEL1 has been connected to mycolate-synthesis and biofilm formation (Ojha et al. 2005). It was shown here with confocal imaging that the anti-GroEL1 and 2 sybodies target mycobacterial biofilm ECM *in vitro* and in *ex vivo* zebrafish granulomas.

In vitro, both *M. marinum* and *M. tuberculosis* biofilms were tested for their sybody binding properties. *M. tuberculosis* strain H37Ra is an avirulent counterpart of the commonly used virulent H37Rv strain. However, it has been reported that the morphology of the colonies differs between these two strains and that the avirulent strain does not form cords similarly to the virulent strain (Middlebrook et al., 1947). The same was seen in the results of this thesis. Both mycobacteria formed biofilms but the organization of the structures were somewhat different, *M. marinum* having longer cords with clearer orientation of the bacteria within the ECM. It is likely that loosing virulence has also altered the formation of the biofilm. Afterall, mycobacteria in biofilm have been shown to be more virulent than cells that have a deficiency in producing biofilm (Arias et al., 2020; Chakraborty et al., 2021).

The granuloma is a structure of mycobacteria surrounded by host's immune cells and fibroblasts that form a tight capsule around the bacterial core. This capsule is rather impermeable and while protecting the bacteria from disseminating it also possess a real challenge when targeting treatments against the bacteria inside the capsule. In the zebrafish *ex vivo* granuloma samples, the fluorescent-labelled sybody clearly targeted the mycobacterial ECM if the granuloma outer layer was removed prior the staining protocol (Figure 17C). This result also shows that *M. marinum* forms biofilm *in vivo*. If intact granulomas with the surrounding host cells were used, anti-GroEL1 and 2 sybodies localized in the space between the biofilm itself and the host cell layer (Figure 17 F&G). It is unclear why the biofilm staining pattern of an intact granuloma did not resemble the biofilm extracted from the granuloma. It is possible that the host cell layer around mycobacteria either prevents the free movement of the sybodies or generates technical issues in the confocal imaging.

To get a stronger binding of the sybody, a more extensive sybody screening could have been done. However, even a highly specific anti-biofilm sybody might struggle in spreading throughout the granuloma. Sybody is a relatively small protein (only 15 kDa) and in this experiment relies on the diffusion which could be only enhanced by fine-tuning incubation time and conditions in the protocol. In a *in vivo* situation, the transportation into the granuloma is not solely dependent on diffusion but factors like granuloma vasculature can contribute the permeability.

The bacterial population inside the granuloma biofilm is likely to include persisters that are not genetically resistant to antimicrobials but are killed slower due to their phenotypic tolerance. Slower killing rate can lead to emerging genetically resistant bacteria by enabling enrichment of spontaneous genetic mutations in the bacterial population. It is also possible to transmit the bacteria if the antimicrobial treatment is ineffective in eliminating the infection, which further increases their clinical relevance. These subpopulations greatly influence the effectiveness of the therapy and new approaches specifically targeting these subpopulations and/or concentrating the drug to the right place could enhance the treatment outcome. Nanobodies are a promising technique that can be designed to target mycobacteria in biofilms and help to transport therapeutic molecules to a specific location.

5.3.4 Limitations of the study

Choosing model organisms and techniques to model any biological phenomenon is always a challenge. Like in the case of infectious diseases, it is often hard to find and use human samples in research, which makes utilizing model organisms the only option to study the complicated network between the host and the microbe. However, using model organisms that are also laboratory strains always comes with a price of inaccuracy.

In this thesis, in addition to possible technical issues that have been considered throughout the discussion section, the limitations of *M. marinum* -infected zebrafish is important to keep in mind. Although *M. marinum*–zebrafish pair is a natural host–pathogen pair and pathological mechanisms in fish tuberculosis resemble the mechanisms seen in human, it might still be far away from the human setting. All the differences between the human and fish immune responses that has been introduced in the literature review section 2.5.3 are very relevant when interpreting the results of this thesis. Zebrafish is a useful model for basic research, and it has given valuable insights to tuberculosis pathogenesis but if aiming for human therapeutics, mammalian models must be used to verify the results.

A similar modelling issue applies for *M. marinum* and for avirulent *M. tuberculosis* as they both differ from virulent human *M. tuberculosis*. *In vitro* microbiological studies, where the microbe can often freely grow in a rich culture media with a fixed atmosphere without attacking immune cells and molecules, can end up with a different outcome than in an *in vivo* situation. For biofilm studies, limited oxygen and carbon sources were used, but it is still not like the biological environment.

Modelling biological systems and environments always requires compromises and it sometimes might be a delicate balance to optimize the experimental settings to have the best possible fit.

5.3.5 Future prospects

This thesis concentrated on how to overcome mycobacterial evasion mechanisms to improve treatment outcomes or even prevent the infection. The next steps for this study would be to better dissect the component(s) that produced the protective responses against mycobacterial infection and can this protective effect be seen in mammalian models as well. Also, in the future it remains to be seen whether the protective immune response can be induced by adaptive immune responses or is trained immunity the best and/or only option.

In the microbiological point of view, the obvious question remains what the exact composition of the mycobacterial extracellular matrix (ECM) is. It is crucial to find ways to ensure that the antimicrobial really finds the mycobacterial biofilm population within granulomas through the ECM and does it quickly. This could significantly enhance the future treatments. It is important to recognize that the course of many bacterial diseases is probably influenced by the ECM or even biofilm formation.

The tuberculosis research is far from done. The limitations of the current treatments and vaccines to end the tuberculosis pandemic is evident and there is a lot to do before this situation changes. If new affordable treatments and diagnostic tools would be available, the incidence numbers would quickly go down. A new effective treatment has been estimated to reduce yearly TB-deaths by 34,000 after six years, new diagnostic method by 52,000 and these two together would save 100,000 lives each year (O'Neill, 2016). Also, it has been estimated that even a vaccine, that gives only 60% protection against active TB, could have a major effect. 60% protection rate is rather poor for a vaccine but if this vaccine is given to only 20% of the adults in risk of having TB, it would reduce the incidence rate by 40% (Knight et al., 2014). This all sounds achievable but has shown to be very difficult especially when the people most badly needing these improvements are in developing countries.

6 SUMMARY AND CONCLUSION

TB remains a significant cause of mortality worldwide and especially developing countries struggle to control the disease. Even though, only 5-10% of the individuals exposed to Mtb get active infection (Comstock et al., 1974), in certain areas of South-Africa, a fifth of the tested children under the year of five had latent TB even without a household contact with active TB, which indicates a high number of untreated and/or undiagnosed TB cases in the society (MacPherson et al., 2020). The same study showed the deadliness of the active TB, especially among young adults as the proportion of latently infected individuals decreased in older age groups (MacPherson et al., 2020). The key to the success of mycobacterium is its ability to professionally evade immune responses. As a result, mycobacteria are sealed in granulomas rather than eradicated by the immune system. The dynamic interaction of the host and the bacteria often leads into this chronic latent disease, which serves as a reservoir for new active TB cases.

In this thesis, heat-killed *L. monocytogenes* (HKLm) was found to be an effective immunomodulator to block or slow *M. marinum* infection in adult zebrafish. HKLm had the greatest effect when it was injected one day prior to the infection. The adult zebrafish population is heterogenous, showing highly similar proportions of active, latent, reactivated and cleared mycobacterial infections as in the human population. HKLm priming was able to increase the percentage of the cleared infection from 10% to 25% and to significantly reduce *M. marinum* loads in the remaining population. The clearance was mediated by innate immune responses, and it was characterized by reduced expression of s*od2* and increased expression of *tnf, nos2b* and *mpeg1*, which indicated that the immune responses responsible for the protective response is due to activated pro-inflammatory macrophages in the early infection.

Interestingly, HKLm did not induce clearance if it was given after the infection. An on-going established mycobacterial infection has already profound immune evasion mechanisms that are tricky to overcome with immune activation. A prophylactic treatment could be, however, used against TB in high endemic areas where daily physical protection is not feasible and having TB carries a stigma.

It is an important question, why boosting immune responses after the infection did not help the immune system to tackle the infection. Strong local

immunosuppression induced by the mycobacteria is one plausible factor to explain the poor performance of the host's immune responses but bacterial extracellular communities in granulomas is another factor. Mycobacterium is capable of producing biofilms in granulomas (Chakraborty et al., 2021) that protect against physical and chemical stress, hampering the effectiveness of both antimicrobials and immune responses.

The biofilm maturation of *M. marinum* did not increase MIC (minimum inhibitory concentration) but affected MBC (minimum bactericidal concentration) indicating an enhanced phenotypic tolerance of the biofilm. It was also possible to reduce the number of live bacteria by treating *M. marinum* biofilm with enzymes degrading the extracellular matrix together with an antimicrobial. *M. marinum* in a biofilm is metabolically active but there is a subpopulation of phenotypically tolerant bacteria, persisters, that can survive in the presence of antimicrobial for a prolonged time. Time-kill curve analysis of *M. marinum* biofilms was used to study persisters. The analysis showed that *M. marinum* biofilm is significantly more tolerant compared to planktonic mycobacteria at one week. *M. marinum* naturally produces two biofilm subtypes in a liquid culture: pellicle and submerged biofilms. However, there was no difference in the antimicrobial susceptibility between these biofilm types.

Finally, sybodies against mycobacterial GroEL1 and GroEL2 in the biofilm extracellular matrix were tested as an approach to specifically target mycobacterial biofilms. This kind of approach could be utilized to carry concentrated amounts of small molecules inside granulomas. The biofilm lifestyle of mycobacteria increases the tolerance against antimicrobials making biofilms clinically highly relevant. Anti-GroEL sybodies were able to bind *M. marinum* and Mtb in *in vitro* biofilms and the biofilms found inside *ex vivo* zebrafish granulomas. The role of persisters in biofilms and the protective ECM structures in infections should be considered when designing new drugs against Mtb.

The mycobacterial evasion mechanisms are well evolved. Some mechanisms could be avoided by right-timed immune activation and some by biofilm-targeted therapies, but the approach has to be chosen depending on the infection state. It has become clear that the heterogenous nature of TB requires heterogenous set of interventions whether those are immunological or pharmacological. The results presented in the thesis open avenues for development of therapeutic interventions to prevent TB.

7 REFERENCES

Aaby, P., Roth, A., Ravn, H., Napirna, B. M., Rodrigues, A., Lisse, I. M., Stensballe, L., Diness, B. R., Lausch, K. R., Lund, N., Biering-Sørensen, S., Whittle, H., & Benn, C. S. (2011). Randomized Trial of BCG Vaccination at Birth to Low-Birth-Weight Children: Beneficial Nonspecific Effects in the Neonatal Period? *The Journal of Infectious Diseases*, *204*(2), 245–252. https://doi.org/10.1093/infdis/jir240

Abdalla, A. E., Lambert, N., Duan, X., & Xie, J. (2016). Interleukin-10 Family and Tuberculosis: An Old Story Renewed. *International Journal of Biological Sciences*, *12*(6), 710–717. https://doi.org/10.7150/ijbs.13881

Abebe, F. (2019). Synergy between Th1 and Th2 responses during Mycobacterium tuberculosis infection: A review of current understanding. *International Reviews of Immunology*, *38*(4), 172–179. https://doi.org/10.1080/08830185.2019.1632842

Abebe, F., Belay, M., Legesse, M., Mihret, A., & Franken, K. S. (2017). Association of ESAT-6/CFP-10-induced IFN-γ, TNF-α and IL-10 with clinical tuberculosis: evidence from cohorts of pulmonary tuberculosis patients, household contacts and community controls in an endemic setting. *Clinical & Experimental Immunology*, *189*(2), 241–249. https://doi.org/10.1111/cei.12972

Abel, L., Fellay, J., Haas, D. W., Schurr, E., Srikrishna, G., Urbanowski, M., Chaturvedi, N., Srinivasan, S., Johnson, D. H., & Bishai, W. R. (2018). Genetics of human susceptibility to active and latent tuberculosis: present knowledge and future perspectives. *Lancet Infectious Diseases*, *18*(3), E64–E75. https://doi.org/10.1016/S1473-3099(17)30623-0

Ackart, D. F., Hascall-Dove, L., Caceres, S. M., Kirk, N. M., Podell, B. K., Melander, C., Orme, I. M., Leid, J. G., Nick, J. A., & Basaraba, R. J. (2014). Expression of antimicrobial drug tolerance by attached communities of Mycobacterium tuberculosis. *Pathogens and Disease*, *70*(3), 359–369. https://doi.org/10.1111/2049-632X.12144

Adams, K. N., Takaki, K., Connolly, L. E., Wiedenhoft, H., Winglee, K., Humbert, O., Edelstein, P. H., Cosma, C. L., & Ramakrishnan, L. (2011). Drug Tolerance in Replicating Mycobacteria Mediated by a Macrophage-Induced Efflux Mechanism. *Cell (Cambridge)*, *145*(1), 39–53. https://doi.org/10.1016/j.cell.2011.02.022

Alcaïs, A., Fieschi, C., Abel, L., & Casanova, J.-L. (2005). Tuberculosis in children and adults: two distinct genetic diseases. *The Journal of Experimental Medicine*, *202*(12), 1617–1621. https://doi.org/10.1084/jem.20052302

Andreu, N., Zelmer, A., Fletcher, T., Elkington, P. T., Ward, T. H., Ripoll, J., Parish, T., Bancroft, G. J., Schaible, U., Robertson, B. D., & Wiles, S. (2010). Optimisation of Bioluminescent Reporters for Use with Mycobacteria. *Plos One*, *5*(5).

Andrews, J. R., Noubary, F., Walensky, R. P., Cerda, R., Losina, E., & Horsburgh, C. R. (2012). Risk of Progression to Active Tuberculosis Following Reinfection With Mycobacterium tuberculosis. *Clinical Infectious Diseases*, *54*(6), 784–791. https://doi.org/10.1093/cid/cir951

Angelidou, A., Diray-Arce, J., Conti, M. G., Smolen, K. K., van Haren, S. D., Dowling, D. J., Husson, R. N., & Levy, O. (2020). BCG as a Case Study for Precision Vaccine Development: Lessons From Vaccine Heterogeneity, Trained Immunity, and Immune Ontogeny. *Frontiers in Microbiology*, *11*, 332. https://doi.org/10.3389/fmicb.2020.00332

Ardain, A., Domingo-Gonzalez, R., Das, S., Kazer, S. W., Howard, N. C., Singh, A., Ahmed, M., Nhamoyebonde, S., Rangel-Moreno, J., Ogongo, P., Lu, L., Ramsuran, D., de la Luz Garcia-Hernandez, M., K Ulland, T., Darby, M., Park, E., Karim, F., Melocchi, L., Madansein, R., … Khader, S. A. (2019). Group 3 innate lymphoid cells mediate early protective immunity against tuberculosis. *Nature*, *570*(7762), 528–532. https://doi.org/10.1038/s41586-019-1276-2

Arias, L., Cardona, P., Català, M., Campo-Pérez, V., Prats, C., Vilaplana, C., Julián, E., & Cardona, P.-J. (2020). Cording Mycobacterium tuberculosis Bacilli Have a Key Role in the Progression towards Active Tuberculosis, Which is Stopped by Previous Immune Response. *Microorganisms*, *8*(2), 228. https://doi.org/10.3390/microorganisms8020228

Aspatwar, A., Hammarén, M., Koskinen, S., Luukinen, B., Barker, H., Carta, F., Supuran, C. T., Parikka, M., & Parkkila, S. (2017). β-CA-specific inhibitor dithiocarbamate Fc14–584B: a novel antimycobacterial agent with potential to treat drug-resistant tuberculosis. *Journal of Enzyme Inhibition and Medicinal Chemistry*, *32*(1), 832–840. https://doi.org/10.1080/14756366.2017.1332056

Augenstreich, J., Arbues, A., Simeone, R., Haanappel, E., Wegener, A., Sayes, F., le Chevalier, F., Chalut, C., Malaga, W., Guilhot, C., Brosch, R., & Astarie-Dequeker, C. (2017). ESX-1 and phthiocerol dimycocerosates of Mycobacterium tuberculosis act in concert to cause phagosomal rupture and host cell apoptosis. *Cellular Microbiology*, *19*(7), e12726-n/a. https://doi.org/10.1111/cmi.12726

Augenstreich, J., & Briken, V. (2020). Host Cell Targets of Released Lipid and Secreted Protein Effectors of Mycobacterium tuberculosis. *Frontiers in Cellular and Infection Microbiology*, *10*. https://doi.org/10.3389/fcimb.2020.595029

Badger, T. L., & Spink, W. W. (1937). First-Infection Type of Tuberculosis in Adults. *The New England Journal of Medicine*, *217*(11), 424–431. https://doi.org/10.1056/NEJM193709092171102

Balik-Meisner, M., Truong, L., Scholl, E., Tanguay, R., & Reif, D. (2018). Population genetic diversity in zebrafish lines. *Mammalian Genome*, *29*(1), 90–100. https://doi.org/10.1007/s00335-018-9735-x

Balla, K. M., Lugo-Villarino, G., Spitsbergen, J. M., Stachura, D. L., Hu, Y., Bañuelos, K., Romo-Fewell, O., Aroian, R. v, & Traver, D. (2010). Eosinophils in the zebrafish: prospective isolation, characterization, and eosinophilia induction by helminth determinants. *Blood*, *116*(19), 3944–3954. https://doi.org/10.1182/blood-2010-03-267419

Barberis, I., Bragazzi, N. L., Galluzzo, L., & Martini, M. (2017). The history of tuberculosis: from the first historical records to the isolation of Koch's bacillus. *Journal of Preventive Medicine and Hygiene*, *58*(1), E9–E12. https://doi.org/10.15167/2421-4248/jpmh2017.58.1.728

Basaraba, R. J., & Hunter, R. L. (2017). Pathology of Tuberculosis: How the Pathology of Human Tuberculosis Informs and Directs Animal Models. *Microbiology Spectrum*, *5*(3). https://doi.org/10.1128/microbiolspec.TBTB2-0029-2016

Bathula, N. v., Bommadevara, H., & Hayes, J. M. (2021). Nanobodies: The Future of Antibody-Based Immune Therapeutics. *Cancer Biotherapy and Radiopharmaceuticals*, *36*(2), 109–122. https://doi.org/10.1089/cbr.2020.3941

Batt, S. M., Minnikin, D. E., & Besra, G. S. (2020). The thick waxy coat of mycobacteria, a protective layer against antibiotics and the host's immune system. *Biochemical Journal*, *477*(10), 1983–2006. https://doi.org/10.1042/BCJ20200194

Belay, M., Legesse, M., Mihret, A., Bekele, Y., Ottenhoff, T. H. M., Franken, K. L. M. C., Bjune, G., & Abebe, F. (2015). Pro- and Anti-Inflammatory Cytokines against Rv2031 Are Elevated during Latent Tuberculosis: A Study in Cohorts of Tuberculosis Patients, Household Contacts and Community Controls in an Endemic Setting. *PloS One*, *10*(4), e0124134. https://doi.org/10.1371/journal.pone.0124134

Belay, M., Legesse, M., Mihret, A., Ottenhoff, T. H. M., Franken, K. L., Bjune, G., & Abebe, F. (2015). IFN- γ and IgA against non-methylated heparin-binding hemagglutinin as markers of protective immunity and latent tuberculosis: Results

of a longitudinal study from an endemic setting. *Journal of Infection*, *72*(2), 189–200. https://doi.org/10.1016/j.jinf.2015.09.040

Bhavanam, S., Rayat, G. R., Keelan, M., Kunimoto, D., & Drews, S. J. (2016). Understanding the pathophysiology of the human TB lung granuloma using in vitro granuloma models. *Future Microbiology*, *11*(8), 1073–1089. https://doi.org/10.2217/fmb-2016-0005

Biraro, I. A., Kimuda, S., Egesa, M., Cose, S., Webb, E. L., Joloba, M., Smith, S. G., Elliott, A. M., Dockrell, H. M., & Katamba, A. (2016). The Use of Interferon Gamma Inducible Protein 10 as a Potential Biomarker in the Diagnosis of Latent Tuberculosis Infection in Uganda. *PloS One*, *11*(1), e0146098. https://doi.org/10.1371/journal.pone.0146098

Bisht, K., & Wakeman, C. A. (2019). Discovery and Therapeutic Targeting of Differentiated Biofilm Subpopulations. *Frontiers in Microbiology*, *10*. https://doi.org/10.3389/fmicb.2019.01908

Bligh, E. G., & Dyer, W. J. (1959). A rapid method of total lipid extraction and purification. *Canadian Journal of Biochemistry and Physiology*, *37*(8), 911. https://www.ncbi.nlm.nih.gov/pubmed/13671378

Bozzano, F., Costa, P., Passalacqua, G., Dodi, F., Ravera, S., Pagano, G., Canonica, G. W., Moretta, L., & de Maria, A. (2009). Functionally relevant decreases in activatory receptor expression on NK cells are associated with pulmonary tuberculosis in vivo and persist after successful treatment. *International Immunology*, *21*(7), 779–791. https://doi.org/10.1093/intimm/dxp046

Brauner, A., Fridman, O., Gefen, O., & Balaban, N. Q. (2016). Distinguishing between resistance, tolerance and persistence to antibiotic treatment. *Nature Reviews. Microbiology*, *14*(5), 320–330. https://doi.org/10.1038/nrmicro.2016.34

Brauner, A., Shoresh, N., Fridman, O., & Balaban, N. Q. (2017). An Experimental Framework for Quantifying Bacterial Tolerance. *Biophysical Journal*, *112*(12), 2664–2671. https://doi.org/10.1016/j.bpj.2017.05.014

Brennan, P. J., & Nikaido, H. (1995). The Envelope of Mycobacteria. *Annual Review of Biochemistry*, *64*(1), 29–63. https://doi.org/10.1146/annurev.bi.64.070195.000333

Brown, K. H., Dobrinski, K. P., Lee, A. S., Gokcumen, O., Mills, R. E., Shi, X., Chong, W. W. S., Chen, J. Y. H., Yoo, P., David, S., Peterson, S. M., Raj, T., Choy, K. W., Stranger, B. E., Williamson, R. E., Zon, L. I., Freeman, J. L., & Lee, C. (2012). Extensive genetic diversity and substructuring among zebrafish strains revealed through copy number variant analysis. *Proceedings of the National Academy of Sciences*

of the United States of America, *109*(2), 529–534. https://doi.org/10.1073/pnas.1112163109

Bryson, D., Hettle, A. G., Boraston, A. B., & Hobbs, J. K. (2020). Clinical Mutations That Partially Activate the Stringent Response Confer Multidrug Tolerance in Staphylococcus aureus. *Antimicrobial Agents and Chemotherapy*, *64*(3). https://doi.org/10.1128/AAC.02103-19

Cadena, A. M., Fortune, S. M., & Flynn, J. L. (2017). Heterogeneity in tuberculosis. *Nature Reviews Immunology*, *17*(11), 691–702. https://doi.org/10.1038/nri.2017.69

Cadena, A. M., Hopkins, F. F., Maiello, P., Carey, A. F., Wong, E. A., Martin, C. J., Gideon, H. P., DiFazio, R. M., Andersen, P., Lin, P. L., Fortune, S. M., & Flynn, J. L. (2018). Concurrent infection with Mycobacterium tuberculosis confers robust protection against secondary infection in macaques. *PLoS Pathogens*, *14*(10), e1007305. https://doi.org/10.1371/journal.ppat.1007305

Cambier, C. J., Takaki, K. K., Larson, R. P., Hernandez, R. E., Tobin, D. M., Urdahl, K. B., Cosma, C. L., & Ramakrishnan, L. (2014). Mycobacteria manipulate macrophage recruitment through coordinated use of membrane lipids. *Nature*, *505*(7482), 218-+. https://doi.org/10.1038/nature12799

Carneiro, P. A. M., Takatani, H., Pasquatti, T. N., Silva, C. B. D. G., Norby, B., Wilkins, M. J., Zumárraga, M. J., Araujo, F. R., & Kaneene, J. B. (2019). Epidemiological Study of Mycobacterium bovis Infection in Buffalo and Cattle in Amazonas, Brazil. *Frontiers in Veterinary Science*, *6*, 434. https://doi.org/10.3389/fvets.2019.00434

Cave, A. J. E., & Demonstrator, A. (1939). The evidence for the incidence of tuberculosis in ancient Egypt. *The British Journal of Tuberculosis*, *33*(3), 142–152. https://doi.org/10.1016/S0366-0850(39)80016-3

Centers for Disease Control and Prevention, (CDC). (2016). *Tuberculosis*. https://www.cdc.gov/tb/default.htm

Chakraborty, P., Bajeli, S., Kaushal, D., Radotra, B. D., & Kumar, A. (2021). Biofilm formation in the lung contributes to virulence and drug tolerance of Mycobacterium tuberculosis. *Nature Communications*, *12*(1), 1606. https://doi.org/10.1038/s41467-021-21748-6

Chakraborty, P., & Kumar, A. (2019). The extracellular matrix of mycobacterial biofilms: could we shorten the treatment of mycobacterial infections? *Microbial Cell*, *6*(2), 105–122. https://doi.org/10.15698/mic2019.02.667

Chávez-Galán, L., Olleros, M. L., Vesin, D., & Garcia, I. (2015). Much More than M1 and M2 Macrophages, There are also CD169+ and TCR+ Macrophages. *Frontiers in Immunology*, *6*(263), 263. https://doi.org/10.3389/fimmu.2015.00263

Chen, Y.-C., Chang, Y.-P., Hsiao, C.-C., Wu, C.-C., Wang, Y.-H., Chao, T.-Y., Leung, S.-Y., Fang, W.-F., Lee, C.-P., Wang, T.-Y., Hsu, P.-Y., & Lin, M.-C. (2020). Blood M2a monocyte polarization and increased formyl peptide receptor 1 expression are associated with progression from latent tuberculosis infection to active pulmonary tuberculosis disease. *International Journal of Infectious Diseases*, *101*, 210–219. https://doi.org/10.1016/j.ijid.2020.09.1056

Cheng, S.-C., Quintin, J., Cramer, R. A., Shepardson, K. M., Saeed, S., Kumar, V., Giamarellos-Bourboulis, E. J., Martens, J. H. A., Rao, N. A., Aghajanirefah, A., Manjeri, G. R., Li, Y., Ifrim, D. C., Arts, R. J. W., van der Meer, B. M. J. W., Deen, P. M. T., Logie, C., O'Neill, L. A., Willems, P., … Netea, M. G. (2014). mTOR- and HIF-1α–mediated aerobic glycolysis as metabolic basis for trained immunity. *Science (American Association for the Advancement of Science)*, *345*(6204), 1579. https://doi.org/10.1126/science.1250684

Choreño-Parra, J. A., Weinstein, L. I., Yunis, E. J., Zúñiga, J., & Hernández-Pando, R. (2020). Thinking Outside the Box: Innate- and B Cell-Memory Responses as Novel Protective Mechanisms Against Tuberculosis. *Frontiers in Immunology*, *11*, 226. https://doi.org/10.3389/fimmu.2020.00226

Clay, H., Davis, J. M., Beery, D., Huttenlocher, A., Lyons, S. E., & Ramakrishnan, L. (2007). Dichotomous Role of the Macrophage in Early Mycobacterium marinum Infection of the Zebrafish. *Cell Host & Microbe*, *2*(1), 29–39. https://doi.org/10.1016/j.chom.2007.06.004

Comstock, G. W., Livesay, V. T., & Woolpert, S. F. (1974). The Prognosis of a Positive Tuberculin Reaction in Childhood and Adolescence. *American Journal of Epidemiology*, *99*(2), 131. https://search.proquest.com/docview/1306652617

Conrad, W. H., Osman, M. M., Shanahan, J. K., Chu, F., Takaki, K. K., Cameron, J., Hopkinson-Woolley, D., Brosch, R., & Ramakrishnan, L. (2017). Mycobacterial ESX-1 secretion system mediates host cell lysis through bacterium contact-dependent gross membrane disruptions. *Proceedings of the National Academy of Sciences of the United States of America*, *114*(6), 1371–1376. https://doi.org/10.1073/pnas.1620133114

Cooper, A. M. (2015). Mouse Model of Tuberculosis. *Cold Spring Harb Perspect Med*, *5*(2). 10.1101/cshperspect.a018556

Cooper, A. M., Dalton, D. K., Stewart, T. A., Griffin, J. P., Russell, D. G., & Orme, I. M. (1993). Disseminated tuberculosis in interferon γ gene-disrupted mice. *The Journal of Experimental Medicine*, *178*(6), 2243–2247. https://doi.org/10.1084/jem.178.6.2243

Corleis, B., Korbel, D., Wilson, R., Bylund, J., Chee, R., & Schaible, U. E. (2012). Escape of Mycobacterium tuberculosis from oxidative killing by neutrophils. *Cellular Microbiology*, *14*(7), 1109–1121. https://doi.org/10.1111/j.1462-5822.2012.01783.x

Corral, D., Charton, A., Krauss, M. Z., Blanquart, E., Levillain, F., Lefrançais, E., Sneperger, T., Vahlas, Z., Girard, J.-P., Eberl, G., Poquet, Y., Guéry, J.-C., Argüello, R. J., Belkaid, Y., Mayer-Barber, K. D., Hepworth, M. R., Neyrolles, O., & Hudrisier, D. (2022). ILC precursors differentiate into metabolically distinct ILC1-like cells during Mycobacterium tuberculosis infection. *Cell Reports*, *39*(3), 110715. https://doi.org/10.1016/j.celrep.2022.110715

Cronan, M. R., Beerman, R. W., Rosenberg, A. F., Saelens, J. W., Johnson, M. G., Oehlers, S. H., Sisk, D. M., Smith, K. L. J., Medvitz, N. A., Miller, S. E., Trinh, L. A., Fraser, S. E., Madden, J. F., Turner, J., Stout, J. E., Lee, S., & Tobin, D. M. (2016). Macrophage Epithelial Reprogramming Underlies Mycobacterial Granuloma Formation and Promotes Infection. *Immunity*, *45*(4), 861–876. https://doi.org/10.1016/j.immuni.2016.09.014

Cronan, M. R., Matty, M. A., Rosenberg, A. F., Blanc, L., Pyle, C. J., Espenschied, S. T., Rawls, J. F., Dartois, V., & Tobin, D. M. (2018). An explant technique for high-resolution imaging and manipulation of mycobacterial granulomas. *Nature Methods*, *15*(12), 1098–1107. https://doi.org/10.1038/s41592-018-0215-8

Cyktor, J. C., Carruthers, B., Kominsky, R. A., Beamer, G. L., Stromberg, P., & Turner, J. (2013). IL-10 Inhibits Mature Fibrotic Granuloma Formation during Mycobacterium tuberculosis Infection. *Journal of Immunology (Baltimore, Md. : 1950)*, *190*(6), 2778–2790. https://doi.org/10.4049/jimmunol.1202722

Daffé, M., & Marrakchi, H. (2019). Unraveling the Structure of the Mycobacterial Envelope. *Microbiology Spectrum*, *7*(4). https://doi.org/10.1128/microbiolspec.GPP3-0027-2018

Darrah, P. A., Zeppa, J. J., Maiello, P., Hackney, J. A., Wadsworth Marc H, 2nd, Hughes, T. K., Pokkali, S., Swanson Phillip A, 2nd, Grant, N. L., Rodgers, M. A., Kamath, M., Causgrove, C. M., Laddy, D. J., Bonavia, A., Casimiro, D., Lin, P. L., Klein, E., White, A. G., Scanga, C. A., … Seder, R. A. (2020). Prevention of tuberculosis in macaques after intravenous BCG immunization. *Nature*, *577*(7788), 95–102. https://doi.org/10.1038/s41586-019-1817-8

Davis, J. M., Clay, H., Lewis, J. L., Ghori, N., Herbomel, P., & Ramakrishnan, L. (2002). Real-Time Visualization of Mycobacterium-Macrophage Interactions Leading to Initiation of Granuloma Formation in Zebrafish Embryos. *Immunity (Cambridge, Mass.)*, *17*(6), 693–702. https://doi.org/10.1016/s1074-7613(02)00475-2

Davis, J. M., & Ramakrishnan, L. (2009). The Role of the Granuloma in Expansion and Dissemination of Early Tuberculous Infection. *Cell*, *136*(1), 37–49. https://doi.org/10.1016/j.cell.2008.11.014

de Martino, M., Lodi, L., Galli, L., & Chiappini, E. (2019). Immune Response to Mycobacterium tuberculosis: A Narrative Review. *Frontiers in Pediatrics*, *7*. https://doi.org/10.3389/fped.2019.00350

Defraine, V., Fauvart, M., & Michiels, J. (2018). Fighting bacterial persistence: Current and emerging anti-persister strategies and therapeutics. *Drug Resistance Updates*, *38*, 12–26. https://doi.org/10.1016/j.drup.2018.03.002

Dhar, N., & Manina, G. (2015). Single-cell analysis of mycobacteria using microfluidics and time-lapse microscopy. *Methods in Molecular Biology (Clifton, N.J.)*, *1285*, 241–256. https://doi.org/10.1007/978-1-4939-2450-9_14

Dhar, N., McKinney, J., & Manina, G. (2016). Phenotypic Heterogeneity in Mycobacterium tuberculosis. *Microbiology Spectrum*, *4*(6). https://doi.org/10.1128/microbiolspec.TBTB2-0021-2016

Dhiman, R., Indramohan, M., Barnes, P. F., Nayak, R. C., Paidipally, P., Rao, L. V. M., & Vankayalapati, R. (2009). IL-22 Produced by Human NK Cells Inhibits Growth of Mycobacterium tuberculosis by Enhancing Phagolysosomal Fusion. *The Journal of Immunology*, *183*(10), 6639–6645. https://doi.org/10.4049/jimmunol.0902587

Dionne, M. S., Ghori, N., & Schneider, D. S. (2003). Drosophila melanogaster Is a Genetically Tractable Model Host for Mycobacterium marinum. *Infection and Immunity*, *71*(6), 3540–3550. https://doi.org/10.1128/iai.71.6.3540-3550.2003

Dionne, M. S., Pham, L. N., Shirasu-Hiza, M., & Schneider, D. S. (2006). Akt and foxo Dysregulation Contribute to Infection-Induced Wasting in Drosophila. *Current Biology*, *16*(20), 1977–1985. https://doi.org/10.1016/j.cub.2006.08.052

Dobos, K. M., Spotts, E. A., Quinn, F. D., & King, C. H. (2000). Necrosis of lung epithelial cells during infection with Mycobacterium tuberculosis is preceded by cell permeation. *Infection and Immunity*, *68*(11), 6300–6310. https://www.ncbi.nlm.nih.gov/pubmed/11035739

Dobson, J. T., Seibert, J., Teh, E. M., Da'as, S., Fraser, R. B., Paw, B. H., Lin, T.-J., & Berman, J. N. (2008). Carboxypeptidase A5 identifies a novel mast cell lineage in the zebrafish providing new insight into mast cell fate determination. *Blood*, *112*(7), 2969–2972. https://doi.org/10.1182/blood-2008-03-145011

Doherty, T. M., Demissie, A., Olobo, J., Wolday, D., Britton, S., Eguale, T., Ravn, P., & Andersen, P. (2002). Immune Responses to the Mycobacterium tuberculosis-Specific Antigen ESAT-6 Signal Subclinical Infection among Contacts of

Tuberculosis Patients. *Journal of Clinical Microbiology*, *40*(2), 704–706. https://doi.org/10.1128/JCM.40.2.704-706.2002

Drain, P. K., Bajema, K. L., Dowdy, D., Dheda, K., Naidoo, K., Schumacher, S. G., Ma, S., Meermeier, E., Lewinsohn, D. M., & Sherman, D. R. (2018). Incipient and Subclinical Tuberculosis: a Clinical Review of Early Stages and Progression of Infection. *Clinical Microbiology Reviews*, *31*(4), 21. https://doi.org/10.1128/CMR.00021-18

Esin, S., Counoupas, C., Aulicino, A., Brancatisano, F. L., Maisetta, G., Bottai, D., Luca, M., Florio, W., Campa, M., & Batoni, G. (2013). Interaction of Mycobacterium tuberculosis Cell Wall Components with the Human Natural Killer Cell Receptors NKp44 and Toll-Like Receptor 2. *Scandinavian Journal of Immunology*, *77*(6), 460–469. https://doi.org/10.1111/sji.12052

Etna, M. P., Giacomini, E., Pardini, M., Severa, M., Bottai, D., Cruciani, M., Rizzo, F., Calogero, R., Brosch, R., & Coccia, E. M. (2015). Impact of Mycobacterium tuberculosis RD1-locus on human primary dendritic cell immune functions. *Scientific Reports*, *5*(1), 17078. https://doi.org/10.1038/srep17078

Eum, S.-Y., Kong, J.-H., Hong, M.-S., Lee, Y.-J., Kim, J.-H., Hwang, S.-H., Cho, S.-N., Via, L. E., & I, C. E. B. I. I. (2010). Neutrophils Are the Predominant Infected Phagocytic Cells in the Airways of Patients With Active Pulmonary TB. *Chest*, *137*(1), 122–128. https://doi.org/10.1378/chest.09-0903

Fehrenbach, H. (2001). Alveolar epithelial type II cell: defender of the alveolus revisited. *Respiratory Research*, *2*(1), 33–46. https://doi.org/10.1186/rr36

Flynn, J. L., Chan, J., Triebold, K. J., Dalton, D. K., Stewart, T. A., & Bloom, B. R. (1993). An essential role for interferon γ in resistance to Mycobacterium tuberculosis infection. *The Journal of Experimental Medicine*, *178*(6), 2249–2254. https://doi.org/10.1084/jem.178.6.2249

Fremond, C. M., Togbe, D., Doz, E., Rose, S., Vasseur, V., Maillet, I., Jacobs, M., Ryffel, B., & Quesniaux, V. F. J. (2007). IL-1 Receptor-Mediated Signal Is an Essential Component of MyD88-Dependent Innate Response to Mycobacterium tuberculosis Infection. *The Journal of Immunology*, *179*(2), 1178–1189. https://doi.org/10.4049/jimmunol.179.2.1178

Frothingham, R., Hills, H. G., & Wilson, K. H. (1994). Extensive DNA sequence conservation throughout the Mycobacterium tuberculosis complex. *Journal of Clinical Microbiology*, *32*(7), 1639–1643. https://doi.org/10.1128/JCM.32.7.1639-1643.1994

Furin, J., Cox, H., & Pai, M. (2019). Tuberculosis. *The Lancet*, *393*(10181), 1642. https://doi.org/10.1016/S0140-6736(19)30308-3

Gallegos, A. M., Pamer, E. G., & Glickman, M. S. (2008). Delayed protection by ESAT-6-specific effector CD4+ T cells after airborne M. tuberculosis infection. *The Journal of Experimental Medicine*, *205*(10), 2359–2368. https://doi.org/10.1084/jem.20080353

Gideon, H. P., Phuah, J., Myers, A. J., Bryson, B. D., Rodgers, M. A., Coleman, M. T., Maiello, P., Rutledge, T., Marino, S., Fortune, S. M., Kirschner, D. E., Lin, P. L., & Flynn, J. L. (2015). Variability in Tuberculosis Granuloma T Cell Responses Exists, but a Balance of Pro- and Anti-inflammatory Cytokines Is Associated with Sterilization. *PLoS Pathogens*, *11*(1), e1004603. https://doi.org/10.1371/journal.ppat.1004603

Glatman-Freedman, A., & Casadevall, A. (1998). Serum therapy for tuberculosis revisited: reappraisal of the role of antibody-mediated immunity against Mycobacterium tuberculosis. *Clinical Microbiology Reviews*, *11*(3), 514–532. https://www.ncbi.nlm.nih.gov/pubmed/9665981

Gold, B., & Nathan, C. (2017). Targeting Phenotypically Tolerant Mycobacterium tuberculosis. *Microbiology Spectrum*, *5*(1). https://doi.org/10.1128/microbiolspec.TBTB2-0031-2016

Gröschel, M. I., Sayes, F., Simeone, R., Majlessi, L., & Brosch, R. (2016). ESX secretion systems: mycobacterial evolution to counter host immunity. *Nature Reviews. Microbiology*, *14*(11), 677–691. https://doi.org/10.1038/nrmicro.2016.131

Guryev, V., Koudijs, M. J., Berezikov, E., Johnson, S. L., Plasterk, R. H. A., van Eeden, F. J. M., & Cuppen, E. (2006). Genetic variation in the zebrafish. *Genome Research*, *16*(4), 491–497. https://doi.org/10.1101/gr.4791006

Gutacker, M. M., Smoot, J. C., Migliaccio, C. A. L., Ricklefs, S. M., Hua, S., Cousins, D. v, Graviss, E. A., Shashkina, E., Kreiswirth, B. N., & Musser, J. M. (2002). Genome-Wide Analysis of Synonymous Single Nucleotide Polymorphisms in Mycobacterium tuberculosis Complex Organisms: Resolution of Genetic Relationships Among Closely Related Microbial Strains. *Genetics*, *162*(4), 1533–1543. http://www.genetics.org/cgi/content/abstract/162/4/1533

Hagedorn, M., Rohde, K. H., Russell, D. G., & Soldati, T. (2009). Infection by Tubercular Mycobacteria Is Spread by Nonlytic Ejection from Their Amoeba Hosts. *Science (American Association for the Advancement of Science)*, *323*(5922), 1729–1733. https://doi.org/10.1126/science.1169381

Hamada, A., Torre, C., Drancourt, M., & Ghigo, E. (2019). Trained Immunity Carried by Non-immune Cells. *Frontiers in Microbiology*, *9*. https://doi.org/10.3389/fmicb.2018.03225

Hamilton, P. T., Votýpka, J., Dostálová, A., Yurchenko, V., Bird, N. H., Lukeš, J., Lemaitre, B., & Perlman, S. J. (2015). Infection Dynamics and Immune Response in a Newly Described Drosophila -Trypanosomatid Association. *MBio*, *6*(5), e01356–e01315. https://doi.org/10.1128/mBio.01356-15

Hammaren, M. M., Oksanen, K. E., Nisula, H. M., Luukinen, B. V., Pesu, M., Ramet, M., & Parikka, M. (2014). Adequate Th2-Type Response Associates with Restricted Bacterial Growth in Latent Mycobacterial Infection of Zebrafish. *Plos Pathogens*, *10*(6), e1004190. https://doi.org/10.1371/journal.ppat.1004190

Harmsen, M. M., van Solt, C. B., Fijten, H. P. D., & van Setten, M. C. (2005). Prolonged in vivo residence times of llama single-domain antibody fragments in pigs by binding to porcine immunoglobulins. *Vaccine*, *23*(41), 4926–4934. https://doi.org/10.1016/j.vaccine.2005.05.017

Hava, D. L., Wel, N. van der, Cohen, N., Dascher, C. C., Houben, D., León, L., Agarwal, S., Sugita, M., Zon, M. van, Kent, S. C., Shams, H., Peters, P. J., & Brenner, M. B. (2008). Evasion of Peptide, but Not Lipid Antigen Presentation, through Pathogen-Induced Dendritic Cell Maturation. *Proceedings of the National Academy of Sciences of the United States of America*, *105*(32), 11281–11286. https://doi.org/10.1073/pnas.0804681105

Hegde, S. R. (2019). Computational Identification of the Proteins Associated With Quorum Sensing and Biofilm Formation in Mycobacterium tuberculosis. *Frontiers in Microbiology*, *10*, 3011. https://doi.org/10.3389/fmicb.2019.03011

Herbomel, P., Thisse, B., & Thisse, C. (1999). Ontogeny and behaviour of early macrophages in the zebrafish embryo. *Development*, *126*(17), 3735. http://dev.biologists.org/content/126/17/3735.abstract

Herbomel, P., Thisse, B., & Thisse, C. (2001). Zebrafish Early Macrophages Colonize Cephalic Mesenchyme and Developing Brain, Retina, and Epidermis through a M-CSF Receptor-Dependent Invasive Process. *Developmental Biology*, *238*(2), 274–288. https://doi.org/10.1006/dbio.2001.0393

Hernández-Pando, R., Marquina-Castillo, B., Barrios-Payán, J., & Mata-Espinosa, D. (2012). Use of mouse models to study the variability in virulence associated with specific genotypic lineages of Mycobacterium tuberculosis. *Infection, Genetics and Evolution*, *12*(4), 725–731. https://doi.org/10.1016/j.meegid.2012.02.013

Hesseling, A. C., Johnson, L. F., Jaspan, H., Cotton, M. F., Whitelaw, A., Schaaf, H. S., Fine, P. E. M., Eley, B. S., Marais, B. J., Nuttall, J., Beyers, N., & Godfrey-Faussett, P. (2009). Disseminated bacille Calmette-Guerin disease in HIV-infected South African infants. *Bulletin of the World Health Organization*, *87*(7), 505–511. https://doi.org/10.2471/BLT.08.055657

Hobby, G. L., Meyer, K., & Chaffee, E. (1942). Observations on the Mechanism of Action of Penicillin. *Proceedings of the Society for Experimental Biology and Medicine*, *50*(2), 281–285. https://doi.org/10.3181/00379727-50-13773

Homolka, S., Projahn, M., Feuerriegel, S., Ubben, T., Diel, R., Nübel, U., & Niemann, S. (2012). High Resolution Discrimination of Clinical Mycobacterium tuberculosis Complex Strains Based on Single Nucleotide Polymorphisms. *PloS One*, *7*(7), e39855. https://doi.org/10.1371/journal.pone.0039855

Houben, R. M. G. J., & Dodd, P. J. (2016). The Global Burden of Latent Tuberculosis Infection: A Re-estimation Using Mathematical Modelling. *Plos Medicine*, *13*(10), e1002152. https://doi.org/10.1371/journal.pmed.1002152

Hult, C., Mattila, J. T., Gideon, H. P., Linderman, J. J., & Kirschner, D. E. (2021). Neutrophil Dynamics Affect Mycobacterium tuberculosis Granuloma Outcomes and Dissemination. *Frontiers in Immunology*, *12*. https://doi.org/10.3389/fimmu.2021.712457

Ilinov, A., Nishiyama, A., Namba, H., Fukushima, Y., Takihara, H., Nakajima, C., Savitskaya, A., Gebretsadik, G., Hakamata, M., Ozeki, Y., Tateishi, Y., Okuda, S., Suzuki, Y., Vinnik, Y. S., & Matsumoto, S. (2021). Extracellular DNA of slow growers of mycobacteria and its contribution to biofilm formation and drug tolerance. *Scientific Reports*, *11*(1), 10953. https://doi.org/10.1038/s41598-021-90156-z

Jasenosky, L. D., Scriba, T. J., Hanekom, W. A., & Goldfeld, A. E. (2015). T cells and adaptive immunity to Mycobacterium tuberculosis in humans. *Immunological Reviews*, *264*(1), 74–87. https://doi.org/10.1111/imr.12274

Johansen, M. D., Kasparian, J. A., Hortle, E., Britton, W. J., Purdie, A. C., & Oehlers, S. H. (2018). Mycobacterium marinum infection drives foam cell differentiation in zebrafish infection models. *Developmental and Comparative Immunology*, *88*, 169–172. https://doi.org/10.1016/j.dci.2018.07.022

Jong, B. C. de, Hill, P. C., Aiken, A., Awine, T., Antonio, M., Adetifa, I. M., Jackson-Sillah, D. J., Fox, A., DeRiemer, K., Gagneux, S., Borgdorff, M. W., McAdam, K. P. W. J., Corrah, T., Small, P. M., & Adegbola, R. A. (2008). Progression to Active Tuberculosis, but Not Transmission, Varies by Mycobacterium tuberculosis

Lineage in the Gambia. *The Journal of Infectious Diseases*, *198*(7), 1037–1043. https://doi.org/10.1086/591504

Joosten, S. A., van Meijgaarden, K. E., Arend, S. M., Prins, C., Oftung, F., Korsvold, G. E., Kik, S. v, Arts, R. J. W., van Crevel, R., Netea, M. G., & Ottenhoff, T. H. M. (2018). Mycobacterial growth inhibition is associated with trained innate immunity. *Journal of Clinical Investigation*, *128*(5), 1837–1851. https://doi.org/10.1172/JCI97508

Joosten, S. A., van Meijgaarden, K. E., del Nonno, F., Baiocchini, A., Petrone, L., Vanini, V., Smits, H. H., Palmieri, F., Goletti, D., & Ottenhoff, T. H. M. (2016). Patients with Tuberculosis Have a Dysfunctional Circulating B-Cell Compartment, Which Normalizes following Successful Treatment. *PLoS Pathogens*, *12*(6), e1005687. https://doi.org/10.1371/journal.ppat.1005687

Jørgensen, L. von G., Korbut, R., Jeberg, S., Kania, P. W., & Buchmann, K. (2018). Association between adaptive immunity and neutrophil dynamics in zebrafish (Danio rerio) infected by a parasitic ciliate. *PloS One*, *13*(9), e0203297. https://doi.org/10.1371/journal.pone.0203297

Jovčevska, I., & Muyldermans, S. (2020). The Therapeutic Potential of Nanobodies. *BioDrugs*, *34*(1), 11–26. https://doi.org/10.1007/s40259-019-00392-z

Jung, S.-H., Ryu, C.-M., & Kim, J.-S. (2019). Bacterial persistence: Fundamentals and clinical importance. *Journal of Microbiology*, *57*(10), 829–835. https://doi.org/10.1007/s12275-019-9218-0

Kaplan, G., Post, F. A., Moreira, A. L., Wainwright, H., Kreiswirth, B. N., Tanverdi, M., Mathema, B., Ramaswamy, S. v, Walther, G., Steyn, L. M., I, C. E. B. I. I., & Bekker, L.-G. (2003). Mycobacterium tuberculosis Growth at the Cavity Surface: a Microenvironment with Failed Immunity. *Infection and Immunity*, *71*(12), 7099–7108. https://doi.org/10.1128/IAI.71.12.7099-7108.2003

Keane, J., Gershon, S., Wise, R. P., Mirabile-Levens, E., Kasznica, J., Schwieterman, W. D., Siegel, J. N., & Braun, M. M. (2001). Tuberculosis Associated with Infliximab, a Tumor Necrosis Factor α–Neutralizing Agent. *The New England Journal of Medicine*, *345*(15), 1098–1104. https://doi.org/10.1056/NEJMoa011110

Kim, M., Wainwright, H. C., Locketz, M., Bekker, L., Walther, G. B., Dittrich, C., Visser, A., Wang, W., Hsu, F., Wiehart, U., Tsenova, L., Kaplan, G., & Russell, D. G. (2010). Caseation of human tuberculosis granulomas correlates with elevated host lipid metabolism. *EMBO Molecular Medicine*, *2*(7), 258–274. https://doi.org/10.1002/emmm.201000079

Kleinnijenhuis, J., Quintin, J., Preijers, F., Joosten, L. A. B., Ifrim, D. C., Saeed, S., Jacobs, C., Loenhout, J. van, Jong, D. de, Stunnenberg, H. G., Xavier, R. J., Meer, J. W. M. van der, Crevel, R. van, & Netea, M. G. (2012). Bacille Calmette-Guérin induces NOD2-dependent nonspecific protection from reinfection via epigenetic reprogramming of monocytes. *Proceedings of the National Academy of Sciences of the United States of America*, *109*(43), 17537–17542. https://doi.org/10.1073/pnas.1202870109

Knight, G. M., Griffiths, U. K., Sumner, T., Laurence, Y. v, Gheorghe, A., Vassall, A., Glaziou, P., & White, R. G. (2014). Impact and cost-effectiveness of new tuberculosis vaccines in low- and middle-income countries. *Proceedings of the National Academy of Sciences of the United States of America*, *111*(43), 15520–15525. https://doi.org/10.1073/pnas.1404386111

Koch, R. (1882). The Aetiology of Tuberculosis. *New York: National Tuberculosis Association*.

Kruk, M. E., Gage, A. D., Arsenault, C., Jordan, K., Leslie, H. H., Roder-DeWan, S., Adeyi, O., Barker, P., Daelmans, B., Doubova, S. v, English, M., Elorrio, E. G., Guanais, F., Gureje, O., Hirschhorn, L. R., Jiang, L., Kelley, E., Lemango, E. T., Liljestrand, J., … Pate, M. (2018). High-quality health systems in the Sustainable Development Goals era: time for a revolution. *The Lancet Global Health*, *6*(11), e1196–e1252. https://doi.org/10.1016/s2214-109x(18)30386-3

Kumar, A., Alam, A., Rani, M., Ehtesham, N. Z., & Hasnain, S. E. (2017). Biofilms: Survival and defense strategy for pathogens. *International Journal of Medical Microbiology*, *307*(8), 481–489. https://doi.org/10.1016/j.ijmm.2017.09.016

Kursar, M., Koch, M., Mittrucker, H.-W., Nouailles, G., Bonhagen, K., Kamradt, T., & Kaufmann, S. H. E. (2007). Cutting Edge: Regulatory T Cells Prevent Efficient Clearance of Mycobacterium tuberculosis. *The Journal of Immunology*, *178*(5), 2661–2665. https://doi.org/10.4049/jimmunol.178.5.2661

Kussell, E., Kishony, R., Balaban, N. Q., & Leibler, S. (2005). Bacterial Persistence: A Model of Survival in Changing Environments. *Genetics*, *169*(4), 1807–1814. https://doi.org/10.1534/genetics.104.035352

Langenau, D. M., Ferrando, A. A., Traver, D., Kutok, J. L., Hezel, J. P. D., Kanki, J. P., Zon, L. I., Look, A. T., & Trede, N. S. (2004). In vivo tracking of T cell development, ablation, and engraftment in transgenic zebrafish. *Proceedings of the National Academy of Sciences of the United States of America*, *101*(19), 7369–7374. https://doi.org/10.1073/pnas.0402248101

Lay, G., Poquet, Y., Salek-Peyron, P., Puissegur, M., Botanch, C., Bon, H., Levillain, F., Duteyrat, J., Emile, J., & Altare, F. (2007). Langhans giant cells from M. tuberculosis-induced human granulomas cannot mediate mycobacterial uptake. *The Journal of Pathology*, *211*(1), 76–85. https://doi.org/10.1002/path.2092

Lehmann, J., Cheng, T., Aggarwal, A., Park, A. S., Zeiler, E., Raju, R. M., Akopian, T., Kandror, O., Sacchettini, J. C., Moody, D. B., Rubin, E. J., & Sieber, S. A. (2018). An Antibacterial β-Lactone Kills Mycobacterium tuberculosis by Disrupting Mycolic Acid Biosynthesis. *Angewandte Chemie International Edition*, *57*(1), 348–353. https://doi.org/10.1002/anie.201709365

Li, W., Deng, G., Li, M., Liu, X., & Wang, Y. (2012). Roles of Mucosal Immunity against Mycobacterium tuberculosis Infection. *Tuberculosis Research and Treatment*, *2012*, 791728. https://doi.org/10.1155/2012/791728

Lieschke, G. J., Oates, A. C., Paw, B. H., Thompson, M. A., Hall, N. E., Ward, A. C., Ho, R. K., Zon, L. I., & Layton, J. E. (2002). Zebrafish SPI-1 (PU.1) Marks a Site of Myeloid Development Independent of Primitive Erythropoiesis: Implications for Axial Patterning. *Developmental Biology*, *246*(2), 274–295. https://doi.org/10.1006/dbio.2002.0657

Lieschke, G. J., & Trede, N. S. (2009). Fish immunology. *Current Biology*, *19*(16), R678–R682. https://doi.org/10.1016/j.cub.2009.06.068

Lin, P. L., Ford, C. B., Coleman, M. T., Myers, A. J., Gawande, R., Ioerger, T., Sacchettini, J., Fortune, S. M., & Flynn, J. L. (2014). Sterilization of granulomas is common in active and latent tuberculosis despite within-host variability in bacterial killing. *Nature Medicine*, *20*(1), 75–79. https://doi.org/10.1038/nm.3412

Lin, P. L., Rodgers, M., Smith, L., Bigbee, M., Myers, A., Bigbee, C., Chiosea, I., Capuano, S. v, Fuhrman, C., Klein, E., & Flynn, J. L. (2009). Quantitative Comparison of Active and Latent Tuberculosis in the Cynomolgus Macaque Model. *Infection and Immunity*, *77*(10), 4631–4642. https://doi.org/10.1128/iai.00592-09

Lipworth, S., Hammond, R. J. H., Baron, V. O., Hu, Yanmin., Coates, A., & Gillespie, S. H. (2016). Defining dormancy in mycobacterial disease. *Tuberculosis*, *99*, 131–142. https://doi.org/10.1016/j.tube.2016.05.006

Liu, Q., Wei, J., Li, Y., Wang, M., Su, J., Lu, Y., López, M. G., Qian, X., Zhu, Z., Wang, H., Gan, M., Jiang, Q., Fu, Y.-X., Takiff, H. E., Comas, I., Li, F., Lu, X., Fortune, S. M., & Gao, Q. (2020). Mycobacterium tuberculosis clinical isolates carry mutational signatures of host immune environments. *Science Advances*, *6*(22), eaba4901. https://doi.org/10.1126/sciadv.aba4901

Liu, Y., Gordesky-Gold, B., Leney-Greene, M., Weinbren, N. L., Tudor, M., & Cherry, S. (2018). Inflammation-Induced, STING-Dependent Autophagy Restricts Zika Virus Infection in the Drosophila Brain. *Cell Host & Microbe*, *24*(1), 57-68.e3. https://doi.org/10.1016/j.chom.2018.05.022

Lu, L. L., Smith, M. T., Yu, K. K. Q., Luedemann, C., Suscovich, T. J., Grace, P. S., Cain, A., Yu, W. H., McKitrick, T. R., Lauffenburger, D., Cummings, R. D., Mayanja-Kizza, H., Hawn, T. R., Boom, W. H., Stein, C. M., Fortune, S. M., Seshadri, C., & Alter, G. (2019). IFN-gamma-independent immune markers of Mycobacterium tuberculosis exposure. *Nature Medicine*, *25*(6), 977-+. https://doi.org/10.1038/s41591-019-0441-3

Ludlow, A. B., Pauling, C. D., Marketon, M. M., & Anderson, D. M. (2019). Drosophila as a Model for Understanding the Insect Host of Yersinia pestis. *Methods in Molecular Biology (Clifton, N.J.)*, *2010*, 167. https://www.ncbi.nlm.nih.gov/pubmed/31177438

MacPherson, P., Lebina, L., Motsomi, K., Bosch, Z., Milovanovic, M., Ratsela, A., Lala, S., Variava, E., Golub, J. E., Webb, E. L., & Martinson, N. A. (2020). Prevalence and risk factors for latent tuberculosis infection among household contacts of index cases in two South African provinces: Analysis of baseline data from a cluster-randomised trial. *PloS One*, *15*(3), e0230376. https://doi.org/10.1371/journal.pone.0230376

Magnadóttir, B. (2006). Innate immunity of fish (overview). *Fish & Shellfish Immunology*, *20*(2), 137–151. https://doi.org/10.1016/j.fsi.2004.09.006

Mahairas, G. G., Sabo, P. J., Hickey, M. J., Singh, D. C., & Stover, C. K. (1996). Molecular analysis of genetic differences between Mycobacterium bovis BCG and virulent M. bovis. *Journal of Bacteriology*, *178*(5), 1274–1282. https://doi.org/10.1128/JB.178.5.1274-1282.1996

Mangtani, P., Abubakar, I., Ariti, C., Beynon, R., Pimpin, L., Fine, P. E. M., Rodrigues, L. C., Smith, P. G., Lipman, M., Whiting, P. F., & Sterne, J. A. (2014). Protection by BCG Vaccine Against Tuberculosis: A Systematic Review of Randomized Controlled Trials. *Clinical Infectious Diseases*, *58*(4), 470–480. https://doi.org/10.1093/cid/cit790

Marakalala, M. J., Raju, R. M., Sharma, K., Zhang, Y. J., Eugenin, E. A., Prideaux, B., Daudelin, I. B., Chen, P.-Y., Booty, M. G., Kim, J. H., Eum, S. Y., Via, L. E., Behar, S. M., Barry III, C. E., Mann, M., Dartois, V., & Rubin, E. J. (2016). Inflammatory signaling in human tuberculosis granulomas is spatially organized. *Nature Medicine*, *22*(5), 531–538. https://doi.org/10.1038/nm.4073

Martin, C. J., Cadena, A. M., Leung, V. W., Lin, P. L., Maiello, P., Hicks, N., Chase, M. R., Flynn, J. L., & Fortune, S. M. (2017). Digitally Barcoding Mycobacterium tuberculosis Reveals In Vivo Infection Dynamics in the Macaque Model of Tuberculosis. *MBio*, *8*(3), 312. https://doi.org/10.1128/mBio.00312-17

Masud, S., Torraca, V., & Meijer, A. H. (2017). Modeling Infectious Diseases in the Context of a Developing Immune System. *Current Topics in Developmental Biology*, *124*, 277. https://www.ncbi.nlm.nih.gov/pubmed/28335862

Mattila, J. T., Ojo, O. O., Kepka-Lenhart, D., Marino, S., Kim, J. H., Eum, S. Y., Via, L. E., Barry Clifton E, 3rd, Klein, E., Kirschner, D. E., Morris Sidney M, J., Lin, P. L., & Flynn, J. L. (2013). Microenvironments in Tuberculous Granulomas Are Delineated by Distinct Populations of Macrophage Subsets and Expression of Nitric Oxide Synthase and Arginase Isoforms. *Journal of Immunology (Baltimore, Md. : 1950)*, *191*(2), 773–784. https://doi.org/10.4049/jimmunol.1300113

Mba Medie, F., ben Salah, I., Henrissat, B., Raoult, D., & Drancourt, M. (2011). Mycobacterium tuberculosis Complex Mycobacteria as Amoeba-Resistant Organisms. *PloS One*, *6*(6), e20499. https://doi.org/10.1371/journal.pone.0020499

McDonough, K. A., Kress, Y., & Bloom, B. R. (1993). Pathogenesis of tuberculosis: interaction of Mycobacterium tuberculosis with macrophages. *Infection and Immunity*, *61*(7), 2763–2773. http://iai.asm.org/content/61/7/2763.abstract

Mckay, A., Kraut, A., Murdzak, C., & Yassi, A. (1999). Determinants of Tuberculin Reactivity among Health Care Workers: Interpretation of Positivity following BCG Vaccination. *The Canadian Journal of Infectious Diseases = Journal Canadien Des Maladies Infectieuses*, *10*(2), 134–139. https://doi.org/10.1155/1999/749765

Medicine, U. S. N. L. of. (2020). *ClinicalTrials.gov*. clinicaltrials.gov

Medina, E., & North, R. J. (1999). Genetically susceptible mice remain proportionally more susceptible to tuberculosis after vaccination. *Immunology*, *96*(1), 16–21. https://search.proquest.com/docview/17153178

Merkul, E., Sijbrandi, N. J., Muns, J. A., Aydin, I., Adamzek, K., Houthoff, H.-J., Nijmeijer, B., & van Dongen, G. A. M. S. (2019). First platinum(II)-based metal-organic linker technology (Lx®) for a plug-and-play development of antibody-drug conjugates (ADCs). *Expert Opinion on Drug Delivery*, *16*(8), 783–793. https://doi.org/10.1080/17425247.2019.1645118

Middlebrook, G., Dubos, R. J., & Pierce, C. (1947). Virulence and Morphological Characteristics of Mammalian Tubercle Bacilli. *Journal of Experimental Medicine*, *86*(2), 175–184. https://doi.org/10.1084/jem.86.2.175

Mills, C. D., Kincaid, K., Alt, J. M., Heilman, M. J., & Hill, A. M. (2000). M-1/M-2 Macrophages and the Th1/Th2 Paradigm. *The Journal of Immunology (1950)*, *164*(12), 6166–6173. https://doi.org/10.4049/jimmunol.164.12.6166

Moreira-Teixeira, L., Tabone, O., Graham, C. M., Singhania, A., Stavropoulos, E., Redford, P. S., Chakravarty, P., Priestnall, S. L., Suarez-Bonnet, A., Herbert, E., Mayer-Barber, K. D., Sher, A., Fonseca, K. L., Sousa, J., Cá, B., Verma, R., Haldar, P., Saraiva, M., & O'Garra, A. (2020). Mouse transcriptome reveals potential signatures of protection and pathogenesis in human tuberculosis. *Nature Immunology*, *21*(4), 464–476. https://doi.org/10.1038/s41590-020-0610-z

Mortaz, E., Adcock, I. M., Tabarsi, P., Masjedi, M. R., Mansouri, D., Velayati, A. A., Casanova, J.-L., & Barnes, P. J. (2015). Interaction of Pattern Recognition Receptors with Mycobacterium Tuberculosis. *Journal of Clinical Immunology*, *35*(1), 1–10. https://doi.org/10.1007/s10875-014-0103-7

Myllymäki, H., Niskanen, M., Luukinen, H., Parikka, M., & Rämet, M. (2018). Identification of protective postexposure mycobacterial vaccine antigens using an immunosuppression-based reactivation model in the zebrafish. *Disease Models & Mechanisms*, *11*(3), dmm033175. https://doi.org/10.1242/dmm.033175

Navarra, S. v, Tang, B., Lu, L., Lin, H., Mok, C. C., Asavatanabodee, P., Suwannalai, P., Hussein, H., & Rahman, M. U. (2014). Risk of tuberculosis with anti-tumor necrosis factor-α therapy: substantially higher number of patients at risk in Asia. *International Journal of Rheumatic Diseases*, *17*(3), 291–298. https://doi.org/10.1111/1756-185X.12188

Nguipdop-Djomo, P., Rodrigues, L. C., Smith, P. G., Abubakar, I., & Mangtani, P. (2020). Drug misuse, tobacco smoking, alcohol and other social determinants of tuberculosis in UK-born adults in England: a community-based case-control study. *Scientific Reports*, *10*(1), 5639. https://doi.org/10.1038/s41598-020-62667-8

Nicol, M. P., & Wilkinson, R. J. (2008). The clinical consequences of strain diversity in Mycobacterium tuberculosis. *Transactions of the Royal Society of Tropical Medicine and Hygiene*, *102*(10), 955–965. https://doi.org/10.1016/j.trstmh.2008.03.025

Oehlers, S. H., Cronan, M. R., Beerman, R. W., Johnson, M. G., Huang, J., Kontos, C. D., Stout, J. E., & Tobin, D. M. (2017). Infection-Induced Vascular Permeability Aids Mycobacterial Growth. *The Journal of Infectious Diseases*, *215*(5), 813–817. https://doi.org/10.1093/infdis/jiw355

Ojha, A., Anand, M., Bhatt, A., Kremer, L., Jacobs, W. R., & Hatfull, G. F. (2005). GroEL1: A Dedicated Chaperone Involved in Mycolic Acid Biosynthesis during

Biofilm Formation in Mycobacteria. *Cell*, *123*(5), 861–873. https://doi.org/10.1016/j.cell.2005.09.012

Ojha, A. K., Baughn, A. D., Sambandan, D., Hsu, T., Trivelli, X., Guerardel, Y., Alahari, A., Kremer, L., Jacobs, W. R., & Hatfull, G. F. (2008). Growth of Mycobacterium tuberculosis biofilms containing free mycolic acids and harbouring drug-tolerant bacteria. *Molecular Microbiology*, *69*(1), 164–174. https://doi.org/10.1111/j.1365-2958.2008.06274.x

Oliveira-Nascimento, L., Massari, P., & Wetzler, L. M. (2012). The Role of TLR2 in Infection and Immunity. *Frontiers in Immunology*, *3*, 79. https://doi.org/10.3389/fimmu.2012.00079

O'Neill, J. (2016). *Tackling drug-resistant infections globally: final report and recommendations*. Government of the United Kingdom.

O'Neill, L. A. J., & Pearce, E. J. (2016). Immunometabolism governs dendritic cell and macrophage function. *The Journal of Experimental Medicine*, *213*(1), 15–23. https://doi.org/10.1084/jem.20151570

Ortalo-Magné, A., Lemassu, A., Lanéelle, M. A., Bardou, F., Silve, G., Gounon, P., Marchal, G., & Daffé, M. (1996). Identification of the surface-exposed lipids on the cell envelopes of Mycobacterium tuberculosis and other mycobacterial species. *Journal of Bacteriology*, *178*(2), 456–461. https://doi.org/10.1128/jb.178.2.456-461.1996

Page, D. M., Wittamer, V., Bertrand, J. Y., Lewis, K. L., Pratt, D. N., Delgado, N., Schale, S. E., McGue, C., Jacobsen, B. H., Doty, A., Pao, Y., Yang, H., Chi, N. C., Magor, B. G., & Traver, D. (2013). An evolutionarily conserved program of B-cell development and activation in zebrafish. *Blood*, *122*(8), E1–E11. https://doi.org/10.1182/blood-2012-12-471029

Palmer, M. v. (2018). Emerging Understanding of Tuberculosis and the Granuloma by Comparative Analysis in Humans, Cattle, Zebrafish, and Nonhuman Primates. *Veterinary Pathology*, *55*(1), 8–10. https://doi.org/10.1177/0300985817712795

Panikar, S. S., Banu, N., Haramati, J., del Toro-Arreola, S., Riera Leal, A., & Salas, P. (2021). Nanobodies as efficient drug-carriers: Progress and trends in chemotherapy. *Journal of Controlled Release*, *334*, 389–412. https://doi.org/10.1016/j.jconrel.2021.05.004

Panteleev, A. v, Nikitina, I. Y., Burmistrova, I. A., Kosmiadi, G. A., Radaeva, T. v, Amansahedov, R. B., Sadikov, P. v, Serdyuk, Y. v, Larionova, E. E., Bagdasarian, T. R., Chernousova, L. N., Ganusov, V. v, & Lyadova, I. v. (2017). Severe Tuberculosis in Humans Correlates Best with Neutrophil Abundance and

Lymphocyte Deficiency and Does Not Correlate with Antigen-Specific CD4 T-Cell Response. *Frontiers in Immunology*, *8*, 963. https://doi.org/10.3389/fimmu.2017.00963

Parikka, M., Hammarén, M. M., Harjula, S. K. E., Halfpenny, N. J. A., Oksanen, K. E., Lahtinen, M. J., Pajula, E. T., Iivanainen, A., Pesu, M., & Rämet, M. (2012). Mycobacterium marinum Causes a Latent Infection that Can Be Reactivated by Gamma Irradiation in Adult Zebrafish. *PLoS Pathog.*, *8*(9), 1–14.

Park, J.-H., Shim, D., Kim, K. E. S., Lee, W., & Shin, S. J. (2021). Understanding Metabolic Regulation Between Host and Pathogens: New Opportunities for the Development of Improved Therapeutic Strategies Against Mycobacterium tuberculosis Infection. *Frontiers in Cellular and Infection Microbiology*, *11*, 635335. https://doi.org/10.3389/fcimb.2021.635335

Pearl, J. E., Saunders, B., Ehlers, S., Orme, I. M., & Cooper, A. M. (2001). Inflammation and Lymphocyte Activation during Mycobacterial Infection in the Interferon-γ-Deficient Mouse. *Cellular Immunology*, *211*(1), 43–50. https://doi.org/10.1006/cimm.2001.1819

Pedrosa, J., Saunders, B. M., Appelberg, R., Orme, I. M., Silva, M. T., & Cooper, A. M. (2000). Neutrophils Play a Protective Nonphagocytic Role in Systemic Mycobacterium tuberculosis Infection of Mice. *Infection and Immunity*, *68*(2), 577–583. https://doi.org/10.1128/IAI.68.2.577-583.2000

Pena, J. C., & Ho, W.-Z. (2015). Monkey Models of Tuberculosis: Lessons Learned. *Infection and Immunity*, *83*(3), 852–862. https://doi.org/10.1128/IAI.02850-14

Peng, X., Knouse, J. A., & Hernon, K. M. (2015). Rabbit Models for Studying Human Infectious Diseases. *Comparative Medicine*, *65*(6), 499–507. https://www.ncbi.nlm.nih.gov/pubmed/26678367

Peterman, E. M., Sullivan, C., Goody, M. F., Rodriguez-Nunez, I., Yoder, J. A., & Kim, C. H. (2015). Neutralization of Mitochondrial Superoxide by Superoxide Dismutase 2 Promotes Bacterial Clearance and Regulates Phagocyte Numbers in Zebrafish. *Infection and Immunity*, *83*(1), 430–440. https://doi.org/10.1128/IAI.02245-14

Peyron, P., Vaubourgeix, J., Poquet, Y., Levillain, F., Botanch, C., Bardou, F., Daffé, M., Emile, J.-F., Marchou, B., Cardona, P.-J., de Chastellier, C., & Altare, F. (2008). Foamy Macrophages from Tuberculous Patients' Granulomas Constitute a Nutrient-Rich Reservoir for M. tuberculosis Persistence. *PLoS Pathogens*, *4*(11), e1000204. https://doi.org/10.1371/journal.ppat.1000204

Phillips, C. J. C., Foster, C. R. W., Morris, P. A., & Teverson, R. (2003). The transmission of Mycobacterium bovis infection to cattle. *Research in Veterinary Science*, *74*(1), 1–15. https://doi.org/10.1016/s0034-5288(02)00145-5

Pietersen, R.-D., du Preez, I., Loots, D. T., van Reenen, M., Beukes, D., Leisching, G., & Baker, B. (2020). Tween 80 induces a carbon flux rerouting in Mycobacterium tuberculosis. *Journal of Microbiological Methods*, *170*, 105795. https://doi.org/10.1016/j.mimet.2019.105795

Pollock, J. M., Girvin, R. M., Lightbody, K. A., Neill, S. D., Clements, R. A., Buddle, B. M., & Andersen, P. (2000). Assessment of defined antigens for the diagnosis of bovine tuberculosis in skin test-reactor cattle. *Veterinary Record*, *146*(23), 659–665. https://doi.org/10.1136/vr.146.23.659

Rani, S. A., Pitts, B., Beyenal, H., Veluchamy, R. A., Lewandowski, Z., Davison, W. M., Buckingham-Meyer, K., & Stewart, P. S. (2007). Spatial Patterns of DNA Replication, Protein Synthesis, and Oxygen Concentration within Bacterial Biofilms Reveal Diverse Physiological States. *Journal of Bacteriology*, *189*(11), 4223–4233. https://doi.org/10.1128/JB.00107-07

Reed, M. B., Gagneux, S., DeRiemer, K., Small, P. M., & I, C. E. B. I. I. (2007). The W-Beijing Lineage of Mycobacterium tuberculosis Overproduces Triglycerides and Has the DosR Dormancy Regulon Constitutively Upregulated. *Journal of Bacteriology*, *189*(7), 2583–2589. https://doi.org/10.1128/JB.01670-06

Reid, M. J. A., Arinaminpathy, N., Bloom, A., Bloom, B. R., Boehm, C., Chaisson, R., Chin, D. P., Churchyard, G., Cox, H., Ditiu, L., Dybul, M., Farrar, J., Fauci, A. S., Fekodu, E., Fujiwara, P. I., Hallett, T. B., Hanson, C. L., Harrington, M., Herbert, N., … Goosby, E. P. (2019). Building a tuberculosis-free world: The Lancet Commission on tuberculosis. *Lancet*, *393*(10178), 1331–1384. https://doi.org/10.1016/S0140-6736(19)30024-8

Renshaw, S. A., & Trede, N. S. (2012). A model 450 million years in the making: zebrafish and vertebrate immunity. *Disease Models & Mechanisms*, *5*(1), 38–47. https://doi.org/10.1242/dmm.007138

Rhoades, E. R., Geisel, R. E., Butcher, B. A., McDonough, S., & Russell, D. G. (2005). Cell wall lipids from Mycobacterium bovis BCG are inflammatory when inoculated within a gel matrix: Characterization of a new model of the granulomatous response to mycobacterial components. *Tuberculosis*, *85*(3), 159–176. https://doi.org/10.1016/j.tube.2004.10.001

Riksen, N. P., & Netea, M. G. (2021). Immunometabolic control of trained immunity. *Molecular Aspects of Medicine*, *77*, 100897. https://doi.org/10.1016/j.mam.2020.100897

Riley, R. L. (1957). Aerial dissemination of pulmonary tuberculosis. *American Review of Tuberculosis*, *76*(6), 931. https://www.ncbi.nlm.nih.gov/pubmed/13488004

Rivas-Santiago, B., Schwander, S. K., Sarabia, C., Diamond, G., Klein-Patel, M. E., Hernandez-Pando, R., Ellner, J. J., & Sada, E. (2005). Human β-Defensin 2 Is Expressed and Associated with Mycobacterium tuberculosis during Infection of Human Alveolar Epithelial Cells. *Infection and Immunity*, *73*(8), 4505–4511. https://doi.org/10.1128/IAI.73.8.4505-4511.2005

Roca, F. J., & Ramakrishnan, L. (2013). TNF Dually Mediates Resistance and Susceptibility to Mycobacteria via Mitochondrial Reactive Oxygen Species. *Cell*, *153*(3), 521–534. https://doi.org/10.1016/j.cell.2013.03.022

Rodrigues, L. C., Diwan, V. K., & Wheeler, J. G. (1993). Protective Effect of BCG against Tuberculous Meningitis and Miliary Tuberculosis: A Meta-Analysis. *International Journal of Epidemiology*, *22*(6), 1154–1158. https://doi.org/10.1093/ije/22.6.1154

Romagnoli, A., Etna, M. P., Giacomini, E., Pardini, M., Remoli, M. E., Corazzari, M., Falasca, L., Goletti, D., Gafa, V., Simeone, R., Delogu, G., Piacentini, M., Brosch, R., Fimia, G. M., & Coccia, E. M. (2014). ESX-1 dependent impairment of autophagic flux by Mycobacterium tuberculosis in human dendritic cells. *Autophagy*, *8*(9), 1357–1370. https://doi.org/10.4161/auto.20881

Roy, A., Eisenhut, M., Harris, R. J., Rodrigues, L. C., Sridhar, S., Habermann, S., Snell, L., Mangtani, P., Adetifa, I., Lalvani, A., & Abubakar, I. (2014). Effect of BCG vaccination against Mycobacterium tuberculosis infection in children: systematic review and meta-analysis. *BMJ : British Medical Journal*, *349*(aug04 5), g4643. https://doi.org/10.1136/bmj.g4643

Sakai, H., Okafuji, I., Nishikomori, R., Abe, J., Izawa, K., Kambe, N., Yasumi, T., Nakahata, T., & Heike, T. (2012). The CD40-CD40L axis and IFN-γ play critical roles in Langhans giant cell formation. *International Immunology*, *24*(1), 5–15. https://doi.org/10.1093/intimm/dxr088

Sakai, S., Kauffman, K. D., Sallin, M. A., Sharpe, A. H., Young, H. A., Ganusov, V. v, & Barber, D. L. (2016). CD4 T Cell-Derived IFN-γ Plays a Minimal Role in Control of Pulmonary Mycobacterium tuberculosis Infection and Must Be Actively Repressed by PD-1 to Prevent Lethal Disease. *PLoS Pathogens*, *12*(5), e1005667. https://doi.org/10.1371/journal.ppat.1005667

Sakamoto, K. (2012). The Pathology of Mycobacterium tuberculosis Infection. *Veterinary Pathology*, *49*(3), 423–439. https://doi.org/10.1177/0300985811429313

Sampaio, A. da G., Gontijo, A. V. L., Araujo, H. M., & Koga-Ito, C. Y. (2018). In Vivo Efficacy of Ellagic Acid against Candida albicans in a Drosophila melanogaster Infection Model. *Antimicrobial Agents and Chemotherapy*, *62*(12). https://doi.org/10.1128/aac.01716-18

Sani, M., Houben, E. N. G., Geurtsen, J., Pierson, J., de Punder, K., van Zon, M., Wever, B., Piersma, S. R., Jiménez, C. R., & Peters, P. J. (2010). Direct Visualization by Cryo-EM of the Mycobacterial Capsular Layer: A Labile Structure Containing ESX-1-Secreted Proteins. *PLoS Pathogens*, *6*(3), e1000794. https://doi.org/10.1371/journal.ppat.1000794

Sarathy, J. P., & Dartois, V. (2020). Caseum: a Niche for Mycobacterium tuberculosis Drug-Tolerant Persisters. *Clinical Microbiology Reviews*, *33*(3). https://doi.org/10.1128/CMR.00159-19

Sarathy, J. P., Via, L. E., Weiner, D., Blanc, L., Boshoff, H., Eugenin, E. A., Barry Clifton E, 3rd, & Dartois, V. A. (2018). Extreme Drug Tolerance of Mycobacterium tuberculosis in Caseum. *Antimicrobial Agents and Chemotherapy*, *62*(2). https://doi.org/10.1128/AAC.02266-17

Schierloh, P., Alemán, M., Yokobori, N., Alves, L., Roldán, N., Abbate, E., Sasiain, M. del C., & de La Barrera, S. (2005). NK cell activity in tuberculosis is associated with impaired CD11a and ICAM-1 expression: a regulatory role of monocytes in NK activation. *Immunology*, *116*(4), 541–552. https://doi.org/10.1111/j.1365-2567.2005.02259.x

Schroeder, E., Souza, O. de, Santos, D., Blanchard, J., & Basso, L. (2002). Drugs that Inhibit Mycolic Acid Biosynthesis in Mycobacterium tuberculosis. *Current Pharmaceutical Biotechnology*, *3*(3), 197–225. https://doi.org/10.2174/1389201023378328

Schwabe, A., & Bruggeman, F. J. (2014). Contributions of Cell Growth and Biochemical Reactions to Nongenetic Variability of Cells. *Biophysical Journal*, *107*(2), 301–313. https://doi.org/10.1016/j.bpj.2014.05.004

Scordo, J. M., Knoell, D. L., & Torrelles, J. B. (2016). Alveolar Epithelial Cells in Mycobacterium tuberculosis Infection: Active Players or Innocent Bystanders? *Journal of Innate Immunity*, *8*(1), 3–14. https://doi.org/10.1159/000439275

Sebastian, J., Nair, R. R., Swaminath, S., & Ajitkumar, P. (2020). Mycobacterium tuberculosis Cells Surviving in the Continued Presence of Bactericidal Concentrations of Rifampicin in vitro Develop Negatively Charged Thickened

Capsular Outer Layer That Restricts Permeability to the Antibiotic. *Frontiers in Microbiology*, *11*, 554795. https://doi.org/10.3389/fmicb.2020.554795

Seshadri, C., Sedaghat, N., Campo, M., Peterson, G., Wells, R. D., Olson, G. S., Sherman, D. R., Stein, C. M., Mayanja-Kizza, H., Shojaie, A., Boom, W. H., & Hawn, T. R. (2017). Transcriptional networks are associated with resistance to Mycobacterium tuberculosis infection. *PloS One*, *12*(4), e0175844. https://doi.org/10.1371/journal.pone.0175844

Sharma, S. K., Mohan, A., & Sharma, A. (2016). Miliary tuberculosis: A new look at an old foe. *Journal of Clinical Tuberculosis and Other Mycobacterial Diseases*, *3*, 13–27. https://doi.org/10.1016/j.jctube.2016.03.003

Shi, C., Shi, J., & Xu, Z. (2011). A review of murine models of latent tuberculosis infection. *Scandinavian Journal of Infectious Diseases*, *43*(11–12), 848–856. https://doi.org/10.3109/00365548.2011.603745

Shi, L., Eugenin, E. A., & Subbian, S. (2016). Immunometabolism in Tuberculosis. *Frontiers in Immunology*, *7*, 150. https://doi.org/10.3389/fimmu.2016.00150

Simmons, J. D., Stein, C. M., Seshadri, C., Campo, M., Alter, G., Fortune, S., Schurr, E., Wallis, R. S., Churchyard, G., Mayanja-Kizza, H., Boom, W. H., & Hawn, T. R. (2018). Immunological mechanisms of human resistance to persistent Mycobacterium tuberculosis infection. *Nature Reviews Immunology*, *18*(9), 575–589. https://doi.org/10.1038/s41577-018-0025-3

Singh, A., & Gupta, U. (2018). Animal models of tuberculosis: Lesson learnt. *Indian Journal of Medical Research (New Delhi, India : 1994)*, *147*(5), 456–463. https://doi.org/10.4103/ijmr.ijmr_554_18

Singh, M., Mynak, M. L., Kumar, L., Mathew, J. L., & Jindal, S. K. (2005). Prevalence and risk factors for transmission of infection among children in household contact with adults having pulmonary tuberculosis. *Archives of Disease in Childhood*, *90*(6), 624–628. https://doi.org/10.1136/adc.2003.044255

Siqueira, M. da S., Ribeiro, R. de M., & Travassos, L. H. (2018). Autophagy and Its Interaction With Intracellular Bacterial Pathogens. *Frontiers in Immunology*, *9*, 935. https://doi.org/10.3389/fimmu.2018.00935

Smith, D. W., McMurray, D. N., Wiegeshaus, E. H., Grover, A. A., & Harding, G. E. (1970). Host-parasite relationships in experimental airborne tuberculosis. IV. Early events in the course of infection in vaccinated and nonvaccinated guinea pigs. *The American Review of Respiratory Disease*, *102*(6), 937. https://www.ncbi.nlm.nih.gov/pubmed/4991996

Solomon, J. M., Leung, G. S., & Isberg, R. R. (2003). Intracellular Replication of Mycobacterium marinum within Dictyostelium discoideum: Efficient Replication in the Absence of Host Coronin. *Infection and Immunity*, *71*(6), 3578–3586. https://doi.org/10.1128/iai.71.6.3578-3586.2003

Spits, H., Artis, D., Colonna, M., Diefenbach, A., di Santo, J. P., Eberl, G., Koyasu, S., Locksley, R. M., McKenzie, A. N. J., Mebius, R. E., Powrie, F., & Vivier, E. (2013). Innate lymphoid cells--a proposal for uniform nomenclature. *Nature Reviews. Immunology*, *13*(2), 145–149. https://doi.org/10.1038/nri3365

Srivastava, S., Ernst, J. D., & Desvignes, L. (2014). Beyond macrophages: the diversity of mononuclear cells in tuberculosis. *Immunological Reviews*, *262*(1), 179–192. https://doi.org/10.1111/imr.12217

Stavnezer, J., & Amemiya, C. T. (2004). Evolution of isotype switching. *Seminars in Immunology*, *16*(4), 257–275. https://doi.org/10.1016/j.smim.2004.08.005

Stinear, T. P., Seemann, T., Harrison, P. F., Jenkin, G. A., Davies, J. K., Johnson, P. D. R., Abdellah, Z., Arrowsmith, C., Chillingworth, T., Churcher, C., Clarke, K., Cronin, A., Davis, P., Goodhead, I., Holroyd, N., Jagels, K., Lord, A., Moule, S., Mungall, K., … Cole, S. T. (2008). Insights from the complete genome sequence of Mycobacterium marinum on the evolution of Mycobacterium tuberculosis. *Genome Research*, *18*(5), 729–741. https://doi.org/10.1101/gr.075069.107

Sturgill-Koszycki, S., Schlesinger, P. H., Chakraborty, P., Haddix, P. L., Collins, H. L., Fok, A. K., Allen, R. D., Gluck, S. L., Heuser, J., & Russell, D. G. (1994). Lack of acidification in Mycobacterium phagosomes produced by exclusion of the vesicular proton-ATPase. *Science*, *263*(5147), 678–681. https://doi.org/10.1126/science.8303277

Subbian, S., Tsenova, L., Kim, M.-J., Wainwright, H. C., Visser, A., Bandyopadhyay, N., Bader, J. S., Karakousis, P. C., Murrmann, G. B., Bekker, L.-G., Russell, D. G., & Kaplan, G. (2015). Lesion-Specific Immune Response in Granulomas of Patients with Pulmonary Tuberculosis: A Pilot Study. *PloS One*, *10*(7), e0132249. https://doi.org/10.1371/journal.pone.0132249

Swaim, L. E., Connolly, L. E., Volkman, H. E., Humbert, O., Born, D. E., & Ramakrishnan, L. (2006). Mycobacterium marinum infection of adult zebrafish causes caseating granulomatous tuberculosis and is moderated by adaptive immunity. *Infection and Immunity*, *74*(11), 6108–6117. https://doi.org/10.1128/IAI.00887-06

Tafalla, C., Bøgwald, J., & Dalmo, R. A. (2013). Adjuvants and immunostimulants in fish vaccines: Current knowledge and future perspectives. *Fish & Shellfish Immunology*, *35*(6), 1740–1750. https://doi.org/10.1016/j.fsi.2013.02.029

Tait, D. R., Hatherill, M., van der Meeren, O., Ginsberg, A. M., van Brakel, E., Salaun, B., Scriba, T. J., Akite, E. J., Ayles, H. M., Bollaerts, A., Demoitié, M.-A., Diacon, A., Evans, T. G., Gillard, P., Hellström, E., Innes, J. C., Lempicki, M., Malahleha, M., Martinson, N., … Roman, F. (2019). Final Analysis of a Trial of M72/AS01E Vaccine to Prevent Tuberculosis. *The New England Journal of Medicine*, *381*(25), 2429–2439. https://doi.org/10.1056/NEJMoa1909953

Takaki, K., Davis, J. M., Winglee, K., & Ramakrishnan, L. (2013). Evaluation of the pathogenesis and treatment of Mycobacterium marinum infection in zebrafish. *Nature Protocols*, *8*(6), 1114–1124. https://doi.org/10.1038/nprot.2013.068

Tobin, D. M., & Ramakrishnan, L. (2008). Comparative pathogenesis of Mycobacterium marinum and Mycobacterium tuberculosis. *Cellular Microbiology*, *10*(5), 1027–1039. https://doi.org/10.1111/j.1462-5822.2008.01133.x

Trede, N. S., Langenau, D. M., Traver, D., Look, A. T., & Zon, L. I. (2004). The use of zebrafish to understand immunity. *Immunity*, *20*(4), 367–379. https://doi.org/10.1016/S1074-7613(04)00084-6

Trivedi, A., Mavi, P. S., Bhatt, D., & Kumar, A. (2016). Thiol reductive stress induces cellulose-anchored biofilm formation in Mycobacterium tuberculosis. *Nature Communications*, *7*(1), 11392. https://doi.org/10.1038/ncomms11392

Tsenova, L., & Singhal, A. (2020). Effects of host-directed therapies on the pathology of tuberculosis. *The Journal of Pathology*. https://doi.org/10.1002/path.5407

Uribe, C., Folch, H., Enriquez, R., & Moran, G. (2011). Innate and adaptive immunity in teleost fish: a review. *Veterinarni Medicina*, *56*(10), 486–503.

van der Meeren, O., Hatherill, M., Nduba, V., Wilkinson, R. J., Muyoyeta, M., van Brakel, E., Ayles, H. M., Henostroza, G., Thienemann, F., Scriba, T. J., Diacon, A., Blatner, G. L., Demoitié, M.-A., Tameris, M., Malahleha, M., Innes, J. C., Hellström, E., Martinson, N., Singh, T., … Tait, D. R. (2018). Phase 2b Controlled Trial of M72/AS01E Vaccine to Prevent Tuberculosis. *The New England Journal of Medicine*, *379*(17), 1621–1634. https://doi.org/10.1056/NEJMoa1803484

van der Sar, A. M., Appelmelk, B. J., Vandenbroucke-Grauls, C., & Bitter, W. (2004). A star with stripes: zebrafish as an infection model. *Trends in Microbiology*, *12*(10), 451–457. https://doi.org/10.1016/j.tim.2004.08.001

van Rhijn, I., Godfroid, J., Michel, A., & Rutten, V. (2008). Bovine tuberculosis as a model for human tuberculosis: advantages over small animal models. *Microbes and Infection*, *10*(7), 711–715. https://doi.org/10.1016/j.micinf.2008.04.005

Vergne, I., Chua, J., & Deretic, V. (2003). Tuberculosis Toxin Blocking Phagosome Maturation Inhibits a Novel Ca2+/Calmodulin-PI3K hVPS34 Cascade. *The Journal of Experimental Medicine*, *198*(4), 653–659. https://doi.org/10.1084/jem.20030527

Vergne, I., Fratti, R. A., Hill, P. J., Chua, J., Belisle, J., & Deretic, V. (2004). Mycobacterium tuberculosis Phagosome Maturation Arrest: Mycobacterial Phosphatidylinositol Analog Phosphatidylinositol Mannoside Stimulates Early Endosomal Fusion. *Molecular Biology of the Cell*, *15*(2), 751–760. https://doi.org/10.1091/mbc.E03-05-0307

Verrall, A. J., Netea, M. G., Alisjahbana, B., Hill, P. C., & van Crevel, R. (2014). Early clearance of Mycobacterium tuberculosis: a new frontier in prevention. *Immunology*, *141*(4), 506–513. https://doi.org/10.1111/imm.12223

Verrall, A. J., Schneider, M., Alisjahbana, B., Apriani, L., Laarhoven, A. van, Koeken, V. A. C. M., Dorp, S. van, Diadani, E., Utama, F., Hannaway, R. F., Inati, A., Netea, M. G., Sharples, K., Hill, P. C., Ussher, J. E., & Crevel, R. van. (2020). Early Clearance of Mycobacterium tuberculosis Is Associated With Increased Innate Immune Responses. *The Journal of Infectious Diseases*, *221*(8), 1342–1350. https://doi.org/10.1093/infdis/jiz147

Vestby, L. K., Grønseth, T., Simm, R., & Nesse, L. L. (2020). Bacterial Biofilm and its Role in the Pathogenesis of Disease. *Antibiotics*, *9*(2), 59. https://doi.org/10.3390/antibiotics9020059

Via, L. E., Fratti, R. A., McFalone, M., Pagan-Ramos, E., Deretic, D., & Deretic, V. (1998). Effects of cytokines on mycobacterial phagosome maturation. *Journal of Cell Science*, *111*(7), 897. http://jcs.biologists.org/cgi/content/abstract/111/7/897

Vijay, S., Nhung, H. N., Bao, N. L. H., Thu, D. D. A., Trieu, L. P. T., Phu, N. H., Thwaites, G. E., Javid, B., & Thuong, N. T. T. (2021). Most-Probable-Number-Based Minimum Duration of Killing Assay for Determining the Spectrum of Rifampicin Susceptibility in Clinical Mycobacterium tuberculosis Isolates. *Antimicrobial Agents and Chemotherapy*, *65*(3). https://doi.org/10.1128/AAC.01439-20

Viola, A., Munari, F., Sánchez-Rodríguez, R., Scolaro, T., & Castegna, A. (2019). The Metabolic Signature of Macrophage Responses. *Frontiers in Immunology*, *10*, 1462. https://doi.org/10.3389/fimmu.2019.01462

Volkman, H. E., Pozos, T. C., Zheng, J., Davis, J. M., Rawls, J. F., & Ramakrishnan, L. (2010). Tuberculous Granuloma Induction via Interaction of a Bacterial Secreted Protein with Host Epithelium. *Science*, *327*(5964), 466–469. https://doi.org/10.1126/science.1179663

Voskuil, M. I., Bartek, I. L., Visconti, K., & Schoolnik, G. K. (2011). The Response of Mycobacterium Tuberculosis to Reactive Oxygen and Nitrogen Species. *Frontiers in Microbiology*, *2*, 105. https://doi.org/10.3389/fmicb.2011.00105

Vugmeyster, Y., Entrican, C. A., Joyce, A. P., Lawrence-Henderson, R. F., Leary, B. A., Mahoney, C. S., Patel, H. K., Raso, S. W., Olland, S. H., Hegen, M., & Xu, X. (2012). Pharmacokinetic, Biodistribution, and Biophysical Profiles of TNF Nanobodies Conjugated to Linear or Branched Poly(ethylene glycol). *Bioconjugate Chemistry*, *23*(7), 1452–1462. https://doi.org/10.1021/bc300066a

Warburg, O. (1956). On the origin of cancer cells. *Science*, *123*(3191), 309–314. https://science.sciencemag.org/content/123/3191/309.long

Westerfield, M. (2000). *The zebrafish book. A guide for the laboratory use of zebrafish (Danio rerio)* (4th ed.). Univ. of Oregon Press, Eugene.

Wolf, A. J., Linas, B., Trevejo-Nunez, G. J., Kincaid, E., Tamura, T., Takatsu, K., & Ernst, J. D. (2007). Mycobacterium tuberculosis Infects Dendritic Cells with High Frequency and Impairs Their Function In Vivo. *The Journal of Immunology*, *179*(4), 2509–2519. https://doi.org/10.4049/jimmunol.179.4.2509

World Health Organization. (2014). *The End TB Strategy*. https://www.who.int/tb/strategy/en/

World Health Organization. (2017). *WHO treatment guidelines for isoniazid-resistant tuberculosis*. https://www.who.int/tb/areas-of-work/drug-resistant-tb/treatment/gdg-meeting-izoniazid-resistant-tb/en/

World Health Organization. (2018). *Latent tuberculosis infection: updated and consolidated guidelines for programmatic management*. https://www.who.int/tb/publications/2018/latent-tuberculosis-infection/en/

World Health Organization. (2019). *Global Tuberculosis Report 2019*. https://www.who.int/tb/publications/global_report/en/

World Health Organization. (2020). *Global Tuberculosis Report 2020*. https://www.who.int/tb/publications/global_report/en/.

World Health Organization. (2021). *Global Tuberculosis Report 2021*. https://www.who.int/tb/publications/global_report/en/.

Xenaki, K. T., Dorresteijn, B., Muns, J. A., Adamzek, K., Doulkeridou, S., Houthoff, H., Oliveira, S., & van Bergen en Henegouwen, P. M. (2021). Homogeneous tumor

targeting with a single dose of HER2-targeted albumin-binding domain-fused nanobody-drug conjugates results in long-lasting tumor remission in mice. *Theranostics*, *11*(11), 5525–5538. https://doi.org/10.7150/thno.57510

Yang, C.-T., Cambier, C. J., Davis, J. M., Hall, C. J., Crosier, P. S., & Ramakrishnan, L. (2012). Neutrophils Exert Protection in the Early Tuberculous Granuloma by Oxidative Killing of Mycobacteria Phagocytosed from Infected Macrophages. *Cell Host & Microbe*, *12*(3), 301–312. https://doi.org/10.1016/j.chom.2012.07.009

Zhang, S., & Cui, P. (2014). Complement system in zebrafish. *Developmental and Comparative Immunology*, *46*(1), 3–10. https://doi.org/10.1016/j.dci.2014.01.010

Zhang, Y.-A., Salinas, I., Li, J., Parra, D., Bjork, S., Xu, Z., LaPatra, S. E., Bartholomew, J., & Sunyer, J. O. (2010). IgT, a primitive immunoglobulin class specialized in mucosal immunity. *Nature Immunology*, *11*(9), 827–835. https://doi.org/10.1038/ni.1913

Zhu, J. (2018). T Helper Cell Differentiation, Heterogeneity, and Plasticity. *Cold Spring Harbor Perspectives in Biology*, *10*(10), a030338. https://doi.org/10.1101/cshperspect.a030338

Zimmerman, A. M., Moustafa, F. M., Romanowski, K. E., & Steiner, L. A. (2011). Zebrafish immunoglobulin IgD: Unusual exon usage and quantitative expression profiles with IgM and IgZ/T heavy chain isotypes. *Molecular Immunology*, *48*(15–16), 2220–2223. https://doi.org/10.1016/j.molimm.2011.06.441

Zimmermann, I., Egloff, P., Hutter, C. A., Arnold, F. M., Stohler, P., Bocquet, N., Hug, M. N., Huber, S., Siegrist, M., Hetemann, L., Gera, J., Gmür, S., Spies, P., Gygax, D., Geertsma, E. R., Dawson, R. J., & Seeger, M. A. (2018). Synthetic single domain antibodies for the conformational trapping of membrane proteins. *ELife*, *7*. https://doi.org/10.7554/eLife.34317

Zimmermann, I., Egloff, P., Hutter, C. A. J., Kuhn, B. T., Bräuer, P., Newstead, S., Dawson, R. J. P., Geertsma, E. R., & Seeger, M. A. (2020). Generation of synthetic nanobodies against delicate proteins. *Nature Protocols*, *15*(5), 1707–1741. https://doi.org/10.1038/s41596-020-0304-x

Zimmermann, N., Thormann, V., Hu, B., Köhler, A., Imai-Matsushima, A., Locht, C., Arnett, E., Schlesinger, L. S., Zoller, T., Schürmann, M., Kaufmann, S. H. E., & Wardemann, H. (2016). Human isotype-dependent inhibitory antibody responses against Mycobacterium tuberculosis. *EMBO Molecular Medicine*, *8*(11), 1325–1339. https://doi.org/10.15252/emmm.201606330

PUBLICATIONS

PUBLICATION I

Modeling Tuberculosis in *Mycobacterium marinum* -Infected Adult Zebrafish

Luukinen H, Hammarén MM, Vanha-aho L-M, Parikka M

J. Vis. Exp. 2018 (140), e58299
doi:10.3791/58299

Video Article

Modeling Tuberculosis in *Mycobacterium marinum* Infected Adult Zebrafish

Hanna Luukinen[1], Milka Marjut Hammarén[1], Leena-Maija Vanha-aho[1], Mataleena Parikka[1,2]

[1]Faculty of Medicine and Life Sciences, University of Tampere

[2]Oral and Maxillofacial Unit, Tampere University Hospital

Correspondence to: Hanna Luukinen at hanna.luukinen@uta.fi

URL: https://www.jove.com/video/58299
DOI: doi:10.3791/58299

Keywords: Immunology and Infection, Issue 140, Zebrafish, tuberculosis, *Mycobacterium marinum*, *Mycobacterium tuberculosis*, mycobacterial infection, qPCR, immune system

Date Published: 10/8/2018

Citation: Luukinen, H., Hammarén, M.M., Vanha-aho, L.M., Parikka, M. Modeling Tuberculosis in *Mycobacterium marinum* Infected Adult Zebrafish. *J. Vis. Exp.* (140), e58299, doi:10.3791/58299 (2018).

Abstract

Mycobacterium tuberculosis is currently the deadliest human pathogen causing 1.7 million deaths and 10.4 million infections every year. Exposure to this bacterium causes a wide disease spectrum in humans ranging from a sterilized infection to an actively progressing deadly disease. The most common form is the latent tuberculosis, which is asymptomatic, but has the potential to reactivate into a fulminant disease. Adult zebrafish and its natural pathogen *Mycobacterium marinum* have recently proven to be an applicable model to study the wide disease spectrum of tuberculosis. Importantly, spontaneous latency and reactivation as well as adaptive immune responses in the context of mycobacterial infection can be studied in this model. In this article, we describe methods for the experimental infection of adult zebrafish, the collection of internal organs for the extraction of nucleic acids for the measurement of mycobacterial loads and host immune responses by quantitative PCR. The in-house-developed, *M. marinum*-specific qPCR assay is more sensitive than the traditional plating methods as it also detects DNA from non-dividing, dormant or recently dead mycobacteria. As both DNA and RNA are extracted from the same individual, it is possible to study the relationships between the diseased state, and the host and pathogen gene-expression. The adult zebrafish model for tuberculosis thus presents itself as a highly applicable, non-mammalian *in vivo* system to study host-pathogen interactions.

Video Link

The video component of this article can be found at https://www.jove.com/video/58299/

Introduction

Zebrafish (*Danio rerio*) is a widely used animal model in biomedical research and it is an accepted model for common vertebrate biology. The zebrafish has been adapted to many fields of research modeling human diseases and disorders ranging from cancer[1] and cardiac disease[2] to infection and immunological studies of several bacterial [3] and viral infections[4,5]. In addition, the *ex utero* development of zebrafish embryos has made the zebrafish a popular model in developmental biology[6] and toxicology[7,8].

In many fields of research, including infection biology, the optically transparent zebrafish larvae are commonly used. The first immune cells appear within 24 h post fertilization (hpf), when primitive macrophages are detected[9]. Neutrophils are the next immune cells to appear around 33 hpf[10]. Zebrafish larvae are thus feasible for studying the early stages of infection and the role of innate immunity in the absence of adaptive immune cells[11]. However, the adult zebrafish with its fully functional adaptive immune system provides an additional layer of complexity for infection experiments. T cells can be detected around 3 days post fertilization[12], and B cells are able to produce functional antibodies by 4 weeks post fertilization[13]. The adult zebrafish has all the main counterparts of the mammalian innate and adaptive immune system. The main differences between the immune systems of fish and humans are found in antibody isotypes as well as in the anatomy of lymphoid tissues. The zebrafish has only three antibody classes[14], whereas humans have five[15]. In the absence of bone marrow and lymph nodes, the primary lymphoid organs in the fish are the kidney and the thymus[16] and the spleen, the kidney and the gut serve as secondary lymphoid organs[17]. Despite these differences, with its full immune arsenal of innate and adaptive cells, the adult zebrafish is a highly applicable, easy-to-use, non-mammalian model for host-pathogen interaction studies.

The zebrafish has lately been established as a feasible model to study tuberculosis[18,19,20,21,22]. Tuberculosis is an airborne disease caused by *Mycobacterium tuberculosis*. According to the World Health Organization, tuberculosis caused *1.7* million deaths in 2016 and is the leading cause of death by a single pathogen worldwide[23]. Mice[24,25], rabbits[26] and non-human primates[27] are the best-known animal models in tuberculosis research but each face their limitations. The non-human primate model of *M. tuberculosis* infection resembles the human disease most closely, but using this model is limited due to serious ethical considerations. Other animal models are hindered by the host-specificity of *M. tuberculosis* that affects the disease pathology. Probably the biggest issue in modeling tuberculosis is the wide spectrum of infection and disease outcomes in the human disease: tuberculosis is a very heterogeneous disease ranging from sterilizing immunity to latent, active and reactivated infection[28], which can be hard to reproduce and model experimentally.

Mycobacterium marinum is a close relative of *M. tuberculosis* with ~3,000 orthologous proteins with 85% amino acid identity[29]. *M. marinum* naturally infects zebrafish producing granulomas, the hallmarks of tuberculosis, in its internal organs[19,30]. Unlike other animal models used

in tuberculosis research, zebrafish produces many offspring, it requires only a limited space and importantly, it is neurophysiologically the least developed vertebrate tuberculosis model available. Additionally, the *M. marinum* infection causes latent infection, active disease or even sterilization of mycobacterial infection in adult zebrafish closely mimicking the spectrum of disease outcomes of human tuberculosis[19,31,32]. Here, we describe methods for the experimental tuberculosis model of adult zebrafish by injecting *M. marinum* into the abdominal cavity and using quantitative PCR to measure the mycobacterial loads and immune responses from zebrafish tissue samples.

Protocol

All zebrafish experiments have been approved by the Animal Experiment Board in Finland (ESAVI/8245/04.10.07/2015). Methods are performed according to the act (497/2013) and the government decree (564/2013) on the protection of animals used for scientific or educational purposes in Finland.

1. Culturing of *Mycobacterium marinum*

NOTE: Since Mycobacterium marinum is a pathogen capable of causing superficial infections in humans, find out the local guidelines for personal safety and biohazard waste disposal before starting to work with this bacterium.

1. Culture *M. marinum* on a 7H10 plate supplemented with 10% OADC (oleic acid, albumin, dextrose, catalase) enrichment and 0.5% v/v of glycerol at 29 °C for at least 5 days. Maintain *M. marinum* cultures by taking fresh bacteria from the freezer every two weeks and transferring onto a new plate every other week.
   NOTE: *M. marinum* is a natural fish pathogen infecting aquatic species and it is important to take precautions not to contaminate zebrafish stocks with the bacteria. Infected zebrafish and items contaminated with bacteria have to be kept separate from the breeding facilities.
2. Use a sterile 1-µL inoculation loop to aseptically transfer a loopful of *M. marinum* bacterial mass into a cell culture flask containing 10 mL of 7H9 medium with 10% ADC (albumin, dextrose, catalase) enrichment, 0.2% v/v polysorbate 80 and 0.2% v/v of glycerol. Culture for 3–4 days to approximately an OD_{600} (optical density) of 0.7 at 29 °C in the dark without shaking. Leave the cap loose, or use a filter cap, to allow for the sufficient exchange of gases.
   NOTE: Polysorbate 80 is added to the medium to prevent the aggregation of bacteria. In addition, exposure to light leads to phenotypic changes in bacterial colonies (*e.g.*, the color changes from white to yellow). To avoid this, keep the cultures in the dark.
3. Measure the OD_{600}value with a spectrophotometer. Dilute the liquid culture to an OD_{600} of 0.07–0.09 and continue culturing for 2 days at 29 °C in the dark without shaking. Leave the cap loose.
   NOTE: During these two days, the bacterial suspension will reach an $OD_{600}$of approximately 0.5 corresponding to an early log-phase.

2. Preparation of Bacterial Solution for Infecting Adult Zebrafish

1. Transfer the bacterial suspension into a big sterile cuvette or a 15 mL tube and place it in the dark at room temperature for 15 min to allow the biggest clumps to settle.
2. Transfer the top 5–7 mL of the suspension into a clean tube or a cuvette and measure the OD_{600}. Use this top phase of the suspension for the infections.
3. Collect 1 mL of *M. marinum* culture into a fresh tube and centrifuge for 3 min at 10,000 x *g*. Remove the supernatant and resuspend the pellet in 1 mL of sterile 1x PBS.
4. Dilute to reach the desired bacterial concentration by using sterile 1x PBS with 0.3 mg/mL phenol red as a tracer. Divide the diluted suspension into three aliquots.
   NOTE: Use a predetermined OD_{600} vs. CFU (colony-forming units)/µL curve to estimate the dilution required to get the wanted number of bacteria in the 5 µL injection volume[34]. The correlation between OD_{600} and concentration of the bacterial suspension needs to be validated before starting the actual infection experiments. Reserve two weeks for collecting this validation data.
5. Using a 1 mL syringe, slowly pull the suspension through a 27 G needle 3x. For each aliquot, perform this step just before use.
   NOTE: Do not use the same bacterial solution for more than 2 h.

3. Experimental *M. marinum* Infection with Intraperitoneal Injection

1. Pipette a 5 µL droplet of the diluted bacterial solution onto a piece of parafilm film and pull the droplet into a 30 G insulin needle.
2. Use 5–8 month-old wild-type fish and rag1−/−hu1999 mutant fish for the experiment. Anesthetize adult zebrafish in the tank water with 0.02% 3-aminobenzoic acid ethyl ester (pH 7.0). Position the fish ventral side up into a slit on a moist foamed plastic.
   NOTE: *Rag-/-* mutant fish are not able to undergo somatic recombination and produce functional T and B cells.
3. Inject the needle between the pelvic fins at an approximately 45° angle. Keep the needle opening upwards to observe that the entire opening is inside the abdominal cavity. Slowly inject the bacterial suspension and carefully remove the needle.
   NOTE: In case the red tracer is leaking out of the fish upon injection, exclude the fish from the experiment.
4. Immediately after injection, transfer the fish into a recovery tank with fresh tank water.
5. Take samples of the bacterial suspension on 7H10 plates every 15 min from the bacterial aliquot in use and incubate the bacteria at 29 °C for 5 days and verify the infection dose by counting the colonies on the plates.
6. Check the well-being of the fish regularly and euthanize any fish with symptoms of the infection with over 0.02% concentration of 3-aminobenzoic acid ethyl ester (pH 7.0).
   NOTE: Approximately, 7% of the adult zebrafish infected with 34 ± 15 CFU and 30% of zebrafish infected with 2029 ± 709 CFU will have had symptoms by 8 weeks[19]. The symptoms may include abnormal swimming, lack of response to touch, gasping, edema or observable wasting.
7. Maintain the zebrafish according to the common standards[35].

4. Collection of Internal Organs

1. Euthanize the zebrafish with an overdose of 3-aminobenzoic acid ethyl ester (over 0.02% concentration, pH 7.0) in the tank water.
2. Insert one pin posterior to the branchiostegal rays and another through the tail to tack the fish onto the platform.
3. Open the whole abdominal cavity with a scalpel and collect the internal organs by using a small spoon and sharp-ended tweezers. Start from the heart and work along the spine towards the tail to detach all internal organs in one block.
   NOTE: Be sure to collect all kidney tissue by scraping along the spine with the spoon.
4. Finally, use tweezers to detach the gut next to the cloaca and transfer the organs into a 1.5 mL homogenization tube with six 2.8 mm ceramic beads. Immediately place on dry-ice to freeze the sample. The sample can be stored at -80 °C until homogenized.
5. Rinse the instruments with 70% ethanol between individuals.

5. Homogenization and RNA extraction from an organ block.

NOTE: The method is modified from the Stanford University protocols[36].

1. Add guanidine thiocyanate-phenol solution used for nucleic acid extraction (**Table of Materials**) on the top of the sample to a total volume of 1,500 µL. Ensure that the sample covers a maximum of 10% of the total volume.
   CAUTION: The expected volume of the harvested tissue is 100 µL. Guanidine thiocyanate-phenol solution contains toxic and irritating compounds and requires protective clothing, nitrile gloves and working in a fume hood. Do not combine with bleach as this will cause formation of toxic gases. Read the material safety data sheet (MSDS) before use.
2. Homogenize samples using a bead-beating homogenizer 3 times for 40 s at 3,200 rpm. Cool on ice for 30 s between the cycles. Sonicate the homogenized samples in a water bath for 9 min.
3. Centrifuge the samples at 12,000 x *g* for 10 min at 4 °C and move 1,000 µL of the cleared homogenate into a fresh microcentrifuge tube.
4. Add 200 µL of chloroform, immediately mix by vortexing for 15 s and incubate for 2 min at room temperature.
   CAUTION: Chloroform is a toxic and irritant compound if inhaled, swallowed or contacted with skin or eyes. Use necessary safety equipment for personal protection and work in a fume hood. Read the material safety data sheet (MSDS) before use.
5. Centrifuge at 12,000 x *g* for 15 min at 4 °C to separate the aqueous and organic phases.
6. Carefully, transfer 500 µL of the top phase to a fresh tube to avoid contaminating the RNA. Remove and discard the rest of the aqueous phase (~100 µL) and store the interphase and organic phase at 4 °C for DNA extraction.
   NOTE: The top phase contains the RNA.
7. Add 500 µL of 2-propanol and immediately mix by vortexing for 15 s. Incubate for 10 min at room temperature to precipitate the RNA.
8. Centrifuge at 12,000 x *g* for 10 min at 4 °C to pellet the RNA. Remove the supernatant by pipetting.
9. Add 1 mL of 75% ethanol and vortex for 10 s.
   NOTE: The protocol can be paused here, and the samples kept overnight at 4 °C.
10. Centrifuge at 7,500 x *g* for 5 min at 4 °C. Remove the supernatant by pipetting.
11. Repeat the wash steps 5.9–5.10. Remove the supernatant carefully by pipetting and let the pellet air-dry in a fume hood.
12. Dissolve the RNA pellet in 500 µL of nuclease-free water and keep the samples on ice. Measure the concentrations with a microvolume spectrophotometer or with equivalent equipment. Store the RNA at -80 °C.

6. Purification of Co-extracted Zebrafish and Mycobacterial DNA

1. Prepare a back-extraction buffer (BEB) by dissolving 118.2 g of guanidine thiocyanate (final concentration 4 M), 3.68 g of sodium citrate (final concentration 50 mM) and 30.29 g of Tris free base (final concentration 1 M) in 120 mL of nuclease-free water (this may require stirring overnight). Add nuclease-free water to a final total volume of 250 mL and filter to sterilize the solution.
   NOTE: This buffer can be stored at room temperature for up to 6 months. Do not combine BEB with bleach as they react to produce toxic gases such as hydrogen chloride and hydrogen cyanide.
2. Use the interphase and organic phase of the sample to extract mycobacterial DNA. Add 500 µL of BEB to each tube. Mix extensively for 10 min by inversion at room temperature.
3. Centrifuge the tubes at 12,000 x *g* for 30 min at room temperature and carefully transfer 500 µL of the upper aqueous phase containing the DNA to a new tube.
4. Add 400 µL of 2-propanol. Mix by inverting and incubate for 10 min at room temperature.
5. Centrifuge the samples at 12,000 x *g* for 15 min at 4 °C. A pellet containing the DNA should be visible at this point. Carefully remove the supernatant by pipetting.
6. Add 800 µL of 70% ethanol. Wash the pellet by inversion. Do not vortex the samples at this point, as genomic DNA breaks down easily.
7. Centrifuge the samples at 12,000 x *g* for 15 min at 4°C and remove the supernatant by pipetting. Repeat the ethanol wash (steps 6.6 and 6.7).
8. Remove the ethanol by carefully pipetting. Let the samples air-dry for 5–10 min. Dissolve the pellet in 200 µL of nuclease-free water.
9. Measure DNA concentrations with a microvolume spectrophotometer or with equivalent equipment. DNA can be stored at 4 °C or at -20 °C for long-term storage.

7. Quantitative PCR for Measuring Mycobacterial Loads

1. Prepare qPCR reaction mixes with no-ROX (carboxy-X-rhodamine) against the *M. marinum* internal transcribed spacer (ITS) between 16S-23S ITS according to the manufacturer's instructions with MMITS1 primers (**Table 1**). Pipette the reaction mix and sample dilutions as duplicates on a 96-well plate suitable for qPCR. Include a DNA standard dilution series of a known amount of bacteria in each run.
   NOTE: The expected *M. marinum* load per fish can range from 0 CFU to 1,000,000 CFU at 4 wpi. The qPCR assay can be also performed with other qPCR kits but the annealing temperature for the primers has to be re-optimized.

2. Seal the plate with an optically transparent film and centrifuge the plate at 2,000 x *g* for 2 min at 4 °C.
3. Run the qPCR program shown in the **Table 2**.
4. Using the standard curve, calculate the number of bacteria in the entire fish sample.

8. DNase Treatment of the RNA Samples

1. To remove any possible remaining traces of genomic DNA from the RNA, carry out DNase I treatment. Thaw the RNA samples on ice. NOTE: Be sure to use only RNase-free equipment and solutions and wipe the working surface and pipettes with a decontamination reagent eliminating RNases (**Table of Materials**) before starting to work. Wear a long-sleeved lab coat and gloves to protect your samples.
2. Prepare 10 µL DNase I reaction mixes on ice according to the manufacturer's instructions. Mix 1 µL of DNase I, 1 µL of 10x DNase buffer and 8 µL of RNA sample including a maximum of 1 µg of RNA.
3. Gently mix the reactions (no vortexing) and incubate for 30 min at 37 °C.
4. Prior to heat-inactivation, add 1 µL of 50 mM EDTA to each 10 µL sample. If EDTA is not added, the RNA will undergo chemical degradation when heated.
5. Incubate for 10 min at 65 °C to heat-inactivate DNase I. Continue directly to cDNA synthesis or store the DNase-treated RNA at -80 °C.

9. cDNA Synthesis

1. Keep all reagents and samples on ice and prepare the reaction mixes according to the manufacturer's instructions. For a 5 µL reaction mix, include 1 µL of Reverse Transcription Master Mix, 3 µL of nuclease-free water and 1 µL of DNase treated RNA.
2. Gently mix the reverse transcription reactions and briefly spin the tube, if needed.
3. Place samples in a PCR machine and use the program shown in **Table 3**.
4. Dilute the cDNA in nuclease-free water for qPCR to a maximum concentration of 2.5 ng/µL, if needed. cDNA can be stored at -20 °C.

10. Measuring Zebrafish Gene Expression by Quantitative PCR

1. Prepare a qPCR master mix on ice according to the manufacturer's instructions and protect from light. Use the primers introduced in **Table 1**. NOTE: To calculate the fold of induction for each gene, measure the expression also from a pooled baseline sample extracted from 6 healthy zebrafish.
2. Prepare replicates of each sample and pipette the reaction mixes onto a qPCR plate. Seal the plate with an optically transparent film and centrifuge the plate at 2,000 x *g* for 2 min at 4 °C before starting the run.
3. Run the qPCR program shown in the **Table 4** with the annealing temperature depending on the primer pair used (**Table 1**).
4. Analyze the gene expression ratio compared to a house-keeping gene (*loopern4*[37]) with the ΔCt method using the equation:

$$\text{ratio} = \frac{2^{Ct(healthy)-Ct(infected)}_{gene}}{2^{Ct(healthy)-Ct(infected)}_{loopern4}}$$

Representative Results

The natural fish pathogen *Mycobacterium marinum* infects the internal organs of the zebrafish and produces a systemic infection with histologically visible granulomas[19]. Adult zebrafish are infected with *M. marinum* by an intraperitoneal injection. The DNA and RNA are extracted, and the mycobacterial load is measured by quantitative polymerase chain reaction (qPCR) using DNA as the template. The outline of the method is shown in **Figure 1**.

The initial number of mycobacteria used for infecting the fish is a critical determinant for the outcome of infection. A high infection dose of *M. marinum* (~2,000 CFU) leads to a progressive disease in which the mycobacterial loads continue to increase until the average bacterial load reaches around five million bacteria (**Figure 2A**) ultimately killing the fish. A low dose (~20–90 CFU) of *M. marinum* leads to the development of a disease spectrum similar to that seen in human tuberculosis (**Figure 2B**). The bacterial load continues to increase until around 4–7 weeks (**Figure 2A** and **Figure 3A**), after which in the majority of the fish the disease reaches a steady-state. **Figure 2B** shows an example of the distribution of disease outcomes with a low dose infection: About 7% of the infected zebrafish were unable to restrict the bacterial growth. These individuals developed a primary progressive disease and they died within two months after the infection. Around 10% of the individuals cleared the mycobacterial infection by 4 weeks. The remaining 65% of the fish population developed a latent mycobacterial infection with steady bacterial burdens. However, between 8 and 32 weeks of infection, in 18%, the latent infection spontaneously reactivated leading to the progression of the disease.

By using *rag-/-* mutant fish, it is possible to study the role of adaptive immune responses in the adult fish. *Rag-/-* mutant fish cannot sufficiently limit the growth of mycobacteria leading to higher bacterial loads (**Figure 3A**) and increased morbidity (**Figure 3B**), clearly demonstrating the importance of adaptive immunity in controlling mycobacterial infection. Also, the importance of adaptive responses in evoking certain cytokine responses in mycobacterial infection can be studied in this model. Here, we show that the adaptive response is required for the efficient induction of interleukin 4 (IL4) (**Figure 3C**) but is dispensable for the induction of interferon-γ (IFNγ) at 4 wpi (**Figure 3D**). Interferon-γ is a cytokine driving the response against intracellular pathogens whereas interleukin 4 is a common mediator in the adaptive immune response against extracellular pathogens. The significantly higher expression levels of *il4* in the wild-type group compared to *rag-/-* mutant fish refers to important adaptive humoral responses in the mycobacterial infection (**Figure 3C**).

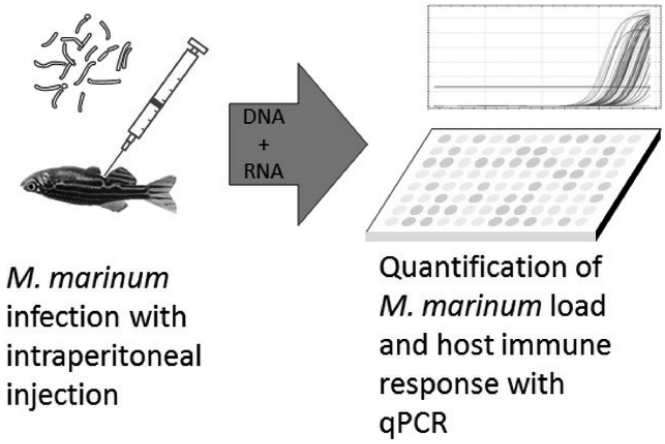

Figure 1: Workflow of studying the development of mycobacterial loads in the adult zebrafish. Adult zebrafish are infected with an intraperitoneal injection of *M. marinum*. DNA and RNA are extracted from the internal organs of the fish and the *M. marinum* load and host's immune responses are analyzed with quantitative polymerase chain reaction (qPCR). Please click here to view a larger version of this figure.

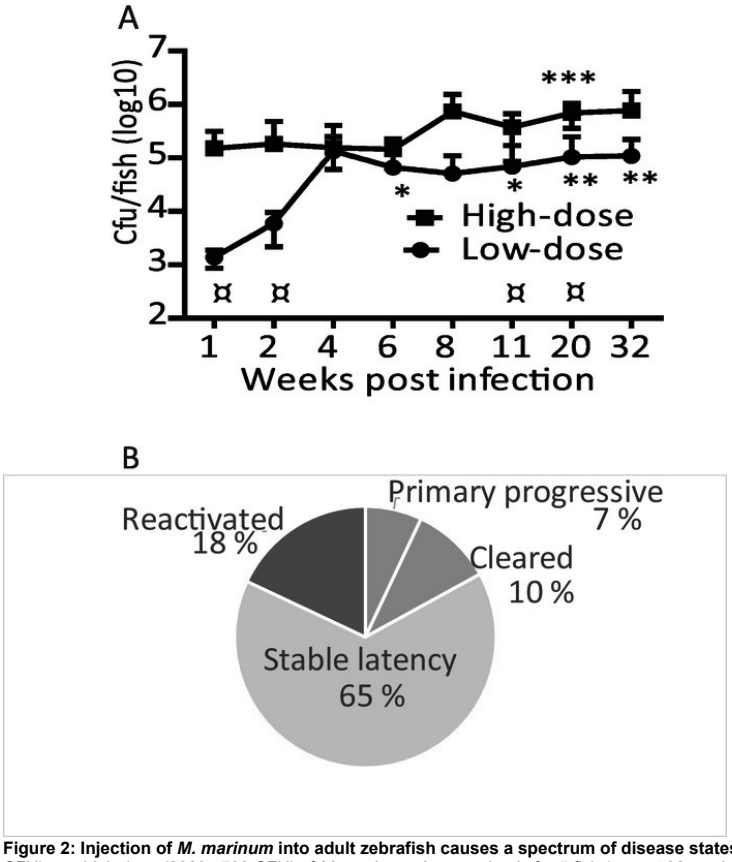

Figure 2: Injection of *M. marinum* into adult zebrafish causes a spectrum of disease states. (**A**) Zebrafish were injected with a low (34 ±15 CFU) or a high dose (2029 ±709 CFU) of *M. marinum*. Average loads for 5 fish (except 32 weeks high dose, n = 2) are shown with SD. Low-dose statistics: * p <0.05 compared with 1 week, ** p <0.05 compared with 1 and 2 week. High-dose statistics: *** p <0.05 compared with 1, 2, 8, 11 and 20 wk. ¤ low dose vs. high dose p<0.05. Modified from Parikka *et al.* 2012[19]. (**B**) Typical distribution of disease outcomes within a wild-type zebrafish population infected with a low-dose of *M. marinum*. Please click here to view a larger version of this figure.

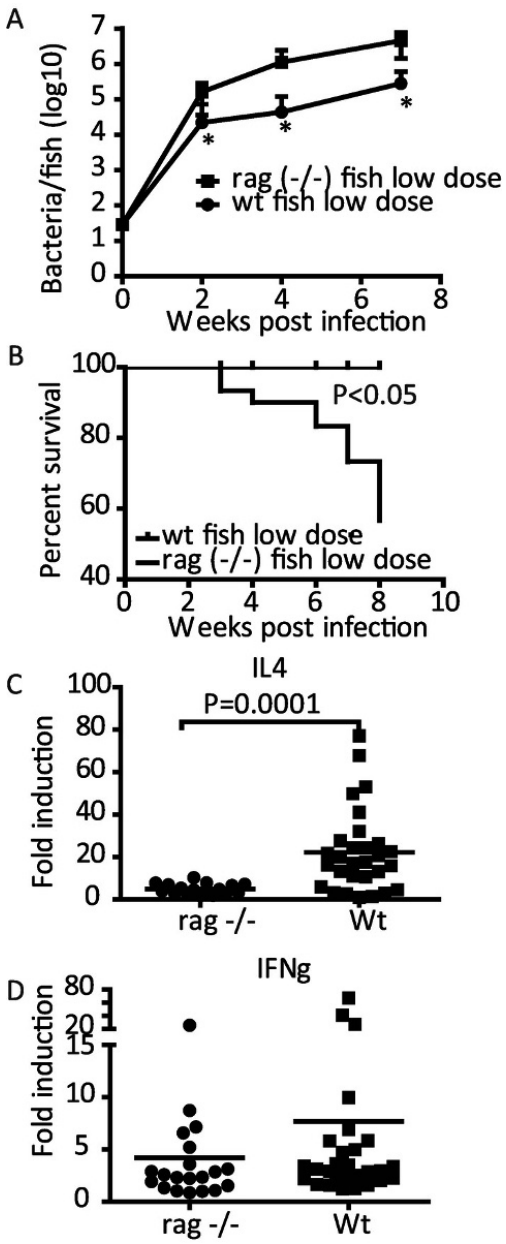

Figure 3: Adaptive immunity affects the course of mycobacterial infection in the adult zebrafish. Adult wild-type (wt) and rag1 (−/−) zebrafish were infected with a low dose (n = 30) of *M. marinum*. (**A**) The average mycobacterial loads were measured by qPCR at 2, 4, and 7 weeks post infection (wpi) (n = 10) *P<0.05. (**B**) The fish were euthanized upon the development of symptoms of the disease and survival plots were created. (**C**). The expression levels of *il4* were measured at 4 wpi. (**D**) The expression levels of *IFNγ* were measured at 4 wpi. (A and B)modified from Parikka *et al.* 2012[19]. (C and D) Modified from Hammarén *et al.* 2014[38]. Please click here to view a larger version of this figure.

Gene	Primer sequence	Annealing temperature
MMITS1	F: CACCACGAGAAACACTCCAA	65
16S–23SITS Locus AB548718 for *M. marinum* quantification	R: ACATCCCGAAACCAACAGAG	
loopern4	F: TGAGCTGAAACTTTACAGACACAT	61
Expressed repetitive elements	R: AGACTTTGGTGTCTCCAGAATG	
il4	GCAGGAATGGCTTTGAAGGG	59.5
ZDB-GENE-100204-1	GCAGTTTCCAGTCCCGGTAT	
ifnγ1-2	F: GGGCGATCAAGGAAAACGACCC,	61
ZDB-GENE-040629-1	R: TAGCCTGCCGTCTCTTGCGT	

Table 1: Primer sequences and annealing temperatures. The sequences of the primers used and their optimized annealing temperatures. The primers for the *M. marinum* 16S-23S rRNA transcript have been optimized for a No-ROX qPCR kit and the other primers for a ROX including qPCR kit.

Step	Time	Temperature
1	3 min	95 °C
2	5 s	95 °C
3	10 s	65 °C
4	5 s	72 °C (fluorescence detection)
5	Go to step 2. 39 times	
6	Melting curve analysis 55-95°C with 0.5°C intervals	
7	Forever	4 °C

Table 2: qPCR program for measuring *M. marinum* DNA. A qPCR protocol designed according to the manufacturer's instructions and optimized for measuring *M. marinum* DNA from zebrafish samples.

Time	Temperature
5 min	25 °C
30 min	42 °C
5 min	85 °C
forever	4 °C

Table 3: cDNA synthesis program. Protocol for synthesizing cDNA from the extracted RNA of an infected zebrafish according to the manufacturer's instructions.

Step	Time	Temperature
1	30 s	95 °C
2	12 s	95 °C
3	30 s	Annealing °C
4	Go to step 2. for 39 times	
5	Melting curve analysis 65–95 °C with 0.5 °C intervals	
6	Forever	4 °C

Table 4: qPCR program for measuring host's gene expression. A qPCR protocol designed according to the manufacturer's instructions and optimized for measuring the expression of different zebrafish genes.

Discussion

Here we describe a qPCR-based application to measure mycobacterial loads from DNA extracted from experimentally infected adult zebrafish tissues. This application is based on primers designed around the 16S-23S rRNA internal transcribed spacer sequence[40]. The total mycobacterial load in a fish sample is estimated using a standard curve prepared from DNA extracted from a known number of cultured mycobacteria and assuming that one bacterium has one copy of its genome at any given moment. The detection limit of the *M. marinum* -qPCR is approximately 100 colony forming units[18]. A clear advantage of the method compared to traditional plating is that both active and non-

dividing dormant bacteria can be detected. In addition, a common problem of contaminating growth on culture plates from zebrafish tissues is circumvented by this approach. However, as DNA is used as the template, it is possible that some of the copies measured can be derived from the DNA of bacteria that have died very recently. A significant advantage of the nucleic acid-based protocol is that as both DNA and RNA (as well as proteins, not described here) can be extracted from the same individual, the mycobacterial load of the individual can be combined with gene expression data of both the host and the bacteria.

The dosing of *M. marinum* is a critical determinant of the outcome of infection. The low *M. marinum* (~20–90 CFU) infection dose produces a spectrum of disease states with latency as the most common form. If the infection dose is in the order of thousands, a more progressive disease develops in the majority of individuals. As the natural infectious dose is known to be low in human tuberculosis[41], using a low dose of *M. marinum* in the zebrafish model is likely to produce a more natural infection. To reach the correct dose, make sure to validate the relation between the OD600 and colony-forming units prior to starting any experiments. The normal variation of the plated infection doses is approximately 30% and is not considered a problem. However, it is important to verify that the entire 5 µL volume of the bacterial suspension remains inside the fish. Leaking of the injection solution will cause extra variation in the infection dose. In addition to the infection dose, the strain of the bacteria can affect the disease progression. It has been shown that the virulence of the different *M. marinum* strains can alter between the strains. The two most commonly used strains are ATCC927 (fish isolated strain used in these experiments) and the M strain. However, these strains differ greatly in their virulence. The human-isolated M strain develops a more progressive disease whereas the fish-isolated strain produces a milder disease well-suitable for studying the latent form of the mycobacterial infection[33]. The virulence of the bacteria within a strain may also alter if the bacteria is serially transferred from one culture to another, which can be prevented by taking fresh mycobacteria from a freezer stock often enough.

In vitro culturing of slowly dividing *M. marinum* without antibiotics is prone to contaminations. Therefore, the handling of the bacteria requires strict aseptic approach carried out in a laminar flow hood. Possible contamination in the culture can be detected as too high an OD_{600} value, odd-looking bacterial suspension or colonies. *M. marinum* colonies are normally fuzzy-edged, flat and matt white in color. *M. marinum* cultures are sensitive to light and they start producing yellow pigment when exposed to light. This yellow pigment can be used to distinguish *M. marinum* colonies from other bacteria after the infections. Contaminants can cause the fish to die soon after infection. Usually, the first symptoms of a low-dose infection do not appear before 3 weeks post infection and any mortalities before this time point are likely due to contamination in the bacterial suspension or trauma induced during injection.

Adult zebrafish are very sensitive to 3-aminobenzoic acid ethyl ester and do not survive if the exposure time is too long or the concentration of the anesthetic is too high. Therefore, when infecting, the zebrafish should be exposed to the anesthetic only for the minimum of time to achieve good anesthesia (~1–2 min). After infection, adult zebrafish are kept in groups at water temperature of 26–28 °C. If the temperature is higher or lower than this, it might affect the *M. marinum* growth rate and kinetics of the infection. Also, the tank water quality (microbiological quality, salt concentration, pH, oxygen saturation) is an important part ensuring a successful experiment. Health monitoring of the fish needs to be carried out daily and fish that show symptoms of infection need to be removed from the group and euthanized. If the fish die in the tank, the other fish may become re-infected through the gut, which will affect the progression of infection.

The commonly used zebrafish larval model of tuberculosis is applicable to study innate immunity, which directs the experiments to a limited subset of host-microbe interactions. The use of adult zebrafish makes it possible to study both innate and adaptive immune responses in a versatile model[18,32,39]. Adult zebrafish presents itself as a convenient vertebrate model to study the entire spectrum of tuberculosis. With a low-dose exposure of *M. marinum*, 7% of the fish population develop primary progressive disease, 10% are able to sterilize the infection, 65% develop latent disease and in 18% spontaneous reactivation occurs (**Figure 2**). The disease spectrum closely resembles that seen in human tuberculosis, in which the vast majority develop a latent disease, approximately 4–14% produce primary active infection within the first five years after the infection[42], 10–20% of heavily exposed persons seem to be able to sterilize the infection[43] and 5–10% of the latent infections reactivate[44]. Differences in hosts' genetics affects the susceptibility to tuberculosis and the disease progression[45]. This is also seen in the zebrafish population that is genetically very heterogeneous unlike many other laboratory animals[46,47]. The natural genetic variation makes it a highly applicable model in the search for optimal immune responses in this multifactorial disease.

Disclosures

The authors have nothing to disclose.

Acknowledgements

This work has been supported by the Finnish Cultural Foundation (H.L.), Tampere Tuberculosis Foundation (H.L., L.-M.V., M.M.H., M.P.), Foundation of the Finnish Anti-Tuberculosis Association (Suomen Tuberkuloosin Vastustamisyhdistyksen Säätiö) (H.L., M.M.H., M.P.), Sigrid Jusélius Foundation (M.P.), Emil Aaltonen Foundation (M.M.H.), Jane and Aatos Erkko Foundation (M.P.) and Academy of Finland (M.P.). Leena Mäkinen, Hanna-Leena Piippo and Jenna Ilomäki are acknowledged for their technical assistance. The authors acknowledge the Tampere Zebrafish Laboratory for their service.

References

1. Zhao, S., Huang, J., & Ye, J. A fresh look at zebrafish from the perspective of cancer research. *Journal of Experimental & Clinical Cancer Research.* **34**, 80 (2015).
2. Bournele, D., & Beis, D. Zebrafish models of cardiovascular disease. *Heart failure reviews.* **21**(6), 803-813 (2016).
3. Torraca, V., & Mostowy, S. Zebrafish Infection: From Pathogenesis to Cell Biology. *Trends in cell biology.* **28**(2), 143-156 (2018).
4. Varela, M., Figueras, A., & Novoa, B. Modelling viral infections using zebrafish: Innate immune response and antiviral research. *Antiviral Research.* **139**, 59-68 (2017).

5. Goody, M.F., Sullivan, C., & Kim, C.H. Studying the immune response to human viral infections using zebrafish. *Developmental and comparative immunology.* **46**(1), 84-95 (2014).
6. Thisse, C., & Zon, L.I. Organogenesis--heart and blood formation from the zebrafish point of view. *Science.* **295**(5554), 457-462 (2002).
7. Eimon, P.M., & Rubinstein, A.L. The use of in vivo zebrafish assays in drug toxicity screening. *Expert Opinion on Drug Metabolism & Toxicology.* **5**(4), 393-401 (2009).
8. Sukardi, H., Chng, H.T., Chan, E.C.Y., Gong, Z., & Lam, S.H. Zebrafish for drug toxicity screening: bridging the in vitro cell-based models and in vivo mammalian models. *Expert Opinion on Drug Metabolism & Toxicology.* **7**(5), 579-589 (2011).
9. Wittamer, V., Bertrand, J.Y., Gutschow, P.W., & Traver, D. Characterization of the mononuclear phagocyte system in zebrafish. *Blood.* **117**(26), 7126-7135 (2011).
10. Harvie, E.A., & Huttenlocher, A. Neutrophils in host defense: new insights from zebrafish. *Journal of leukocyte biology.* **98**(4), 523-537 (2015).
11. Yoshida, N., Frickel, E., & Mostowy, S. Macrophage-Microbe interactions: Lessons from the Zebrafish Model. *Frontiers in Immunology.* **8**, 1703 (2017).
12. Langenau, D.M.*, et al.* In vivo tracking of T cell development, ablation, and engraftment in transgenic zebrafish. *Proceedings of the National Academy of Sciences of the United States of America.* **101**(19), 7369-7374 (2004).
13. Lewis, K.L., Del Cid, N., & Traver, D. Perspectives on antigen presenting cells in zebrafish. *Developmental and comparative immunology.* **46**(1), 63-73 (2014).
14. Hu, Y., Xiang, L., & Shao, J. Identification and characterization of a novel immunoglobulin Z isotype in zebrafish: Implications for a distinct B cell receptor in lower vertebrates. *Molecular immunology.* **47**(4), 738-746 (2010).
15. Danilova, N., Bussmann, J., Jekosch, K., & Steiner, L.A. The immunoglobulin heavy-chain locus in zebrafish: identification and expression of a previously unknown isotype, immunoglobulin Z. *Nature immunology.* **6**(3), 295-302 (2005).
16. Zapata, A., Diez, B., Cejalvo, T., Frias, C.G., & Cortes, A. Ontogeny of the immune system of fish. *Fish & shellfish immunology.* **20**(2), 126-136 (2006).
17. Traver, D., Paw, B.H., Poss, K.D., Penberthy, W.T., Lin, S., & Zon, L.I. Transplantation and in vivo imaging of multilineage engraftment in zebrafish bloodless mutants. *Nature immunology.* **4**(12), 1238-1246 (2003).
18. Hammaren, M.M.*, et al.* Adequate Th2-Type Response Associates with Restricted Bacterial Growth in Latent Mycobacterial Infection of Zebrafish. *Plos Pathogens.* **10**(6), e1004190 (2014).
19. Parikka, M.*, et al.* Mycobacterium marinum Causes a Latent Infection that Can Be Reactivated by Gamma Irradiation in Adult Zebrafish. *PLoS Pathog.* **8**(9), 1-14 (2012).
20. Tobin, D.M.*, et al.* Host Genotype-Specific Therapies Can Optimize the Inflammatory Response to Mycobacterial Infections. *Cell.* **148**(3), 434-446 (2012).
21. Lesley, R., & Ramakrishnan, L. Insights into early mycobacterial pathogenesis from the zebrafish. *Current opinion in microbiology.* **11**(3), 277-283 (2008).
22. Berg, R.D., & Ramakrishnan, L. Insights into tuberculosis from the zebrafish model. *Trends in molecular medicine.* **18**(12), 689-690 (2012).
23. World Health Organization. *WHO Global tuberculosis report 2017.* http://www.who.int/tb/publications/global_report/en/ (2017).
24. Ordonez, A.A.*, et al.* Mouse model of pulmonary cavitary tuberculosis and expression of matrix metalloproteinase-9. *Disease Models & Mechanisms.* **9**(7), 779-788 (2016).
25. Kramnik, I., & Beamer, G. Mouse models of human TB pathology: roles in the analysis of necrosis and the development of host-directed therapies. *Seminars in Immunopathology.* **38**(2), 221-237 (2016).
26. Manabe, Y.C.*, et al.* The aerosol rabbit model of TB latency, reactivation and immune reconstitution inflammatory syndrome. *Tuberculosis.* **88**(3), 187-196 (2008).
27. Pena, J.C., & Ho, W. Monkey Models of Tuberculosis: Lessons Learned. *Infection and immunity.* **83**(3), 852-862 (2015).
28. Cadena, A.M., Fortune, S.M., & Flynn, J.L. Heterogeneity in tuberculosis. *Nature Reviews Immunology.* **17**(11), 691-702 (2017).
29. Stinear, T.P.*, et al.* Insights from the complete genome sequence of Mycobacterium marinum on the evolution of Mycobacterium tuberculosis. *Genome research.* **18**(5), 729-741 (2008).
30. Swaim, L.E., Connolly, L.E., Volkman, H.E., Humbert, O., Born, D.E., & Ramakrishnan, L. Mycobacterium marinum infection of adult zebrafish causes caseating granulomatous tuberculosis and is moderated by adaptive immunity. *Infection and immunity.* **74**(11), 6108-6117 (2006).
31. Myllymaki, H., Bauerlein, C.A., & Ramet, M. The Zebrafish Breathes new Life into the Study of Tuberculosis. *Frontiers in Immunology.* **7**, 196 (2016).
32. Luukinen, H.*, et al.* Priming of Innate Antimycobacterial Immunity by Heat-killed Listeria monocytogenes Induces Sterilizing Response in Adult Zebrafish Tuberculosis Model. *Disease Models and Mechanisms.* **11** (2018).
33. Sar, A M, Abdallah, A.M., Sparrius, M., Reinders, E., Vandenbroucke-Grauls, C., & Bitter, W. Mycobacterium marinum strains can be divided into two distinct types based on genetic diversity and virulence. *Infection and immunity.* **72**(11), 6306-6312 (2004).
34. Madigan, M., & Martinko, J. *Brock Biology of Microorganisms.* (2016).
35. Nüsslein-Volhard, C., & Dahm, R. *Zebrafish:a practical approach.* Oxford University Press, Oxford (2002).
36. *Anonymous Stanford University Protocols.* http://med.stanford.edu/labs/vanderijn-west/Protocols.html (2018).
37. Vanhauwaert, S.*, et al.* Expressed Repeat Elements Improve RT-qPCR Normalization across a Wide Range of Zebrafish Gene Expression Studies. *Plos One.* **9**(10), e109091 (2014).
38. Hammaren, M.M.*, et al.* Adequate Th2-Type Response Associates with Restricted Bacterial Growth in Latent Mycobacterial Infection of Zebrafish. *Plos Pathogens.* **10**(6), e1004190 (2014).
39. Oksanen, K.E.*, et al.* An adult zebrafish model for preclinical tuberculosis vaccine development. *Vaccine.* **31**(45), 5202-5209 (2013).
40. Roth, A., Fischer, M., Hamid, M.E., Michalke, S., Ludwig, W., & Mauch, H. Differentiation of phylogenetically related slowly growing mycobacteria based on 16S-23S rRNA gene internal transcribed spacer sequences. *Journal of clinical microbiology.* **36**(1), 139-147 (1998).
41. Rajararna, M.V.S., Ni, B., Dodd, C.E., & Schlesinger, L.S. Macrophage immunoregulatory pathways in tuberculosis. *Seminars in immunology.* **26**(6), 471-485 (2014).
42. Vynnycky, E., & Fine, P. The natural history of tuberculosis: the implications of age-dependent risks of disease and the role of reinfection. *Epidemiology and infection.* **119**(2), 183-201 (1997).
43. Cobat, A.*, et al.* Two loci control tuberculin skin test reactivity in an area hyperendemic for tuberculosis. *Journal of Experimental Medicine.* **206**(12), 2583-2591 (2009).
44. Delogu, G., & Goletti, D. The Spectrum of Tuberculosis Infection: New Perspectives in the Era of Biologics. *Journal of Rheumatology.* **41**, 11-16 (2014).

45. Abel, L., *et al.* Genetics of human susceptibility to active and latent tuberculosis: present knowledge and future perspectives. *Lancet Infectious Diseases.* **18**(3), E75 (2018).
46. Guryev, V., *et al.* Genetic variation in the zebrafish. *Genome research.* **16**(4), 491-497 (2006).
47. Brown, K.H., *et al.* Extensive genetic diversity and substructuring among zebrafish strains revealed through copy number variant analysis. *Proceedings of the National Academy of Sciences of the United States of America.* **109**(2), 529-534 (2012).

PUBLICATION II

Priming of Innate Antimycobacterial Immunity by Heat-killed *Listeria monocytogenes* Induces Sterilizing Response in the Adult Zebrafish Tuberculosis Model

Luukinen H, Hammarén MM, Vanha-aho L-M, Svorjova A, Kantanen L, Järvinen S, Luukinen BV, Dufour E, Rämet M, Hytönen VP, Parikka M

Disease Models & Mechanisms 2018 11: dmm031658
doi: 10.1242/dmm.031658

© 2018. Published by The Company of Biologists Ltd | Disease Models & Mechanisms (2018) 11, dmm031658. doi:10.1242/dmm.031658

RESEARCH ARTICLE

Priming of innate antimycobacterial immunity by heat-killed *Listeria monocytogenes* induces sterilizing response in the adult zebrafish tuberculosis model

Hanna Luukinen[1], Milka Marjut Hammarén[1,*,‡], Leena-Maija Vanha-aho[1,*], Aleksandra Svorjova[1], Laura Kantanen[1], Sampsa Järvinen[1], Bruno Vincent Luukinen[1], Eric Dufour[1,2], Mika Rämet[1,2,3,4], Vesa Pekka Hytönen[1,2,5] and Mataleena Parikka[1,6]

ABSTRACT

Mycobacterium tuberculosis remains one of the most problematic infectious agents, owing to its highly developed mechanisms to evade host immune responses combined with the increasing emergence of antibiotic resistance. Host-directed therapies aiming to optimize immune responses to improve bacterial eradication or to limit excessive inflammation are a new strategy for the treatment of tuberculosis. In this study, we have established a zebrafish-*Mycobacterium marinum* natural host-pathogen model system to study induced protective immune responses in mycobacterial infection. We show that priming adult zebrafish with heat-killed *Listeria monocytogenes* (HKLm) at 1 day prior to *M. marinum* infection leads to significantly decreased mycobacterial loads in the infected zebrafish. Using *rag1*$^{-/-}$ fish, we show that the protective immunity conferred by HKLm priming can be induced through innate immunity alone. At 24 h post-infection, HKLm priming leads to a significant increase in the expression levels of macrophage-expressed gene 1 (*mpeg1*), tumor necrosis factor α (*tnfa*) and nitric oxide synthase 2b (*nos2b*), whereas superoxide dismutase 2 (*sod2*) expression is downregulated, implying that HKLm priming increases the number of macrophages and boosts intracellular killing mechanisms. The protective effects of HKLm are abolished when the injected material is pretreated with nucleases or proteinase K. Importantly, HKLm priming significantly increases the frequency of clearance of *M. marinum* infection by evoking sterilizing immunity (25 vs 3.7%, P=0.0021). In this study, immune priming is successfully used to induce sterilizing immunity against mycobacterial infection. This model provides a promising new platform for elucidating the mechanisms underlying sterilizing immunity and to develop host-directed treatment or prevention strategies against tuberculosis.

[1]Faculty of Medicine and Life Sciences, FI-33014 University of Tampere, Tampere, Finland. [2]BioMediTech Institute, FI-33014 University of Tampere, Tampere, Finland. [3]PEDEGO Research Unit, and Medical Research Center Oulu, FI-90014 University of Oulu, Oulu, Finland. [4]Department of Children and Adolescents, Oulu University Hospital, FI-90220 Oulu, Finland. [5]Fimlab Laboratories, Pirkanmaa Hospital District, FI-33520 Tampere, Finland. [6]Oral and Maxillofacial Unit, Tampere University Hospital, FI-33521 Tampere, Finland.
*These authors contributed equally to this work

‡Author for correspondence (milka.hammaren@uta.fi)

M.M.H., 0000-0001-9076-8782; B.V.L., 0000-0003-3578-782X; M.P., 0000-0001-5555-3815

Received 7 August 2017; Accepted 21 November 2017

This article has an associated First Person interview with the first author of the paper.

KEY WORDS: *Listeria monocytogenes*, *Mycobacterium marinum*, Mycobacterial infection, Sterilizing immunity, Tuberculosis, Zebrafish

INTRODUCTION

Tuberculosis (TB) is an airborne respiratory disease caused by the intracellular bacterium *Mycobacterium tuberculosis* (Mtb). As few as one to five bacteria can lead to an infection (Rajaram et al., 2014; Cambier et al., 2014). The outcome of TB is highly variable, ranging from rapid clearance by innate immune mechanisms to development of active disease or the formation of a latent infection that can be actively contained inside granulomas but not eradicated. According to Centers for Disease Control and Prevention (CDC) estimates, even one third of the world population is infected with Mtb. However, only 5-10% of this population develops active, primary TB. Commonly, infection with Mtb leads to a latent, asymptomatic disease with the inherent ability to reactivate and disseminate into an active disease even decades after initial exposure, for example in the case of immunosuppression. In 2015, 1.4 million people died of TB and a total of 10.4 million new cases were reported along with an increasing number of multidrug-resistant strains (World Health Organization, 2016; http://www.who.int/tb/publications/2016/en/). Despite available multidrug therapies and the Bacille Calmette–Guérin (BCG) vaccine, TB remains one of the leading infectious killers worldwide. According to a recent study, the standard 6-month antibiotic treatment against TB is ineffective in the eradication of Mtb even in patients with a successful follow through of the antibiotic treatment (Malherbe et al., 2016). As the current preventive and treatment strategies have proven insufficient, new approaches to control the global TB epidemic are urgently needed. Host-directed therapies offer a promising approach to improve the outcome of anti-TB treatments. Host-directed therapies are a form of adjunctive therapy that aim to modulate the host immune responses to eradicate or limit mycobacterial infection (Tobin, 2015).

Mycobacteria are especially successful in evading immune responses. Macrophages are known to limit mycobacterial growth in early infection to some extent (Clay et al., 2007). However, in many cases, the early events of mycobacterial infections are characterized by bacterial dominance. Pathogenic mycobacteria are able to avoid recognition by pattern-recognition receptors and can lure mycobacterium-permissive macrophages to the sites of infection (Cambier et al., 2014). Upon phagocytosis, they block the fusion of phagosomes with lysosomes (Russell, 2011), translocate

to the cytoplasm (Simeone et al., 2012; Houben et al., 2012) and neutralize nitric oxide (NO) species (Flynn and Chan, 2003), allowing them to survive within macrophages. Astonishingly, mycobacteria are even capable of exploiting macrophages for tissue dissemination (Clay et al., 2007). In addition to avoiding innate killing mechanisms, mycobacteria also inhibit transportation of mycobacterial antigens to lymph nodes (Wolf et al., 2008; Reiley et al., 2008; Gallegos et al., 2008), thereby hampering the initiation of adaptive responses (Chackerian et al., 2002). Aggregates of innate and adaptive immune cells, called granulomas, are formed to contain the bacteria and to localize the infection to a limited area without eradicating the bacteria. Depending on the immune status of the host, either an active infection or a latent infection with a life-long risk of reactivation ensues (Barry et al., 2009).

Despite Mtb being good at evading host immune responses and having the ability to cause aggressive active or persistent latent infections, some people are known to be naturally protected against TB. There are significant differences in the ability of individuals to resist mycobacterial infection, reflecting the heterogenic nature of the human population. According to epidemiological data, a 7-43% proportion of heavily exposed individuals are able to clear the infection before the onset of adaptive immunity, resulting in negative tuberculin skin tests and interferon-gamma (Ifnγ) release assays (reviewed in Verrall et al., 2014). With this in mind, it should be possible to shift the balance of host-pathogen interactions in favor of the host by directing the immune response to the right immune activation at the early stages of infection, when the bacterial loads are rather small. Optimal immune activation could prevent mycobacterial evasion strategies, enhance killing of mycobacteria and ideally lead to sterilization of infection. However, to our knowledge, sterilizing antimycobacterial immunity has not been successfully induced *in vivo*.

In this study, we used the zebrafish model to study protective immune responses against mycobacteria at the early stages of infection. The zebrafish has recently become a well-accepted genetically tractable vertebrate model for human TB pathogenesis. Zebrafish are naturally susceptible to *Mycobacterium marinum*, a close genetic relative of Mtb. *M. marinum* causes a disease that shares the main pathological and histological features of human TB, including the formation of macrophage aggregates and granulomas (reviewed in Meijer, 2016; van Leeuwen et al., 2014). As the basic mechanisms of innate and adaptive immunity are conserved from zebrafish to humans, the innate immune responses to *M. marinum* can be studied in zebrafish larvae (Ramakrishnan, 2013), while the adult zebrafish has been proven an applicable model to study also the adaptive responses in TB (Hammarén et al., 2014; Parikka et al., 2012; Oksanen et al., 2013). Even the transition of an acute primary infection to latency and its reactivation can be modeled in the adult zebrafish (Parikka et al., 2012), which has been difficult in other models. Our previous studies have shown that an infection with a low dose of *M. marinum* causes a latent mycobacterial disease with steady bacterial counts in the majority of the fish population, whereas, in a small proportion of the fish (<1.5%), primary active disease leads to mortality (Parikka et al., 2012). Around 10% of the fish are able to clear the mycobacterial infection (Hammarén et al., 2014). The spectrum of different disease outcomes in the *M. marinum*-zebrafish model thus resembles that of human TB.

Here, we have used the zebrafish model to test whether the number of individuals sterilizing the infection can be increased through injection with different priming agents to circumvent mycobacterial virulence strategies, which generally lead to persistent, latent infections (Parikka et al., 2012). Our study shows that the priming of zebrafish with heat-killed *Listeria monocytogenes* results in the sterilization of *M. marinum* infection in one fourth of individuals. The protective effect is caused by a protein and/or nucleic acid component of *L. monocytogenes* and is accompanied by the induction of *tumor necrosis factor α* (*tnfα*) and *nitric oxide synthase 2b* (*nos2b*), and downregulation of *superoxide dismutase 2* (*sod2*). Hereby, we show that the adult zebrafish is a feasible model for deciphering the mechanisms of sterilizing immunity, knowledge of which is crucial for the development of new preventive strategies and adjunctive therapies against TB.

RESULTS

Immune activation by heat-killed *L. monocytogenes* leads to lower mycobacterial burdens in adult zebrafish

In this study, we set out to investigate protective immune responses at the early stages of an *M. marinum* infection. Our hypothesis is that the right immune activation at the early stages of an infection prevents mycobacterial evasion strategies and leads to protective immune responses, increased killing of mycobacteria or even clearing of mycobacteria. To study our hypothesis, we wanted to direct the zebrafish immune response towards an optimal anti-TB response before the onset of an *M. marinum* infection. To find a factor that promotes a protective immune response in the early stages of an infection in adult zebrafish, fish were intraperitoneally (i.p.) injected with different priming agents 1 day before a low-dose i.p. *M. marinum* infection (Fig. 1A,B). Mycobacterial loads of the fish were determined with quantitative real-time PCR (qPCR) from internal organs at 7 weeks post-infection (wpi). We tested eight different agents, including Toll-like receptor (TLR) ligands, vaccine adjuvants and heat-killed bacteria, namely: heat-killed *M. marinum* (HKMm), *L. monocytogenes* (HKLm), *Streptococcus iniae* (HKSi) and *Escherichia coli* (HKEc), lipopolysaccharide (LPS), paclitaxel, muramyl dipeptide (MDP) and zymosan.

In this preliminary experiment, the tested priming agents had variable effects on mycobacterial loads. Priming of the adult fish with HKLm led to a clear decrease in median mycobacterial loads at 7 wpi compared to phosphate-buffered saline (PBS) controls. However, with most of the other tested priming agents, including HKMm, the reduction in mycobacterial loads was not as dramatic as with HKLm (Fig. 1B). Importantly, HKLm priming was the most efficient way to induce bacterial clearance. The frequency of clearance increased by 4.8-fold compared to PBS-primed controls. For paclitaxel, priming led to an increase in mycobacterial loads. With the right dosing, paclitaxel can induce proinflammatory responses (Bracci et al., 2014) but can also be toxic to immune cells (Tang et al., 2017), which might explain the increase in mycobacterial load by paclitaxel. Our results indicate that early immune priming affects mycobacterial loads at 7 wpi and that HKLm is the most promising priming agent with our experimental setup.

To ensure that the reduction in mycobacterial loads in adult fish was not due to direct bactericidal effects of HKLm priming, we incubated *M. marinum* in 7H9 medium together with different concentrations of HKLm (Fig. S1). Based on *in vitro* culturing, HKLm does not kill *M. marinum*, indicating that the lowered mycobacterial burdens in zebrafish induced by HKLm priming is not due to direct killing of the mycobacteria by HKLm, but is mediated through effects on the host immune system.

To characterize the duration of the effect after HKLm priming, we injected fish at either 1 or 7 days prior to infection with *M. marinum*. The mycobacterial loads were determined already at 4 wpi because, at this stage of the infection, bacterial counts have generally reached a steady state and they are easily measurable. Priming 1 day prior to infection was most efficient, increasing the frequency of a clearing

Disease Models & Mechanisms (2018) 11, dmm031658. doi:10.1242/dmm.031658

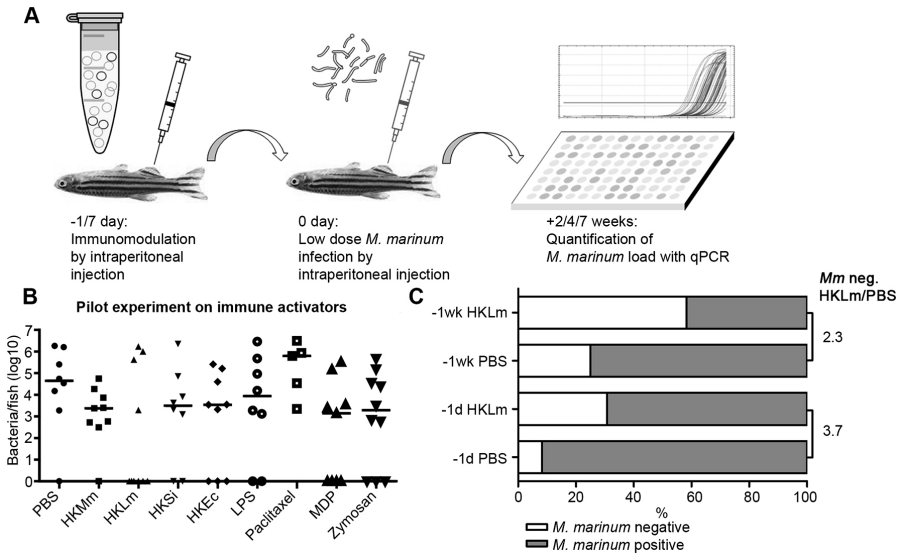

Fig. 1. The effect of priming agents on *M. marinum* loads in adult zebrafish. (A) Outline of the study. Adult wild-type zebrafish were primed with 0.5×10^7-1×10^7 colony-forming units (cfu) per fish of heat-killed bacteria or with other priming agents (13.5 µg per fish, except MDP 4.5 µg) 1 or 7 days prior to *M. marinum* infection (−1/7 day) with an i.p. injection. Sterile 1× PBS was used as an injection control. The following day (0 day), a low dose of *M. marinum* was injected i.p. into the zebrafish. Internal organs were collected either 2, 4 or 7 weeks post infection (wpi), DNA was extracted and the bacterial counts were measured with *M. marinum*-specific qPCR. (B) Priming with heat-killed *L. monocytogenes* (HKLm) reduces mycobacterial loads at 7 wpi. Zebrafish were primed with either PBS (*n*=8), heat-killed *M. marinum* (HKMm; *n*=9), HKLm (*n*=10), heat-killed *S. iniae* (HKSi; *n*=8), heat-killed *E. coli* (KHEc; *n*=9), lipopolysaccharide (LPS; *n*=8), paclitaxel (*n*=5), muramyl dipeptide (MDP; *n*=9) or zymosan (*n*=10) 1 day prior to *M. marinum* infection (16±4 cfu). Organs were collected at 7 wpi. Priming with HKLm led to a bigger decrease in the mycobacterial loads in adult zebrafish compared to other tested priming agents. Paclitaxel increased the mycobacterial loads in adult zebrafish. Medians are shown in the figure. (C) Priming with HKLm 1 day prior to *M. marinum* infection increases the frequency of clearance. The fold change in the percentage of fish that were able to clear the *M. marinum* infection was higher in the group that was primed with HKLm 1 day prior (3.7-fold; PBS: *n*=12, HKLm: *n*=13) to infection compared to group that was primed 7 days (2.3-fold; PBS: *n*=12, HKLm: *n*=12) before the infection.

response by 3.7-fold compared to the control group (7 days: 2.3-fold) in this preliminary experiment (Fig. 1C). Based on these results, we continued with HKLm priming at 1 day before *M. marinum* infection.

Priming with HKLm increases the frequency of clearance of mycobacterial infection in adult zebrafish

To verify our finding from the preliminary priming experiments, zebrafish were primed with an injection of HKLm (Fig. 2A) 1 day prior to *M. marinum* infection, and PBS was used as a negative control. Compared to control treatments, priming with HKLm 1 day before infection consistently led to a significant decrease (14.1-fold decrease, on average) in mycobacterial loads in adult zebrafish at 4 wpi (Fig. 2A shows a representative result of four separate experiments).

From our previous study, we know that, without priming, approximately 10% of *M. marinum*-infected zebrafish are able to naturally clear the mycobacterial infection (Hammarén et al., 2014). Combining the results from four different experiments shows that priming with HKLm 1 day prior to *M. marinum* infection increases the frequency of sterilizing response by 6.8-fold in the wild-type fish at 4 wpi [PBS 3.7% (*n*=54) vs HKLm 25% (*n*=56), *P*=0.0021] (Fig. 2B). However, individuals that have been unable to clear the infection also benefit from HKLm priming in terms of lowered bacterial loads (Fig. S2). In a wild-type population with sustained infection, HKLm reduced the median bacterial load by 11.1-fold (*P*<0.0001).

Innate immune mechanisms mediate HKLm-induced protection against mycobacterial infection

Our results show a beneficial effect of HKLm priming on mycobacterial loads and clearance at 7 wpi (Fig. 1B) and 4 wpi (Fig. 2A), as well as at 2 wpi (Fig. 2C), all of which are late enough stages for both innate and adaptive responses to be active, although it is known that virulent mycobacteria cause a delay in the activation of T-cell responses (Gallegos et al., 2008). To test whether HKLm priming has the same reducing effect on mycobacterial loads in the absence of an adaptive immune response, we used *rag1*$^{-/-}$ mutant fish. Fish lacking *rag1* do not undergo V(D)J recombination, which is essential for the production of the full variety of T- and B-cell receptors. The *rag1*$^{-/-}$ mutants therefore rely solely on their innate immune mechanisms for protection against infections (Wienholds et al., 2002).

When *rag1*$^{-/-}$ mutants were primed with HKLm 1 day before *M. marinum* infection and bacterial loads were measured with qPCR at 4 wpi, HKLm priming caused a similar reduction in bacterial loads in *rag1*$^{-/-}$ mutants (30-fold, *P*=0.0089) as in wild-type fish (9.7-fold, *P*=0.0013) (Fig. 2D,A). Also in *rag1*$^{-/-}$ mutants, priming with HKLm increased the frequency of sterilizing response from 0% (*n*=26) to 17% (*n*=23) (*P*=0.0418) (Fig. 2E). Looking at the fish with a sustained infection (unable to clear the infection), HKLm priming reduced the bacterial load in *rag1* mutants by 7.2-fold (Fig. S2B, not statistically significant). HKLm priming did not affect the cumulative mortality of low-dose-infected wild-type adult fish

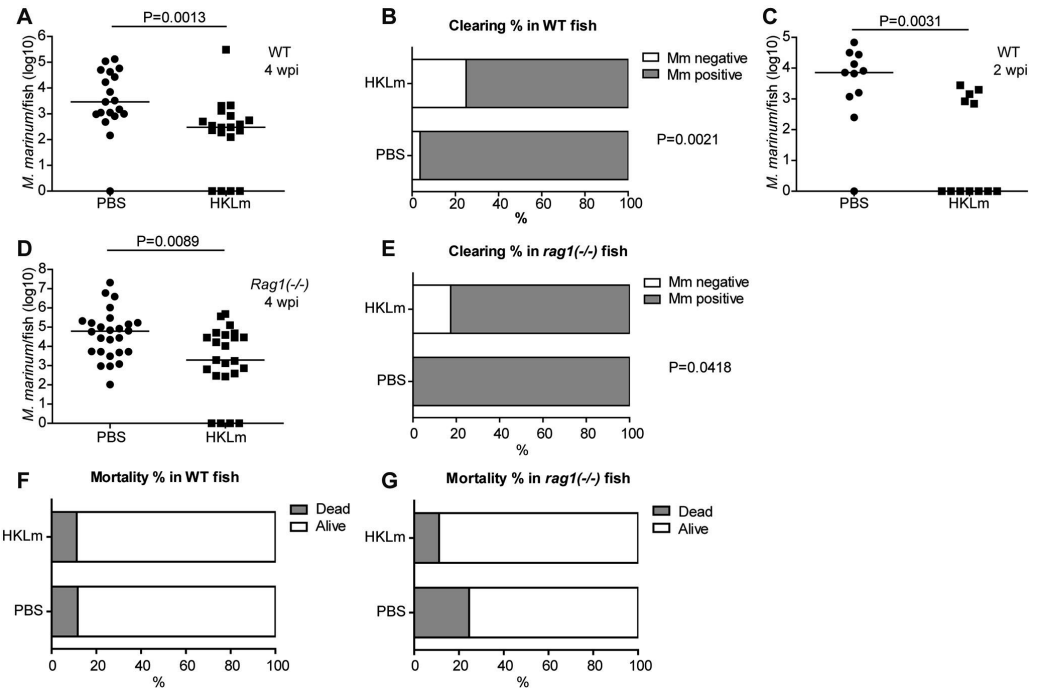

Fig. 2. Priming with HKLm significantly reduces mycobacterial loads in adult zebrafish via innate responses. (A) Priming of adult zebrafish with 0.5×10^7 cfu of HKLm 1 day prior to *M. marinum* infection (27±2 cfu) led to a significant decrease in mycobacterial loads compared to control injection of sterile 1× PBS. The graph shows one representative experiment. Samples were collected at 4 wpi (PBS: *n*=19, HKLm: *n*=19). (B) Priming with HKLm 1 day prior to *M. marinum* infection leads to sterilization of *M. marinum* in 25% of the wild-type (WT) zebrafish. Clearance percentage in the WT PBS control group was 3.7%. The data were collected from four independent experiments. *M. marinum* infection doses in the independent experiments were 27±2 cfu, 26±13 cfu, 75±13 cfu and 26±8 cfu. PBS: *n*=54, HKLm: *n*=56. (C) Priming of adult zebrafish with HKLm leads to a significant decrease in mycobacterial loads compared to PBS controls already at 2 wpi. Infection dose: 48±8 cfu. PBS: *n*=11, HKLm: *n*=12. (D) HKLm priming 1 day prior to *M. marinum* infection significantly reduced mycobacterial loads in *rag1*$^{-/-}$ mutant fish compared to the PBS control group at 4 wpi, indicating a role for innate immune responses. The graph contains a combined result from two separate experiments. *M. marinum* infection doses were 48±8 cfu and 27±2 cfu. (E) Priming with HKLm 1 day prior to *M. marinum* infection leads to sterilization of *M. marinum* in 17% of the *rag1*$^{-/-}$ mutant fish. Clearance percentage in the PBS control group was 0%. Data are pooled from two independent experiments. PBS: *n*=26, HKLm: *n*=23. (F,G) HKLm priming did not affect cumulative mortality in WT adult fish (F; PBS: *n*=152, HKLm: *n*=170), but caused a trend of reduced mortality in HKLm-injected *rag1*$^{-/-}$ mutant fish (PBS: *n*=53, HKLm: *n*=55). *P*-values in A, C and D were calculated with a two-tailed non-parametric Mann–Whitney test with GraphPad Prism. Medians for the individual experiments are shown in the figures. The *P*-values in B, E, F and G were calculated with Fisher's test using GraphPad (QuickCalcs) online software.

(PBS: 11.7%; HKLm: 11.2%) but caused a trend of reduced mortality in *rag1*$^{-/-}$ mutant fish (PBS: 24.5%; HKLm: 11.1%) (Fig. 2F,G). Together, these results imply an important role for innate immunity in the formation of protective HKLm-induced immune responses against mycobacterial infection. Importantly, they show that an optimal response induced by HKLm priming significantly increases the frequency of clearance of mycobacterial infection also in the absence of adaptive immunity.

Protective effects of HKLm priming are not seen in the larval *M. marinum*-infection model

As our results showed that the protective effects of HKLm priming can be mediated through innate immune responses alone, we next used zebrafish larvae to test the effect of HKLm priming on *M. marinum* infection. During the first weeks of development, zebrafish lack adaptive immune responses and rely solely on innate immune responses, making it possible to study mechanisms of mycobacterial infection that arise from innate immunity. To this end, zebrafish larvae were primed with HKLm to induce a protective immune response against *M. marinum* infection. Zebrafish were primed by intravenous injection either at 1 day post-fertilization (dpf) (Fig. S3A) or at 2 dpf (Fig. S3B). *M. marinum* infection was carried out intravenously at 2 dpf. Within this experimental setting, mycobacterial loads were not reduced in zebrafish larvae after priming with HKLm (Fig. S3), possibly due to the immaturity of immune responses in the young larvae or due to the relatively lower HKLm dose that could be delivered into the larvae. As we were unable to see any protective effect in the zebrafish larvae, we continued using adult zebrafish for subsequent experiments.

Protective immunity against *M. marinum* infection is mediated by a protein and/or nucleic acid component of HKLm

Based on the results of the preliminary experiment with different priming agents, HKLm seemed to contain a specific component responsible for the induction of sterilizing immunity. To characterize

Disease Models & Mechanisms (2018) 11, dmm031658. doi:10.1242/dmm.031658

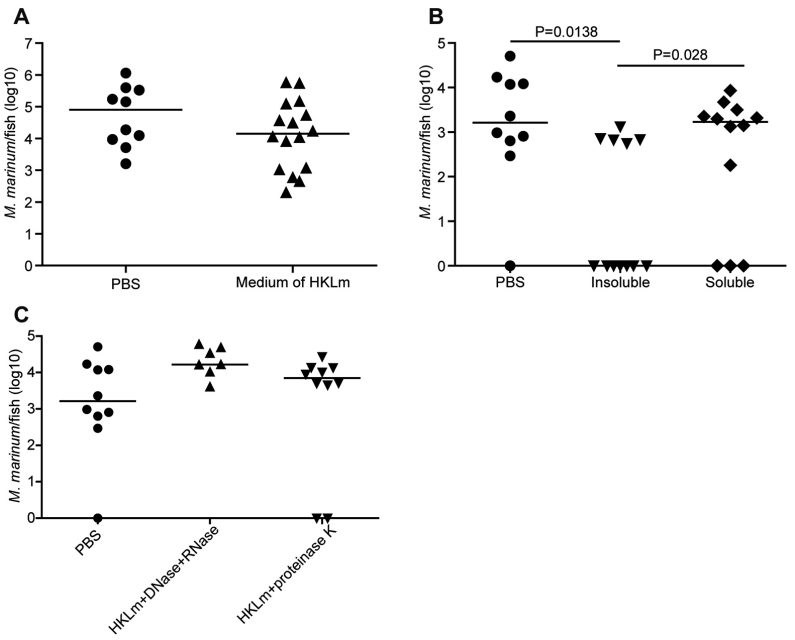

Fig. 3. Protective immunity against *M. marinum* is mediated by a protein and/or nucleic acid component of HKLm. (A-C) Zebrafish were primed with different components of HKLm and *L. monocytogenes* 1 day prior to *M. marinum* infection and mycobacterial loads were determined with *M. marinum*-specific qPCR at 4 wpi. (A) Protective immunity is not mediated by a secreted component in the *L. monocytogenes* growth medium. Infection dose: 26±6 cfu; PBS: *n*=10, medium: *n*=16. (B) Protective immunity is mediated by a component that was found in the insoluble phase. Infection dose: 33±11 cfu; PBS: *n*=10, insoluble: *n*=12, soluble: *n*=12. (C) Protective effect of HKLm priming was lost when HKLm was treated with DNase and RNase, or proteinase K. Infection dose: 33±11 cfu; PBS: *n*=10, DNase and RNase: *n*=7, proteinase K: *n*=8. *P*-values for all experiments were calculated with a two-tailed non-parametric Mann–Whitney test with GraphPad Prism and corrected with the Bonferroni's method. Medians for each experiment are shown.

the protective component(s), we carried out a set of experiments in which zebrafish were primed with different preparations of HKLm 1 day prior to *M. marinum* infection and bacterial growth was analyzed at 4 wpi. Priming with spent *L. monocytogenes* medium did not cause a significant reduction in the mycobacterial loads of the fish, indicating that a secreted factor was not the causative agent behind the activation of antimycobacterial immune responses (Fig. 3A). We also found that, after autoclavation of *L. monocytogenes*, priming with the insoluble material provided a protective effect against *M. marinum* infection, whereas the soluble material was not protective (Fig. 3B). However, we were able to show that treatment of the HKLm extract with either proteinase K or a cocktail of RNase and DNase abolished the protective effect (Fig. 3C). These results indicate that the protective component is stable, resistant to high temperature and pressure, non-secreted, insoluble, and likely consists of both a protein and nucleic acid component.

Therapeutic potential of HKLm treatment

To further characterize the features of HKLm treatment, a 30-fold higher HKLm dose was injected 1 day prior to low-dose *M. marinum* infection. With such a high dose, HKLm lost its beneficial effects (Fig. 4A) and there was a trend of increased mortality of the fish by 4 wpi (PBS: 22.7%; HKLm: 41.7%) (Fig. 4B). According to these results, it was concluded that, by increasing the HKLm dose, it is not possible to further boost the protective effect but rather *vice versa*. The optimal dosage thus plays a crucial role in inducing a protective response.

We then tested whether priming with HKLm 1 day prior to infection could protect fish against a high-dose infection challenge with 4883±919 colony-forming units (cfu) of *M. marinum*. In the context of a high-dose infection, HKLm did not induce significant difference in the mycobacterial loads, clearance or cumulative end-point mortality at 4 wpi (Fig. 4C,D).

We next wanted to test whether HKLm can induce protective immune responses if the mycobacterial infection is already established. We have previously shown in adult zebrafish that, at 2 wpi, *M. marinum* infection is well established and granulomas have already started to form (Parikka et al., 2012). We infected adult zebrafish with a low dose of *M. marinum*, injected HKLm at 2 wpi and measured mycobacterial loads, as well as determined the cumulative mortality at 4 wpi. Based on our results, at a time point in which the mycobacteria have already multiplied substantially and started forming granulomas, HKLm injection was not able to lower the bacterial loads, increase bacterial clearance or affect cumulative mortality (Fig. 4E,F).

Priming adult zebrafish with HKLm induces *mpeg1*, *tnfα* and *nos2* expression, and downregulates *sod2*, at the early phase of mycobacterial infection

We were interested in further characterizing the nature of the immune response induced by HKLm priming in adult zebrafish. We hypothesized that the protective effect could be mediated through enhanced killing of mycobacteria at the early phase of the infection due to changes in the numbers or activity of innate immune cells. To study the details of HKLm-induced immune activation by qPCR, the fish were primed with HKLm or PBS, infected with a low dose of *M. marinum* 1 day after priming and the total RNA was extracted from zebrafish organs collected 1 day post-infection (dpi). First, the possible effects of HKLm treatment on the number of macrophages and neutrophils were assessed by measuring the expression of *macrophage expressed gene 1* (*mpeg1*) (Ellett et al., 2011) and *myeloid-specific peroxidase* (*mpx*) (Lieschke et al., 2001), respectively. In the HKLm group, *mpeg1* expression was significantly higher than in the control group (Fig. 5A; HKLm: 59.9-fold; PBS: 39.3-fold; P=0.0352), suggesting that the number of macrophages was increased due to HKLm priming. The expression of *mpx* was not affected by HKLm (Fig. 5B).

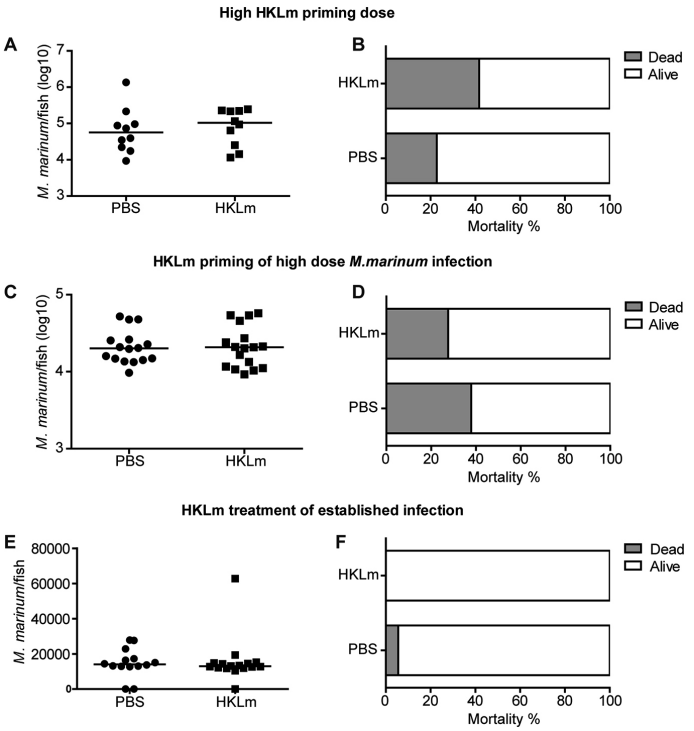

Fig. 4. HKLm treatment does not protect against high-dose or established *M. marinum* infection. (A,B) Protective effect of HKLm priming is lost with high-dose priming. Fish were injected with a high dose of HKLm (15.6×10^7 cfu, 30-fold compared to previous dose) 1 day prior to *M. marinum* infection (34±11 cfu). Priming with a high dose of HKLm did not reduce mycobacterial numbers (A) and led to an increase in the mortality of the fish at 4 wpi (B). PBS: *n*=10, HKLm: *n*=10. (C,D) HKLm priming does not protect from high-dose *M. marinum* infection. Fish were primed with HKLm 1 day prior to high-dose *M. marinum* infection (4883±919 cfu). No effect was observed on bacterial loads (C) or cumulative end-point mortality (D). PBS: *n*=16, HKLm: *n*=17. (E,F) HKLm does not protect against an established *M. marinum* infection. Fish were injected with HKLm 2 weeks after an *M. marinum* infection (22±6 cfu). No effect on mycobacterial loads (E) or cumulative end-point mortality (F) was observed. PBS: *n*=14, HKLm: *n*=16. *P*-values for bacterial loads were calculated with a two-tailed non-parametric Mann–Whitney test with GraphPad Prism (A,C,E). Medians for the experiments are shown.

To assess the HKLm-induced changes at the level of immune cell activation, we measured the expression of a selection of markers related to the effective antimycobacterial functions of innate immune cells 1 day after *M. marinum* infection. Based on literature on the mechanisms limiting intracellular mycobacterial growth, the genes chosen for analysis were *tnfα* (Cobat et al., 2015; Roca and Ramakrishnan, 2013), *ifnγ* (Flynn et al., 1993) and *nos2b* (Nicholson et al., 1996; Thoma-Uszynski et al., 2001). Expression of *ifnγ* was not differentially induced between PBS- and HKLm-treated groups (Fig. 5C,D). The median expression levels of *tnfα* (Fig. 5F; HKLm 10.3-fold vs PBS 1.1-fold, *P*=0.0043) and *nos2b* (Fig. 5G; HKLm 10.7-fold vs 0.6-fold PBS, *P*=0.0001) were significantly increased in the HKLm-primed group compared to the PBS control group. We also analyzed the expression levels of *sod2*, which encodes a mitochondrial protein that converts the byproducts of oxidative phosphorylation to hydrogen peroxide and oxygen, leading to neutralization of mitochondrial reactive oxygen species (ROS) (Pias et al., 2003) and *arg1*, which is an alternative macrophage activation marker (Gordon and Martinez, 2010). In the HKLm group, *sod2* expression was significantly more downregulated as compared to the PBS group, indicating increased levels of ROS due to HKLm priming (PBS 0.59-fold vs HKLm 0.27-fold, *P*=0.0022) (Fig. 5H). *Arg1*, however, was not induced in HKLm-primed fish, suggesting that alternative activation does not have an impact on the early mycobacterial elimination (Fig. 5E). Together, these results suggest that HKLm induces M1-type classical macrophage activation leading to enhanced intracellular killing at the early stages of a mycobacterial infection.

Priming of macrophages with HKLm leads to decreased oxygen consumption *in vitro*

Classically activated M1 macrophages have been shown to change their metabolism upon immune activation (Cheng et al., 2014). To test whether this is also the case with HKLm priming, we set up a RAW264.7 cell culture and primed them either with LPS (50 ng/µl) or HKLm (MOI: 530). At 19-24 h later, oxygen consumed by these cells was measured using a Clark electrode. We used LPS as a positive control and showed that both treatments lower the oxygen consumption significantly (Fig. 5I). Pooled result from three independent experiments concluded that HKLm- or LPS-primed mouse macrophages consume, respectively, 1.8-times (*P*=0.008) and 2.3-times (*P*=0.0042) less oxygen compared to untreated cells, *in vitro* (Fig. 5I). This result implies that HKLm-treated macrophages exhibit metabolic changes indicative of diminished oxygen similar to those observed during classical macrophage activation.

DISCUSSION

Despite substantial progress in the field of medicine, TB still kills millions of people every year and has been declared a global public health crisis (World Health Organization, 2016; http://www.who.int/tb/publications/2016/en/). The advances in the battle against TB have been hindered by the complex nature of the disease and the limitations of tuberculosis animal models. TB manifests itself in a wide spectrum of disease, with most affected individuals being unable to eradicate the causative bacteria (Mtb), leading to the development of latent TB infection, which has a lifetime risk of reactivation in 5-10% of cases. The World Health Organization has

Disease Models & Mechanisms (2018) 11, dmm031658. doi:10.1242/dmm.031658

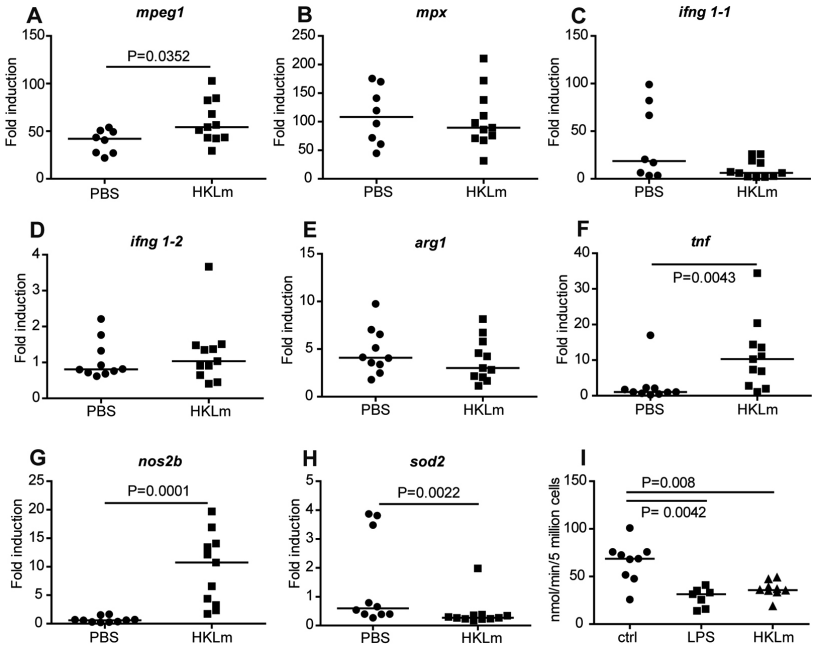

Fig. 5. HKLm priming induces *mpeg*, *tnfα* and *nos2b* expression, downregulates *sod2* expression in adult zebrafish and leads to decreased oxygen consumption *in vitro*. (A-H) The expression levels of *mpeg* (A), *mpx* (B), *ifnγ1-1* (C), *ifnγ1-2* (D), *arg1* (E), *tnfα* (F), *nos2b* (G) and *sod2* (H) were measured with qPCR from wild-type fish primed with HKLm or sterile PBS buffer as a control. At 1 day after the priming, the fish were infected with a low dose (67±16 cfu) of *M. marinum*. Samples for qPCR analysis were collected at 1 dpi. The results were normalized to uninfected wild-type baseline control. PBS: *n*=10, HKLm: *n*=11. (I) HKLm priming leads to metabolic changes *in vitro*. RAW264.7 cells were primed with LPS or HKLm and oxygen consumption was measured 19-24 h after priming. HKLm priming leads to a 1.8-fold decrease (*P*=0.008) in oxygen consumption compared to control. LPS was used as a positive control (2.3-fold decrease, *P*=0.0042). PBS: *n*=9, LPS: *n*=7, HKLm: *n*=9. *P*-values for all experiments were calculated with a two-tailed non-parametric Mann–Whitney test with GraphPad Prism. Medians for each experiment are shown. Bonferroni correction was used in C.

estimated that 2-3 billion people are latently infected with Mtb (World Health Organization, 2016), creating a huge pool of individuals with a potential to develop an active, transmissive disease. As current vaccination and antibiotic schemes have proven insufficient for controlling the global TB epidemic, host-directed therapies inducing protective immune responses are emerging as a novel strategy to treat TB (Tobin, 2015). Efficient host-directed therapies used either alone or in combination with antibiotics are an approach that could potentially lead to sterilization of TB.

Although genome-wide association studies carried out in humans have given important clues on the nature of protective immune responses against TB (Azad et al., 2012; Wilkinson et al., 2000; Cobat et al., 2009, 2015), animal models are essential for the execution of more mechanistic studies. The mouse, rabbit and macaque have been widely used to study TB (Myllymäki et al., 2015). To the best of our knowledge, spontaneous or induced sterilizing immunity has not been observed at the organismal level in mammalian animal models of TB. Clearance of cultivable mycobacteria occurs in the rabbit model (Subbian et al., 2012). However, standard bacterial culturing methods only detect the actively replicating mycobacterial populations, but not dormant bacteria (Chao and Rubin, 2010), and, in the rabbit, the clearance of cultivable mycobacteria indicates the establishment of a truly latent disease instead of sterilization (Subbian et al., 2012). The zebrafish has recently become a well-accepted genetically tractable vertebrate model for human TB pathogenesis to complement the more traditional mammalian models (Myllymäki et al., 2015). In our previous study, using a qPCR-based method, we were able to see spontaneous clearance of mycobacterial infection in the zebrafish-*M. marinum* infection model in approximately 10% of the fish at 4 wpi (Hammarén et al., 2014). As we observed no clearance at 2 wpi (Hammarén et al., 2014), spontaneous early clearance (likely induced by innate mechanisms) in our wild-type zebrafish population is a rare event. In this current study, we were able to increase the frequency of sterilizing mycobacterial infection by priming the innate immune response prior to *M. marinum* infection.

Our hypothesis was that priming or stimulation of the immune response in the adult zebrafish before *M. marinum* infection could lead to a sterilizing immune response instead of a lethal primary active disease or a latent infection that is prone to reactivation later in life (Parikka et al., 2012). By using an array of different priming agents, we wanted to study whether we could create a climate that would allow the immune response to circumvent their efficient virulence strategies and even eradicate the mycobacteria. Priming approaches have been successful in inducing protective responses against various other bacterial infections in the fruit fly, *Drosophila melanogaster*, which relies solely on innate immunity (Pham et al., 2007). Indeed, our results showed that sterilizing immunity can be induced in the *M. marinum* zebrafish model. In our hands, priming with HKLm induces a sterilizing response in 25% of *M. marinum*-

infected fish at 4 wpi, whereas the percentage of spontaneous clearance was 3.7% in the PBS-primed control group.

The *M. marinum*-specific qPCR used to quantify bacterial loads is a sensitive method, with a detection limit of approximately 100 bacterial genomes in the entire fish (Parikka et al., 2012; Hammarén et al., 2014). The major advantage of a qPCR-based method over culturing methods is that qPCR detects all bacterial genomes irrespective of metabolic state so that dormant bacteria are also detected. An advantage of the zebrafish is that, due to its small size, all infection target organs can be collected for determination of bacterial load, which is not practically feasible in larger animals. Based on the qPCR results, we are able to say that 25% of the wild-type fish were able to clear the infection, indicating that HKLm priming indeed increases the frequency of sterilizing immune response. This model provides tools for elucidating the detailed mechanisms behind sterilizing immunity against TB.

To study whether the protective effects of HKLm priming require a functional adaptive immune system, we used *rag1* mutant zebrafish. Although *rag1* mutant zebrafish are known to be hypersusceptible to *M. marinum* infection due to a failure in the development of functional T and B cells (Swaim et al., 2006; Parikka et al., 2012), their bacterial loads were significantly lowered and even cleared by HKLm priming, suggesting that the protective response can be mediated by innate immunity alone. The role of innate immunity is also supported by the significant HKLm-induced reduction in bacterial loads as early as 2 wpi in wild-type fish, by which time adaptive responses are only starting to arise in mycobacterial infections (Andersen and Woodworth, 2014). Despite the clear involvement of innate responses in HKLm-induced protective responses in adult fish, the results could not be reproduced in young zebrafish larvae that have only innate immunity, probably due to an immature immune response and technical difficulties to deliver high enough doses of HKLm by microinjection methods. As adaptive responses are centrally involved in the pathogenesis of mycobacterial infections, using the adult zebrafish will likely better model the effects of immunomodulatory treatments on the immune response as a whole. On top of the protective effects of HKLm mediated through innate immunity, an additional level of protection was observed in the presence of a functional adaptive immune system in zebrafish. However, the observation that activation of innate immunity alone by immune priming with HKLm in some cases was sufficient for induction of a protective or sterilizing immunity opens new avenues for host-directed therapies or preventive strategies even in the absence of a fully functional adaptive immune system, such as in patients with an HIV co-infection.

At the moment, there is no immunotherapy that could cure an ongoing mycobacterial infection by simply boosting the immune system. Therefore, we wanted to study whether HKLm could induce a protective response during an established mycobacterial infection. A single dose of HKLm was injected 2 weeks after *M. marinum* infection, when early granulomas have started to form and are visible in various organs (Parikka et al., 2012). However, this single injection of HKLm did not decrease mycobacterial loads at 4 wpi (Fig. 4E,F). By this time point, *M. marinum* has already had plenty of time to exert its early virulence strategies leading to effective avoidance of the pro-inflammatory host immune response (Elks et al., 2014; Queval et al., 2016; Bhat et al., 2017; Cambier et al., 2014). Having gained a foothold within its host, mycobacteria are not as prone to the effects caused by a single therapeutic injection of HKLm as they are when entering a primed host. Adult zebrafish have also been used to model active fulminant TB by infecting individuals with a high *M. marinum* dose (Parikka et al., 2012). Individuals infected with a high *M. marinum* dose did not benefit from HKLm priming. The high infection dose of a few thousand mycobacteria leads to a disease state in which the capacity of the immune system rapidly becomes saturated, allowing the bacteria to grow almost logarithmically (Parikka et al., 2012) possibly due to the limited number of macrophages (Pagán et al., 2015) compared to the low infection dose; a situation too challenging to overcome even in the presence of HKLm priming. However, in our preliminary experiments, we saw that, in addition to priming 1 day prior to infection, protective effects were still visible when HKLm priming was delivered 1 week prior to *M. marinum* infection (Fig. 1C), suggesting that this type of protective response could be considered in designing new preventive strategies.

The protective effects of HKLm treatment delivered prior to infection could be mediated through the induction of trained immunity. It is known that innate immune cells can mediate an enhanced immune response upon reinfection with the same pathogen (Quintin et al., 2012). The innate immune system can also cross-react with a new pathogen according to previous stimuli (Kleinnijenhuis et al., 2014). It has been reported that some vaccines can produce durable cross-protection that cannot be explained by adaptive responses (Aaby et al., 2014). This type of nonspecific innate memory is referred to as trained immunity. Mechanisms of trained immunity have also been shown to be responsible for BCG-induced by-stander protection against *Candida albicans* in the mouse (Van't Wout et al., 1992). Innate memory is mediated through reversible epigenetic changes rather than irreversible genetic recombination seen during the formation of classical immunological memory in adaptive immune cells and can last for weeks to months (reviewed by Netea et al., 2016). The effects of trained immunity in the context of susceptibility to TB is an interesting area of research and can yield new approaches in the development of preventive strategies based on innate immunity.

It has been reported that the number of macrophages is critical for the disease outcome and that macrophage deficiency is connected to accelerated progression of mycobacterial infection (Pagán et al., 2015). To assess the effect of HKLm priming on the number of macrophages and neutrophils, we measured the expression of the commonly used markers *mpeg1* (Ellett et al., 2011) and *mpx* (Lieschke et al., 2001), respectively. Based on the expression of these markers, the number of macrophages was significantly higher in HKLm-primed fish (P=0.0352), whereas the amount of neutrophils remained unchanged (Fig. 5A,B). This change seen in macrophages is potentially mediating the protective response against mycobacteria.

To decipher the type of protective immune response induced by HKLm priming, we measured an array of genes related to innate immune activation in the organs of *M. marinum*-infected zebrafish at 1 dpi. In line with *in vitro* studies on *Listeria* (Barbuddhe et al., 1998; Mirkovitch et al., 2006), *in vivo* priming with HKLm caused a significant increase in *nos2b* and *tnfα* with a simultaneous decrease in *sod2* expression. *nos2b* is one of the NO synthases in zebrafish (Lepiller et al., 2009). NO is known to be mycobacteriocidal (Nicholson et al., 1996) but, as pathogenic mycobacteria have developed evasion strategies to inhibit the production of NO (Elks et al., 2014; Queval et al., 2016; Bhat et al., 2017), the NO levels naturally induced in Mtb-infected macrophages seem to be insufficient for lysing mycobacteria (Jung et al., 2013). Thus, the additional production of Nos caused by HKLm prior to infection likely potentiates the intracellular killing mechanisms. The beneficial effects of increased NO in neutrophils (Elks et al., 2013) as well as in

macrophages (Cambier et al., 2014) during early *M. marinum* infection have previously been demonstrated in zebrafish larvae. Cambier and colleagues showed that virulent mycobacteria avoid NO-mediated intracellular killing during the early phase of infection by hiding their TLR ligands under a phthiocerol dimycoceroserate coat (Cambier et al., 2014). Co-infecting zebrafish larvae with *M. marinum* and *Staphylococcus aureus* or *Pseudomonas aeruginosa* leads to attenuation of mycobacterial infection (Cambier et al., 2014). Also, co-injection of live *M. marinum* with heat-killed *M. marinum* or with a mutant with exposed TLR ligands caused similar attenuation (Cambier et al., 2014). It is likely that at least part of the protective effects caused by HKLm in the adult zebrafish are mediated through TLR ligands. The component analysis of HKLm suggested that nucleotides were important for HKLm-mediated protection against *M. marinum*. TLR9, which recognizes double-stranded DNA and leads to the induction of Nos2 (Ito et al., 2005), is a receptor potentially responsible for the protection. However, detailed analysis of the signaling pathways activated by HKLm treatment was beyond the scope of this study.

Tnfα is also known to mediate intracellular killing of mycobacteria by macrophages (Roca and Ramakrishnan, 2013) and optimal levels of this cytokine have been proposed to lead to early clearance of TB in humans (Cobat et al., 2015). Studies in zebrafish larvae have shown that high Tnfα levels alongside high ROS levels within macrophages, during the early days of mycobacterial infection, is bactericidal (Roca and Ramakrishnan, 2013). Sod2 is an enzyme that acts through neutralization of mitochondrial ROS (Pias et al., 2003). Its downregulation by HKLm should thus cause an increase in mitochondrial ROS, the high levels of which have been shown to enhance intracellular killing mechanisms within macrophages (reviewed in Hall et al., 2014). Recently, in a human population study, a genetic variant leading to reduced activity of *Sod2* was found to be associated with increased resistance to leprosy, a disease caused by *Mycobacterium leprae* (Ramos et al., 2016). Therefore, a likely mechanism of clearing the mycobacterial infection by HKLm priming in the adult zebrafish model is mediated through increased Tnfα and decreased Sod2 production that together lead to higher, mycobacteriocidal, levels of ROS within macrophages.

Roca and Ramakrishnan also showed that, when the expression of Tnfα is endogenously high, continuously high ROS levels after the first days of infection lead to excessive inflammation, necrosis and exacerbation of the disease (Roca and Ramakrishnan, 2013). This probably also explains the increased mortality with the higher HKLm dose. With a single small dose of HKLm used in our study, the effects of the treatment were undoubtedly positive, but it must be kept in mind that excessive or prolonged induction of Tnfα and ROS can also have detrimental effects. The dosage of treatment as well as the genotype of the host, affecting the baseline production of inflammatory cytokines, will also need to be carefully considered in the development of host-directed immunomodulatory treatments.

Based on the gene expression data, the changes in the innate immunity induced by HKLm in the adult zebrafish seem to be mediated through an increased number and activation of M1-type macrophages. Recent research on the metabolism of different innate immune cells has shown that M1 macrophages have decreased oxygen consumption, and increased glycolysis and lactate production (Cheng et al., 2014). In our experiments, the oxygen consumption of mouse macrophages was significantly decreased by HKLm priming (Fig. 5I), providing a further piece of evidence of M1 macrophages playing a central role in HKLm-mediated protection against mycobacterial infection. The result also implies that the types of activation caused by HKLm in the zebrafish are similar to those induced in mammalian macrophages.

Overall, we show that protective and even sterilizing immune responses can be induced in the zebrafish model for TB by priming with HKLm. The response is induced even in the absence of adaptive immunity and is accompanied by the increase in the number of macrophages, the induction of *tnfα* and *nos2b*, and the downregulation of *sod2*, likely leading to increased production of radical nitrogen and oxygen species and enhanced intracellular killing of mycobacteria. Based on our results, it seems that the type of activation induced by HKLm treatment is only effective when delivered at an early enough time point prior to exposure to pathogenic mycobacteria. The model provides a platform in which both innate and adaptive mechanisms leading to sterilization of mycobacterial infection can be reliably studied. Such knowledge will contribute to the development of new vaccination strategies as well as host-directed therapies aimed at prevention of transmission and sterilizing treatment of TB disease.

MATERIALS AND METHODS

Zebrafish lines and housing

Adult 5- to 10-month-old male and female AB wild-type zebrafish (*Danio rerio*) and *rag1*$^{-/-}$ (hu1999) mutant zebrafish (from Zebrafish International Resource Center, University of Oregon, OR, USA) were used in the experiments. The fish were housed in flow-through water-circulation systems with a 14 h/10 h light/dark cycle.

Ethics statement

All experiments were conducted according to the Finnish Act on Animal Experimentation (62/2006) and the Act on the Protection of Animals Used for Scientific or Educational Purposes (497/2013). ELLA (Eläinkoelautakunta; the National Animal Experiment Board in Finland under the Regional State Administrative Agency for Southern Finland) approved the Tampere zebrafish facility and the animal experiments carried out in this project under the licenses ESAVI/6407/04.10.03/2012, ESAVI/8245/04.10.07/2015 and ESAVI/10079/04.10.06/2015.

Experimental *M. marinum* infections

Mycobacterium marinum (ATCC 927) was first pre-cultured on Middlebrook 7H10 plates with OADC enrichment (Fisher Scientific, NH, USA) at 29°C for 1 week. After plate culturing, *M. marinum* was transferred into Middlebrook 7H9 medium with ADC enrichment (Fisher Scientific, NH, USA) with 0.2% Tween-80 (Sigma-Aldrich, MO, USA), cultured for 3-4 days, diluted 1:10 and cultured for a further 2 days until OD600 nm reached 0.460-0.650. For adult zebrafish infections, *M. marinum* was first harvested by centrifuging for 3 min at 10,000 ***g*** and was then resuspended and diluted in sterile 1× PBS with 0.3 mg/ml of Phenol Red (Sigma-Aldrich, MO, USA). A total of 5 µl of the suspension (33±19 cfu/fish) was injected i.p. with an Omnican 100 30 G insulin needle (Braun, Melsungen, Germany) under 0.02% 3-aminobenzoic acid ethyl ester (pH 7.0) (Sigma-Aldrich, MO, USA) anesthesia. Infection doses were verified by plating 5 µl of the injection suspension on a 7H10 plate.

For larval infections, the *M. marinum* pTEC15 strain was used. This in-house-made *M. marinum* wasabi-fluorescent strain was made by transforming a pTEC15 plasmid (Addgene plasmid #30174, deposited by Lalita Ramakrishnan; Takaki et al., 2013) into the *M. marinum* ATCC 927 strain by electroporation. For larval infections, the *M. marinum* pTEC15 strain was cultured for 4-5 days in supplemented 7H9 medium with 75 µg/ml hygromycin (Merck, Darmstadt, Germany), diluted 1:10, cultured for 3 days until the OD600 nm was 0.407-0.537 and harvested for infection by centrifugation.

Zebrafish larval infection experiments

To study the effect of HKLm priming in zebrafish larvae, 1 nl of HKLm (240 cfu) or PBS control were injected into the caudal vein at 1 dpf under

0.0045% 1-phenyl-2-thiourea (Sigma-Aldrich, MO, USA) anesthesia. At 2 dpf the larvae were infected with 1 nl of *M. marinum* (39±13 cfu) into the blood circulation valley, transferred to fresh E3 medium and kept at 29°C. At 8 dpi, larvae were collected for DNA extraction with TRI Reagent (Fisher Scientific, NH, USA). DNA extraction was performed according to the manufacturer's instructions, after which *M. marinum*-specific qPCR was used to quantify mycobacteria.

For the quantification of pTEC15 fluorescence, 1-dpf wild-type AB embryos were dechorionated and kept in E3 medium with 0.0045% 1-phenyl-2-thiourea (Sigma-Aldrich, MO, USA) at 29°C to prevent pigmentation. A total of 1 nl of wasabi-fluorescent *M. marinum* suspension (39±16 cfu) with 0.6 mg/ml of Phenol Red (Sigma-Aldrich, MO, USA) and 490 cfu of HKLm were microinjected into the blood circulation valley at 2 dpf with a glass microcapillary. *M. marinum* infection doses were verified by plating the injection doses on a 7H10 agar plate. After infection, the larvae were kept in E3 medium with 0.0045% 1-phenyl-2-thiourea (Sigma-Aldrich, MO, USA) on 24-well plates at 29°C.

At 7 dpi, larvae were anesthetized with 0.02% 3-aminobenzoic acid ethyl ester (pH 7.0) (Sigma-Aldrich, MO, USA). The larvae were embedded on their side in 1% low-melt agarose in E3 medium on black 96-proxiplates (Perkin-Elmer, MA, USA). Extra E3 medium with the anesthetic was added on top of the solidified low-melt agarose to prevent the larvae from drying. The wasabi-fluorescent signal was measured three times using the EnVision plate reader (Perkin-Elmer, MA, USA) scanning program. The scan measurement was carried out on five horizontal and five vertical dots 0.5 mm apart from 6.5 mm height with 100% excitation at 493 nm, 509 nm emission and 500 flashes per point. The fluorescent signals of individual zebrafish larvae were normalized with the average signal from healthy non-infected larvae.

Preparation of heat-killed bacteria and priming injections

For the preparation of heat-killed bacteria, *L. monocytogenes* (10403S), *E. coli* (ATCC 25922), *S. aureus* (ATCC 29213), *S. typhimurium* (ATCC 14028) and *S. iniae* (ATCC 29178) were inoculated from glycerol stocks or blood agar plates and cultured in brain heart broth (BHB) (Sigma-Aldrich, MO, USA) at 37°C until the OD600 nm reached 0.9-1.0. Bacterial suspensions were plated on LB agar plates to verify bacterial concentrations. To heat-kill bacteria, the bacterial suspensions were autoclaved in BHB at 120°C for 20 min and the sterility was confirmed by plating on LB plates after autoclaving. Injection doses of heat-killed bacteria for adult zebrafish were 0.5×10^7-1×10^7 cfu. Injection doses for other priming agents were 13.5 µg/fish for LPS (Sigma-Aldrich, MO, USA), paclitaxel (Sigma-Aldrich, MO, USA) and zymosan (Sigma-Aldrich, MO, USA), and 4.5 µg/fish for muramyl-dipeptide (Sigma-Aldrich, MO, USA). Priming i.p. injections (5 µl) were injected with an Omnican 100 30 G insulin needle (Braun, Melsungen, Germany) under 0.02% 3-aminobenzoic acid ethyl ester (pH 7.0) anesthesia.

DNase, RNase and proteinase K treatment of HKLm

DNase and RNase treatments were performed for autoclaved *L. monocytogenes* in BHB medium. Heat-killed bacterial suspension was incubated with 10 µg/ml of RNase A (Thermo Fisher Scientific, NH, USA) at 37°C for 18 h. After RNase treatment, the suspension was treated with 83 U/ml DNase I (Thermo Fisher Scientific, NH, USA) according to the manufacturer's instructions. Accordingly, HKLm was treated with 10 µg/ml of proteinase K (Thermo Fisher Scientific, NH, USA) at 37°C for 18 h and inactivated at 70°C for 15 min before injections.

RNA and DNA extractions from zebrafish samples

For RNA and DNA extractions, adult zebrafish were first euthanized with an overdose of 3-aminobenzoic acid ethyl ester anesthetic and then internal organs were collected from the body cavity. Organs were homogenized in TRI Reagent (Thermo Fisher Scientific, NH, USA) with ceramic beads using the PowerLyzer24 (Mobio, CA, USA) bead beater at 3200 rpm for 3×40 s. Samples were cooled on ice between the cycles. After homogenization, samples were sonicated for 9 min and the RNA and DNA were extracted according to the manufacturer's instructions.

Gene expression studies and quantifying mycobacterial loads by qPCR

Prior to qPCR analysis, RNA was treated with DNase I (Thermo Fisher Scientific, NH, USA) to remove possible traces of genomic DNA according to the manufacturer's instructions. After DNase treatment, RNA was reverse transcribed into cDNA with a Reverse Transcription kit (Fluidigm, CA, USA) according to the manufacturer's instructions. Gene expression was measured by using SsoFast EvaGreen Supermix with Low ROX qPCR kit (Bio-Rad, CA, USA) with the CFX96 qPCR system (Bio-Rad, CA, USA). Zebrafish genes were normalized with expressed repetitive element *loopern4* (Vanhauwaert et al., 2014) and compared with the average induction of pooled baseline sample of healthy non-infected zebrafish. Results were analyzed using the ΔCt method and are shown as fold induction.

Mycobacterial loads were measured with the SensiFAST SYBR No-ROX qPCR kit (Bioline, London, UK) from genomic DNA according to the manufacturer's instructions. Each bacterial quantification qPCR run included standard curve of known amounts of *M. marinum* DNA. Primer sequences and gene association numbers are shown in Table 1.

Table 1. Primer pairs used in qPCR

Name	Gene	Primer sequences (5′-3′)
ifnγ1-2	ZDB-GENE-040629-1	F: GGGCGATCAAGGAAAACGACCC R: TAGCCTGCCGTCTCTTGCGT
ifnγ1-1	ZDB-GENE-060210-1	F: CCAGGATATTCACTCAGTCAAGGC R: TGTGGAGGCCCGATAATACACC
loopern4	Expressed repetitive elements	F: TGAGCTGAAACTTTACAGACACAT R: AGACTTTGGTGTCTCCAGAATG
nos2b	ZDB-GENE-080916-1	F: TCACCACAAAAGAGCTGGAATTCGG R: ACGCGCATCAAACAACTGCAAA
sod2	ZDB-GENE-030131-7742	F: GGCCATAAAGCGTGACTTTG R: GCTGCAATCCTCAATCTTCC
tnf	ZDB-GENE-050317-1	F: GGGCAATCAACAAGATGGAAG R: GCAGCTGATGTGCAAAGACAC
arg1	ZDB-GENE-040724-181	F: TGGGAATAATAGGCGCTCCGTTC R: TCCTTCACCACACAACCTTGC
mpeg1	ZDB-GENE-081105-5	F: CTTCTGTTTCAGCATCAGCCG R: ATAAAGCTCCTCCGTGGCTC
mpx	ZDB-GENE-030131-9460	F: AACACTGAACTAGCCCGCAA R: CAACCTATCGCCATCTCGGA
16S–23S ITS	Locus AB548718 for *M. marinum* quantification	F: CACCACGAGAAACACTCCAA R: ACATCCCGAAACCAACAGAG

F, forward; R, reverse.

Measurement of oxygen consumption in HKLm-primed RAW264.7 cells

To measure oxygen consumption, RAW264.7 cells (ATCC TIB-71) were cultured in Dulbecco's modified Eagle's medium with 4.5 g/l D-glucose and L-glutamine (Gibco, Thermo Fisher Scientific, NH, USA) supplemented with 10% of heat-inactivated fetal bovine serum (Gibco, Thermo Fisher Scientific, NH, USA) and 100 U/ml penicillin-streptomycin (Thermo Fisher Scientific, NH, USA) at 37°C with 5% CO_2. The cells were primed either with 50 ng/ml of LPS or HKLm to correspond to an MOI of 530. At 19-24 h later the media was changed to fresh media including priming agents. A minimum of 30 min later the oxygen consumption from 5 million cells was measured at 37°C in their culture media using a Clark electrode (Hansatech, UK). Mitochondrial respiration was measured as the total minus the background oxygen consumption; the latter being determined by exposing the cell suspension to 150-270 nM of antimycin A (Sigma-Aldrich, MO, USA), a potent inhibitor of the respiratory chain complex III.

Statistical analyses

GraphPad Prism software (5.02) was used to carry out statistical analysis. A non-parametric two-tailed Mann–Whitney test was used to compare differences between experimental groups. Bonferroni's post-test was used to correct *P*-values for multiple comparisons. *P*-values smaller than 0.05 were considered as significant. The sample sizes for experimental fish groups were calculated with power and sample size program (version 3.1.2) by using data from our preliminary studies (Dupont and Plummer, 1998).

Acknowledgements

We thank Leena Mäkinen, Hanna-Leena Piippo and Jenna Ilomäki for technical assistance, Timo Kauppila and Johanna Kauppila for discussions on mitochondrial ROS production, and Jack George for proof-reading the manuscript.

Competing interests

The authors declare no competing or financial interests.

Author contributions

Conceptualization: H.L., M.M.H., E.D., V.P.H., M.P.; Methodology: H.L., M.M.H., E.D., V.P.H., M.P.; Validation: H.L., M.M.H.; Formal analysis: H.L., M.M.H., L.-M.V., L.K., S.J., B.V.L., E.D., M.P.; Investigation: H.L., M.M.H., L.-M.V., A.S., L.K., S.J., B.V.L., M.P.; Resources: H.L., M.M.H., M.R., V.P.H., M.P.; Data curation: H.L., M.M.H.; Writing - original draft: H.L., M.M.H., L.-M.V., M.P.; Writing - review & editing: H.L., M.M.H., L.-M.V., A.S., L.K., S.J., B.V.L., E.D., M.R., V.P.H., M.P.; Visualization: H.L., M.M.H., L.-M.V., A.S.; Supervision: H.L., M.M.H., V.P.H., M.P.; Project administration: H.L., M.M.H., M.P.; Funding acquisition: H.L., M.M.H., M.R., V.P.H., M.P.

Funding

This work has been supported by the Finnish Cultural Foundation (H.L.), Tampere Tuberculosis Foundation (H.L., L.-M.V., M.M.H., B.V.L., M.R., M.P.), Foundation of the Finnish Anti-Tuberculosis Association (Suomen Tuberkuloosin Vastustamisyhdistyksen Säätiö) (H.L., M.M.H., B.V.L., M.P.), Sigrid Jusélius Foundation (M.P.), Emil Aaltonen Foundation (M.M.H.), Jane and Aatos Erkko Foundation (M.R.) and AFM-Téléthon (#17424, E.D.)

Supplementary information

Supplementary information available online at
http://dmm.biologists.org/lookup/doi/10.1242/dmm.031658.supplemental

References

Aaby, P., Kollmann, T. R. and Benn, C. S. (2014). Nonspecific effects of neonatal and infant vaccination: public-health, immunological and conceptual challenges. *Nat. Immunol.* **15**, 895-899.

Andersen, P. and Woodworth, J. S. (2014). Tuberculosis vaccines–rethinking the current paradigm. *Trends Immunol.* **35**, 387-395.

Azad, A. K., Sadee, W. and Schlesinger, L. S. (2012). Innate immune gene polymorphisms in tuberculosis. *Infect. Immun.* **80**, 3343-3359.

Barbuddhe, S., Malik, S. and Gupta, L. K. (1998). Effect of in vitro monocyte activation by Listeria monocytogenes antigens on phagocytosis and production of reactive oxygen and nitrogen radicals in bovines. *Vet. Immunol. Immunopathol.* **64**, 149-159.

Barry, C. E., Boshoff, H. I., Dartois, V., Dick, T., Ehrt, S., Flynn, J. A., Schnappinger, D., Wilkinson, R. J. and Young, D. (2009). The spectrum of latent tuberculosis: rethinking the biology and intervention strategies. *Nature Reviews Microbiology* **7**, 845-855.

Bhat, K. H., Srivastava, S., Kotturu, S. K., Ghosh, S. and Mukhopadhyay, S. (2017). The PPE2 protein of Mycobacterium tuberculosis translocates to host nucleus and inhibits nitric oxide production. *Sci. Rep.* **7**, 39706.

Bracci, L., Schiavoni, G., Sistigu, A. and Belardelli, F. (2014). Immune-based mechanisms of cytotoxic chemotherapy: implications for the design of novel and rationale-based combined treatments against cancer. *Cell Death Differ.* **21**, 15-25.

Cambier, C. J., Takaki, K. K., Larson, R. P., Hernandez, R. E., Tobin, D. M., Urdahl, K. B., Cosma, C. L. and Ramakrishnan, L. (2014). Mycobacteria manipulate macrophage recruitment through coordinated use of membrane lipids. *Nature* **505**, 218-222.

Chackerian, A. A., Alt, J. M., Perera, T. V., Dascher, C. C. and Behar, S. M. (2002). Dissemination of Mycobacterium tuberculosis is influenced by host factors and precedes the initiation of T-cell immunity. *Infect. Immun.* **70**, 4501-4509.

Chao, M. C. and Rubin, E. J. (2010). Letting sleeping dos lie: does dormancy play a role in tuberculosis? *Annu. Rev. Microbiol.* **64**, 293-311.

Cheng, S., Quintin, J., Cramer, R. A., Shepardson, K. M., Saeed, S., Kumar, V., Giamarellos-Bourboulis, E. J., Martens, J. H. A., Rao, N. A., Aghajanirefah, A. et al. (2014). mTOR- and HIF-1 alpha-mediated aerobic glycolysis as metabolic basis for trained immunity. *Science* **345**, **345**, 1250684.

Clay, H., Davis, J. M., Beery, D., Huttenlocher, A., Lyons, S. E. and Ramakrishnan, L. (2007). Dichotomous role of the macrophage in early Mycobacterium marinum infection of the zebrafish. *Cell Host Microbe* **2**, 29-39.

Cobat, A., Gallant, C. J., Simkin, L., Black, G. F., Stanley, K., Hughes, J., Doherty, T. M., Hanekom, W. A., Eley, B., Jais, J. P. et al. (2009). Two loci control tuberculin skin test reactivity in an area hyperendemic for tuberculosis. *J. Exp. Med.* **206**, 2583-2591.

Cobat, A., Poirier, C., Hoal, E., Boland-Auge, A., De La Rocque, F., Corrard, F., Grange, G., Migaud, M., Bustamante, J., Boisson-Dupuis, S. et al. (2015). Tuberculin skin test negativity is under tight genetic control of chromosomal region 11p14-15 in settings with different tuberculosis endemicities. *J. Infect. Dis.* **211**, 317-321.

Dupont, W. D. and Plummer, W. D. (1998). Power and sample size calculations for studies involving linear regression. *Control. Clin. Trials* **19**, 589-601.

Elks, P. M., Brizee, S., Van Der Vaart, M., Walmsley, S. R., Van Eeden, F. J., Renshaw, S. A. and Meijer, A. H., (2013). Hypoxia inducible factor signaling modulates susceptibility to mycobacterial infection via a nitric oxide dependent mechanism. *PLoS Pathog.* **9**, e1003789.

Elks, P. M., Van Der Vaart, M., Van Hensbergen, V., Schutz, E., Redd, M. J., Murayama, E., Spaink, H. P. and Meijer, A. H., (2014). Mycobacteria counteract a TLR-mediated nitrosative defense mechanism in a zebrafish infection model. *PloS One* **9**, e100928.

Ellett, F., Pase, L., Hayman, J. W., Andrianopoulos, A. and Lieschke, G. J. (2011). Mpeg1 promoter transgenes direct macrophage-lineage expression in zebrafish. *Blood* **117**, E49-E56.

Flynn, J. A. L. and Chan, J. (2003). Immune evasion by Mycobacterium tuberculosis: living with the enemy. *Curr. Opin. Immunol.* **15**, 450-455.

Flynn, J. L., Chan, J., Triebold, K. J., Dalton, D. K., Stewart, T. A. and Bloom, B. R. (1993). An essential role for interferon gamma in resistance to Mycobacterium tuberculosis infection. *J. Exp. Med.* **178**, 2249.

Gallegos, A. M., Pamer, E. G. and Glickman, M. S. (2008). Delayed protection by ESAT-6-specific effector CD4+ T cells after airborne M. tuberculosis infection. *J. Exp. Med.* **205**, 2359-2368.

Gordon, S. and Martinez, F. O. (2010). Alternative activation of macrophages: mechanism and functions. *Immunity* **32**, 593-604.

Hall, C. J., Sanderson, L. E., Crosier, K. E. and Crosier, P. S. (2014). Mitochondrial metabolism, reactive oxygen species, and macrophage function-fishing for insights. *J. Mol. Med.* **92**, 1119-1128.

Hammarén, M. M., Oksanen, K. E., Nisula, H. M., Luukinen, B. V., Pesu, M., Rämet, M. and Parikka, M. (2014). Adequate Th2-type response associates with restricted bacterial growth in latent mycobacterial infection of zebrafish. *PLoS Pathog.* **10**, e1004190.

Houben, D., Demangel, C., Van Ingen, J., Perez, J., Baldeón, L., Abdallah, A. M., Caleechurn, L., Bottai, D., Van Zon, M. and De Punder, K., (2012). ESX-1-mediated translocation to the cytosol controls virulence of mycobacteria. *Cell. Microbiol.* **14**, 1287-1298.

Ito, T., Wang, Y. and Liu, Y. (2005). Plasmacytoid dendritic cell precursors/type I interferon-producing cells sense viral infection by Toll-like receptor (TLR) 7 and TLR9. *Springer Semin. Immunopathol.* **26**, 221-229.

Jung, J.-Y., Madan-Lala, R., Georgieva, M., Rengarajan, J., Sohaskey, C. D., Bange, F. C. and Robinson, C. M. (2013). The intracellular environment of human macrophages that produce nitric oxide promotes growth of mycobacteria. *Infect. Immun.* **81**, 3198-3209.

Kleinnijenhuis, J., Quintin, J., Preijers, F., Joosten, L. A. B., Jacobs, C., Xavier, R. J., Van Der Meer, J. W. M., Van Crevel, R. and Netea, M. G., (2014). BCG-induced trained immunity in NK cells: role for non-specific protection to infection. *Clin. Immunol.* **155**, 213-219.

Lepiller, S., Franche, N., Solary, E., Chluba, J. and Laurens, V. (2009). Comparative analysis of zebrafish nos2a and nos2b genes. *Gene* **445**, 58-65.
Lieschke, G. J., Oates, A. C., Crowhurst, M. O., Ward, A. C. and Layton, J. E. (2001). Morphologic and functional characterization of granulocytes and macrophages in embryonic and adult zebrafish. *Blood* **98**, 3087-3096.
Malherbe, S. T., Shenai, S., Ronacher, K., Loxton, A. G., Dolganov, G., Kriel, M., Van, T., Chen, R. Y., Warwick, J. and Via, L. E. (2016). Persisting positron emission tomography lesion activity and Mycobacterium tuberculosis mRNA after tuberculosis cure. *Nat. Med.* **23**, 526.
Meijer, A. H. (2016). Protection and pathology in TB: learning from the zebrafish model *Semin. Immunopathol.* **38**, 261-273.
Mirkovitch, J., König, A., Sauter, K., Brcic, M., Hope, J., Howard, C. and Jungi, T. (2006). Single-cell analysis divides bovine monocyte-derived dendritic cells into subsets expressing either high or low levels of inducible nitric oxide synthase. *Vet. Immunol. Immunopathol.* **114**, 1-14.
Myllymäki, H., Niskanen, M., Oksanen, K. E. and Rämet, M. (2015). Animal models in tuberculosis research–where is the beef? *Expert Opin. Drug Discov.* **10**, 871-883.
Netea, M. G., Joosten, L. A. B., Latz, E., Mills, K. H. G., Natoli, G., Stunnenberg, H. G., O'neill, L. A. J. and Xavier, R. J. (2016). Trained immunity: a program of innate immune memory in health and disease. *Science* **352**, aaf1098.
Nicholson, S., Bonecini-Almeida, M.da G., Lapa e Silva, J. R., Nathan, C., Xie, Q. W., Mumford, R., Weidner, J. R., Calaycay, J., Geng, J., Boechat, N., et al. (1996). Inducible nitric oxide synthase in pulmonary alveolar macrophages from patients with tuberculosis. *J. Exp. Med.* **183**, 2293-2302.
Oksanen, K. E., Halfpenny, N. J., Sherwood, E., Harjula, S. E., Hammarén, M. M., Ahava, M. J., Pajula, E. T., Lahtinen, M. J., Parikka, M. and Rämet, M. (2013). An adult zebrafish model for preclinical tuberculosis vaccine development. *Vaccine* **31**, 5202-5209.
Pagán, A. J., Yang, C., Cameron, J., Swaim, L. E., Ellett, F., Lieschke, G. J. and Ramakrishnan, L. (2015). Myeloid growth factors promote resistance to mycobacterial infection by curtailing granuloma necrosis through macrophage replenishment. *Cell Host Microbe* **18**, 15-26.
Parikka, M., Hammarén, M. M., Harjula, S. E., Halfpenny, N. J., Oksanen, K. E., Lahtinen, M. J., Pajula, E. T., Ivanainen, A., Pesu, M. and Rämet, M., (2012). Mycobacterium marinum causes a latent infection that can be reactivated by gamma irradiation in adult zebrafish. *PLoS Pathog.* **8**, e1002944.
Pham, L. N., Dionne, M. S., Shirasu-Hiza, M. and Schneider, D. S. (2007). A specific primed immune response in Drosophila is dependent on phagocytes. *PLoS Pathog.* **3**, e26.
Pias, E. K., Ekshyyan, O. Y., Rhoads, C. A., Fuseler, J., Harrison, L. and Aw, T. Y. (2003). Differential effects of superoxide dismutase isoform expression on hydroperoxide-induced apoptosis in PC-12 cells. *J. Biol. Chem.* **278**, 13294-13301.
Queval, C. J., Song, O.-R., Deboosère, N., Delorme, V., Debrie, A., Iantomasi, R., Veyron-Churlet, R., Jouny, S., Redhage, K. and Deloison, G. (2016). STAT3 represses nitric oxide synthesis in human macrophages upon Mycobacterium tuberculosis infection. *Sci. Rep.* **6**, 29297.
Quintin, J., Saeed, S., Martens, J. H. A., Giamarellos-Bourboulis, E. J., Ifrim, D. C., Logie, C., Jacobs, L., Jansen, T., Kullberg, B., Wijmenga, C. et al. (2012). Candida albicans infection affords protection against reinfection via functional reprogramming of monocytes. *Cell Host Microbe* **12**, 223-232.
Rajaram, M. V., Ni, B., Dodd, C. E. and Schlesinger, L. S. (2014). Macrophage immunoregulatory pathways in tuberculosis, *Sem. Immunol.* **26**, 471-485.
Ramakrishnan, L., (2013). Looking within the zebrafish to understand the tuberculous granuloma. *Adv. Exp. Med. Biol.* **783**, 251-266.
Ramos, G. B., Salomao, H., Francio, A. S., Fava, V. M., Werneck, R. I. and Mira, M. T. (2016). Association analysis suggests SOD2 as a newly identified candidate gene associated with leprosy susceptibility. *J. Infect. Dis.* **214**, 475-478.
Reiley, W. W., Calayag, M. D., Wittmer, S. T., Huntington, J. L., Pearl, J. E., Fountain, J. J., Martino, C. A., Roberts, A. D., Cooper, A. M., Winslow, G. M. et al. (2008). ESAT-6-specific CD4 T cell responses to aerosol Mycobacterium tuberculosis infection are initiated in the mediastinal lymph nodes. *Proc. Natl. Acad. Sci. USA* **105**, 10961-10966.
Roca, F. J. and Ramakrishnan, L. (2013). TNF dually mediates resistance and susceptibility to mycobacteria via mitochondrial reactive oxygen species. *Cell* **153**, 521-534.
Russell, D. G. (2011). Mycobacterium tuberculosis and the intimate discourse of a chronic infection. *Immunol. Rev.* **240**, 252-268.
Simeone, R., Bobard, A., Lippmann, J., Bitter, W., Majlessi, L., Brosch, R. and Enninga, J. (2012). Phagosomal rupture by Mycobacterium tuberculosis results in toxicity and host cell death. *PLoS Pathog.* **8**, e1002507.
Subbian, S., Tsenova, L., O'brien, P., Yang, G., Kushner, N. L., Parsons, S., Peixoto, B., Fallows, D. and Kaplan, G. (2012). Spontaneous latency in a rabbit model of pulmonary tuberculosis. *Am. J. Pathol.* **181**, 1711-1724.
Swaim, L. E., Connolly, L. E., Volkman, H. E., Humbert, O., Born, D. E. and Ramakrishnan, L. (2006). Mycobacterium marinum infection of adult zebrafish causes caseating granulomatous tuberculosis and is moderated by adaptive immunity. *Infect. Immun.* **74**, 6108.
Takaki, K., Davis, J. M., Winglee, K. and Ramakrishnan, L. (2013). Evaluation of the pathogenesis and treatment of Mycobacterium marinum infection in zebrafish. *Nat. Protoc.* **8**, 1114-1124.
Tang, Y.C., Yuwen, H., Wang, K., Bruno, P. M., Bullock, K., Deik, A., Santaguida, S., Trakala, M., Pfau, S. J., Zhong, N. et al. (2017). Aneuploid cell survival relies upon sphingolipid homeostasis. *Cancer Res.*, **77**, 5272-5286.
Thoma-Uszynski, S., Stenger, S., Takeuchi, O., Ochoa, M. T., Engele, M., Sieling, P. A., Barnes, P. F., Rollinghoff, M., Bolcskei, P. L., Wagner, M. et al. (2001). Induction of direct antimicrobial activity through mammalian toll-like receptors. *Science (New York, N.Y.)* **291**, 1544-1547.
Tobin, D. M., (2015). Host-directed therapies for tuberculosis. *Cold Spring Harb. Perspect. Med.* **5**, a021196.
Van Leeuwen, L.M., Van der Sar, A. M. and Bitter, W., (2014). Animal models of tuberculosis: zebrafish. *Cold Spring Harbor Perspect. Med.* **5**, a018580.
Vanhauwaert, S., Van Peer, G., Rihani, A., Janssens, E., Rondou, P., Lefever, S., De Paepe, A., Coucke, P. J., Speleman, F. and Vandesompele, J., (2014). Expressed repeat elements improve RT-qPCR normalization across a wide range of zebrafish gene expression studies. *PloS ONE* **9**, e109091.
Van't Wout, J., Poell, R. and Van Furth, R., (1992). The role of Bcg/ppd-activated macrophages in resistance against systemic candidiasis in mice. *Scand. J. Immunol.* **36**, 713-719.
Verrall, A. J., Netea, M., Alisjahbana, B., Hill, P. C. and van Crevel, R., (2014). Early clearance of Mycobacterium tuberculosis: a new frontier in prevention. *Immunology* **141**, 506-513.
Wienholds, E., Schulte-Merker, S., Walderich, B. and Plasterk, R. H. A. (2002). Target-selected inactivation of the zebrafish rag1 gene. *Science* **297**, 99.
Wilkinson, R. J., Llewelyn, M., Toossi, Z., Patel, P., Pasvol, G., Lalvani, A., Wright, D., Latif, M. and Davidson, R. N. (2000). Influence of vitamin D deficiency and vitamin D receptor polymorphisms on tuberculosis among Gujarati Asians in west London: a case-control study. *Lancet* **355**, 618-621.
Wolf, A. J., Desvignes, L., Linas, B., Banaiee, N., Tamura, T., Takatsu, K. and Ernst, J. D. (2008). Initiation of the adaptive immune response to Mycobacterium tuberculosis depends on antigen production in the local lymph node, not the lungs. *J. Exp. Med.* **205**, 105-115.

Figure S1

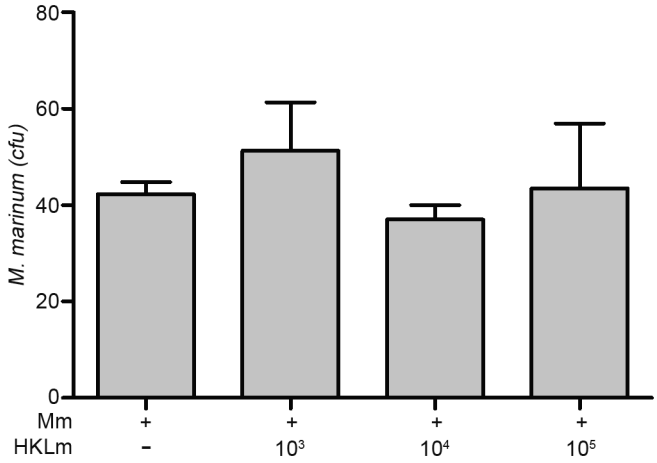

Figure S1. HKLm does not exhibit bactericidal effects on *Mycobacterium marinum* in vitro. *M. marinum* was incubated for 12 days in 7H9 medium together with different concentrations of HKLm. The bacterial cultures were plated on 7H10 plates and the colony forming units (cfu) of *M. marinum* were determined. 10^3, 10^4, and 10^5 denote the ratio of HKLm compared to the initial cfu in the *M. marinum* culture. Mm= *Mycobacterium marinum*, HKLm= Heat-killed *Listeria monocytogenes*. n=3 for each sample.

Figure S2

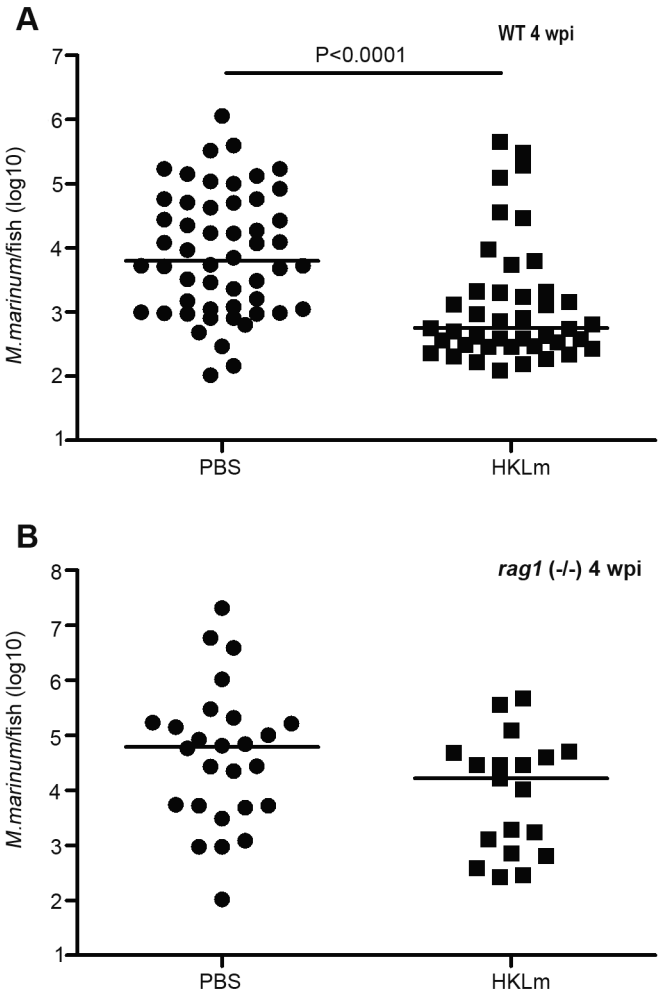

Figure S2. HKLm priming decreases the mycobacterial loads also in non-cleared populations. The data represented in A and B exclude those individuals that had bacterial counts below the detection limit of the *M. marinum* -specific qPCR method i.e. had cleared the infection. Also the wild-type individuals that were unable to clear the infection benefit from HKLm by showing significantly lowered mycobacterial loads (A). *Rag1* (-/-) fish show a similar trend (B). P-values were calculated with a two-tailed non-parametric Mann-Whitney test with GraphPad Prism. Medians for the experiments are shown in the figures. Data are pooled from 4 individual experiments for A (representative experiment shown in Fig 2A, n=52 for PBS and n=42 for HKLm) and from 2 individual experiments in Fig. 2D for B (n=26 for PBS and n=19 for HKLm).

Figure S3

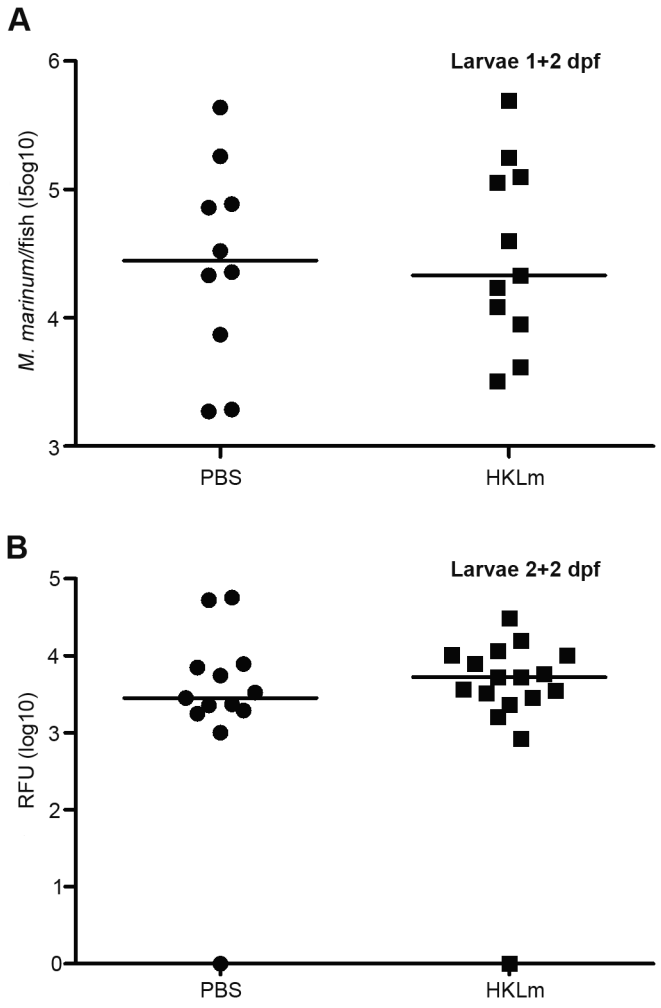

Figure S3. HKLm priming does not protect zebrafish larvae from mycobacterial infection. Zebrafish larvae were primed with 240 cfu of HKLm 1 day post-fertilization (dpf) (A) or 490 cfu of HKLm 2 dpf (B). *M. marinum* infections (39±13 cfu for A and 39±16 cfu for B) were carried out 2 dpf. Mycobacterial loads were determined with an *M. marinum* -specific qPCR (A) or by measuring the fluorescent signal of a wasabi-*M. marinum* strain (B) with a plate reader. n=10 for PBS and n=11 for HKLm in A and n=13 for PBS and n=17 for HKLm in B.

FIRST PERSON

First person – Hanna Luukinen

First Person is a series of interviews with the first authors of a selection of papers published in Disease Models & Mechanisms, helping early-career researchers promote themselves alongside their papers. Hanna Luukinen is first author on 'Priming of innate antimycobacterial immunity by heat-killed *Listeria monocytogenes* induces sterilizing response in the adult zebrafish tuberculosis model', published in DMM. Hanna is a PhD student in the lab of Mataleena Parikka at the University of Tampere, Finland, investigating the mechanisms behind mycobacterial persistence both in the context of evading the host immune responses as well as phenotypic tolerance to antibiotic treatment.

How would you explain the main findings of your paper to non-scientific family and friends?

When I tell my family and friends that I am doing a PhD on tuberculosis the discussion quite often changes very quickly to what we should eat next. Nourishment is an important topic of course, but if the conversation would continue with my favorite subject, tuberculosis, there are couple of points I would like to make. The causative agent of tuberculosis, mycobacterium, is a master of dampening the immune system and hiding from it, which has made the bacteria hard to eliminate the bacteria. These evasion strategies have also affected vaccine development to the point, that currently, there is no vaccine that is able to protect against the infection. In this study, we found that with a bacterial booster we were able to help individuals to cope with mycobacterial infection and even get rid of this ingenious bacteria. This booster seems to work via the very basic mechanisms of the immune system. It's like margherita pizza – it just works without any additional toppings.

What are the potential implications of these results for your field of research?

The World Health Organization (WHO) has set a goal of reducing tuberculosis deaths by 90% by 2030. Still, it is unknown what kinds of immune responses are needed to eliminate the pathogen. Also, conventional antimicrobial treatments for tuberculosis last several months and multidrug-resistant mycobacteria are becoming more and more common. Therefore, new therapeutic and prophylactic treatments are strongly needed. It is likely that different kinds of responses are beneficial in early, established or reactivated disease states. Our current study concentrates on the early responses against mycobacterial infection. Here, we show that innate immune responses can protect against mycobacterial infection, through the increased transcription levels of *macrophage-expressed gene 1* (*mpeg1*), *tumor necrosis factor α* (*tnfα*) and *nitric oxide synthase 2b* (*nos2b*) and downregulation of *superoxide dismutase 2* (*sod2*). Our results can help to give new ideas on how immune mechanisms should be optimally modulated in the early mycobacterial infection.

Hanna Luukinen's contact details: Faculty of Medicine and Life Sciences, University of Tampere, Finland.
E-mail: hanna.luukinen@staff.uta.fi

Hanna Luukinen

"[…] I am still most amazed by the result that the protective mechanisms in mycobacterial infection operate via the innate immune system in our model."

What are the main advantages and drawbacks of the model system you have used as it relates to the disease you are investigating?

In this study, we used the zebrafish and *Mycobacterium marinum* to model human tuberculosis. *M. marinum* is a natural pathogen of ectothermic animals and with this model, we are able to follow the natural course of the infection of this host-specific pathogen. *M. marinum* causes a granulomatous disease with necrotic granulomas in adult zebrafish, closely resembling human tuberculosis. Adult zebrafish has both an innate and adaptive immune system, which makes them ideal for immunological studies. Zebrafish also develop fast, produce offspring abundantly, are cheap to maintain and, most importantly, are the least neuro-physiologically developed organisms of the known tuberculosis models. However, zebrafish have anatomical and physiological differences compared to humans

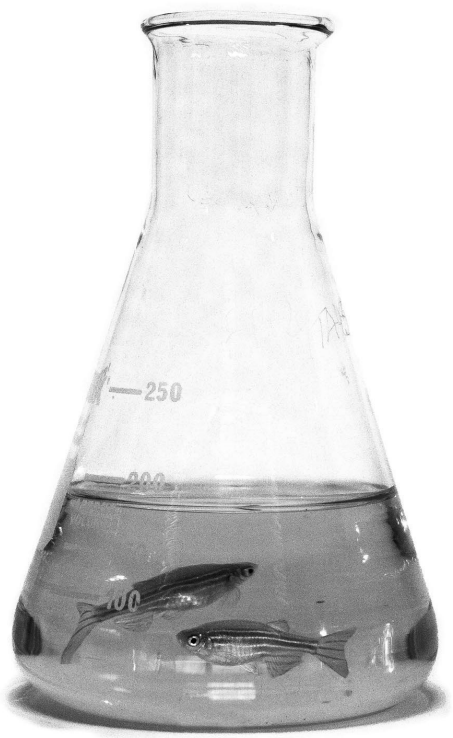

Adult zebrafish used in the research (picture by Lauri Paulamäki).

and lack some commonly used antibody-based techniques, which affected the study design.

What has surprised you the most while conducting your research?

Of all surprises we had during this project, I am still most amazed by the result that the protective mechanisms in mycobacterial infection operate via the innate immune system in our model. How beautiful!

Describe what you think is the most significant challenge impacting your research at this time and how will this be addressed over the next 10 years?

In my opinion, scientists are just scratching the surface of understanding mycobacteria and their different lifestyles. It is a real challenge to fight successfully against this ancient disease. Tuberculosis is mostly seen in developing countries where malnutrition and AIDS are serious problems. However, as people travel around the world actively, I could bet that this disease, including multidrug-resistant forms of mycobacteria, is spreading more broadly. It has been noticed on several occasions that traditional vaccines and treatments are not working perfectly against mycobacteria. If it were easy to protect against tuberculosis, an effective treatment would have already been discovered. I think that the eradication of tuberculosis really requires thinking outside the box and new experimental approaches. Hopefully in 10 years, we have made significant progress.

What's next for you?

The work with these challenging bacteria continues and if I finish my PhD while trying to crack the code, it would be great.

Reference

Luukinen, H., Hammarén, M. M., Vanha-aho, L.-M., Svorjova, A., Kantanen, L., Järvinen, S., Luukinen, B. V., Dufour, E., Rämet, M., Hytönen, V. P. and Parikka, M. (2018). Priming of innate antimycobacterial immunity by heat-killed *Listeria monocytogenes* induces sterilizing response in the adult zebrafish tuberculosis model. *Dis. Model. Mech.* **11**, doi:10.1242/dmm.031658.

PUBLICATION III

Surface-Shaving Proteomics of *Mycobacterium marinum* Identifies Biofilm Subtype-Specific Changes Affecting Virulence, Tolerance and Persistence

Savijoki K, Myllymäki H, Luukinen H, Paulamäki L, Vanha-aho LM, Svorjova A, Miettinen I, Fallarero A, Ihalainen TO, Yli-Kauhaluoma J, Nyman T, Parikka M

mSystems 2021 29;6(3):e0050021
doi: 10.1128/mSystems.00500-21

AMERICAN SOCIETY FOR MICROBIOLOGY | mSystems®

RESEARCH ARTICLE

Surface-Shaving Proteomics of *Mycobacterium marinum* Identifies Biofilm Subtype-Specific Changes Affecting Virulence, Tolerance, and Persistence

Kirsi Savijoki,[a] Henna Myllymäki,[b]* Hanna Luukinen,[b] Lauri Paulamäki,[b] Leena-Maija Vanha-aho,[b] Aleksandra Svorjova,[b] Ilkka Miettinen,[a] Adyary Fallarero,[a]* Teemu O. Ihalainen,[b] Jari Yli-Kauhaluoma,[c] Tuula A. Nyman,[d] Mataleena Parikka[b]

[a]Drug Research Program, Division of Pharmaceutical Biosciences, Faculty of Pharmacy, University of Helsinki, Helsinki, Finland
[b]Faculty of Medicine and Health Technology, Tampere University, Tampere, Finland
[c]Drug Research Program, Division of Pharmaceutical Chemistry and Technology, Faculty of Pharmacy, University of Helsinki, Helsinki, Finland
[d]Institute of Clinical Medicine, Department of Immunology, Rikshospitalet, Oslo University Hospital, Oslo, Norway

Kirsi Savijoki and Henna Myllymäki contributed equally to this work. Author order was determined in order of increasing seniority.

ABSTRACT The complex cell wall and biofilm matrix (ECM) act as key barriers to antibiotics in mycobacteria. Here, the ECM and envelope proteins of *Mycobacterium marinum* ATCC 927, a nontuberculous mycobacterial model, were monitored over 3 months by label-free proteomics and compared with cell surface proteins on planktonic cells to uncover pathways leading to virulence, tolerance, and persistence. We show that ATCC 927 forms pellicle-type and submerged-type biofilms (PBFs and SBFs, respectively) after 2 weeks and 2 days of growth, respectively, and that the increased CelA1 synthesis in this strain prevents biofilm formation and leads to reduced rifampicin tolerance. The proteomic data suggest that specific changes in mycolic acid synthesis (cord factor), Esx1 secretion, and cell wall adhesins explain the appearance of PBFs as ribbon-like cords and SBFs as lichen-like structures. A subpopulation of cells resisting 64× MIC rifampicin (persisters) was detected in both biofilm subtypes and already in 1-week-old SBFs. The key forces boosting their development could include subtype-dependent changes in asymmetric cell division, cell wall biogenesis, tricarboxylic acid/glyoxylate cycle activities, and energy/redox/iron metabolisms. The effect of various ambient oxygen tensions on each cell type and nonclassical protein secretion are likely factors explaining the majority of the subtype-specific changes. The proteomic findings also imply that Esx1-type protein secretion is more efficient in planktonic (PL) and PBF cells, while SBF may prefer both the Esx5 and nonclassical pathways to control virulence and prolonged viability/persistence. In conclusion, this study reports the first proteomic insight into aging mycobacterial biofilm ECMs and indicates biofilm subtype-dependent mechanisms conferring increased adaptive potential and virulence of nontuberculous mycobacteria.

IMPORTANCE Mycobacteria are naturally resilient, and mycobacterial infections are notoriously difficult to treat with antibiotics, with biofilm formation being the main factor complicating the successful treatment of tuberculosis (TB). The present study shows that nontuberculous *Mycobacterium marinum* ATCC 927 forms submerged- and pellicle-type biofilms with lichen- and ribbon-like structures, respectively, as well as persister cells under the same conditions. We show that both biofilm subtypes differ in terms of virulence-, tolerance-, and persistence-conferring activities, highlighting the fact that both subtypes should be targeted to maximize the power of antimycobacterial treatment therapies.

KEYWORDS biofilm matrix, biofilms, cell surface proteomics, *Mycobacterium marinum*, persistence, tolerance

Citation Savijoki K, Myllymäki H, Luukinen H, Paulamäki L, Vanha-aho L-M, Svorjova A, Miettinen I, Fallarero A, Ihalainen TO, Yli-Kauhaluoma J, Nyman TA, Parikka M. 2021. Surface-shaving proteomics of *Mycobacterium marinum* identifies biofilm subtype-specific changes affecting virulence, tolerance, and persistence. mSystems 6:e00500-21. https://doi.org/10.1128/mSystems.00500-21.

Editor Tricia A. Van Laar, California State University, Fresno

Address correspondence to Mataleena Parikka, mataleena.parikka@tuni.fi.

* Present address: Henna Myllymäki, UoE Centre for Inflammation Research, Queen's Medical Research Institute, University of Edinburgh, Edinburgh, United Kingdom; Adyary Fallarero, Thermo Fischer Scientific, Vantaa, Finland.

Received 25 April 2021
Accepted 27 May 2021
Published 22 June 2021

Tuberculosis (TB) remains a major global health issue, with approximately 10 million new cases and 1.4 million deaths in 2019 (1). The causative agent, *Mycobacterium tuberculosis* (Mtb), is carried by an estimated one-quarter of the human population as a latent infection, which has a 5% to 10% lifetime risk of developing into TB disease. In addition, the emergence of drug-resistant Mtb strains continues to be a public health threat, with approximately half a million new cases in 2019. Even in the case of drug-sensitive Mtb strains, the first-line antibiotic treatment requires the use of four antimicrobials over a course of at least 6 months (WHO, 2020). Moreover, despite successful treatment, the recurrence of TB carries a substantial risk, especially among immunocompromised patients (2, 3). The heterogeneity of the standard treatment outcome is also evident in positron emission tomography-computed tomography (PET-CT) images showing nonresolving and active lesions and the presence of Mtb mRNA in sputum samples. This suggests that a significant proportion of patients generate viable mycobacteria in their lungs even after clinically curative antibiotic treatment (4). In a rabbit TB model, it was further shown that the caseum of granulomas contains Mtb that is highly tolerant to most anti-TB drugs (5). The complex mycobacterial cell wall, involving capsule and outer/inner membranes connected by a dense mycolyl-arabinogalactan-peptidoglycan with high lipid levels, is the main barrier that protects the bacterial cells against drugs (6). While the mechanisms leading to drug tolerance in TB have remained poorly understood, biofilm formation was recently indicated as one of the strategies to increase viability, tolerance, and persistence (7–10).

Biofilm formation is defined as adherent growth within self-produced extracellular matrix (ECM) consisting of proteins, polysaccharides, and DNA/RNA, and it is the strategy bacteria use to escape the effects of antibiotics and host defense systems (11–13). Mycobacteria use phenotypically distinct biofilm subtypes for growth, which physiologically differ from planktonic-type growth. These include (i) floating/pellicle-type biofilms (PBFs) at the air-liquid interface having an ECM rich in free mycolic acids (MAs) and with a frequent cord/ribbon-like appearance, while (ii) submerged-type biofilms (SBFs) show adherent growth on a solid substratum (11, 14–16). The capsule layer plays a vital role in triggering biofilm growth in mycobacteria, as Tween 80 (nonionic surfactant) has been shown to detach the capsule layer and prevent biofilm formation of culture cells (17). Thus, this labile layer forming the first molecular interaction with the host/environment is likely to involve key factors contributing to persistence/adaptation and search of anti-TB targets. Although several studies on mycobacteria have pinpointed cellular pathways and proteins that affect the capsule/cell wall and biofilm formation (9, 14, 17–25), systematic investigation of the factors that directly interact with the surrounding environment is necessary to be able to maximize the power of antimycobacterial treatment therapies.

Mycobacterium marinum (Mmr) has proven to be an excellent alternative model pathogen for slow-growing Mtb, as it allows for the investigation of TB-like chronic and latent infections in its natural host, the zebrafish (26–29). Cultured mycobacterial biofilms have been used to understand resilient bacterial phenotypes emerging in mycobacterial infections. However, the distinct phenotypic profiles associated with PBFs and SBFs, including marker proteins discriminating the two biofilm subtypes, have remained poorly understood. To shed light on the specific attributes linking these biologically different biofilm subtypes to their phenotypes, we first cultured Mmr strain ATCC 927 to create *in vitro* biofilms. These biofilms were then imaged using widefield deconvolution microscopy (WDeM) to investigate temporal effects on biofilm architectures. Label-free quantitative (LFQ) proteomics was next used to uncover the ECM proteome dynamics in maturing Mmr biofilms and to identify the cell surface proteins (proteome) on Mmr cells grown in Tween 80, a detergent known to prevent cells from clumping and forming a biofilm (17). The key proteome findings were validated by gene overexpression studies to indicate cellulose-dependent biofilm formation as well as by biofilm killing assays to confirm the formation of persister cells in both biofilm subtypes. To the best of our knowledge, this is the first study monitoring mycobacterial

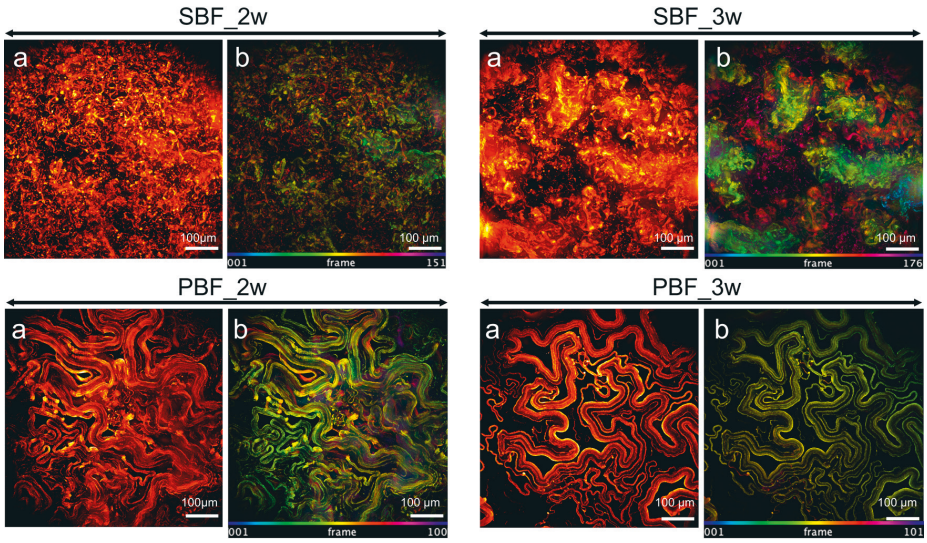

FIG 1 Mmr biofilms show distinct growth morphologies after 2-weeks of growth. SBFs grow with lichen-like structures, whereas PBFs have a ribbon-like cords morphology, which becomes more defined with maturation (after 3 weeks). The WDeM images are maximum-intensity projections of 2- and 3-week-old biofilms (a) together with an image where the *z* position is color coded (b); frame interval is 2 μm.

ECM proteomes over 3 months' time as well as protein and morphological phenotypic markers for distinguishing defined biofilm subtypes.

RESULTS

SBFs and PBFs show distinct morphological characteristics. The kinetics of development and maturation as well as the morphology of mycobacterial PBFs and SBFs have been reported to differ substantially (8). Here, we first show that that Mmr forms PBFs at the air-liquid interphase and that SBFs attached to the bottom of the culture well under the same physiological *in vitro* conditions after 2 weeks of growth (see Fig. S1A in the supplemental material). The SBF subtype developed earlier (visible already after 2 days of culture) than the PBF, which was not clearly distinguishable before 2 weeks of growth. Next, we investigated the three-dimensional morphology of Mmr biofilms in more detail by culturing Mmr cells carrying the pTEC27 plasmid with the tdTomato fluorescent marker gene (29) for 2 and 3 weeks to produce PBFs and SBFs and analyzing the biofilms by widefield deconvolution microscopy (WDeM). Figure 1 shows that Mmr forms organized three-dimensional structures with distinctive subtype-specific morphological features. For the SBF, the structures displayed a lichen- or moss-like appearance, having tens-of-microns-high feature structures rising from the biofilm base after 2 weeks (Fig. 1, top). In comparison, the morphology of the PBF subtype was very different by the first time point, showing flat ribbon-like structures without any protruding structures (Fig. 1, bottom). Defined, extensive structures in all dimensions, although less dense than those detected at the 2-week time point, were found for both biofilm subtypes also after 3 weeks of growth.

Submerged biofilms exhibit the greatest ECM proteome diversity. As the phenotypic profiles of PBFs and SBFs are clearly different, their ECM proteomes were next quantitatively monitored and compared during the development and maturation stages. To this end, the PBF and SBF cells at the points shown in Fig. 2A were subjected to trypsin/Lys-C digestion as well as liquid chromatography-tandem mass spectrometry (LC-MS/MS)-based protein identification and LFQ proteomics (all data available via PRIDE with identifier PXD02010). Logarithmic state planktonic cells (PL_log), representing single-cell cultures,

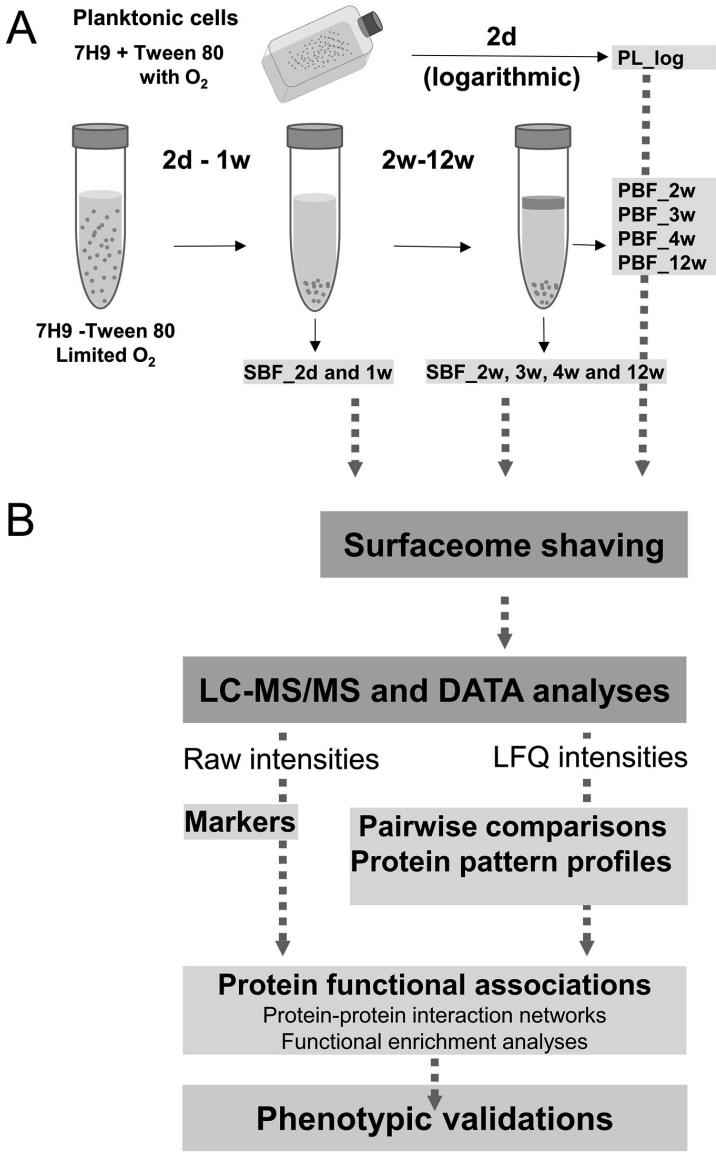

FIG 2 (A) Workflow depicting the conditions and time points used for preparing the planktonic and biofilm cells of Mmr. Gray arrows indicate sampling time points for pellicle (PBF) and submerged (SBF) biofilms. (B) Workflow used for identification of surface proteins associated with planktonic (PL_log) cells, PBFs, and SBFs. Marker proteins were identified by comparing the raw intensity data, statistically significant protein abundance changes by pairwise comparisons of the $\log_2$-converted LFQ data, and the protein coabundance patterns by subjecting the LFQ data to imputation and Z-score normalization. STRING and pathway enrichment analyses were conducted on the selected heat map clusters and necessary phenotypic assays to validate the key proteome differences.

were obtained by growing the Mmr strain in the presence of Tween 80. The quality of each data set was high: 84.7% or all proteins were identified with at least three or more matching peptides, with an average sequence coverage of approximately 31%, and only 11% of proteins were categorized as single-peptide hits. In addition, a broad overlap in

protein identifications was detected within the four biological replica samples; 41% to 89% of the proteins were shared by each replicate, with the 2-week PBF and the 3-week SBF showing the highest variation between replicates (Fig. S1B). Table S1 lists the proteins detected in at least two of four replica samples. An outlier replicate associated with one of the SBF identification replica sets at the 3-week time point was excluded from subsequent data analyses. The numbers of detected proteins were 1,132, 1,957, and 2,133 for the PL, PBF, and SBF cells, respectively.

Cytoplasmic protein export/release is most efficient in submerged biofilms. Figure S2A shows the distributions of all identified proteins according to their predicted secretion motif (Sec/SPII, TatP/SPI, LIPO/SPII, and type VII secretion [T7SS]; SecretomeP) and the number of transmembrane spanning domains (TMDs). The most notable differences were detected for membrane proteins with six to ten TMDs as well as in the number of cytoplasmic proteins. Nearly 2-fold more trehalose dimycolate (TDM) proteins were detected from the PL cells than from the biofilm cells. In contrast, 2-fold more cytoplasmic proteins predicted to be exported out of the cells via a nonclassical route (SecretomeP) were identified from the biofilm ECMs (*n*, 300) in comparison to that from the PL cells (*n*, 150). For many of these proteins, a secondary function as a moonlighting protein (30) was indicated (Table S1). In addition, more than 900, 1,600, and 1,800 cytoplasmic proteins identified in the PL, PBF, and SBF cells, respectively, contained no motifs for classical or nonclassical secretion and were assigned here as "others" (Table S1).

Most significant protein abundance changes specific to planktonic and biofilm cells. The Venn diagram in Fig. S2B indicates the highest number of specifically identified proteins in the SBFs (*n*, 173) and the lowest in the PBFs (*n*, 16), while no unique identifications were detected for the PL cells. The uniquely detected proteins with the highest raw intensity values included a signal transduction-associated serine/threonine-protein kinase (PknL), an LGFP-repeat protein specific to SBFs, and a β-1,3-endoglucanase and bacterioferritin BfrA specific to PBFs (see Table S2). The proteins detected with the highest intensity values and only in the biofilm ECMs included an error-prone polymerase DinB, a preprotein sec-translocase subunit YajC, a cytochrome P-450 monooxygenase, a PE family immunogen, and a signal transduction-related adenylate cyclase involved in cyclic di-AMP biosynthesis (Table S2).

Next, the $\log_2$ transformed MaxLFQ data were subjected to pairwise comparisons to indicate statistically significant protein abundance changes (see Table S3). Figure 3 shows the greatest growth mode- and time-dependent fold changes related to the PL versus biofilm cells, PBF versus SBF cells, and each biofilm subtype at different time points. Comparison of the PL and both biofilm cells at their first time points of growth (PBF_2w and SBF_2d) indicated the most prominent changes for PPE family proteins (e.g., PPE61) and enzymes involved in cell envelope biogenesis/metabolism (MurE, CwlM, cutinase, and CelA1). Among these, the PPE61 immunogen was ca. 6,000- and 1,800-times more abundant on the PL cells than on the PBF_2w and SBF_2d cells, respectively. CelA1, a β-1,4-cellobiohydrolase known to prevent biofilm growth in *Mycobacterium smegmatis* and Mtb (11, 18, 19), was detected with 50- and 130-fold higher abundances on the PL cells than on the PBFs at the 1-week time point and the SBFs at the 2-day time point, respectively (Table S3).

Comparison of the PBF_2w and SBF_2d cells indicated Esx1-associated virulence factors (i.e., EspF, EspA/EspE, and ESAT-6) and PPE family immunogens as 30- to 130-fold more abundant from the PBF than from the SBF cells; meanwhile, tricarboxylic acid (TCA)/glyoxylate cycle-associated isocitrate lyase (ICL1) was >200-fold more produced by the SBF than the PBF cells. After 12 weeks, the proteins more abundant in the SBF than in the PBF included an LppP/LprE lipoprotein (ca. 16-fold), HemD involved in the synthesis of vitamin B_{12} (ca. 15-fold), FadD29 contributing to the synthesis of phenolic glycolipids (~13-fold), β-lactamase able to hydrolase β-lactam antibiotics (ca. 9-fold), and ICL1 catalyzing the glyoxylate shunt-mediated activities (ca. 8-fold). More abundant proteins in the PBF at this time point were identified as a polysaccharide (*N*-acetylmuramic acid [MurNAc]) deacetylase PdaC (ca. 15-fold) and a translocase subunit, SecE (ca. 11-fold).

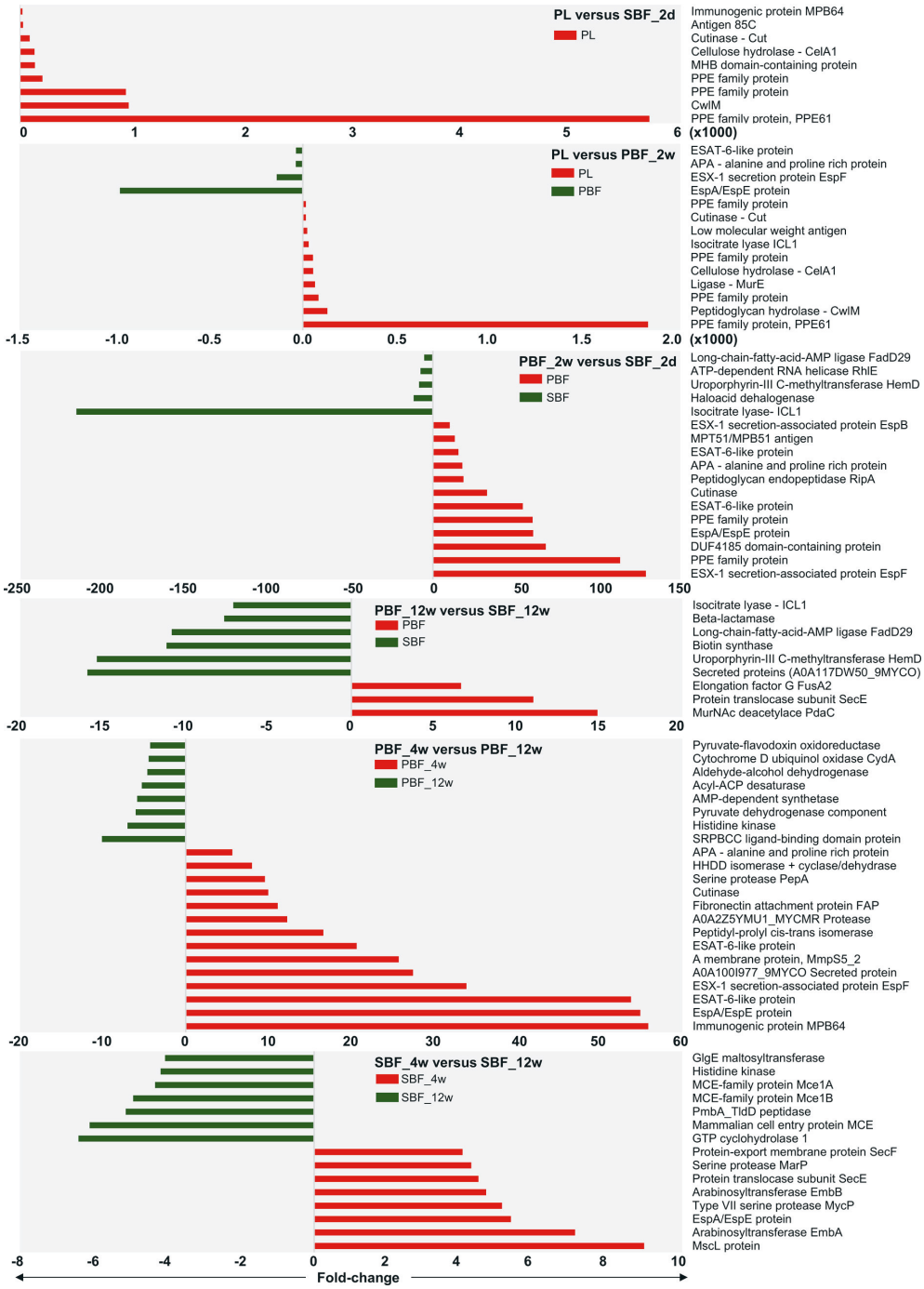

FIG 3 Most significant protein abundance fold changes between the indicated cell types at selected time points. The $\log_2$-transformed LFQ data were analyzed using Student's *t* test with permutation-based FDR adjustment. In two top panels, the fold change is times 1,000.

In the PBF, an MPB64 immunogen, siderophore export accessory protein MmpS5, several Esx1-associated proteins (EspA/EspE and EspF) and adhesins (Ala-Pro-Ala-rich protein APA and fibronectin-binding protein FAP) displayed the most significant abundance decreases at the 12-week time point. In the SBFs, these proteins included a large-conductance mechanosensitive channel protein, Msc, a membrane protein acting as the cells' safety valve to relieve osmotic pressure, arabinosyltransferases EmbA and EmbB, the Esx1-associated EspA/EspE, and the MycP1 protease. Proteins with the greatest abundance changes after 12 weeks in the SBFs included mammalian entry proteins (MCEs) and an α-1,4-glucan:maltose-1-phosphate maltosyltransferase.

Decreased CelA1 synthesis is also required for biofilm formation in *M. marinum*. As our findings suggest that a lack of CelA could also promote biofilm formation of Mmr, we tested this hypothesis by overexpressing the *celA1* gene in an Mmr strain equipped with pTEC27 with the tdTomato fluorescent marker (29). First, the *celA1* expression level in the transformed Mmr strain was confirmed by quantitative PCR (qPCR), indicating ca. 150-times higher *celA1* transcription than in the control strain carrying an empty pTEC27 (Fig. 4A). Then we analyzed the morphology of both the SBFs and PBFs after 2 weeks using the CelA1 strain with WDeM. As seen in Fig. 4B, the CelA1 strain showed altered morphology compared to that of the Mmr with pTEC27 (wild-type [WT] control strain). After 2 weeks of growth, the CelA1 strain SBF showed a less defined/loss of the lichen-like morphology and lower total thickness than the SBF control with pTEC27. Similarly, CelA1 overproduction in Mmr resulted in disrupted and fuzzy ribbon-like cords associated with PBF-type biofilm growth, as the PBF cells with pTEC27 had well-defined and tight ribbon-like structures.

CelA1 expression was recently linked with biofilm formation, antibiotic tolerance, and virulence in Mtb (9). Therefore, Mmr cells in planktonic and biofilm forms with/without CelA1 overexpression were also exposed to rifampicin to determine the MIC and minimum bactericidal concentration (MBC) for this bactericidal first-line TB drug. Figure 4C shows that in both the planktonic and biofilm cultures, CelA1 overexpression decreased the MIC and MBC, with a clear impact on 2-day-old and 4-day-old biofilms. These results indicate that CelA1 in Mmr impedes biofilm formation and increases the susceptibility of the residing cells to rifampicin.

Functional pathways specifically induced in planktonic and biofilm cells. The LFQ proteomic data were next subjected to a principal-component analysis (PCA) for comparing growth mode- and time-dependent protein abundance patterns in the PL cells and aging biofilms. The PCA in Fig. 5A shows clear clustering for each data set except for replicates associated with 2-week-old PBF proteomes, which show greater variation. PC1, separating the samples according to the growth mode, explains 15% of the total variation, while 39% (PC2) of the variation can be explained by the age of the culture. The 2-day-old SBF proteomes formed a clearly distinguishable cluster, while the PL proteomes and proteomes associated with the PBFs between the 2- and 4-week time points showed close clustering. Although the SBF and PBF proteomes differed greatly within the first 4 weeks of growth, these biofilm subtypes appeared to undergo similar proteome changes during the later stages of growth, as proteomes of both subtypes clustered more closely at the 12-week time point. Notably, PBFs during the first weeks (2 to 3 weeks) of growth shared a more similar ECM proteome with that of the PL cells than that of the SBFs under the same conditions.

Next, a multisample test (analysis of variance [ANOVA]) was conducted on the normalized LFQ intensity data to investigate growth mode-dependent proteome differences at time points between 2 days and 3 months. A dendrogram/heat map in Fig. 5B shows hierarchically clustered coabundance data for 690 proteins having a statistically significant abundance change in at least one of the conditions tested (see Table S4). Six major clusters were clearly distinguished, among which cluster 1 (*n*, 375) and cluster 6 (*n*, 125) contained the greatest number of proteins, with higher abundances in 1- to 4-week-old SBFs (cluster 1) and 2-day- to 2-week-old SBFs (cluster 6), respectively. STRING (Search Tool for the Retrieval of Interacting Genes/Proteins) enrichment analyses performed on both clusters (see Table S5) indicated the greatest changes for pathways coordinating cell envelope biogenesis/metabolism,

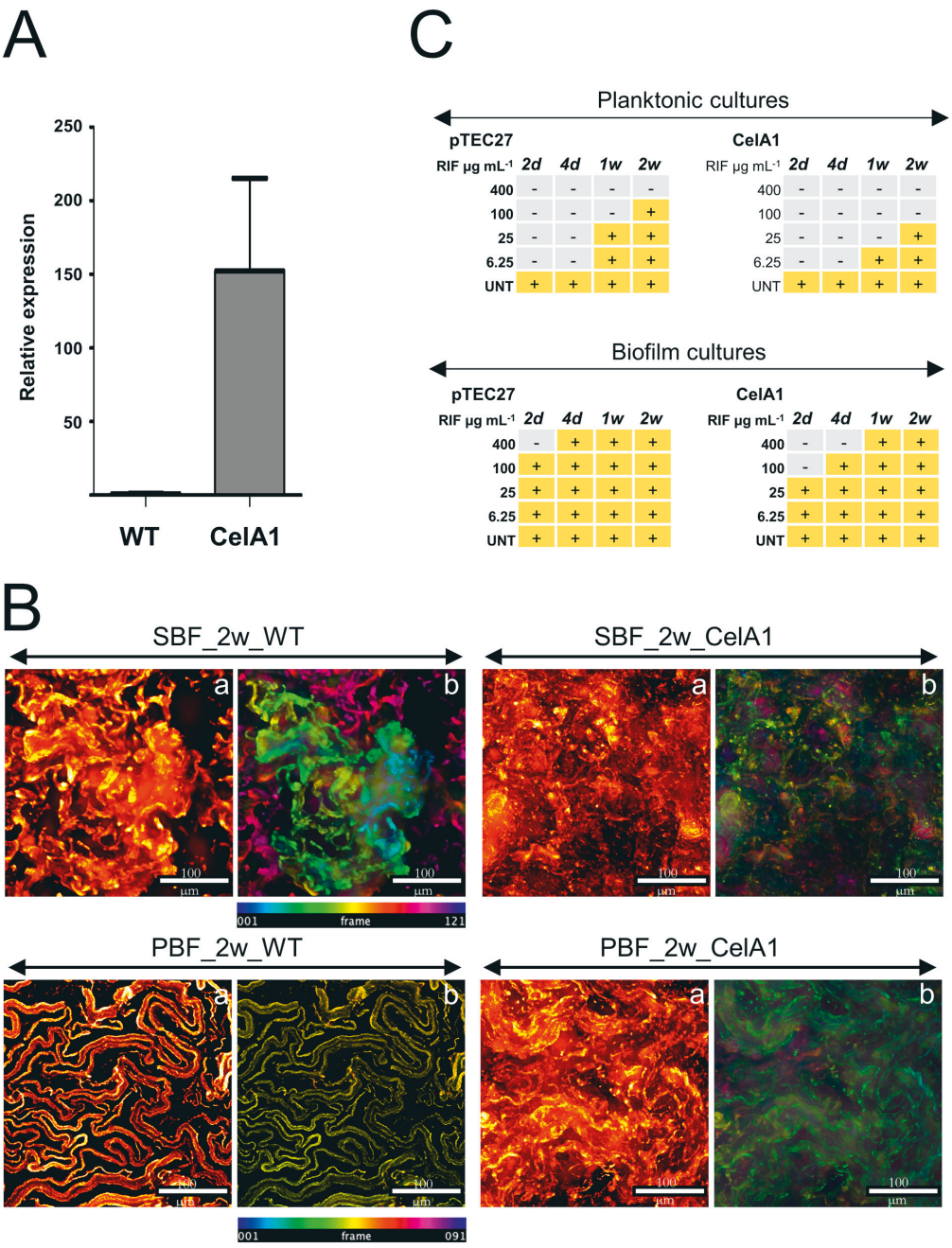

FIG 4 (A) Comparison of relative transcript abundance for *celA1* between the Mmr-CelA1 overexpression strain and the Mmr control strain with pTEC27 (WT). The CelA1 overexpression levels were normalized to the expression level of CelA1 in the WT control. The data were obtained from two technical replicates from two different bacterial clones. The bars represent the standard deviations. CelA1 expression was normalized to the amount of Mmr DNA in each sample. (B) CelA1 overexpression disrupts the biofilm development and the formation of the subtype-specific growth morphologies. The WDeM images are maximum-intensity projections of the 2-week-old Mmr control biofilms

(Continued on next page)

energy metabolism, and protein secretion/export. Figure 6A shows a protein-protein interaction (PPI) network for cluster 1 proteins: (i) cytoplasmic proteins with a primary function in amino acid biosynthesis (e.g., Gly, Asp, Tyr, Arg, His, Thr, Ser, Lys, and Phe), purine/pyrimidine metabolism (e.g., PyrG, PurD/L/H, and GuaB), and stress response (HrcA, ClpC/X, DnaJ, HtpG, AhpC, SodC, RecA, and Trx), (ii) proteins involved in cell wall/outer layer and mycomembrane biogenesis/metabolism (e.g., PknA/B, Weg31, CwsA, CwlM, PbpA1a, EmbA/B, KasA, DesA1/2, PpsA/B/D, PcaA, and Fad enzymes), (iii) components of the respiratory electron transport chain (SDH, FMR, and Qcr complex) and ATP synthesis (F_1F_o ATP synthase complex), and (iv) proteins involved in iron storage/homeostasis (ferritin). The PPI network analysis of the cluster 6 proteins indicated the enrichment of metabolic activities related to translation (ribosomal proteins/r proteins), stress response (GroEL/ES, GrpE, DnaK, TF, and ClpB) and the TCA/glyoxylate cycle (e.g., CitA, ICL1, fructose-bisphosphate aldolase [FBA], and GlcB) (Fig. 6B).

Clusters 2, 4, and 5 (*n*, 144) share coabundance patterns, which indicate increased protein abundances during the first weeks of growth in the PBFs compared to that in the SBFs. These contain virulence-, invasion-, and viability/persistence-related proteins, such as EsxA/B, ESX-EspB/G/M/P/N, Esx5 secretion-associated protease MycP, cutinase (Cut), a lysophospholipase (YtpA), endopeptidase (Lon), heparin binding hemagglutinin (HbhA), and fibronectin binding (Apa), catalase-peroxidase (KatG), and mammalian entry proteins (MCEs). Cytoplasmic proteins were also detected in these clusters (e.g., ICL2, aconitase [ACN], enolase [ENO], glyceraldehyde-3-phosphate dehydrogenase [GAPDH], GPD, Tpi, PGK, malate dehydrogenase [MDH], ClpP1/2, CpsA/D, Trp, Cys, Met, and an 18-kDa β-CA), but their composition differs clearly from those in clusters 1 and 6. In addition, cluster 2 contains virulence-associated ESAT-6-like proteins, TDM-cord factor synthesis-associated Ag85A/C (mycolyltransferases), and an MPT64 immunogen, with higher overall abundancies in the PL and PBF cells than in the SBFs. The remaining cluster 3 (*n*, 47) differs from the other five by proteins with its overall higher abundancies in the PL cells and/or in 4- to 12-week-old PBFs than in the SBFs at the same time points. One of these was identified as a potential trehalase (A0A2Z5YJK7_MYCMR), a glycoside hydrolase that catalyzes the conversion of trehalose to glucose, which had a high abundancy in 4- and 12-week-old PBFs.

The protein identifications most relevant to biofilm growth and viability identifications are listed in Table S6 according to their predicted functions. The major growth mode-dependent changes associate with the following five functional groups: (i) secretion mechanisms, virulence, and adherence; (ii) cell wall/membrane/lipid biogenesis and metabolism and biofilm formation; (iii) stress response; (iv) TCA/glyoxylate cycles and carbohydrate metabolism; and (v) maintaining redox balance and energy metabolism. An additional schematic model of the mycobacterial cell envelope in Fig. 7 illustrates the key proteome changes relevant to the PL-, SBF-, and PBF-type growth of Mmr.

Time-kill curve analysis for indicating persister cells in maturing biofilms. As growth mode-dependent differences imply higher persistence/tolerance-associated activities in biofilms than in planktonic cultures, we next validated these findings by exposing both the planktonic and biofilm cells to rifampicin and monitored cell death using a time-kill curve analysis. This method enables the demonstration of an overall slower killing efficacy for tolerant populations or a bimodal time-kill curve that indicates the presence of a persistent bacterial subpopulation (31, 32).

First, we used a bacterial killing assay with bioluminescence as a readout to quantify the tolerance/persistence in the planktonic cultures and 2-week-old biofilms. The planktonic and biofilm cells were treated with 400 μg ml^{-1} rifampicin (64× MIC), and the rate of bacterial

FIG 4 Legend (Continued)
(pTEC27, WT) and the Mmr-CelA1 cultures (a), together with color coded by *z* position images (b). Frame interval is 2 μm. (C) The MIC/MBC of rifampicin is reduced in both the PL and biofilms formed with the CelA1 overexpressing strain compared to that in the Mmr control cultures (PTEC27, WT). Rifampicin was added to the liquid cultures 2, 4, 7, and 14 days after the start of the culture. Ten microliters per sample (in triplicates) was plated 7 days after the addition of rifampicin, and CFU were counted 7 days thereafter. One hundred CFU per sample was used as the cutoff limit for bacterial growth. The experiment was carried out three times. The figure shows a representative experiment. −, no growth; +, bacterial growth; UNT, untreated.

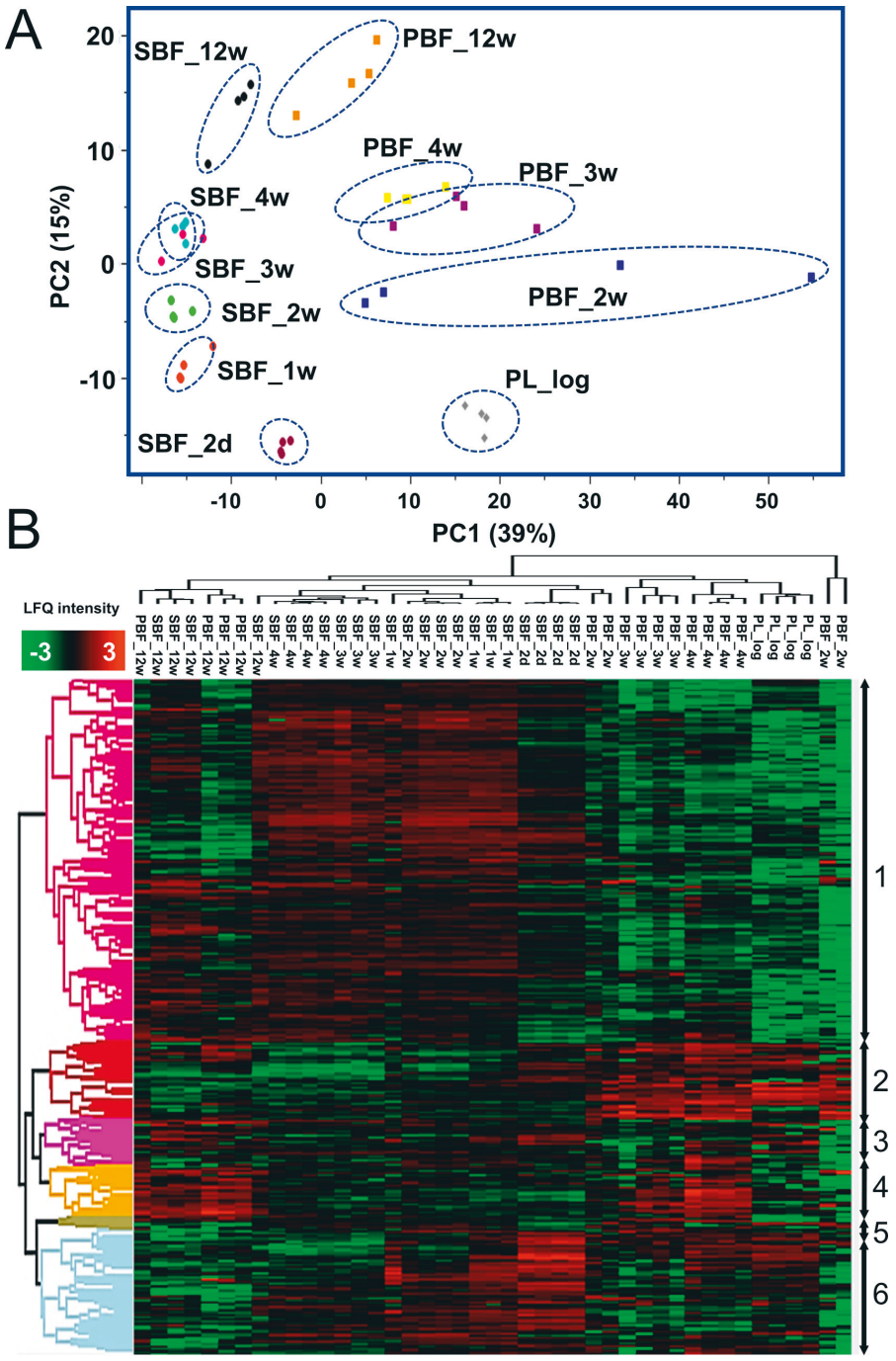

FIG 5 (A) PCA analysis of all detected proteins (based on LFQ intensities excluding one SBF_3w outlier), with PC1 and PC2 indicating growth mode- and time point-dependent changes. (B) Hierarchical clustering of proteins (complete linkage; *n*, 690) with significantly changed expression profiles. Color intensity: red and green indicate higher and lower protein abundances, respectively.

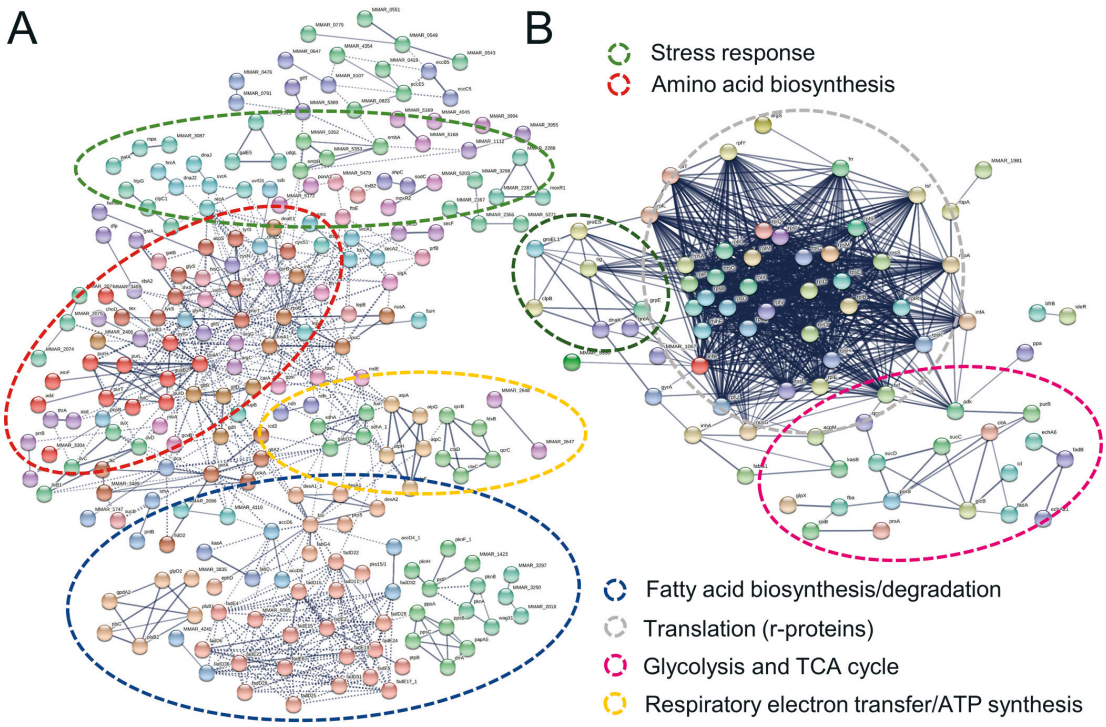

FIG 6 (A) PPI network analysis of cluster 1 proteins (Fig. 5B) with higher abundancies on SBFs between 2 and 4 weeks. Number (no.) of nodes, 368; no. of edges, 3,256; PPI enrichment, $P < 1.0e{-}16$. (B) PPI network analysis of cluster 6 proteins with higher abundancies in SBFs between 2 days and 2 weeks. Proteins were clustered using MCL with the inflation parameter set to 4.0 (cluster 6) and 6.0 (cluster 1). No. of nodes, 155; no. of edges, 3,024; PPI enrichment, $P < 1.0e{-}16$. Circles indicate the most enriched protein interactions.

killing was monitored for 7 days. The use of bioluminescence as a readout for killing biofilm-associated bacteria was also assessed using an optical density at 600 nm (OD_{600})-based method (see Fig. S3A). The time-kill curve for the biofilm population was bimodal, showing the faster killing of a susceptible subpopulation followed by slower killing of a persistent subpopulation of cells (Fig. 8A). These results indicate that Mmr biofilms harbor significantly more persister cells than logarithmic phase planktonic populations.

Next, the development of persistence in the biofilms was monitored by killing 2-day-, 4-day-, and 1-week-old biofilm cells with 64× MIC rifampicin. Analysis of the time-kill curves showed that persistence increased gradually in the maturing biofilms, reaching a statistically significant increase in 1-week-old biofilms compared to that in the planktonic cells ($P = 0.0002$) (Fig. 8B). In untreated biofilms, the bioluminescence signal level continued to increase well past the 1-week time point, showing that the biofilm-associated mycobacterial population was replicating and/or metabolically active at this stage (Fig. S3B). This indicates that increased persistence is not (mainly) caused by the induction of dormancy or metabolic inactivity. According to our experimental settings, PBFs form later than SBFs and are visually detectable only after 2 weeks. Thus, these data show that a substantial persister subpopulation develops in SBFs by the first week of biofilm development.

To test if the formation of persister cells differs between the two biofilm subtypes, PBFs and SBFs were collected separately and tested with the time-kill assay under 64× MIC rifampicin. After 7 days, the time-kill curves indicated no significant differences in the rates of persistence between the 2-week-old pellicle and submerged biofilms ($P = 0.51$) (Fig. 8C). Thus, our results indicate that the proportion of persisters is greater in >1-week-old Mmr biofilms

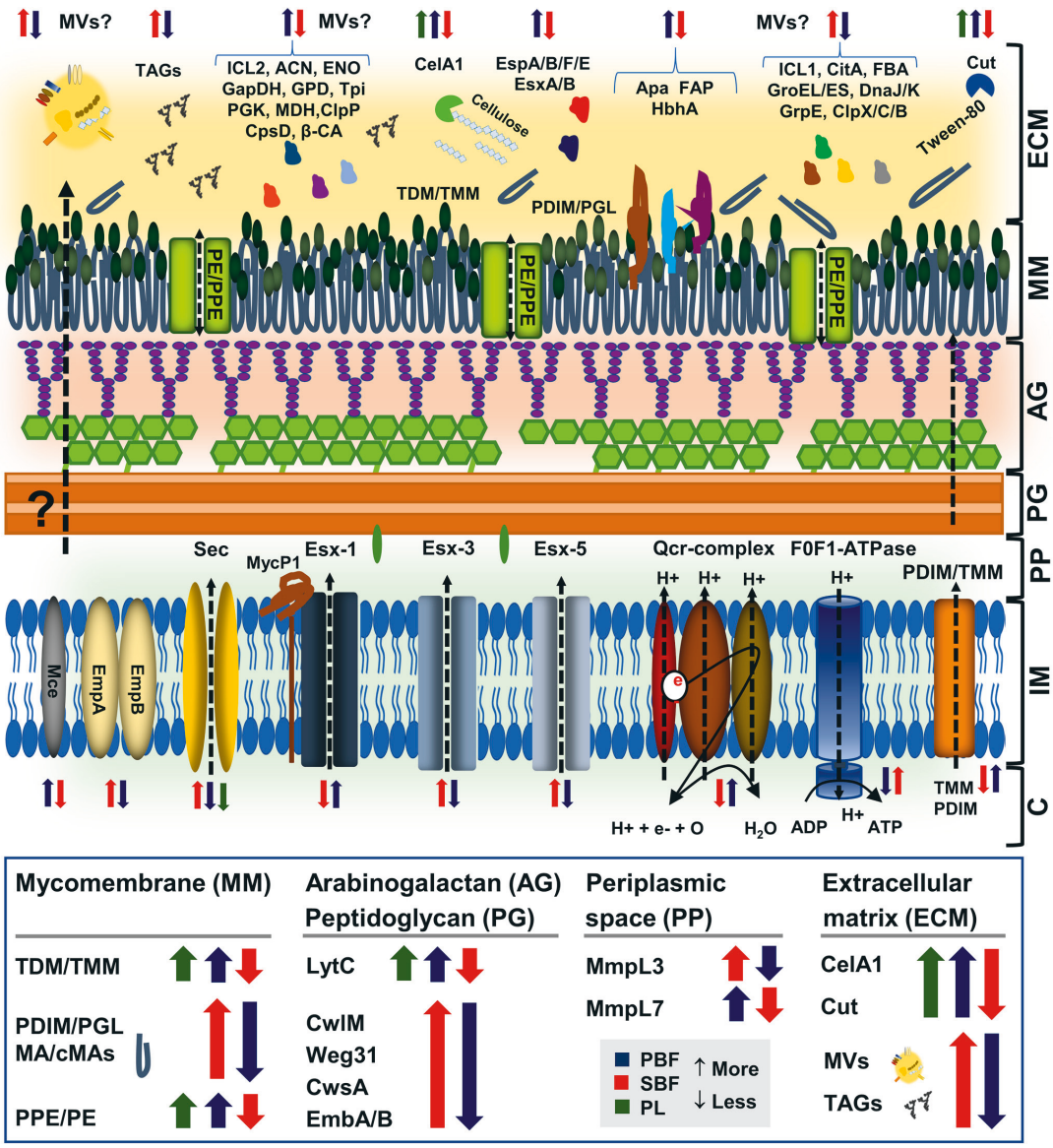

FIG 7 Schematic model of the Mmr cell envelope with key protein abundance changes specific to PL, PBF, and SBF cells. Colored arrows pointing up/down refer to protein abundances/abundance changes within the indicated cell sample types (green, PL; blue, PBFs; red, SBFs). MA, mycolic acids; cMAs, cyclopropanated mycolic acids; TDM/TMM, trehalose-6,6-dimycolate/trehalose monomycolate; PDIM/PGL, phthiocerol dimycocerosates/phenolic glycolipids. C, cytoplasm; IM, inner membrane; PP, periplasmic space; AG, arabinogalactan; PG, peptidoglycan; MM, mycomembrane; ECM, extracellular matrix.

than in logarithmic planktonic cell populations and that the biofilm-associated persistence increases over time.

DISCUSSION

Mmr grows in morphologically distinct biofilm subtypes *in vitro*. A recent study confirmed that Mtb forms biofilm-like communities *in vivo*, which confers increased

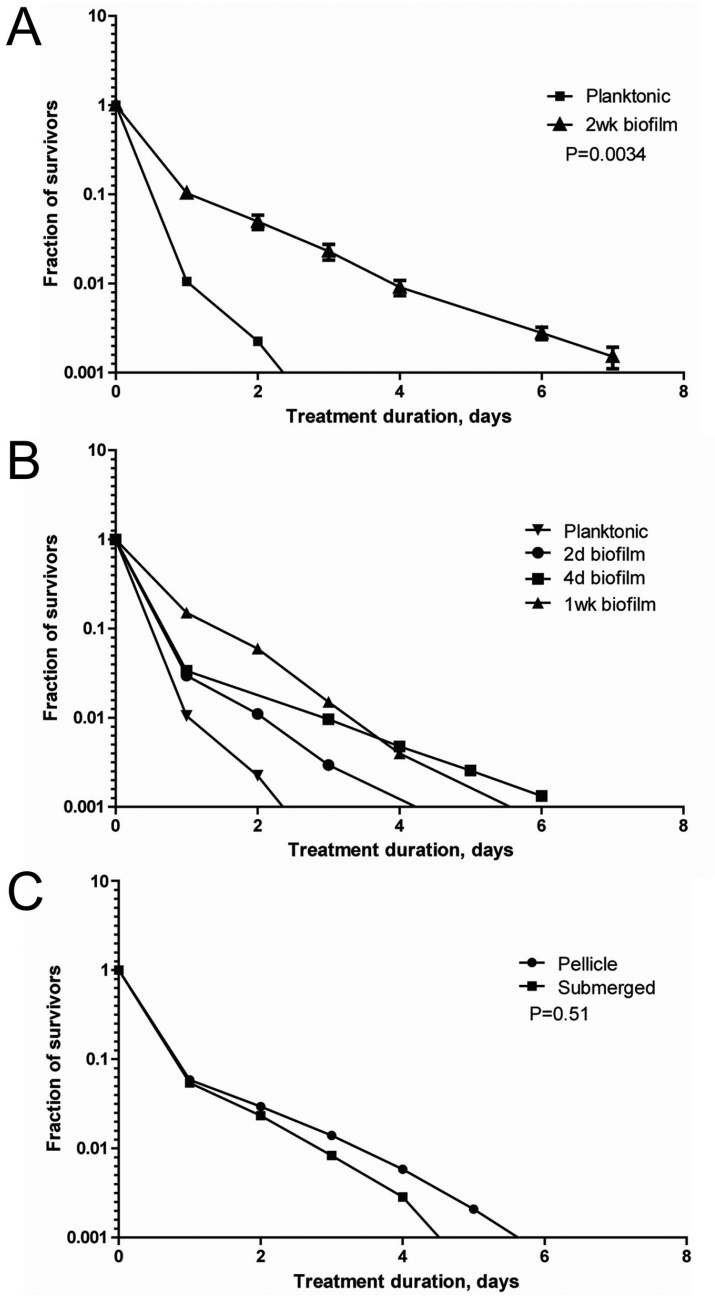

FIG 8 The proportion of persistent bacterial cells increases in Mmr biofilms. Time-kill curve analysis was performed by culturing biofilms from 2 days to 2 weeks and treating the bacteria with 400 μg ml^{-1} rifampicin. The killing kinetics were monitored for 7 days by measuring the bioluminescence signal produced by Lux-Mmr daily. (A) Logarithmic growth phase planktonic cells and 2-week-old biofilm Mmr were treated with 400 μg ml^{-1} of rifampicin. The time-kill curves of the planktonic and biofilm-associated bacteria were significantly different ($P < 0.0034$, log rank test). The means and

(Continued on next page)

tolerance to rifampicin and thus provides an explanation for the chronic nature of TB (11). The present study shows that Mmr grows in two different biofilm subtypes and that reduced CelA1 hydrolase activity is one of the main triggers of biofilm growth and increased tolerance to rifampicin in both biofilm subtypes. Studies on Mtb and *M. smegmatis* have demonstrated that cellulose filaments are vital structural constituents of mycobacterial biofilm ECMs as well as essential for biofilm formation and the development of tolerance/persistence (9, 11, 18, 19). We also show that the Mmr biofilm subtypes show distinct morphologies, with SBFs containing lichen-like structures and PBFs consisting of ribbon-like cords under the same *in vitro* conditions. Biofilm growth accompanied by cording-like growth morphology is also reported for other mycobacteria and Mtb, in which the surface interactions mediated by, e.g., mycolic acids modulating the mycomembrane/capsule hydrophobicity (11, 33). The proteomic data presented here suggest that subtype-specific changes in cord factor TDM synthesis (mycolyltransferase Ag85), Esx1 secretion, phthiocerol dimycocerosate (PDIM) export (MmpL7), MA cyclopropanation (PcaA/Cma2), and lectin synthesis (33–37) may have affected the mycomembrane composition and thereby contributed to distinct biofilm growth morphologies in Mmr.

Mmr may use membrane vesicles to deliver proteins in the biofilm ECM. The LFQ proteomics identified cytoplasmic proteins and proteins associated with the inner membrane/mycomembrane as the largest protein group in both the planktonic and biofilm cells. These findings are supported by studies identifying cytoplasmic proteins in the capsule of another Mmr strain (E11) and by showing that their number increases when mycobacterial cells grow in the biofilms, as demonstrated for *Mycobacterium bovis* (17, 20). Membrane vesiculation is the most likely explanation for their presence on Mmr cells and within the biofilm ECM, as several reports have demonstrated the presence of membrane vesicles (MVs) on mycobacterial cells (38) as well as trapped in biofilm ECMs in other bacteria (39). In addition, several of the cytoplasmic and inner membrane/mycomembrane proteins detected here, including, e.g., enzymes involved in cell wall synthesis and lipid/fatty acid metabolism, were previously identified in MVs released by *Mycobacterium avium* 104 in response to starvation (40). Mycobacteria have been shown to form MVs from mycomembrane (mMV) during normal growth (cell lysis/death) and/or from the inner membrane (iMV) by blebbing in response to stress (e.g., iron limitation and anoxia) (38). This report supports the idea that the identified mycomembrane/inner membrane proteins could have also entered the biofilm ECMs by MVs in our study. We further propose that CwlM, an *N*-acetylmuramoyl-L-alanine amidase (41, 42), detected in 1-week-old SBFs, is involved in this process, as weakening the link between the mycomembrane and peptidoglycan has been suggested to stimulate MV blebbing in the mycobacteria (38). Taken together, these findings may explain why more cytoplasmic proteins were detected in this biofilm subtype, as the maturing biofilm cells grow under reduced oxygen tension and anoxia is one of the factors able to trigger membrane vesiculation.

Bacterial MVs are involved in, i.e., cell-cell communication, biofilm formation, virulence, antibiotic resistance, iron scavenging, nutrient acquisition, and modulating the host immune system (43). We detected several cytoplasmic proteins involved in signal transduction (e.g., PknL specific to SBFs and an adenylate cyclase detected only in biofilm ECMs) and enzymes involved in biofilm formation. GroEL1 and fatty-acid synthase system (FAS-I and FAS-II) enzymes were among the detected proteins that coordinate

FIG 8 Legend (Continued)
standard errors of the means (SEMs) from three biological replicates are shown. (B) In biofilms, persistence increases over time and is significantly higher after 1 week than that in planktonic bacteria ($P = 0.0002$, log rank test). Planktonic culture and 2-day-old biofilm show similar killing curves. Means and SEMs from three biological replicates are shown. (C) Two-week-old PBFs and SBFs were tested separately for persistence. The two different biofilm types show no difference in their persistence levels ($P = 0.51$, log rank test). Means and SEMs from three biological replicates are shown.

biofilm formation in mycobacteria. The GroEL1 chaperone is involved in the synthesis of mycolic acids (MAs) that eventually become inserted in the mycomembrane as trehalose dimycolates (TDMs) and monomycolates (TMMs) beneath the capsule (14, 21). This chaperone interacts with ketoacyl-acyl carrier protein (ACP) synthase KasA (FAS-II) to modulate the synthesis of short-chain MAs specifically during biofilm formation (21). A lack of GroEL1 has been reported to prevent the biofilm formation and to affect the biosynthesis and composition of MAs in *Mycobacterium bovis* BCG, whereas the GroEL1 deficiency blocks the formation of mature biofilms of *M. smegmatis* (21, 24). In addition, the overexpression of KasA and the inactivation of other FAS-II enzymes, such as enoyl-ACP reductase (InhA) and 3-oxoacyl-[acyl-carrier-protein] synthase 2 (KasB), have also been reported to prevent biofilm formation and formation of cords by reducing the cyclopropanation of MAs (14, 21, 25). Here, GroEL1, KasA, and InhA were detected as more abundant in the SBFs, implying that these enzymes could support the initial stages of SBF-type biofilm growth, as GroEL and KasA were detected with the highest abundancies already in the 2-day-old SBFs.

Although no cell lysis was seen during the sample preparation for proteomic analysis (see Table S7 in the supplemental material), we cannot exclude the possibility that some of the cytoplasmic or inner membrane/mycomembrane proteins were released by autolysis during growth. In other Gram-positive bacteria, cytoplasmic proteins reach the extracellular space via regulated autolysis (involving autolysins/peptidoglycan hydrolases), and as soon as the pH of the culture medium drops (due to the active metabolism of the growing cells), many of the released proteins show an enhanced ability to bind to the cell wall and biofilm ECM structures (43–48). SBF cells are exposed to hypoxic conditions, and oxygen limitation acidifies the biofilm matrix (48), allowing for a more efficient interaction between the cytoplasmic proteins and biofilm ECM structures. Thus, this could explain the presence of r proteins as the largest cytoplasmic protein group already in 2-day-old SBFs; the strong positive charge of these proteins has been proposed to mediate electrostatic interactions with anionic cell surface components, which promotes cell aggregation and biofilm stabilization (48). Since the exposed mycomembranes with MAs as the major components create a condition stimulating an interaction with many cytoplasmic proteins, pH-dependent binding with the cell surface components could also explain why cytoplasmic proteins were detected in Mmr cells grown on Tween 80.

Biofilm subtypes differ in terms of secreted virulence and adhesion factors. The proteomics data indicated that the mycomembrane-associated PPE/PE family proteins were remarkably greater in number in the PL cells than in the PBFs or SBFs, indicating that Mmr in a single-cell state could more readily interact with the host and modulate the host immune response and/or nutrient transport (49, 50). PL cells were cultured in the presence of Tween 80, which, in detaching the mycobacterial capsule (17), most likely helped identify these immunogens. Tween 80 can also induce alterations in the morphology, pathogenicity, and virulence of mycobacteria (51). For example, genes encoding lipases and cutinases have been shown to be significantly upregulated in Mtb in response to this nonionic surfactant. Our data are in line with this by showing that several lipases/cutinases, with a likely ability to hydrolyze Tween 80, were more abundant in PL cells than in biofilms. As Tween 80 is considered to mimic a lipid-rich milieu of macrophages (51), the detected PL proteome changes here may reflect a metabolic adaption to conditions faced *in vivo*.

Our findings also suggest that Mmr uses different T7SS pathways in SBFs and PBFs for virulence and adherence. For example, the Esx1 secretion components and substrates (EsxA/B, EspB, EspF, EccA1, EspG1, EspH, EspL, and MycP) were detected as more abundant in the PBFs, while those associated with Esx5-type secretion were overall more abundant in the SBFs (Ecc, EspG, and PPE/PE proteins). Both secretion pathways can contribute to virulence and subverting the host immune system in Mtb (52). The major subtype-dependent differences between the PBFs and SBFs were related to invasion and adherence, including the MCE proteins, fibronectin-binding APA, and

HphA, which can modulate host cell signaling as well as aid adhesion or entry into host cells (53–55). All these proteins were significantly more produced by the PBFs than the SBFs, and, in the case of MCEs, may also involve MVs, as these adhesins are located on the inner membrane of the mycobacterial cell wall. HphA also has implications in promoting cell-cell aggregation in Mtb (56), suggesting that this adhesin could also contribute to cording during PBF-type growth.

Biofilm subtypes use different tolerance- and persistence-conferring mechanisms. Tolerance is defined as the extent of time that bacteria can survive in the presence of a high antibiotic concentration (31), whereas persisters are a subpopulation of phenotypically drug-tolerant cells that do not grow in the presence of an antibiotic (32). We show that antibiotic killing of biofilm cells occurs at a significantly lower rate than for PL cells. The time-kill curve indicated the temporally increased formation of a persistent subpopulation with slower killing kinetics as well as the formation of persisters in SBFs already after 1 week. At this stage, Mmr biofilms remained metabolically active and replicating, indicating that persistence develops due to phenotypic differentiation during biofilm growth rather than via the induction of dormancy.

The proteomic findings suggest that Mmr could use both overlapping and subtype-specific mechanisms for increasing its tolerance and persistence, in which MVs or other nonclassical routes for protein export may play a role. Here, most significant proteome changes related to cytoplasmic and inner membrane/mycomembrane proteins and included enzymes/proteins involved in the TCA cycle and glyoxylate shunt, mycolic acid synthesis stress response, and energy and redox metabolisms. A recent transcriptome analysis of another nontuberculous mycobacterial model, *Mycobacterium abscessus*, supports our findings; biofilm growth activated the glyoxylate shunt, redox metabolism, and the MA synthesis-associated elongation and desaturation pathways. The TCA cycle-associated enzyme CitA was recently reported to control the asymmetric cell division in *Caulobacter crescentus* (57). This process has also been shown in mycobacteria to lead to the formation of heterogenous cell populations in biofilms, macrophages, and granulomatous lesions (7, 58, 59). Here, our findings indicated the presence of this enzyme in 1-week-old SBFs, suggesting that asymmetric cell division occurs before the PBFs are formed. Moreover, arabinosyltransferases EmbA and EmbB, involved in the polymerization of arabinogalactan, were also detected with high abundances in SBFs by 1 week onward, suggesting that strengthening the arabinogalactan could further help residing cells, including the persisters, increase their tolerance to rifampicin, as demonstrated with Mtb persisters under hypoxia (60). Taken together, these findings strengthen the hypothesis that persisters are indeed formed in 1-week-old SBFs and support the results obtained with the biofilm killing assay in SBFs at this time point.

We also suggest that cells in PBFs use different TCA cycle enzymes, such as aconitase (ACN), malate dehydrogenase (MDH), enolase (ENO), and/or fructose-bisphosphate aldolase (FBA), to maintain long-term survival. In other Gram-positive bacteria, these enzymes belong to known moonlighting proteins with established secondary roles outside the bacterial cell (e.g., adhesion) (30). In mycobacteria, these enzymes have been reported to contribute to increased viability or persistence (61–63). The associated glyoxylate shunt could also be involved (64), as isocitrate lyase 1 (ICL1) was detected as more abundant in the SBFs, implying that this enzyme could help residing cells increase their antioxidant defense and antibiotic tolerance (65). In contrast, ICL2 was produced more in the PBFs, which may help the cells to survive under starvation conditions when fatty acids are used as the primary carbon source (66). This is in line with the temporally increased production of diacylglycerol *O*-acyltransferase (Tgs1) in PBFs, which can promote the accumulation of triacylglycerols (TAGs), a process that has been considered a hallmark feature of persisting Mtb/latent TB and a long-term energy source for Mtb and has been found in substantial amounts in the mycobacterial cell wall (67, 68). The detection of trehalase as significantly more abundant in 4- to 12-week-old PBFs strengthens the idea that cells within this biofilm subtype suffer from nutrient stress and activate trehalose salvage/recycling to promote redox and energy

homeostasis, as seen under carbon limitations in Mtb (69). These findings may also explain the detection of proteases, chaperones, and assisting stress proteins in high numbers in the biofilm ECMs, including, e.g., the proteases Clp/Lon and the cold shock protein CpsD, with known implications in stringent response, persistence, and/or post-antibiotic recovery (70–72). These proteins were detected here as more abundant in the PBFs than in the SBFs, implying that these pathways are preferred in PBFs to maintain viability.

A recent study comparing high numbers of persister Mtb mutants using genomics and transcriptomics indicated a significant upregulation of energy production pathways and pathways involved in redox reactions (oxidoreductase) (73). The ECM proteome changes occurring during SBF-type growth are in line with this report, as the components of the respiratory electron transfer chain (cytochrome bc_1 complex, cytochrome *c* terminal oxidase, and F_oF_1 ATPase synthase) were detected as more abundant in the SBFs facing more hypoxic conditions than in the PBFs. Our findings also agree with previous reports showing that the electron transfer chain is essential for maintaining ATP homeostasis and the viability of nonreplicating/persistent Mtb cells under hypoxia (74–76). In addition, we show that both redox and iron metabolism could also play a biofilm subtype-specific role in helping the cells cope with hypoxia/aeration-related stress (77); several oxidoreductases, thioredoxin, and a superoxide dismutase (SOD) were overall more abundant in the SBFs, and a catalase-peroxidase (KatG) and alkyl hydroxyperoxidases (AhpCF) were more abundant in the PBFs. These enzymes have been shown to protect Mtb against oxidative stress by the reduction of superoxide radicals into less toxic intermediates for inhibiting autophagy, apoptosis, and cellular damage (78). Iron-storing proteins ferritin (BfrB) and bacterioferritin (BfrA) can confer increased redox resistance to Mtb and protect the cells against oxidative stress and hypoxia, respectively (79). Here, these iron-storing proteins displayed biofilm subtype-specific abundance changes, implying that SBFs could rely on BfrB to cope with hypoxia and PBFs could rely on BrfA to help cells grow at the air-liquid interface.

Conclusions. The present study reports an in-depth view of ECM proteome changes occurring in Mmr ATCC 927 during biofilm growth *in vitro* from 2 days to 3 months. We show that this nontuberculous mycobacterial model forms SBFs already after 2 days, whereas the formation of detectable PBFs was observed after 2 weeks of growth in the absence of Tween 80. Both biofilm subtypes were formed physically under the same conditions with clearly distinct growth morphologies: SBFs with lichen-like structures and PBFs with ribbon-like cords. We show that reduced CelA1-mediated cellulose hydrolysis is necessary to establish proper biofilm growth, growth morphology, and increased tolerance to rifampicin for both biofilm subtypes. The formation of persisters in both biofilm subtypes and increased tolerance were further confirmed by the newly established bioluminescence-based time-kill assay, which provides an effective tool for quantifying tolerance and persistence of Mmr. The proteomic findings imply that subtype-dependent changes in MA synthesis and modification, Esx1-type secretion, and the production of specific adhesins were the major drivers of distinct biofilm growth morphologies. We also propose that pathways associated with MA biosynthesis, development of tolerance/persistence, and oxidative/redox stress are differentially used in PBFs and SBFs to maintain prolonged viability. Possible explanations for these differences include the different oxygen tensions encountered by the biofilm subtypes, differences in membrane vesiculation activities, and/or other nonclassical pathways for protein export. Taken together, this is the first study reporting on ECM proteome dynamics in maturing mycobacterial biofilms and predicting biofilm subtype-specific changes in cell-cell communication, biofilm matrix formation, virulence, and tolerance/persistence. This is also the first time that the kinetics of persistence have been explicitly measured from mycobacterial biofilms.

MATERIALS AND METHODS

Preparing bacterial cells for surface proteomics. *Mycobacterium marinum* (ATCC 927) with the pTEC27 plasmid expressing the red fluorescent protein tdTomato (Addgene number 30182, http://n2t.net/addgene:30182) (29) was precultured on Middlebrook 7H10 plates with 10% (vol/vol) oleic albumin

dextrose catalase (OADC) enrichment (Fisher Scientific, NH, USA) and 0.5% (vol/vol) glycerol at 29°C for 1 week. For planktonic cultures, an inoculum of Mmr was transferred into a Middlebrook 7H9 medium supplemented with 10% (vol/vol) ADC (Fisher Scientific, NH, USA), 0.2% (vol/vol) glycerol, and 0.2% (vol/vol) Tween 80 (Sigma-Aldrich, MO, USA), and the cells were cultured at 29°C in cell culture flasks with filter caps. After 3 days of incubation, the cell cultures were diluted to obtain an OD_{600} of 0.042, and the dilutions were cultured for an additional 2 days at 29°C until harvesting. For the biofilm cultures, a Middlebrook 7H9 medium with the ADC growth supplement but without Tween 80 or glycerol was used. The inoculum was cultured for 3 days at 29°C until the OD_{600} reached 0.45. The cell cultures were diluted 1:40, and the dilutions were divided into 10-ml aliquots. The cap of each tube was sealed with Parafilm M laboratory wrapping film, and the cultures were incubated at 29°C. Planktonic and biofilm cell samples (SBFs and PBFs separately) were collected at the time points indicated in Fig. 2A. All the cultures were performed in quadruplicates. Planktonic cells were harvested by centrifugation (3 min, 5,000 × *g*, 4°C), and the pelleted cells were suspended gently in ice-cold buffer (100 mM bis-Tris, pH 6.5) to remove interfering/nonspecifically bound proteins. This step prevents the detachment/removal of cytoplasmic moonlighters bound to the cell surfaces/biofilm ECM (43–46, 79, 80). The PBFs were collected with an inoculation loop, the extra medium was removed by pipetting to avoid cross-biofilm-type contamination, and the SBFs were harvested by pipetting/scraping. The PBFs and SBFs were collected in separate Eppendorf tubes in ice-cold buffer (100 mM bis-Tris, pH 6.5). Cells (planktonic and biofilm cultures) were pelleted by centrifugation (3 min, 5,000 × *g*, 4°C), and the washed cells were suspended gently in 95 μl of 100 mM triethylammonium bicarbonate (TEAB; pH 8.5) for the enzymatic shaving reaction.

Trypsin/Lys-C shaving of planktonic and biofilm cells. Peptides from cell surface/biofilm ECM-associated proteins were released via a trypsin/Lys-C mix (Promega) at a final concentration of 50 ng μl^{-1}, and the digestions were incubated at 37°C for 20 min. The method was validated by counting the number of colonies formed by the planktonic/single and biofilm cells treated with/without the enzyme mix (see Table S7 in the supplemental material). The released peptides and the enzymes were recovered by filtration through a 0.2-μm acetate membrane (Costar Spin-X centrifuge tube filter; Corning Inc., Corning, NY, USA) by centrifugation (8,000 × *g*, 3 min, 20°C). Flowthroughs were incubated for 16 h at 37°C. The concentration of released peptides in each sample was measured with a NanoDrop 2000 spectrophotometer (Thermo Scientific). Digestions were terminated with 0.6% (vol/vol) trifluoroacetic acid (TFA) (Sigma-Aldrich), and the peptides were purified using ZipTip C_{18} (Millipore) according to the manufacturer's instructions and dried using a miVac centrifugal vacuum concentrator (Genevac).

LC-MS/MS analysis. The peptides were dissolved in 0.1% (vol/vol) formic acid (FA) and analyzed with nanoscale LC-MS/MS using an Easy-nLC 1000 nano-LC system (Thermo Scientific) coupled with a quadrupole Orbitrap mass spectrometer (Q Exactive; ThermoElectron, Bremen, Germany) as previously reported (80). The obtained MS raw data were processed via MaxQuant software (version v.1.6.1.0) with the built-in search engine Andromeda (81, 82), using a protein database comprising all 5,564 Mmr protein sequences (UniProt proteome up000257451, genome accession PEDF01000000), both forward and reverse. Carbamidomethyl (C) was set as fixed, and methionine oxidation was set as a variable modification. Tolerance was set to 20 ppm in the first search and 4.5 ppm in the main search. Trypsin without the proline restriction enzyme option and with two allowed miscleavages was used. The minimal unique plus+ razor peptide number was set to 1, the false-discovery rate (FDR) was set to 0.01 (1%) for peptide and protein identification, and LFQ with default settings was used. The mass spectrometry proteomics data were deposited in the ProteomeXchange Consortium via the PRIDE (83) partner repository with the data set identifier PXD02010.

Proteome statistics and bioinformatics. The identified Mmr proteins were manually curated by characterizing hypothetical and tentatively annotated proteins with the aid of the Basic Local Alignment Search Tool (BLAST) program from the National Center for Biotechnology Information (NCBI) (84–86) combined with CDD/SPARCLE conserved domain identification (87) and SmartBLAST (UniProt) searches. General protein functions were annotated using the Gene Ontology (GO) database (88). Isoelectric points (pIs) and molecular weights (MWs) for the identified proteins were predicted using EMBOSS Pepstats (89) at https://www.ebi.ac.uk/Tools/seqstats/emboss_pepstats/. The presence of possible protein secretion motifs (classical and nonclassical) for all the predicted and identified proteins was obtained with SignalP4.1 (90) (http://www.cbs.dtu.dk/services/SignalP/) and SecretomeP 2.0/SecP (91) (http://www.cbs.dtu.dk/services/SecretomeP/). The presence of transmembrane spanning domains/helices (TMDs) was determined with the TMHMM Server v. 2.0 at http://www.cbs.dtu.dk/services/TMHMM/ (92, 93) for the identified proteins.

For indicating statistically significant abundance changes, the log_2-transformed LFQ data were analyzed in Perseus v.1.6.2.3 (94) using a Student's *t* test with permutation-based FDR adjustment. For the multivariate analyses, the missing values were replaced by imputed values from the normal distribution (width, 0.3; down shift, 1.8) and then normalized (Z-score) prior to ANOVA for multisample testing (S0 set to 0.1 and a permutation-based FDR of 5%) and hierarchical clustering/PCA. STRING protein interaction network and functional enrichment analyses (GO, KEGG, InterPro, and Pham) were studied using the STRING database v. 11 (95). Interaction scores were set to high (0.700) confidence, and the interacting proteins were clustered using Markov clustering (MCL) with the inflation parameter set to 4.0 to 6.0. Functional enrichments were statistically assessed with both rank- and gene set-based approaches (FDR of 0.05).

Creation of the CelA1 overexpression construct in Mmr. The Mmr CelA1 overexpression strain was created by ordering the MMAR_0107 open reading frame in the pUC57 vector with appropriate restriction sites from GenScript and subcloning the construct into the pTEC27 vector (Addgene) (29),

which carries the red fluorescent protein tdTomato. The sequence of the plasmid was confirmed by sequencing. The resulting plasmid was transformed into an electrocompetent Mmr ATCC 927 strain. Transformants were selected on Middlebrook 7H10 agar plates containing 10% (vol/vol) OADC enrichment, 0.5% (vol/vol) glycerol, and 75 μg ml^{-1} hygromycin.

RNA and DNA extractions. For RNA and DNA extractions, the *celA1* overexpression strain and Mmr were precultured on Middlebrook 7H10 plates and transferred into the Middlebrook 7H9 medium described above (75 μg ml^{-1} hygromycin for the CelA1 strain). After 3 days, the bacterial cells were harvested, pelleted, and homogenized in TRI reagent (Thermo Fisher Scientific, NH, USA) with ceramic beads using a PowerLyzer24 (MO BIO, CA, USA). After homogenization, the samples were sonicated for 9 min, and the RNA and DNA were extracted according to the manufacturer's instructions.

***celA1* expression and the quantification of mycobacterial loads by qPCR.** Prior to qPCR analysis, RNA was reverse transcribed into cDNA with a reverse transcription kit (Fluidigm, CA, USA) according to the manufacturer's instructions. *celA1* expression was measured using soFast EvaGreen supermix with the low ROX qPCR kit (Bio-Rad, CA, USA) and the CFX96 qPCR system (Bio-Rad). The primers used for *celA1* were (forward) 5′-ACACTCCGCAGTCCTACT-3′ and (reverse) 5′-TAGAGCGTCAGAATCGGC-3′. The number of mycobacterial cells in the sample was quantified using the SensiFAST SYBR no-ROX qPCR kit (Bioline, London, UK) on bacterial DNA according to the manufacturer's instructions. The primers used for Mmr quantification were targeted against the 16S-23S locus AB548718 (forward, 5′-CACCACGAGAAACACTCCAA-3′; reverse, 5′-CACCACG AGAAACACTCCAA-3′). Each bacterial quantification qPCR run included a standard curve of the known amounts of Mmr DNA. The mycobacterial cell number in each sample was used to normalize *celA1* expression.

Widefield deconvolution microscopy of Mmr biofilms. PBFs and SBFs formed by Mmr with pTEC27 (WT), expressing the red fluorescent protein tdTomato (29), and Mmr overexpressing CelA1 were prepared as follows. Briefly, the cells were incubated at 29°C, and the surface-attached cells were imaged at 7, 14, and 21 days after dilution. *In situ* imaging of the SBFs was conducted with Nikon FN1 upright epifluorescence microscope equipped with a 20×/0.8 dry lens objective, Hamamatsu ORCA-Flash4.0 V3 digital complementary metal-oxide-semiconductor (CMOS) camera, and CoolLED pE-4000 light source. tdTomato was excited with a 550-nm light-emitting diose (LED), and fluorescence was collected with a 617/73 band-pass emission filter. Image stacks were collected with 2-μm intervals (*x-y* pixel size, 325 nm). The data were deconvolved with Huygens Essential deconvolution software (SVI, Amsterdam, Netherlands) using a 200-iteration limit, signal-to-noise ratio of 30, and quality threshold of 0.01.

Biofilm tolerance assays. The role of CelA1 overexpression in the antibiotic tolerance of Mmr was assessed as follows. First, the *celA1* overexpression strain and pTEC27 control strain were cultured for 1 week on 7H10 plates (10% OADC and 0.5% glycerol plus 75 μg ml^{-1} hygromycin) and then transferred in a Middlebrook 7H9 medium supplemented with 10% ADC and 75 μg ml^{-1} hygromycin) at an OD_{600} of 0.1 to initiate biofilm growth. Aliquots of bacterial suspension (192 μl per well) were added to 96-well-plates in triplicates, sealed with parafilm, and incubated at 29°C in the dark. Planktonic cultures grown in the presence of 0.2% (vol/vol) Tween 80 were used as controls. Eight microliters of antibiotics per well was added 2, 4, 7, and 14 days after the start of the liquid culture. The final antibiotic concentrations used were 400, 100, 25, and 6.25 μg ml^{-1} for the rifampicin TOKU-E solution. Untreated wells were used as controls. Ten microliters per sample was plated on 7H9 plates (10% OADC, 75 μg ml^{-1} hygromycin) 1 week after the addition of antibiotics. The plates were incubated at 29°C for 7 to 9 days, and the colonies were counted.

Biofilm persistence assays. Mmr (ATCC 927) with a bioluminescence cassette in the pMV306hsp+LuxG13 plasmid was used for antibiotic tolerance assays. pMV306hsp+LuxG13 was provided by Brian Robertson and Siouxsie Wiles (Addgene plasmid number 26161; http://n2t.net/addgene:26161). To measure the kinetics of bacterial killing, the bioluminescent Mmr strain was first cultured on Middlebrook 7H10 agar (Sigma-Aldrich) supplemented with 0.5% (vol/vol) glycerol (Sigma-Aldrich) and 10% (vol/vol) OADC enrichment (Becton, Dickinson) at 29°C for 7 days in the dark. To initiate biofilm formation, the Mmr cells were suspended in Middlebrook 7H9 broth (Sigma-Aldrich) supplemented with 10% (vol/vol) ADC enrichment (Becton, Dickinson) at a starting OD_{600} of 0.1. Planktonic cultures were prepared in the same way except that the medium contained 0.2% (vol/vol) glycerol (Sigma-Aldrich) and 0.2% (vol/vol) Tween 80 (Sigma-Aldrich). Bacterial suspensions (192 μl per well in triplicates) were divided into white 96-well plates (Perkin Elmer). The biofilm cultures were sealed with laboratory film and incubated at 29°C in the dark to the desired ages. Rifampicin solution (TOKU-E) in water at a final concentration of 400 μg ml^{-1} corresponding to 64× MIC was added to the bacterial suspensions and incubated for 7 days at 29°C in the dark. The bioluminescence signal was measured with an EnVision plate reader (Perkin Elmer) as a readout for bacterial survival three times for 3 s per well daily from a white 96-well plate for 7 days. The background signal from medium-only wells was first subtracted from the sample wells, and an average of the three measurements normalized with the starting bioluminescence signal was used to draw time-kill curves of the bacterial population in the biofilms at different maturation stages.

To compare the level of persistence/tolerance in the PBFs and SBFs, Mmr was cultured in a total volume of 10 ml at the starting OD_{600} value of 0.1. After 2 weeks, the biofilms were collected separately from the tubes by lifting the pellicle with a 1-μl inoculation loop coupled with careful pipetting. The pellicle and submerged biofilms were centrifuged at 10,000 × *g* for 3 min, the supernatants were collected, and the wet weight of the bacterial mass was measured. The bacterial cells were suspended into previously collected spent medium at the concentration of 15 mg ml^{-1}, vortexed briefly, and divided into white 96-well plates (Perkin Elmer) with 192 μl of cell suspension per well in triplicates. Eight microliters of TOKU-E solution at a final concentration of 400 μg ml^{-1} was pipetted into the bacterial suspension. Liquid cultures were incubated for 7 days at 29°C in the dark, and the bioluminescence signal was

measured daily with an EnVision plate reader (Perkin Elmer) three times for 3 s per well. The background signal from the medium-only wells was first subtracted from the sample wells, and an average of the three measurements was normalized with the starting bioluminescence signal measured just before adding the rifampicin. The statistical significance of the differences between the time-kill curves was tested with a log rank test using Prism5 software (GraphPad).

SUPPLEMENTAL MATERIAL

Supplemental material is available online only.

FIG S1, PDF file, 0.1 MB.

FIG S2, PDF file, 0.1 MB.

FIG S3, PDF file, 0.1 MB.

TABLE S1, XLSX file, 1.9 MB.

TABLE S2, XLSX file, 0.3 MB.

TABLE S3, XLSX file, 2.5 MB.

TABLE S4, XLSX file, 0.9 MB.

TABLE S5, XLSX file, 0.04 MB.

TABLE S6, DOCX file, 0.1 MB.

TABLE S7, XLSX file, 0.1 MB.

ACKNOWLEDGMENTS

This work received financial support from the Academy of Finland (project no. 322010 to A.F., J.Y.-K., and M.P. and no. 326674 to M.P.), the Jane and Aatos Erkko Foundation (to M.P.), the Sigrid Jusélius Foundation (to M.P.), the Foundation of the Finnish Anti-Tuberculosis Association (Suomen Tuberkuloosin Vastustamisyhdistyksen Säätiö; to H.L., L.-M.V.-A., and K.S.), and the Tampere Tuberculosis Foundation (to M.P., K.S., H.M., H.L., and L.-M.V.-A.). Mass spectrometry-based proteomic analyses were performed by the Proteomics Core Facility, Department of Immunology, University of Oslo/Oslo University Hospital, which is supported by the Core Facilities program of the South-Eastern Norway Regional Health Authority. This core facility is also a member of the National Network of Advanced Proteomics Infrastructure (NAPI), which is funded by the Research Council of Norway INFRASTRUKTUR-program (project number 295910 to T.A.N.).

REFERENCES

1. World Health Organization. 2020. Global tuberculosis report 2020. License CC BY-NC-SA 3.0 IGO. World Health Organization, Geneva, Switzerland.
2. Panjabi R, Comstock GW, Golub JE. 2007. Recurrent tuberculosis and its risk factors: adequately treated patients are still at high risk. Int J Tuberc Lung D 11:828–837.
3. Rosser A, Marx FM, Pareek M. 2018. Recurrent tuberculosis in the pre-elimination era. Int j Tuber Lung Dis 22:139–150. https://doi.org/10.5588/ijtld.17.0590.
4. Aldridge BB, Fernandez-Suarez M, Heller D, Ambravaneswaran V, Irimia D, Toner M, Fortune SM. 2012. Asymmetry and aging of mycobacterial cells lead to variable growth and antibiotic susceptibility. Science 335:100–104. https://doi.org/10.1126/science.1216166.
5. Malherbe ST, Shenai S, Ronacher K, Loxton AG, Dolganov G, Kriel M, Van T, Chen RY, Warwick J, Via LE, Song T, Lee M, Schoolnik G, Tromp G, Alland D, Barry CE, III, Winter J, Walzl G, Catalysis TB–Biomarker Consortium, Lucas L, van der Spuy G, Stanley K, Thiart L, Smith B, Du Plessis N, Beltran CGG, Maasdorp E, Ellmann A, Choi H, Joh J, Dodd LE, Allwood B, Koegelenberg C, Vorster M, Griffith-Richards S. 2016. Persisting positron emission tomography lesion activity and *Mycobacterium tuberculosis* mRNA after tuberculosis cure. Nat Med 22:1094–1100. https://doi.org/10.1038/nm.4177.
6. Jankute M, Cox JA, Harrison J, Besra GS. 2015. Assembly of the mycobacterial cell wall. Annu Rev Microbiol 69:405–423. https://doi.org/10.1146/annurev-micro-091014-104121.
7. Sarathy JP, Via LE, Weiner D, Blanc L, Boshoff H, Eugenin EA, Barry CE, 3rd, Dartois VA. 2018. Extreme drug tolerance of *Mycobacterium tuberculosis* in caseum. Antimicrob Agents Chemother 62:e02266-17. https://doi.org/10.1128/AAC.02266-17.
8. Basaraba RJ, Ojha AK. 2017. Mycobacterial biofilms: revisiting tuberculosis bacilli in extracellular necrotizing lesions. Microbiol Spectr 5:TBTB2-0024-2013. https://doi.org/10.1128/microbiolspec.TBTB2-0024-2016.
9. Chakraborty P, Bajeli S, Kaushal D, Radotra BD, Kumar A. 2021. Biofilm formation in the lung contributes to virulence and drug tolerance of *Mycobacterium tuberculosis*. Nat Commun 12:1606. https://doi.org/10.1038/s41467-021-21748-6.
10. Handwerger S, Tomasz A. 1985. Antibiotic tolerance among clinical isolates of bacteria. Annu Rev Pharmacol Toxicol 25:349–380. https://doi.org/10.1146/annurev.pa.25.040185.002025.
11. Chakraborty P, Kumar A. 2019. The extracellular matrix of mycobacterial biofilms: could we shorten the treatment of mycobacterial infections? Microb Cell 6:105–122. https://doi.org/10.15698/mic2019.02.667.
12. Marrakchi H, Laneelle MA, Daffe M. 2014. Mycolic acids: structures, biosynthesis, and beyond. Chem Biol 21:67–85. https://doi.org/10.1016/j.chembiol.2013.11.011.
13. Flemming HC, Wingender J, Szewzyk U, Steinberg P, Rice SA, Kjelleberg S. 2016. Biofilms: an emergent form of bacterial life. Nat Rev Microbiol 14:563–575. https://doi.org/10.1038/nrmicro.2016.94.
14. Ojha AK, Baughn AD, Sambandan D, Hsu T, Trivelli X, Guerardel Y, Alahari A, Kremer L, Jacobs WR, Jr, Hatfull GF. 2008. Growth of *Mycobacterium tuberculosis* biofilms containing free mycolic acids and harbouring drug-tolerant bacteria. Mol Microbiol 69:164–174. https://doi.org/10.1111/j.1365-2958.2008.06274.x.
15. Caceres N, Vilaplana C, Prats C, Marzo E, Llopis I, Valls J, Lopez D, Cardona P-J. 2013. Evolution and role of corded cell aggregation in *Mycobacterium tuberculosis* cultures. Tuberculosis (Edinb) 93:690–699. https://doi.org/10.1016/j.tube.2013.08.003.

16. Kalsum S, Braian C, Koeken VACM, Raffetseder J, Lindroth M, van Crevel R, Lerm M. 2017. The cording phenotype of *Mycobacterium tuberculosis* induces the formation of extracellular traps in human macrophages. Front Cell Infect Microbiol 7:278. https://doi.org/10.3389/fcimb.2017.00278.
17. Sani M, Houben EN, Geurtsen J, Pierson J, de Punder K, van Zon M, Wever B, Piersma SR, Jiménez CR, Daffé M, Appelmelk BJ, Bitter W, van der Wel N, Peters PJ. 2010. Direct visualization by cryo-EM of the mycobacterial capsular layer: a labile structure containing ESX-1-secreted proteins. PLoS Pathog 6:e1000794. https://doi.org/10.1371/journal.ppat.1000794.
18. Trivedi A, Mavi PS, Bhatt D, Kumar A. 2016. Thiol reductive stress induces cellulose-anchored biofilm formation in *Mycobacterium tuberculosis*. Nat Commun 7:11392. https://doi.org/10.1038/ncomms11392.
19. Van Wyk N, Navarro D, Blaise M, Berrin J-G, Henrissat B, Drancourt M, Kremer L. 2017. Characterization of a mycobacterial cellulase and its impact on biofilm- and drug-induced cellulose production. Glycobiology 27:392–399. https://doi.org/10.1093/glycob/cwx014.
20. Pagani TD, Guimarães ACR, Waghabi MC, Corrêa PR, Kalume DE, Berrêdo-Pinho M, Degrave WM, Mendonça-Lima L. 2019. Exploring the potential role of moonlighting function of the surface-associated proteins from *Mycobacterium bovis* BCG Moreau and Pasteur by comparative proteomic. Front Immunol 10:716. https://doi.org/10.3389/fimmu.2019.00716.
21. Ojha A, Anand M, Bhatt A, Kremer L, Jacobs WR, Jr, Hatfull GF. 2005. GroEL1: a dedicated chaperone involved in mycolic acid biosynthesis during biofilm formation in mycobacteria. Cell 123:861–873. https://doi.org/10.1016/j.cell.2005.09.012.
22. McNamara M, Tzeng S-C, Maier C, Wu M, Bermudez LE. 2013. Surface-exposed proteins of pathogenic mycobacteria and the role of Cu-Zn superoxide dismutase in macrophages and neutrophil survival. Proteome Sci 11:45. https://doi.org/10.1186/1477-5956-11-45.
23. McNamara M, Tzeng S-C, Maier C, Zhang L, Bermudez LE. 2012. Surface proteome of *Mycobacterium avium* subsp. *hominissuis* during the early stages of macrophage infection. Infect Immun 80:1868–1880. https://doi.org/10.1128/IAI.06151-11.
24. Wang X-M, Lu C, Soetaert K, S'Heeren C, Peirs P, Lanéelle M-A, Lefèvre P, Bifani P, Content J, Daffé M, Huygen K, De Bruyn J, Wattiez R. 2011. Biochemical and immunological characterization of a cpn60.1 knockout mutant of *Mycobacterium bovis* BCG. Microbiology (Reading) 157:1205–1219. https://doi.org/10.1099/mic.0.045120-0.
25. Bhatt A, Fujiwara N, Bhatt K, Gurcha SS, Kremer L, Chen B, Chan J, Porcelli SA, Kobayashi K, Besra GS, Jacobs WM, Jr. 2007. Deletion of *kasB* in *Mycobacterium tuberculosis* causes loss of acid-fastness and subclinical latent tuberculosis in immunocompetent mice. Proc Natl Acad Sci U S A 104:5157–5162. https://doi.org/10.1073/pnas.0608654104.
26. Luukinen H, Hammaren MM, Vanha-Aho LM, Parikka M. 2018. Modeling tuberculosis in *Mycobacterium marinum* infected adult zebrafish. J Vis Exp 8:58299. https://doi.org/10.3791/58299.
27. Parikka M, Hammarén MM, Harjula S-KE, Halfpenny NJA, Oksanen KE, Lahtinen MJ, Pajula ET, Iivanainen A, Pesu M, Rämet M. 2012. *Mycobacterium marinum* causes a latent infection that can be reactivated by gamma irradiation in adult zebrafish. PLoS Pathog 8:e1002944. https://doi.org/10.1371/journal.ppat.1002944.
28. Tobin DM, Ramakrishnan L. 2008. Comparative pathogenesis of *Mycobacterium marinum* and *Mycobacterium tuberculosis*. Cell Microbiol 10:1027–1760. https://doi.org/10.1111/j.1462-5822.2008.01133.x.
29. Takaki K, Davis JM, Winglee K, Ramakrishnan L. 2013. Evaluation of the pathogenesis and treatment of *Mycobacterium marinum* infection in zebrafish. Nat Protoc 8:1114–11124. https://doi.org/10.1038/nprot.2013.068.
30. Chen C, Liu H, Zabad S, Rivera N, Rowin E, Hassan M, Gomez De Jesus SM, Llinás Santos PS, Kravchenko K, Mikhova M, Ketterer S, Shen A, Shen S, Navas E, Horan B, Raudsepp J, Jeffery C. 2021. MoonProt 3.0: an update of the moonlighting proteins database. Nucleic Acids Res 49:D368–D372. https://doi.org/10.1093/nar/gkaa1101.
31. Brauner A, Shoresh N, Fridman O, Balaban NQ. 2017. An Experimental framework for quantifying bacterial tolerance. Biophys J 112:2664–2671. https://doi.org/10.1016/j.bpj.2017.05.014.
32. Brauner A, Fridman O, Gefen O, Balaban NQ. 2016. Distinguishing between resistance, tolerance and persistence to antibiotic treatment. Nat Rev Microbiol 14:320–330. https://doi.org/10.1038/nrmicro.2016.34.
33. Glickman MS, Cox JS, Jacobs WR, Jr. 2000. A novel mycolic acid cyclopropane synthetase is required for cording, persistence, and virulence of *Mycobacterium tuberculosis*. Mol Cell 5:717–727. https://doi.org/10.1016/s1097-2765(00)80250-6.
34. Anton V, Rougé P, Daffé M. 1996. Identification of the sugars involved in mycobacterial cell aggregation. FEMS Microbiol Lett 144:167–170. https://doi.org/10.1111/j.1574-6968.1996.tb08525.x.
35. Glickman MS, Cahill SM, Jacobs WR, Jr. 2001. The *Mycobacterium tuberculosis cmaA2* gene encodes a mycolic acid trans-cyclopropane synthetase. J Biol Chem 276:2228–2233. https://doi.org/10.1074/jbc.C000652200.
36. Warrier T, Tropis M, Werngren J, Diehl A, Gengenbacher M, Schlegel B, Schade M, Oschkinat H, Daffe M, Hoffner S, Eddine AN, Kaufmann SHE. 2012. Antigen 85C Inhibition restricts *Mycobacterium tuberculosis* growth through disruption of cord factor biosynthesis. Antimicrob Agents Chemother 56:1735–1743. https://doi.org/10.1128/AAC.05742-11.
37. Lerner TR, Queval CJ, Lai RP, Russell MRG, Fearns A, Greenwood DJ, Collinson L, Wilkinson RJ, Gutierrez MG. 2020. *Mycobacterium tuberculosis* cords within lymphatic endothelial cells to evade host immunity. JCI Insight 5:e136937. https://doi.org/10.1172/jci.insight.136937.
38. Nagakubo T, Tahara YO, Miyata M, Nomura N, Toyofuku M. 2021. Mycolic acid-containing bacteria trigger distinct types of membrane vesicles through different routes. iScience 24:102015. https://doi.org/10.1016/j.isci.2020.102015.
39. Schooling SR, Beveridge TJ. 2006. Membrane vesicles: an overlooked component of the matrices of biofilms. J Bacteriol 188:5945–5957. https://doi.org/10.1128/JB.00257-06.
40. Chiplunkar SS, Silva CA, Bermudez LE, Danelishvili L. 2019. Characterization of membrane vesicles released by *Mycobacterium avium* in response to environment mimicking the macrophage phagosome. Future Microbiol 14:293–313. https://doi.org/10.2217/fmb-2018-0249.
41. Deng LL, Humphries DE, Arbeit RD, Carlton LE, Smole SC, Carroll JD. 2005. Identification of a novel peptidoglycan hydrolase CwlM in *Mycobacterium tuberculosis*. Biochim Biophys Acta 1747:57–66. https://doi.org/10.1016/j.bbapap.2004.09.021.
42. Wang C, Zhang Q, Tang X, An Y, Li S, Xu H, Li Y, Wang X, Luan W, Wang Y, Liu M, Yu L. 2019. Effects of CwlM on autolysis and biofilm formation in *Mycobacterium tuberculosis* and *Mycobacterium smegmatis*. Int J Med Microbiol 309:73–83. https://doi.org/10.1016/j.ijmm.2018.12.002.
43. Antikainen J, Kuparinen V, Kupannen V, Lähteenmäki K, Korhonen TK. 2007. pH-dependent association of enolase and glyceraldehyde-3-phosphate dehydrogenase of *Lactobacillus crispatus* with the cell wall and lipoteichoic acids. J Bacteriol 189:4539–4543. https://doi.org/10.1128/JB.00378-07.
44. Kainulainen V, Loimaranta V, Pekkala A, Edelman S, Antikainen J, Kylväjä R, Laaksonen M, Laakkonen L, Finne J, Korhonen TK. 2012. Glutamine synthetase and glucose-6-phosphate isomerase are adhesive moonlighting proteins of *Lactobacillus crispatus* released by epithelial cathelicidin LL-37. J Bacteriol 194:2509–2519. https://doi.org/10.1128/JB.06704-11.
45. Foulston L, Elsholz AKW, DeFrancesco AS, Losick R. 2014. The extracellular matrix of *Staphylococcus aureus* biofilms comprises cytoplasmic proteins that associate with the cell surface in response to decreasing pH. mBio 5:e01667-14. https://doi.org/10.1128/mBio.01667-14.
46. Dengler V, Foulston L, DeFrancesco AS, Losick R. 2015. An electrostatic net model for the role of extracellular DNA in biofilm formation by *Staphylococcus aureus*. J Bacteriol 197:3779–3787. https://doi.org/10.1128/JB.00726-15.
47. Ebner P, Götz F. 2019. Bacterial excretion of cytoplasmic proteins (ECP): occurrence, mechanism, and function. Trends Microbiol 27:176–187. https://doi.org/10.1016/j.tim.2018.10.006.
48. Graf AC, Leonard A, Schäuble M, Rieckmann LM, Hoyer J, Maass S, Lalk M, Becher D, Pané-Farré J, Riedel K. 2019. Virulence factors produced by *Staphylococcus aureus* biofilms have a moonlighting function contributing to biofilm integrity. Mol Cell Proteomics 18:1036–1053. https://doi.org/10.1074/mcp.RA118.001120.
49. Qian J, Chen R, Wang H, Zhang X. 2020. Role of the PE/PPE family in host–pathogen interactions and prospects for anti-tuberculosis vaccine and diagnostic tool design. Front Cell Infect Microbiol 10:594288. https://doi.org/10.3389/fcimb.2020.594288.
50. Wang Q, Boshoff HIM, Harrison JR, Ray PC, Green SR, Wyatt PG, Barry CE, III. 2020. PE/PPE proteins mediate nutrient transport across the outer membrane of *Mycobacterium tuberculosis*. Science 367:1147–1151. https://doi.org/10.1126/science.aav5912.
51. Pietersen R-D, Du Preez I, Loots DT, van Reenen N, Beukes D, Leisching G, Baker B. 2020. Tween 80 induces a carbon flux rerouting in *Mycobacterium tuberculosis*. J Microbiol Methods 170:105795. https://doi.org/10.1016/j.mimet.2019.105795.

52. Gröschel MI, Sayes F, Simeone R, Majlessi L, Brosch R. 2016. ESX secretion systems: mycobacterial evolution to counter host immunity. Nat Rev Microbiol 14:677–691. https://doi.org/10.1038/nrmicro.2016.131.
53. Schorey JS, Li Q, McCourt DW, Bong-Mastek M, Clark-Curtiss JE, Ratliff TL, Brown EJ. 1995. A *Mycobacterium leprae* gene encoding a fibronectin binding protein is used for efficient invasion of epithelial cells and Schwann cells. Infect Immun 63:2652–2657. https://doi.org/10.1128/IAI.63.7.2652-2657.1995.
54. Fenn K, Wong CT, Darbari VC. 2019. *Mycobacterium tuberculosis* uses Mce proteins to interfere with host cell signaling. Front Mol Biosci 6:149. https://doi.org/10.3389/fmolb.2019.00149.
55. Vinod V, Vijayrajratnam S, Vasudevan AK, Biswas R. 2020. The cell surface adhesins of *Mycobacterium tuberculosis*. Microbiol Res 232:126392. https://doi.org/10.1016/j.micres.2019.126392.
56. Delogu G, Brennan MJ. 1999. Functional domains present in the mycobacterial hemagglutinin, HBHA. J Bacteriol 181:7464–7469. https://doi.org/10.1128/JB.181.24.7464-7469.1999.
57. Berge M, Pezzatti J, Gonzalez-Ruiz V, Degeorges L, Mottet-Osman G, Rudaz S, Viollier PH. 2020. Bacterial cell cycle control by citrate synthase independent of enzymatic activity. Elife 9:e52272. https://doi.org/10.7554/eLife.52272.
58. Rego EH, Audette RE, Rubin EJ. 2017. Deletion of a mycobacterial divisome factor collapses single-cell phenotypic heterogeneity. Nature 546:153–157. https://doi.org/10.1038/nature22361.
59. Kieser KJ, Rubin EJ. 2014. How sisters grow apart: mycobacterial growth and division. Nat Rev Microbiol 12:550–562. https://doi.org/10.1038/nrmicro3299.
60. Jakkala K, Ajitkumar P. 2019. Hypoxic non-replicating persistent *Mycobacterium tuberculosis* develops thickened outer layer that helps in restricting rifampicin entry. Front Microbiol 10:2339. https://doi.org/10.3389/fmicb.2019.02339.
61. Banerjee S, Nandyala AK, Raviprasad P, Ahmed N, Hasnain SE. 2007. Iron-dependent RNA-binding activity of *Mycobacterium tuberculosis* aconitase. J Bacteriol 189:4046–4052. https://doi.org/10.1128/JB.00026-07.
62. Rahi A, Dhiman A, Singh D, Lynn AM, Rehan M, Bhatnagar R. 2018. Exploring the interaction between *Mycobacterium tuberculosis* enolase and human plasminogen using computational methods and experimental techniques. J Cell Biochem 119:2408–2417. https://doi.org/10.1002/jcb.26403.
63. de la Paz Santangelo M, Gest PM, Guerin ME, Coinçon M, Pham H, Ryan G, Puckett SE, Spencer JS, Gonzalez-Juarrero M, Daher R, Lenaerts AJ, Schnappinger D, Therisod M, Ehrt S, Sygusch J, Jackson M. 2011. Glycolytic and non-glycolytic functions of *Mycobacterium tuberculosis* fructose-1,6-bisphosphate aldolase, an essential enzyme produced by replicating and non-replicating bacilli. J Biol Chem 286:40219–40231. https://doi.org/10.1074/jbc.M111.259440.
64. Gengenbacher M, Rao SPS, Pethe K, Dick T. 2010. Nutrient-starved, non-replicating *Mycobacterium tuberculosis* requires respiration, ATP synthase and isocitrate lyase for maintenance of ATP homeostasis and viability. Microbiology (Reading) 156:81–87. https://doi.org/10.1099/mic.0.033084-0.
65. Nandakumar M, Nathan C, Rhee K. 2014. Isocitrate lyase mediates broad antibiotic tolerance in *Mycobacterium tuberculosis*. Nat Commun 5:4306. https://doi.org/10.1038/ncomms5306.
66. Bhusal RP, Jiao W, Kwai BXC, Reynisson J, Collins AJ, Sperry J, Bashiri G, Leung IKH. 2019. Acetyl-CoA-mediated activation of *Mycobacterium tuberculosis* isocitrate lyase 2. Nat Commun 10:4639. https://doi.org/10.1038/s41467-019-12614-7.
67. Daniel J, Maamar H, Deb C, Sirakova TD, Kolattukudy PE. 2011. *Mycobacterium tuberculosis* uses host triacylglycerol to accumulate lipid droplets and acquires a dormancy-like phenotype in lipid-loaded macrophages. PLoS Pathog 7:e1002093. https://doi.org/10.1371/journal.ppat.1002093.
68. Maurya RK, Bharti S, Krishnan MY. 2018. Triacylglycerols: fuelling the hibernating *Mycobacterium tuberculosis*. Front Cell Infect Microbiol 8:450. https://doi.org/10.3389/fcimb.2018.00450.
69. Pohane AA, Carr CR, Garhyan J, Swarts BM, Siegrist MS. 2021. Trehalose recycling promotes energy-efficient biosynthesis of the mycobacterial cell envelope. mBio 12:e02801-20. https://doi.org/10.1128/mBio.02801-20.
70. Langklotz S, Narberhaus F. 2011. The *Escherichia coli* replication inhibitor CspD is subject to growth-regulated degradation by the Lon protease. Mol Microbiol 80:1313–1325. https://doi.org/10.1111/j.1365-2958.2011.07646.x.
71. Uppal S, Shetty DM, Jawali N. 2014. Cyclic AMP receptor protein regulates *cspD*, a bacterial toxin gene, in *Escherichia coli*. J Bacteriol 196:1569–1577. https://doi.org/10.1128/JB.01476-13.
72. Spanka DT, Konzer A, Edelmann D, Berghoff BA. 2019. High-throughput proteomics identifies proteins with importance to postantibiotic recovery in depolarized persister cells. Front Microbiol 10:378. https://doi.org/10.3389/fmicb.2019.00378.
73. Torrey HL, Keren I, Via LE, Lee JS, Lewis K. 2016. High persister mutants in *Mycobacterium tuberculosis*. PLoS One 11:e0155127. https://doi.org/10.1371/journal.pone.0155127.
74. Beites T, O'Brien K, Tiwari D, Engelhart CA, Walters S, Andrews J, Yang H-J, Sutphen ML, Weiner DM, Dayao EK, Zimmerman M, Prideaux B, Desai PV, Masquelin T, Via LE, Dartois V, Boshoff HI, Barry CE, Ehrt S, Schnappinger D. 2019. Plasticity of the *Mycobacterium tuberculosis* respiratory chain and its impact on tuberculosis drug development. Nat Commun 10:4970. https://doi.org/10.1038/s41467-019-12956-2.
75. Rao SPS, Alonso S, Rand L, Dick T, Pethe K. 2008. The protonmotive force is required for maintaining ATP homeostasis and viability of hypoxic, non-replicating *Mycobacterium tuberculosis*. Proc Natl Acad Sci U S A 105:11945–11950. https://doi.org/10.1073/pnas.0711697105.
76. Cook GM, Hards K, Vilchèze C, Hartman T, Berney M. 2014. Energetics of respiration and oxidative phosphorylation in mycobacteria. Microbiol Spectr 2:MGM2-0015-2013. https://doi.org/10.1128/microbiolspec.MGM2-0015-2013.
77. Ganguli G, Mukherjee U, Sonawane A. 2019. Peroxisomes and oxidative stress: their implications in the modulation of cellular immunity during mycobacterial infection. Front Microbiol 10:1121. https://doi.org/10.3389/fmicb.2019.01121.
78. Khare G, Nangpal P, Tyagi AK. 2017. Differential roles of iron storage proteins in maintaining the iron homeostasis in *Mycobacterium tuberculosis*. PLoS One 12:e0169545. https://doi.org/10.1371/journal.pone.0169545.
79. Savijoki K, Nyman TA, Kainulainen V, Miettinen I, Siljamäki P, Fallarero A, Sandholm J, Satokari R, Varmanen P. 2019. Growth mode and carbon source impact the surfaceome dynamics of *Lactobacillus rhamnosus* GG. Front Microbiol 10:1272. https://doi.org/10.3389/fmicb.2019.01272.
80. Savijoki K, Miettinen I, Nyman TA, Kortesoja M, Hanski L, Varmanen P, Fallarero A. 2020. Growth mode and physiological state of cells prior to biofilm formation affect immune evasion and persistence of *Staphylococcus aureus*. Microorganisms 8:106. https://doi.org/10.3390/microorganisms8010106.
81. Cox J, Mann M. 2008. MaxQuant enables high peptide identification rates, individualized p.p.b.-range mass accuracies and proteome-wide protein quantification. Nat Biotechnol 26:1367–1372. https://doi.org/10.1038/nbt.1511.
82. Cox J, Neuhauser N, Michalski A, Scheltema RA, Olsen JV, Mann M. 2011. Andromeda: a peptide search engine integrated into the MaxQuant environment. J Proteome Res 10:1794–1805. https://doi.org/10.1021/pr101065j.
83. Deutsch EW, Csordas A, Sun Z, Jarnuczak A, Perez-Riverol Y, Ternent T, Campbell DS, Bernal-Llinares M, Okuda S, Kawano S, Moritz RL, Carver JJ, Wang M, Ishihama Y, Bandeira N, Hermjakob H, Vizcaino JA. 2017. The ProteomeXchange consortium in 2017: supporting the cultural change in proteomics public data deposition. Nucleic Acids Res 45:D1100–D1106. https://doi.org/10.1093/nar/gkw936.
84. Altschul SF, Gish W, Miller W, Myers EW, Lipman DJ. 1990. Basic local alignment search tool. J Mol Biol 215:403–410. https://doi.org/10.1016/S0022-2836(05)80360-2.
85. Altschul SF, Madden TL, Schaffer AA, Zhang J, Zhang Z, Miller W, Lipman DJ. 1997. Gapped BLAST and PSI-BLAST: a new generation of protein database search programs. Nucleic Acids Res 25:3389–3402. https://doi.org/10.1093/nar/25.17.3389.
86. Altschul SF, Wootton JC, Gertz EM, Agarwala R, Morgulis A, Schaffer AA, Yu YK. 2005. Protein database searches using compositionally adjusted substitution matrices. FEBS J 272:5101–5109. https://doi.org/10.1111/j.1742-4658.2005.04945.x.
87. Marchler-Bauer A, Bo Y, Han L, He J, Lanczycki CJ, Lu S, Chitsaz F, Derbyshire MK, Geer RC, Gonzales NR, Gwadz M, Hurwitz DI, Lu F, Marchler GH, Song JS, Thanki N, Wang Z, Yamashita RA, Zhang D, Zheng C, Geer LY, Bryant SH. 2017. CDD/SPARCLE: functional classification of proteins via subfamily domain architectures. Nucleic Acids Res 45:D200–D203. https://doi.org/10.1093/nar/gkw1129.
88. Ashburner M, Ball CA, Blake JA, Botstein D, Butler H, Cherry JM, Davis AP, Dolinski K, Dwight SS, Eppig JT, Harris MA, Hill DP, Issel-Tarver L, Kasarskis A, Lewis S, Matese JC, Richardson JE, Ringwald M, Rubin GM, Sherlock G. 2000. Gene ontology: tool for the unification of biology. The Gene Ontology Consortium. Nat Genet 25:25–29. https://doi.org/10.1038/75556.
89. Rice P, Longden I, Bleasby A. 2000. EMBOSS: the European Molecular Biology Open Software Suite. Trends Genet 16:276–277. https://doi.org/10.1016/s0168-9525(00)02024-2.
90. Petersen TN, Brunak S, von Heijne G, Nielsen H. 2011. SignalP 4.0: discriminating signal peptides from transmembrane regions. Nat Methods 8:785–786. https://doi.org/10.1038/nmeth.1701.

91. Bendtsen JD, Kiemer L, Fausboll A, Brunak S. 2005. Non-classical protein secretion in bacteria. BMC Microbiol 5:58. https://doi.org/10.1186/1471-2180-5-58.
92. Krogh A, Larsson B, von Heijne G, Sonnhammer EL. 2001. Predicting transmembrane protein topology with a hidden Markov model: application to complete genomes. J Mol Biol 305:567–580. https://doi.org/10.1006/jmbi.2000.4315.
93. Sonnhammer EL, von Heijne G, Krogh A. 1998. A hidden Markov model for predicting transmembrane helices in protein sequences. Proc Int Conf Intell Syst Mol Biol 6:175–182.
94. Tyanova S, Temu T, Sinitcyn P, Carlson A, Hein MY, Geiger T, Mann M, Cox J. 2016. The Perseus computational platform for comprehensive analysis of (prote)omics data. Nat Methods 13:731–740. https://doi.org/10.1038/nmeth.3901.
95. Szklarczyk D, Gable AL, Lyon D, Junge A, Wyder S, Huerta-Cepas J, Simonovic M, Doncheva NT, Morris JH, Bork P, Jensen LJ, von Mering C. 2019. STRING v11: protein-protein association networks with increased coverage, supporting functional discovery in genome-wide experimental datasets. Nucleic Acids Res 47:D607–D613. https://doi.org/10.1093/nar/gky1131.

MANUSCRIPT

Proteomic Analysis of Mycobacterial Biofilm Matrix and Development of Biofilm-binding Synthetic Nanobodies

Hammarén MM*, Luukinen H*, Sillanpää A, Remans K, Lapouge K, Custodio T, Löw C, Myllymäki H, Montonen T, Seeger MA, Robertson J, Nyman T, Savijoki K, Parikka M

*equal contribution

Submitted 2022